TRACE ELEMENT GEOCHEMICAL CHARACTERIZATION OF SOUTHEASTERN PEGMATITIC MUSCOVITE AND RESULTANT IMPLICATIONS FOR THE PROVENANCING OF ARCHAEOLOGICAL MICA

by

MICHAEL F. BONOMO

(Under the Direction of Samuel E. Swanson)

ABSTRACT

Pegmatitic muscovite is a common component of Mississippian period archaeological sites. Where encountered, such archaeological muscovite has often been attributed to an assumed Spruce Pine (North Carolina) source. Large crystals of pegmatitic muscovite, however, occur over a wide geographic range throughout the southeastern United States from Virginia through Alabama. In the case of muscovite artifacts from the Etowah mounds in northwest Georgia, Georgia's muscovite-bearing pegmatite districts provide a local alternative source to Spruce Pine. Non-destructive portable X-ray fluorescence spectroscopy (pXRF) has been utilized in both the trace element geochemical characterization of muscovite from two of Georgia's pegmatite districts (as well as from Spruce Pine) and in the quantitative analysis of Etowah muscovite artifacts. On the basis of principal components analysis (PCA) and discriminant function analysis (DFA), the Etowah micas have been shown to display a geochemical signature more consistent with a local Georgia source than a Spruce Pine source.

INDEX WORDS: Muscovite mica, Pegmatites, Etowah, Provenance, Trace elements, Principal components analysis, Discriminant function analysis

TRACE ELEMENT GEOCHEMICAL CHARACTERIZATION OF SOUTHEASTERN PEGMATITIC MUSCOVITE AND RESULTANT IMPLICATIONS FOR THE PROVENANCING OF ARCHAEOLOGICAL MICA

by

MICHAEL F. BONOMO

B.S., The University of Miami, 2009

A Thesis Submitted to the Graduate Faculty of The University of Georgia in Partial Fulfillment of the Requirements for the Degree

MASTER OF SCIENCE

ATHENS, GEORGIA

2011

TRACE ELEMENT GEOCHEMICAL CHARACTERIZATION OF SOUTHEASTERN PEGMATITIC MUSCOVITE AND RESULTANT IMPLICATIONS FOR THE PROVENANCING OF ARCHAEOLOGICAL MICA

by

MICHAEL F. BONOMO

Major Professor: Samuel E. Swanson

Committee: Douglas E. Crowe
Paul A. Schroeder

Electronic Version Approved:

Maureen Grasso
Dean of the Graduate School
The University of Georgia
August 2011

ACKNOWLEDGEMENTS

First and foremost, I thank my advisor, Sam Swanson, for his constant support and guidance throughout my academic endeavors. I would also like to thank my committee, Doug Crowe and Paul Schroeder, for their patience and support. My gratitude is extended to both Steve Holland and Max Christie for their assistance with matters relating to the statistical aspects of this research.

Several acknowledgements are in order for all those who assisted me (either directly or indirectly) throughout the course of my field work. Particular thanks go to Katrina Ostrowicki, Heather Veasey, Jason Jones and Eric Porter for assisting with sample collection; the Spruce Pine samples utilized in this research were left over from Brian Veal's thesis work conducted years prior. In addition, a number of property owners and community members were gracious enough to point me in the direction of some of the old mine workings or to allow sample collection on their property; for this, I especially thank Ogden Persons and George Wilson of Forsyth, Georgia, and Al Cleveland of Holly Springs, Georgia.

Robert Tykot of the University of South Florida was gracious enough to allow me to test the applicability of a portable XRF system on some of my samples, free of charge.

Thomas Foster of the Antonio J. Waring, Jr. Archaeological Laboratory and Bryan Tucker of Georgia DNR's Historic Preservation Division were responsible for granting the necessary permission to analyze the Etowah mica artifacts stored in the collections at the Waring Lab. The Waring Lab's Susan Fishman-Armstrong and Kitty Lee provided assistance in accessing the artifacts from within the collections.

This research was made possible through funding from a research grant from the Geological Society of America, as well as multiple research grants from the Department of Geology at the University of Georgia's Miriam Watts-Wheeler Scholarship Fund. I am beyond grateful for the generosity of both institutions.

TABLE OF CONTENTS

Page

LIST OF TABLES

PAGE

LIST OF FIGURES

PAGE

CHAPTER 1

INTRODUCTION

Research Question and Objectives

Muscovite mica [$KAl_2(AlSi_3O_{10})(OH)_2$] is a typical component of Mississippian period archaeological sites. Artifacts frequently consist of scraps of sheet mica, though cut mica artifacts or mica caches are occasionally uncovered (Ferguson 1974). The discovery of sheets of mica in burials in the Mississippi Valley, laid over the face, breast, or entire body of the deceased, signifies use in religious rites or in a sacred context in addition to simple ornamentation and mirrors (Smith 1877). The Etowah site (9BR1), located along the Etowah River's northern bank near Cartersville in northwestern Georgia (Figure 1), is one Mississippian mound site from which muscovite mica artifacts have been recovered. Mica artifacts have been recovered from the site's elite burial mound, Mound C (King 2003) (Figure 2); artifacts referenced in the literature include mica ornaments excavated from Grave 37, as well as fragments of mica from Grave 76 (Moorehead 1932). The University of West Georgia's Antonio J. Waring, Jr. Archaeological Laboratory serves as a repository for perforated and otherwise worked muscovite discs, crosses and ornaments from Mound C and the village area east of Mound A, along with numerous cut fragments and strips (Thomas Foster, personal communication, 2011); these artifacts were collected during excavations by Sears (1953) and Larson (1954-1958, 1961 and 1964) (excavations referenced in Hally & Langford 1988). Cut mica artifacts from a non-burial context have also been recovered from Mound B (King 2001).

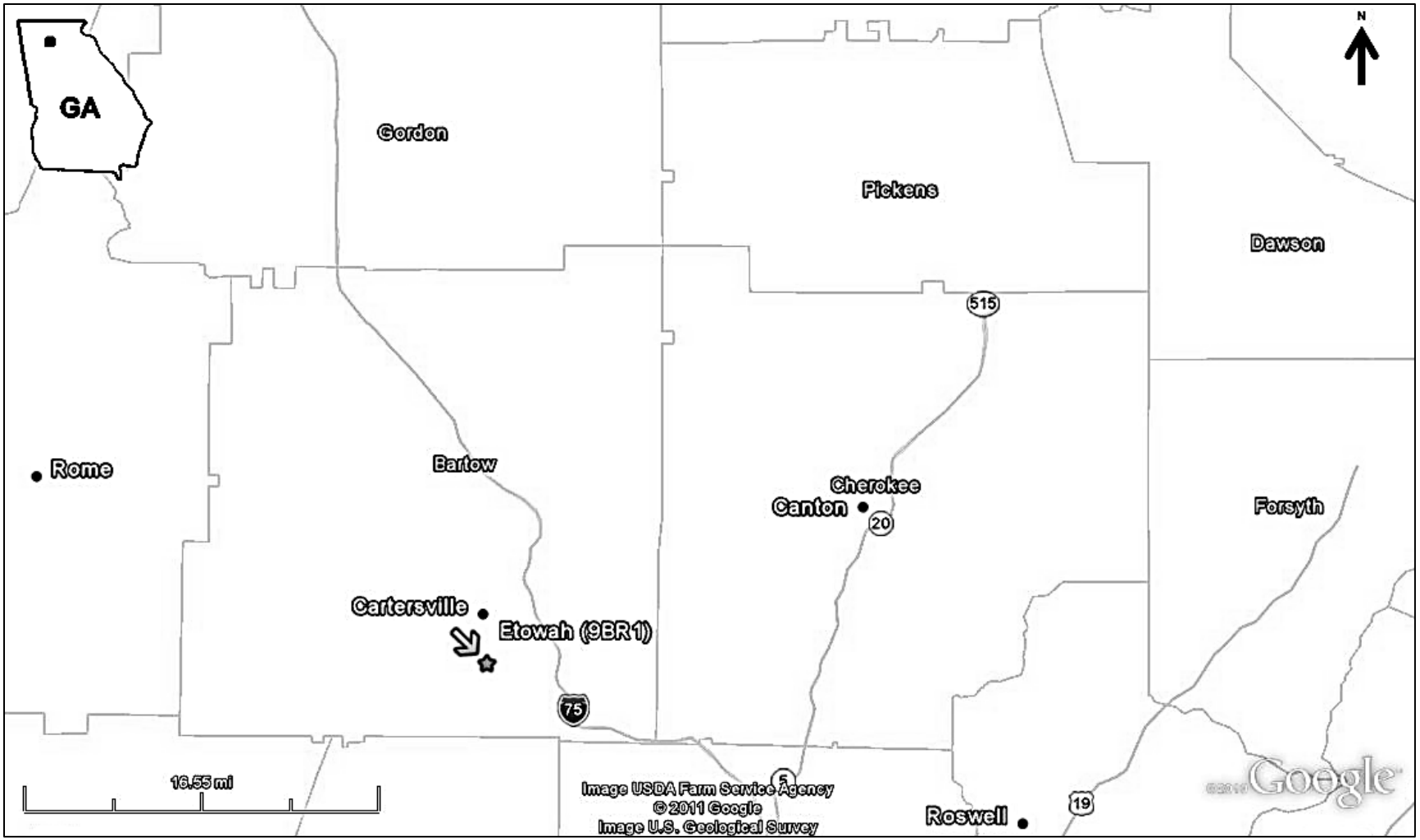

Figure 1: The Etowah site (9BR1).

Figure 2: The Etowah mounds (A, B & C).

King (2003:1) attributes the objects and artifacts from Etowah "to the suite of ceremonial objects and symbolic themes known as the Southeastern Ceremonial Complex". In doing so, he attributes the discoveries of Thomas (1894), Moorehead (1932), and Larson (1971) of numerous Southeastern Ceremonial Complex goods at Mound C as a sign that the inhabitants of Etowah, much like the Hopewell, "participated heavily in the exchange of exotic materials," and that such a system was as "fundamental to the operation of" the Middle Mississippian period chiefdoms as it was to those of the Hopewell (King 2003:3). The source of the Etowah micas is a topic which has not received much, if any, scientific consideration (Vin Steponaitis, personal communication, 2009). While the well-known prehistoric mica mines of western North Carolina, particularly those in the Spruce Pine district, seem to be the obvious potential sources, prehistoric mica mines are known from northern Georgia and eastern Alabama as well, and provide closer alternative sources to Spruce Pine (Thomas 1891; Sterrett 1923; Ferguson 1974). The focus of this research will be to establish a non-destructive methodology for discriminating amongst muscovite-bearing pegmatites primarily on the basis of trace element geochemistry. The resulting methodology may then lend itself to future provenance studies of muscovite artifacts from archaeological sites in the Southeast.

Archaeological Muscovite

Notable Occurrences of Muscovite Artifacts

The most prominent sites indicative of the Mississippian culture, the large earthen mounds scattered throughout the American Midwest and Southeast, were originally described in Garcilaso de la Vega's (1605) *La Florida del Inca*, in which de la Vega provides an account of Hernando de Soto's expedition throughout the American Southeast during a time in which the mound-building tradition was still in practice (Silverberg 1968). De la Vega writes that at

Cofachiqui in present-day Columbia, South Carolina, the Native Americans had presented de Soto and his men with a variety of "metals… of the colors the Spaniards were seeking," including what de la Vega describes as "great slabs of iron pyrites which were thick as boards" (qtd. in Silverberg 1968:15). Silverberg (1968) proposes that these were not iron pyrites, however, but thick sheets of mica.

Archaeological evidence of the extraction and utilization of mica by prehistoric Native Americans predates de la Vega's account. Mica artifacts have been excavated from some of the earliest burial mounds in the Ohio Valley, those of the Adena culture and Hopewell tradition. These artifacts include spectacular figures of hands, claws, talons, geometric designs, and human torsos cut from large sheets of mica, as well as perforated mica disks and elliptical shapes that may have been backed and used as mirrors (Figure 3). At the Mound City Group in Chillicothe, Ohio, several hundred disks of mica, speculated to have been strung together as part of a medicine man or shaman's ritual costume, were discovered (Margolin 2000). Work by Mills (1922) at Mound City's Mica Grave Mound discovered graves containing thick sheets of mica cut into rectangular sheets measuring up to 25-x-35 cm and covering an area approximately 2.4-x-1.2 m (see also Silverberg [1968] and Margolin [2000]); at the nearby Seip Mound site, the foundations of two workshops were unearthed in which the floors were found to be covered with mica trimmings and blades left over from the cutting process (Baby & Langlois 1979; see also Margolin 2000). In the Southeast, Dickens (1976) and Wilson (1986) describe the discovery of funerary objects made of mica at the Warren Wilson and Garden Creek sites (North Carolina), though "in quantities that pale in comparison with those found in the Ohio Valley Mounds" (Margolin 2000:43). Excavations by Gail Wagner of a house in a Mississippian center in central South Carolina discovered a covering of mica debris over the floor (Adam King, personal

Figure 3: Muscovite artifacts from the Ohio Valley. Artifacts not scaled relative to one another: bird claw cutout, h. ~27.9 cm; hand cutout, h. ~29 cm; headless torso, h. ~20.3 cm; serpent effigy, w. ~35.6 cm; atlatl effigy, dimensions not given. From Townsend (2004).

communication, 2009). At Moundville in Alabama, a pit was excavated and found to contain approximately 208 g of mica debris, remnants of the manufacture of artifacts (Welch 1991). Scarry (1998:75) references personal communications in which mica from Moundville was surmised to "have been used to make a glitterlike pigment".

Prehistoric Mining Practices

Hopewellian tradition and Mississippian period mica mining practices have been documented, to a limited extent. Since modern historic commercial mica mining operations were begun in North Carolina in 1867, evidence of prehistoric pits and trenches has been sufficiently disturbed, to the extent that much of the information regarding prehistoric Native American mining practices is only available through written historic records (Kerr 1875; Stuckey 1965; Ferguson 1974). Native Americans had extensively utilized mica deposits in the southern Appalachians, particularly in western North Carolina, over the past 2,000 years or more (Ferguson 1974; Margolin 2000); reports by Thomas (1891) and Sterrett (1923) identify at least 24 prehistoric mica mines across North Carolina, Georgia, and Alabama (Figure 4; Appendix A).

One of the earliest accounts of the extent and skill with which Native Americans mined the Southeast comes from Kerr's (1875:300-301) *Reports of the North Carolina Geological Survey* in which it is stated that the mica mining industry "is not really new [in North Carolina], it is only revived":

> Since the development of mica-mining on a large scale in Mitchell and the adjoining counties it has been ascertained that there are hundreds of old pits and connecting tunnels among the spurs and knobs and ridges of this rugged region; and there remains no doubt that mining was carried on here for ages, and in a very systematic and skillful way; for among all the scores of mines recently opened, I am informed that scarcely one has turned out profitably which did not follow the old workings, and strike the ledges wrought by these ancient miners.

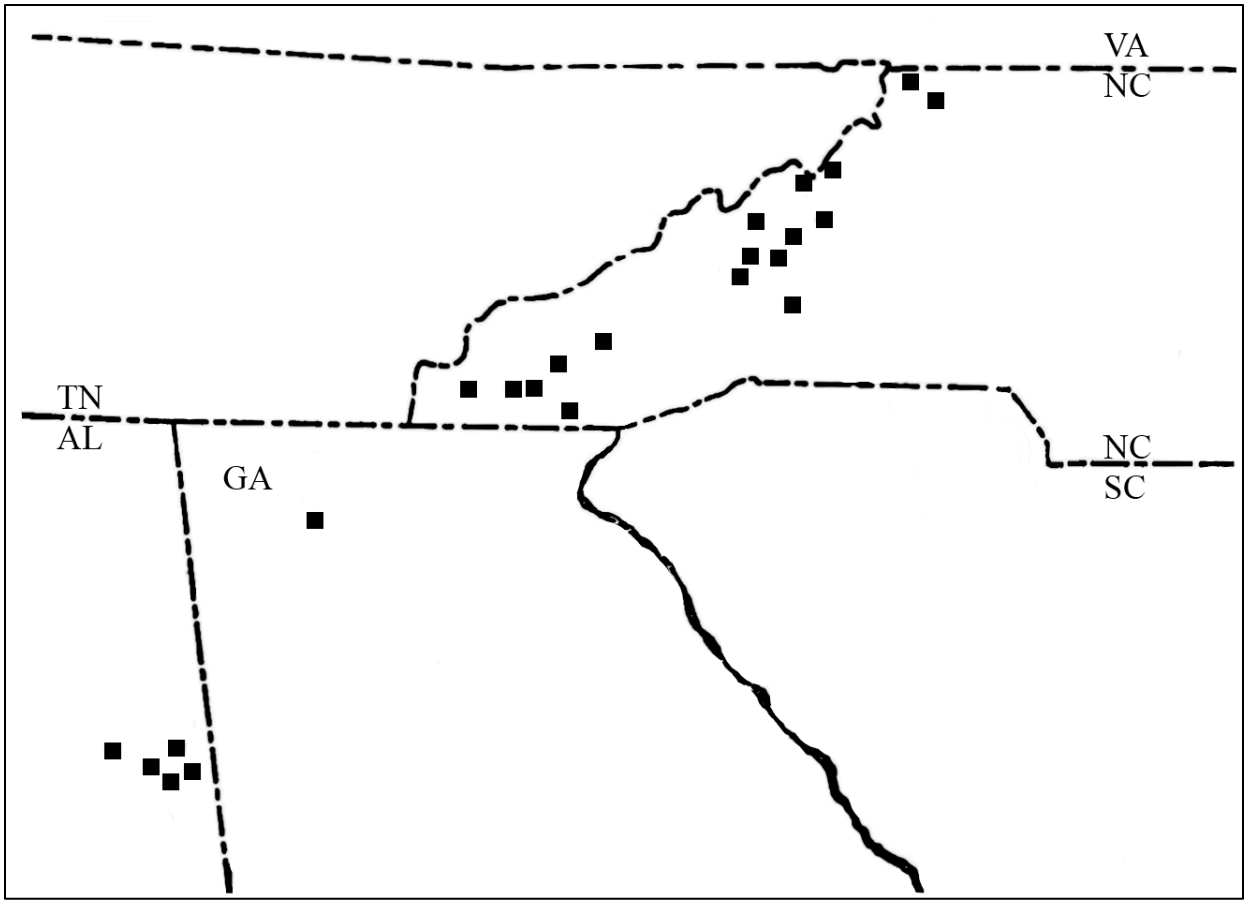

Figure 4: Prehistoric mica mines in the southern Appalachians. Modified from Ferguson 1974.

Kerr (1880:457) further claims that "the largest and most profitable mines of the present day are simply the ancient Mound Builders' mines reopened and pushed into the hard undecomposed granite by powder and steel". Smith (1877) echoes Kerr's assessments:

> There are several ancient mica diggings in Mitchell County, North Carolina. Gen. T.L. Clingman, some twenty-five or thirty years ago, supposing that these old diggings were the work of De Soto in search for silver, had one of the old pits opened, and instead of finding silver, he found a vein containing large crystals of mica (pp. 441-442).
>
> It is manifest that the ancient miners understood their business well. Indeed, they seldom committed a mistake. In every instance which has come under my observation, where they did work along the mica zone, mica veins have been found by opening the old works. It is also a noteworthy fact that where the old excavations are extensive, the veins yield usually large crystals of firm mica of good cleavage and in every way of excellent quality (pp. 442).

With regard to the mining techniques used by the Native Americans, Kerr (1875, 1880) and Smith (1877) provide detailed observations of the methods employed. Smith (1877:442) attests to seeing "very clearly corroborative evidence that the people who did this ancient work had no implements superior to stone," stating that "[t]hey only operated upon such veins as contain a decomposed and consequently soft feldspar". For this reason, when extracting mica from veins, the Native Americans simply worked around rather than through hard points in the vein. Smith (1877:443) observes that the stone implements used by the Native Americans in their ancient diggings left blunt tool marks in their shafts. Kerr's (1880:457) descriptions of the aboriginal works at several mines in western North Carolina agree accordingly:

> They opened and worked a great many veins down to or near water level… as far as the action of atmospheric chemistry had softened the rock so that it was workable without metal tools. …Blocks of mica have often been found half imbedded in the face of the vein, with the tool-marks about it, showing the exact limit of the efficiency of those prehistoric mechanical appliances.

Smith (1877:441) characterizes the nature of these diggings as open excavations, some of which were "of large proportions, and must have employed a large force and a series of years in their accomplishment".

Kerr (1875:301) similarly describes the prehistoric mining tunnels at Cane Creek in Mitchell County, North Carolina:

> The pits are always open "diggings," never regular shafts, and the earth and debris often amounts to enormous heaps. …The tunnels are much smaller than such workings in modern mining, generally only three to three and a half feet in height and considerably less in width. Some have been followed for fifty and a hundred feet and upwards.

Sterrett (1923), possibly in reference to the same mining operations at Cane Creek, describes a "large amphitheatral cut in the side of the ridge" (qtd. in Ferguson 1974:213). Smith (1877:443) points out that the practice of tunneling to extract mica was only "seldom attempted… and where there is any evidence of such work it is more like burrowing in than cutting a tunnel", and provides one example of such a hole which "does not exceed 15 feet in length".

Smith (1877:442-443) also provides one of the more detailed accounts of an ancient Native American mining operation located on his farm in Macon County, North Carolina:

> The old excavation commences at a small branch and runs at a right angle from it into a ridge that juts down with a gentle slope. The dump material has been thrown right and left for the first hundred feet. I tunneled in diagonally and struck the vein 60 feet from the branch, and have drifted along it 40 feet. Here we reach an immense dump-rim, 65 feet higher than the level of the branch, and which seems to have been thrown back upon their works. It forms at this end a circular rim to the continued excavations higher up the ridge. The whole length of the excavation from the branch to the upper end of the cut is about 320 feet. The material removed from the upper part of the cut was carried up the hill as well as down it. The dump on the upper side of this upper part of the cut, and at the widest point, is about 25 feet above the present bottom of the excavation, and at this point dump and excavation measure about 150 feet across. At the upper end of my tunnel the old digging has been carried down about 30 feet below the surface. If the excavation at the point just mentioned was carried as deep as the work at the upper end of the tunnel, it would make the dump heap on the upper side 55 feet higher than the bottom of the old works. I have been thus particular,

> in order to show that with mere stone implements it must have required a series of years and a large force to have accomplished such results.

At the Sink Hole (also Sinkhole, or Silvers) mine in Bandana in Mitchell County, North Carolina, prehistoric workings consisted of several overgrown pits dug into the hillsides opposite the Sink Hole Creek. One line of excavations extended for over 365 m, reaching depths from approximately 9 m to 12 m (Margolin 2000). Kerr (1875:300), upon witnessing the Sink Hole workings, described them as "a dozen or more open pits 40 to 50 feet wide, by 75 to 100 long, filled up to 15 or 20 feet of depth". While Clingman had attributed these workings to the Native Americans as early as 1873 (Margolin 2000:47), Kerr (1875:301) only later learned that "mica was of common occurrence in the tumuli of the Mound Builders, among the utensils and ornaments which [Native Americans] are in the habit of inhuming with their dead" and that "cut forms similar to those found in the mounds were occasionally discovered among the rubbish and refuse heaps about, and in the old pits".

The Southern Appalachians in Prehistoric Mica Exchange Networks

Connections like those made by Clingman and Kerr have led many to suggest that the southern Appalachians, particularly in North Carolina, were integral to prehistoric trade networks; Ferguson (1974:212) suggests this on the basis of "[t]he distribution of artifacts of large sheet mica in the eastern United States, especially in the area of the Hopewellian climax". Keel (1967), citing the discovery of Ohio Flint Ridge material at the Garden Creek site in Hayward County, North Carolina, speculates that these networks may have extended as far as the Ohio Valley (Ferguson 1974). This notion, however, was hardly new; Holmes (1919) believed the North Carolina mica deposits to be the source of mica utilized by the architects of the burial mounds in the Ohio Valley (see also Margolin 2000). Prior to Holmes, Smith (1877:441) had surmised that mica found in the mounds of the western Mississippi Valley had origins in "the

southern spurs of the Alleghanies" and cites the religious significance associated with mica as being the reason the Native Americans went to such lengths to obtain it:

> The supposition that much of the mica found in those ancient mounds was employed in the religious ceremonies of the race, suggests the high value placed upon it, and the immense labor employed in procuring it, as well as the great distance to which it was transported, sustain the idea that there was more than an economical or commercial value attached to it.

Prufer (1965) extends this notion to the Ohio Valley, claiming that the entire Hopewellian exchange network and its "emphasis on exotic raw materials" was established solely to provide objects for religious ceremonies:

> These exotic materials – copper from the Upper Great Lakes regions, mica from the Appalachians, fancy flints from various sources, obsidian from the Rockies or from the Southwest, large conch shells from the Gulf Coast, various sea shells from the Atlantic and Gulf Coasts, Grizzly Bear canine teeth from the Rockies, silver, meteoric iron, fossil shark teeth, to mention only a few – seem to have been crucial components in the material maintenance of the Hopewellian idea system. In order to obtain these materials a vast, and undoubtedly complex, exchange network had to be maintained through large areas of the United States. The exchange network itself seems to have provided the mechanical basis upon which this system spread, leading to a vast dynamic interaction sphere, the aim of which appears to have been exclusively the production of ceremonial objects primarily intended for deposition with the dead (qtd. in Silverberg 1968:265).

Margolin (2000:51-52) supports the view of a far-reaching trade network, arguing that in the case of the inhabitants of the Ohio Valley, "this conclusion appears incontestable, for although they are hundreds of miles apart, North Carolina [mica] deposits are nearer to the mounds than any others available to the prehistoric miners". The extraction and careful transportation of large sheets of mica (some up to one meter in diameter) which were prized for ritual purposes from the deposits in North Carolina would have required an investment of time and effort similar to that required to obtain their other exotic materials. In some instances, the Native Americans dug pits or caches with the exclusive purpose of stockpiling mica until it was ready to be transported to fabrication sites or workshops like those at the Seip Mound to be cut "into designs of ritual

significance" (Margolin 2000:54). Such pits were discovered by Smith (1877) near the prehistoric mines in Macon County (see also Stuckey 1965); the Smithsonian Institution's collections house large elliptical sheets of mica which may have been excavated from pits in Mitchell County (Margolin 2000).

The Etowah Site

The Etowah site (9BR1) consists of six mounds, the largest of which (Mound A) stands over 18 m in height and is the second largest American earthwork by volume at over 121,762 m^3, covering an area over 12,140.5 m^2 (Silverberg 1968; King 2003). Its shape is that of a rectangular pyramid with the top having been leveled off, with a graded ramp situated on the east side of the mound (Silverberg 1968). It is possible that de Soto and his men, in the mid-sixteenth century, were the first Europeans to have viewed the mounds at Etowah. It is also possible that William Bartram, in 1773, was the first to describe them, though doubts exist as to whether the mounds he described were those at Etowah. The Reverend Elias Cornelius's description of them in *Silliman's Journal/American Journal of Science* (1819) is thus regarded as the first definitive account (Silverberg 1968). The following is that which Cornelius wrote of the "stupendous pile" he encountered at Etowah:

> I had at the time no means of taking an accurate admeasurement. To supply my deficiency I cut a long vine, which was preserved until I had an opportunity of ascertaining its exact length. In this manner I found the distance from the margin of the summit to the base to be 111 feet. And, judging from the degree of its declivity, the perpendicular height can not be less than 75 feet. The circumference of the base, including the feet of three parapets, measured 1,114 feet. One of these parapets extends from the base to the summit, and can be ascended, though with difficulty, on horseback. The other two, after rising 30 or 40 feet, terminate in a kind of triangular platform. Its top is level and, at the time I visited it, was so completely covered with weeds, bushes, and trees of most luxuriant growth that I could not examine it as well as I wished. Its diameter, I judged, must be 150 feet…. At a short distance to the southeast is another mound, in ascending which I took 30 steps. Its top is encircled by a breastwork 3 feet high, intersected through the middle with another elevation of a similar kind. A

> little farther is another mound, which I had not time to examine (qtd. in Silverberg 1968:307).

Archaeological excavations by the Smithsonian Institution's Bureau of Ethnology began at Etowah in 1883, with excavations occurring intermittently over subsequent years (Silverberg 1968, Hally & Langford 1988). The Etowah micas at the Antonio J. Waring Jr. Archaeological Laboratory were collected primarily during excavations carried out by Sears in 1953 and Larson from 1954-1958, 1961 and 1964 (excavations referenced in Hally & Langford 1988).

CHAPTER 2

THE GEOLOGY OF MUSCOVITE-BEARING PEGMATITES

Distribution of Pegmatite Districts and Pegmatite Terminology

Within the eastern United States, there are a number of prominent pegmatite mining districts which occur along a 965-km stretch from east-central Alabama northeast through northern Georgia, the western Carolinas, and central Virginia (Figure 5). London (2008:4) defines pegmatites as homogeneous to zoned igneous rocks, typically granitic in composition, which display "extremely coarse but variable grain-size". Combining the words of Černỳ (1982:9) and Cocker (1992a:2), a *pegmatite district* can be defined as a "spatially and/or genetically definable" clustering of "several associated pegmatite fields, which are separated from other pegmatite fields either territorially or geologically", with a *pegmatite field* being "an area containing pegmatites which include a single formation type with a common geological-structural environment, age and igneous source"; *pegmatite belts* consist "of pegmatite fields or districts which are related to each other by a large scale linear geologic structure and occur in a common structural position and geological environment". The Blue Ridge belt encompasses North Carolina's Jefferson-Boone, Wilkes, Spruce Pine, and Buncombe districts; North Carolina and Georgia's Franklin-Sylva district; and Georgia's North Georgia and Cherokee-Pickens districts. The Piedmont belt encompasses Virginia's Amelia district; Virginia and North Carolina's Ridgeway-Sandy Ridge district; North Carolina's Shelby-Hickory district; South Carolina and Georgia's Hartwell district; Georgia's Thomaston-Barnesville and Troup district; and three districts in Alabama, collectively referred to as the Alabama district (Jahns and

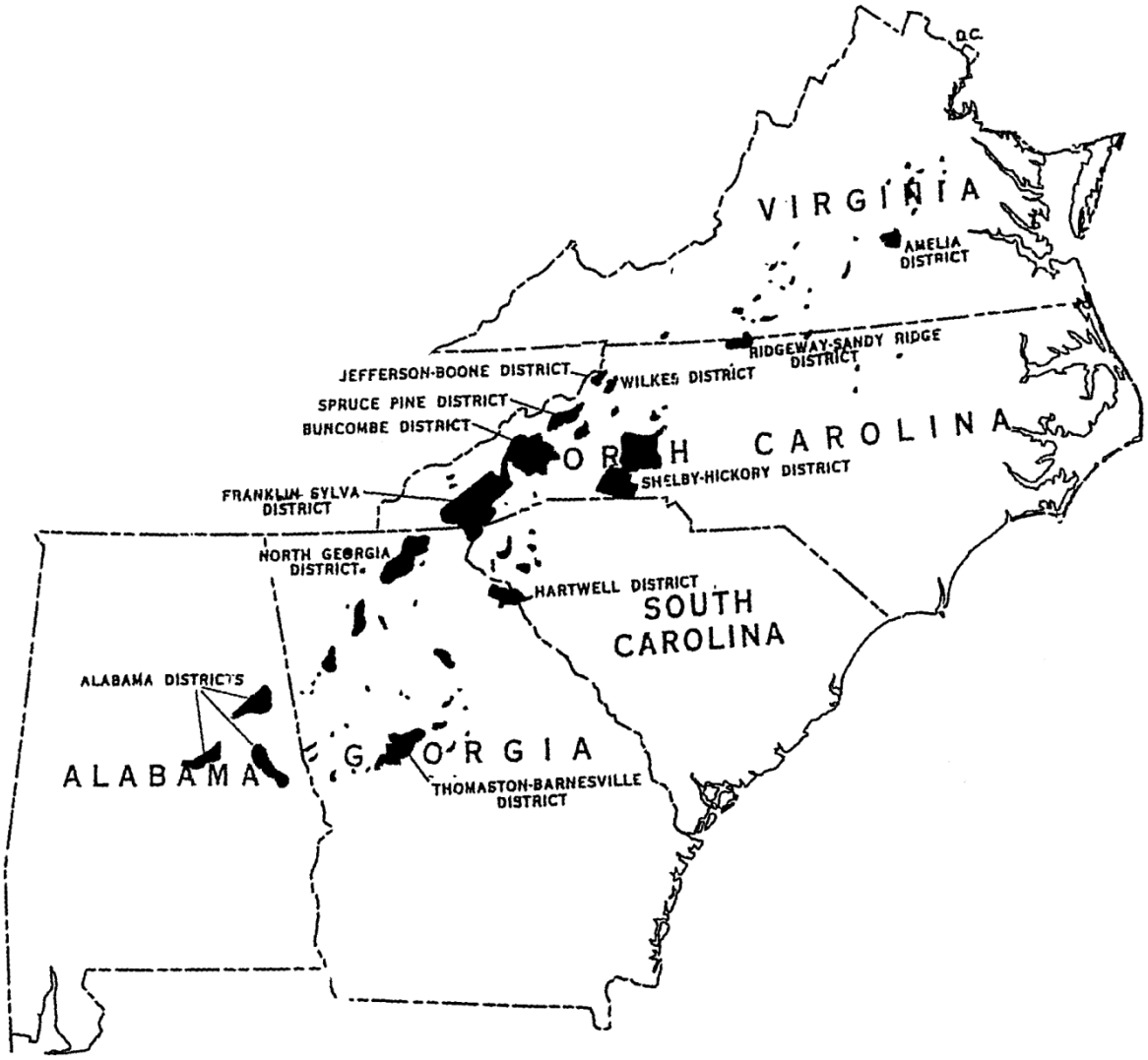

Figure 5: Prominent pegmatite mining districts in the southeastern United States. From Cameron et al. (1949).

Lancaster 1950; Gunow & Bonn 1989). The region also encompasses numerous other smaller deposits (Jahns & Lancaster 1950). The Blue Ridge pegmatite belt averages approximately 65 km in width, while the Piedmont belt is approximately 160 km wide (Gunow & Bonn 1989).

Distribution and Occurrence of Pegmatitic Mica in Georgia

Muscovite-bearing pegmatites, like the majority of Georgia's economic mineral resources, are confined primarily to the granites, gneisses, schists, and slates of Georgia's Crystalline Belt (Galpin 1915; Furcron et al. 1938). The belt trends in a northeast-southwest direction with a southeast-prevailing dip, extending for over 160 km in width across the northwestern part of the state, and encompasses both the physiographic subdivisions of the Appalachian Mountains and the Piedmont Plateau (McCallie 1910). The Cartersville fault zone bounds the western Piedmont to the north. It is an area where phyllites and metagraywackes have been thrust over Paleozoic rocks in Polk and Bartow counties. To the south it is bounded by the Fall Line, the unconformity separating sedimentary rocks of Cretaceous age and younger from the crystalline rocks to the north (Long 1971).

Pegmatitic muscovite in particular is one of the most widely distributed economic minerals in the crystalline rocks of Georgia, being found in some quantity in all of the counties of the Crystalline Belt (Furcron et al. 1938). It is found in association with granitic pegmatites, which are associated with micaceous schists and gneisses and also, though less frequently, in hornblende gneisses and granites (McCallie 1910; Galpin 1915; Long 1971). In general, the strike and dip of the pegmatites conforms to that of the enclosing country rock, though some will cut across the schistosity of the surrounding rock (Galpin 1915; Furcron & Teague 1943). In Georgia's northern and eastern mica-producing regions (Rabun, Hart, Elbert, Union, and Lumpkin Counties), the Carolina gneiss and schist serves as the country rock within which the

mica-bearing pegmatites are hosted; those in Cherokee and Pickens counties occur in both the Carolina gneiss and the Talladega series mica schists (Furcron & Teague 1943), or in more updated terminology, within the metamorphosed schists and gneisses of the Murphy Belt Group and Great Smoky Group (for the Ball Ground pegmatites in Cherokee and Pickens counties) and the Powers Ferry Formation of the Sandy Springs Group (the Holly Springs pegmatites in Cherokee County) (Gunow & Bonn 1989).

Furcron & Teague (1943), Lester (1946) Jahns & Lancaster (1950), and Long (1971) identify five primary mica-producing districts in Georgia (Figure 6): (1) the Hartwell District (Hart and Elbert counties); (2) the Franklin-Sylva District (Rabun County); (3) the North Georgia District (parts of Union, Lumpkin, Towns, Fannin, and White counties); (4) the Cherokee-Pickens District (parts of Cherokee, Pickens, and Fulton counties); and (5) the Thomaston-Barnesville District (southeastern Lamar County, central Monroe County, parts of Pike County, and central and eastern Upson County). In the more recent literature, Cocker (1992a) recognizes 12 pegmatite districts in Georgia (Thomaston-Barnesville, Troup, Jasper, Putnam, Crawford-Jones-Baldwin, Cherokee-Pickens, Carroll-Paulding, Hartwell, Rabun, Lumpkin-Union-Towns, Habersham, and Oconee).

Review of the literature has resulted in the compilation of a database containing references to at least 591 described occurrences of pegmatitic muscovite in the state of Georgia alone (Galpin 1915; The Geological Survey 1941, 1943, 1950, 1954, 1956, 1961, 1963, 1968; Furcron & Teague 1943; Jahns & Lancaster 1950; Heinrich et al. 1953; Long 1971; Steele & O'Connor 1987; Gunow & Bonn 1989; Cocker 1992a); three additional localities not referenced in the literature were found while conducting fieldwork/sample collection. These 594 muscovite occurrences have been compiled in Appendix B. Those cases in which multiple occurrences are

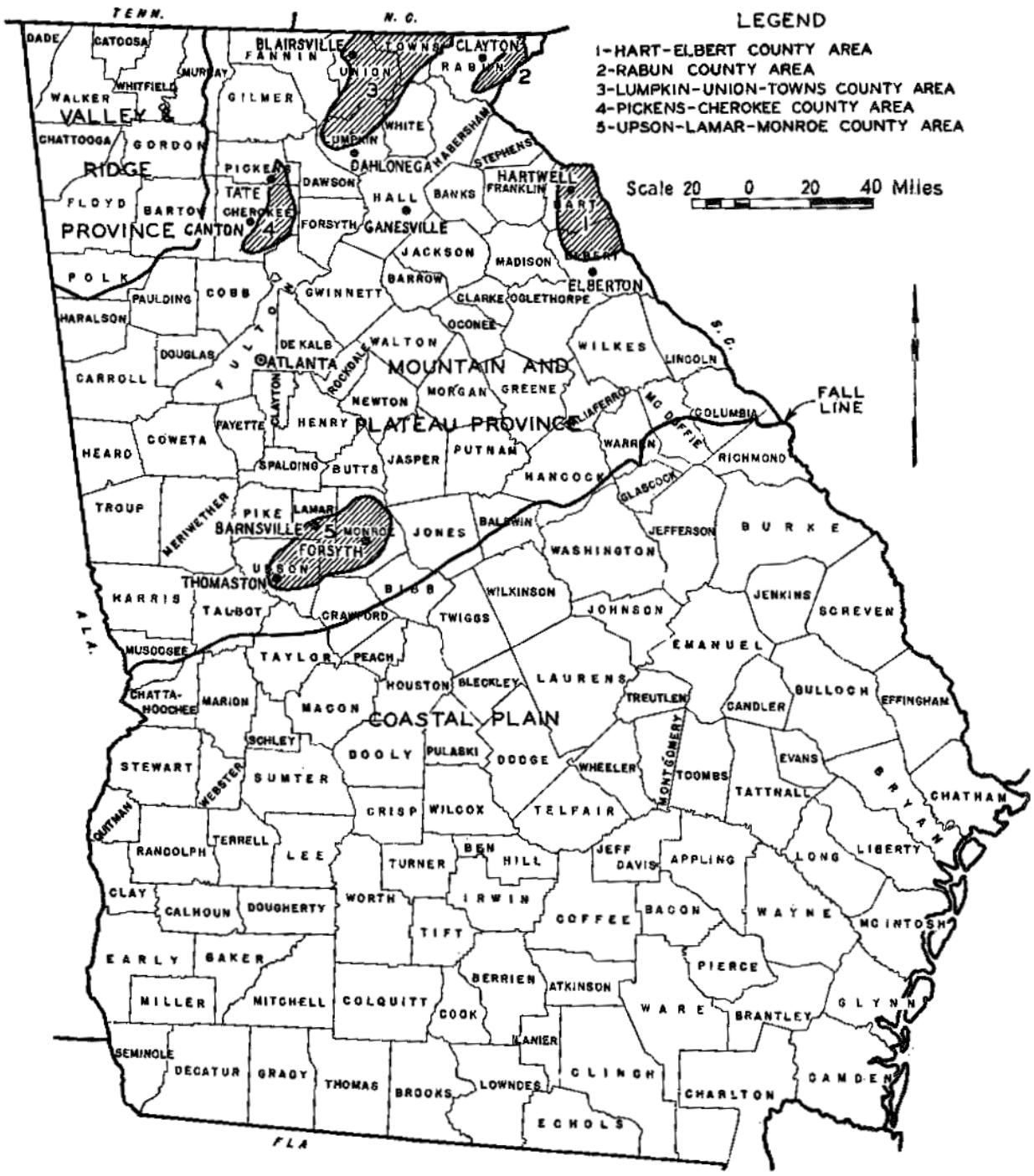

Figure 6: Georgia's principal mica-producing districts. From Furcron & Teague (1943).

identified at a single mine/prospect are the result of either (1) multiple mining loci at the mine/prospect or (2) mica of notably differing characteristics (e.g., color, flatness, spotting) having been encountered at the mine/prospect. Mines were identified from all five of Georgia's principal mica-producing regions, as well as from most of Cocker's (1992a) additional districts and several outlying deposits in Bartow, Carroll, Clarke, Cobb, Coweta, Dawson, DeKalb, Douglas, Fannin, Fayette, Forsyth, Franklin, Fulton, Gordon, Greene, Habersham, Hall, Haralson, Heard, Henry, Jackson, Jasper, Jones, Lincoln, Meriwether, Morgan, Oconee, Paulding, Pike, Rockdale, Spaulding, Talbot, Towns, Troup, Walton, and Wilkes counties.

Pegmatite Overview, Classification and Structure

While most mica grains occurring in igneous and metamorphic rock types are generally fine grained flakes, those occurring in coarse-grained granitic pegmatites sometimes form significantly larger sheets of commercial value (termed *sheet mica*) (Furcron et al. 1938; Ferguson 1974; Klein 2002) (Figure 7). One pegmatite locality in Mantawan Township, Ontario, Canada, has produced crystals measuring nearly 3 m in diameter (Klein 2002).

The pegmatitic variety of muscovite can occur in either dikes or veins; McCallie (1910:148-149) differentiates between the two features, stating that:

> [t]he veins differ from the dikes chiefly in being smaller in size and in having a banded structure, due to the arrangements of the mica, feldspar, and quartz, the three principal minerals present. In the dikes, on the other hand, the different minerals have no definite order of arrangement. They may occur in bunches or segregations or may even be pretty evenly distributed throughout the dike.

Large blocks of muscovite crystals, termed *books*, tend to be located along the sides of pegmatite dikes and veins; while these dikes and veins are variable in terms of length and thickness, "neither the abundance nor the quality of mica is dependent upon the size of the dike or vein in which it is found" (Whitlatch 1962:60).

Figure 7: Sheet muscovite from the Ridgeway mine (Henry Co., Virginia). From Jahns et al. (1952).

Mica-bearing pegmatites cluster around granitic bodies or along the contacts between different rock formations, and can take on tabular, pod-like, or irregular shapes ranging in thickness from less than 2.5 cm to over 40 m, though those which have been mined historically tend to have been at least approximately 1 m thick (Long 1971). The tabular bodies tend to form in well-developed joints at slight depth; the irregular and lens-like bodies result from injection in fracture zones. *Pinch and swell* structures are common in pegmatites, occurring where series of large lenses lying within a plane are connected by narrow stringers (Galpin 1915).

As per Černỳ & Burt (1984), granitic pegmatites are classified into four principal categories: (1) abyssal-class, or maximal depth, pegmatites; (2) muscovite-class, or mica-bearing, pegmatites; (3) rare-element-class pegmatites; and (4) miarolitic-class pegmatites. Muscovite mica is typically associated with the muscovite, rare-element, and miarolitic classes. Muscovite-class pegmatites have a strictly orogenic derivation, while the rare-element- and miarolitic-class pegmatites may have either orogenic or anorogenic derivations. Jahns et al. (1952) identify the pegmatites of the southeastern Piedmont as being overwhelmingly muscovite-class pegmatites; similarly, Cocker (1992a) states that the mica-bearing and maximal depth types are the most abundant pegmatite classes in the southeastern United States. No miarolitic pegmatites are known in the Southeast (Cocker 1992a).

Pegmatite bodies may be further classified as either unzoned or zoned, with zoned bodies consisting of core zones, as many as three intermediate zones (though most typically display only one), wall zones, and border zones (Figure 8); a typical wall-to-core sequence will display a progressive increase in mineral grain size, along with increasing concentrations of K-feldspar and decreasing amounts of plagioclase (Long 1971). Jahns et al. (1952) identify a general sequence within texturally well-differentiated muscovite-class pegmatites in the Southeast of:

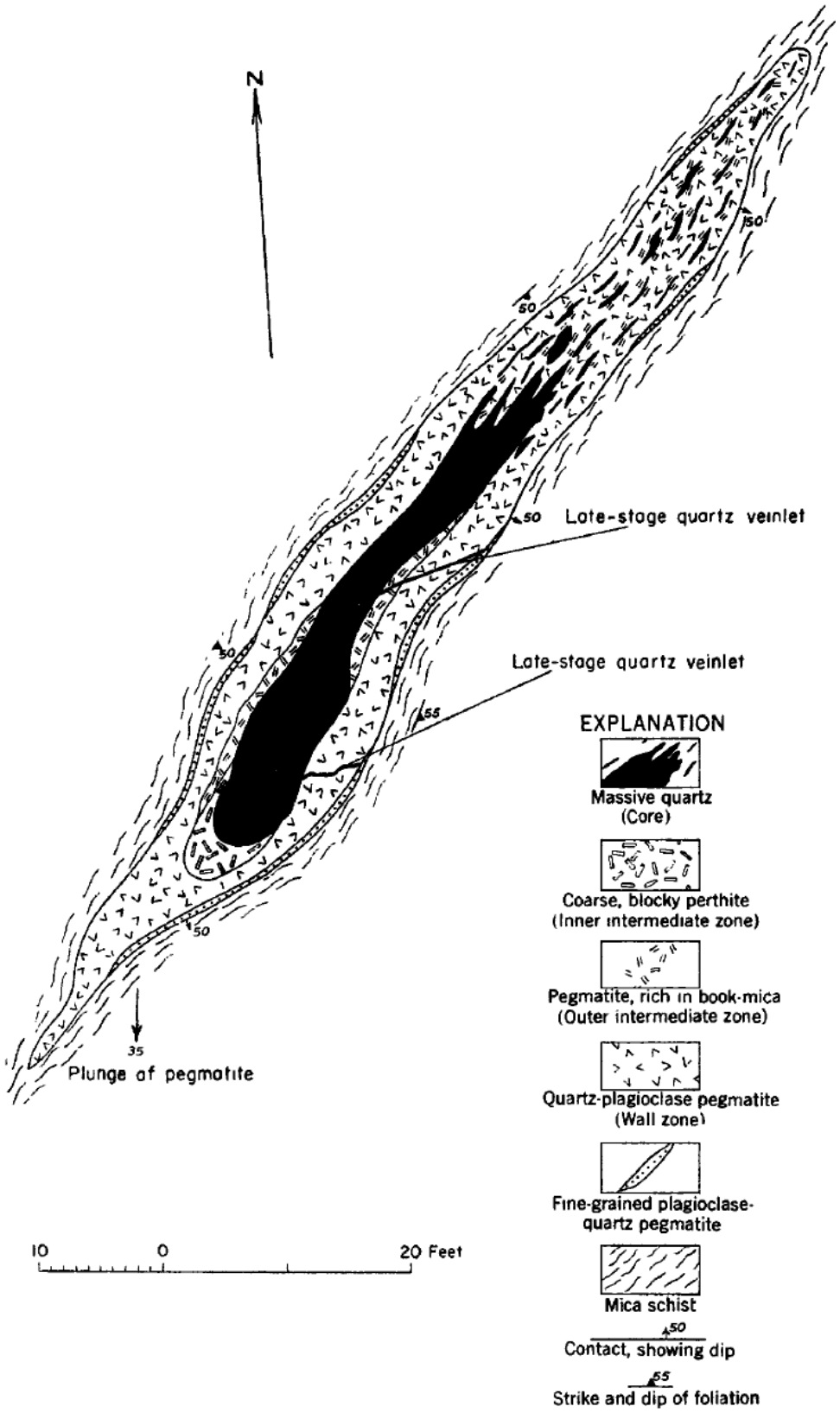

Figure 8: Typical zonation pattern observed in zoned pegmatites. From Heinrich & Olson (1953).

(1) a quartz ± plagioclase border zone containing biotite + muscovite; (2) a quartz + K-feldspar wall zone containing muscovite + biotite; and (3) a K-feldspar + quartz core, the margins of which contain muscovite + biotite. While muscovite can also occur as a film covering fracture surfaces within pegmatites (Galpin 1915; Jahns et al. 1952) or as an alteration/metasomatic replacement mineral (Jahns et al. 1952; Černỳ & Burt 1984), it possesses no economic value in this form (Galpin 1915). While Černỳ & Burt (1984) reference the presence of muscovite in most zones of the zoned pegmatites, the minerals of economic value are characteristically found in specific zones or in association with specific types of pegmatites, occasionally concentrated in shoots; for example, "[f]lat mica that yields an average of 5 percent sheet mica occurs in unzoned deposits and the wall zones of zoned deposits" (Long 1971:63).

Rare-element-class pegmatites are typically enriched in one or more of the elements Li, Rb, Cs, Ta, Sn and Nb (Cocker 1992a). Černỳ & Burt (1984) identify gadolinite, beryl-columbite, spodumene, and lepidolite types depending on the mineralogy of the pegmatites, and Cocker (1992a) identifies cassiterite as a commonly occurring phase as well. While some muscovite-class pegmatites may be important sources of minerals with high concentrations of rare-elements (e.g., the beryl-bearing Ball Ground pegmatite field in Georgia's Cherokee-Pickens district [Gunow & Bonn 1989; Cocker 1992a]), references to rare-element minerals are not typically encountered in the Georgia literature outside of Troup County; Virginia's Amelia district, North Carolina's Shelby-Hickory/King's Mountain district and Alabama's Rockford district are the only other prominent rare-element-bearing pegmatite districts in the Southeast and are important sources of Be and Li (Gunow & Bonn 1989).

CHAPTER 3

HISTORICAL CONSIDERATIONS

Uses for Muscovite

Owing to the substitution of Al^{3+} cations for Si^{4+} cations in the tetrahedral sheets of the mica crystal structure, a negative charge imbalance is created and subsequently compensated for by the incorporation of K^{+} cations in the interlayer sites in the structure (Figure 9); weaker bond strengths associated with bonds involving these interlayer K^{+} cations, relative to those of the Si-O bonds in the tetrahedral sheets, are responsible for the diagnostic perfect cleavage of muscovite. The ability to split books of mica into fine, flexible single cleavage plates, along with the chemical stability of muscovite (particularly its high dielectric and heat-resisting properties, low conductivity of heat and electricity, and non-flammability), have traditionally made it a desirable component in a wide array of commercial and industrial products (Jahns & Lancaster 1950; Long 1971; Klein 2002): as electrical insulation in heaters, electric irons and toasters; as washers in fuses, lamp sockets, and radios; in wallpaper, paints, tiles, plastics, and as a filler in rubber; in the manufacture of asphalt roofing, concrete, and stucco; as a dusting powder for rubber tires, molded insulation, and fireproofing materials; as stove doors and lamp chimneys; as a mineral lubricant; in microwave ovens as the windows on microwave tubes; in the manufacture of vacuum tubes, capacitors, and transistors; as a constituent of drilling mud; and even in cosmetic creams, nail polish, lipstick, and eye shadow (McCallie 1910; Furcron et al. 1938; Jahns & Lancaster 1950; Whitlatch 1962; Long 1971; Nesse 2000; Klein 2002).

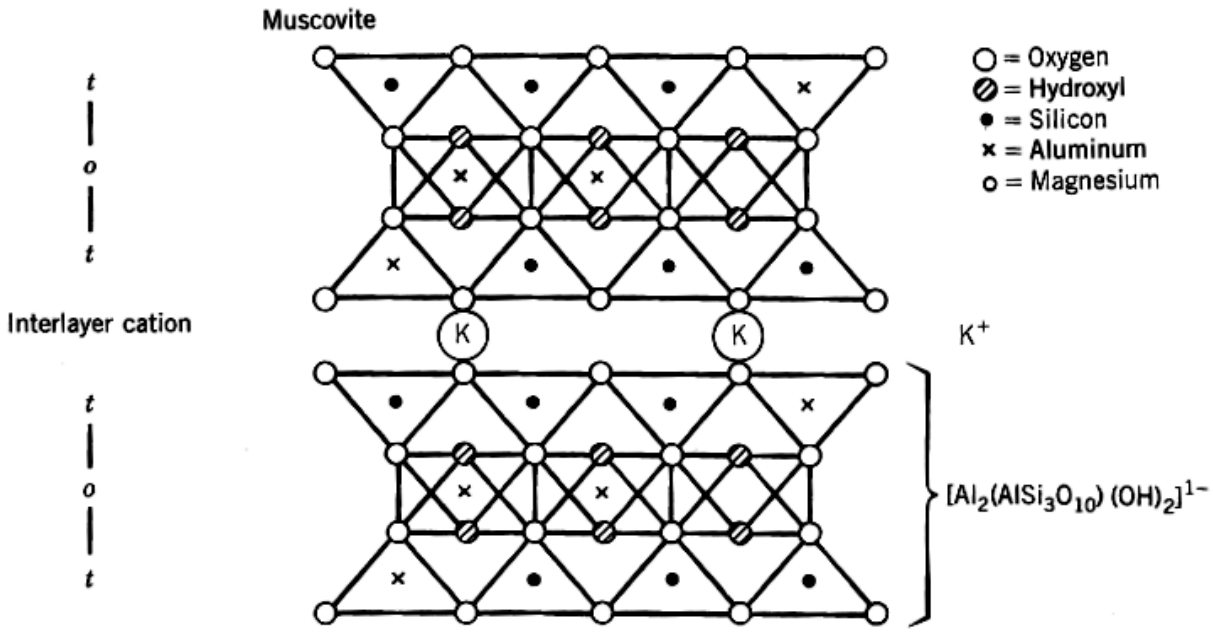

Figure 9: Diagram of the structure and composition of muscovite. *t* = tetrahedrally-coordinated cations; *o* = octahedrally-coordinated cations. From Klein (2002:Figure 12.62).

Periods of national crises have been associated with surges in the mining of mica due to additional war-time applications as condensers in military radios and other electronic equipment, built-up commutator segments, and as coil insulation in transformers, switchboards, spark plugs, aircraft generators, and blasting apparatuses (Jahns & Lancaster 1950; Long 1971). The need for *strategic mica* or *mica of military grade* (mica suitable for the manufacture of military equipment) had been one of the driving forces behind much of the early mica prospecting/research (e.g., Kesler & Olson 1942). As of 1971, over 1,600 mica deposits in the southeastern Piedmont had been mined, with many of those having been mined during World War II; high quality clear sheet mica was obtained from at least 595 of these deposits throughout the war (Long 1971).

Hart and Upson counties were once Georgia's main producers of full- trimmed mica, while sericite mica suitable for grinding came primarily from Cherokee County (Whitlatch 1962). During World War II, a large portion of the mica produced in the southeastern Piedmont came from Georgia's Thomaston-Barnesville district (Cocker 1992a).

Physical Properties of Muscovite in the Context of Historical Mining

The economic value of sheet mica has been influenced not only by demand, but by a number of additional factors relating to the size and quality of the books (Long 1971). Qualities of particular importance are the size of individual sheets able to be split from the book, possession of perfect uniform cleavage, color, clarity/transparency, flexibility, natural distortion, a low electric power factor, and freedom from impurities and foreign materials (e.g., mineral inclusions and stains) (McCallie 1910; Furcron et al. 1938; Kesler & Olson 1942; Whitlatch 1962); such properties are discussed in detail in the subsequent subsections.

Owing to the effect these properties had on the value of the mica, an appreciable portion of the literature is devoted to the character of the mica present at any particular locality; as such, at least some of these properties may potentially assist in the characterization of muscovite from different sources. Information regarding the maximum reported or observed dimensions of crystals at a given locality (given as either grain size or yield), color and mineral inclusions are in included in Appendix B, where such information was available in the original literature. Information relating to the relative proportions of mica displaying "A" structures, stains, and spots or specks has been largely excluded, as these properties tend not to be characteristic of the muscovite from a given locality; for example, very rarely will every book collected from a given pegmatite display the same degree of staining or spotting or the same structural features. For the most part, all books from a given pegmatite will be of similar color. While the entire suite of mineral inclusions identified in all books from a given pegmatite will not be manifest within every book, it is found that some mineral inclusions have not been observed within certain districts, and thus they may serve as discriminating variables when present.

Size

For obvious reasons, larger sheet mica was valued more than smaller sheet and punch mica. Many of the historic descriptions of pegmatitic mica occurrences provide measurements of the largest crystals observed or reported from that locality in terms of either grain size or yield; the former refers to the natural size of the crystal, with the latter referring to the size of trimmed sheets able to be obtained from the uncut crystal. Those attributing a Spruce Pine source to prehistoric mica artifacts generally cite the large grain size of mica in the pegmatites of the Spruce Pine district. However, mica of substantial grain size is found in local abundance throughout the entire Southeast (Figure 10; Table 1); for the maximum dimensions observed at

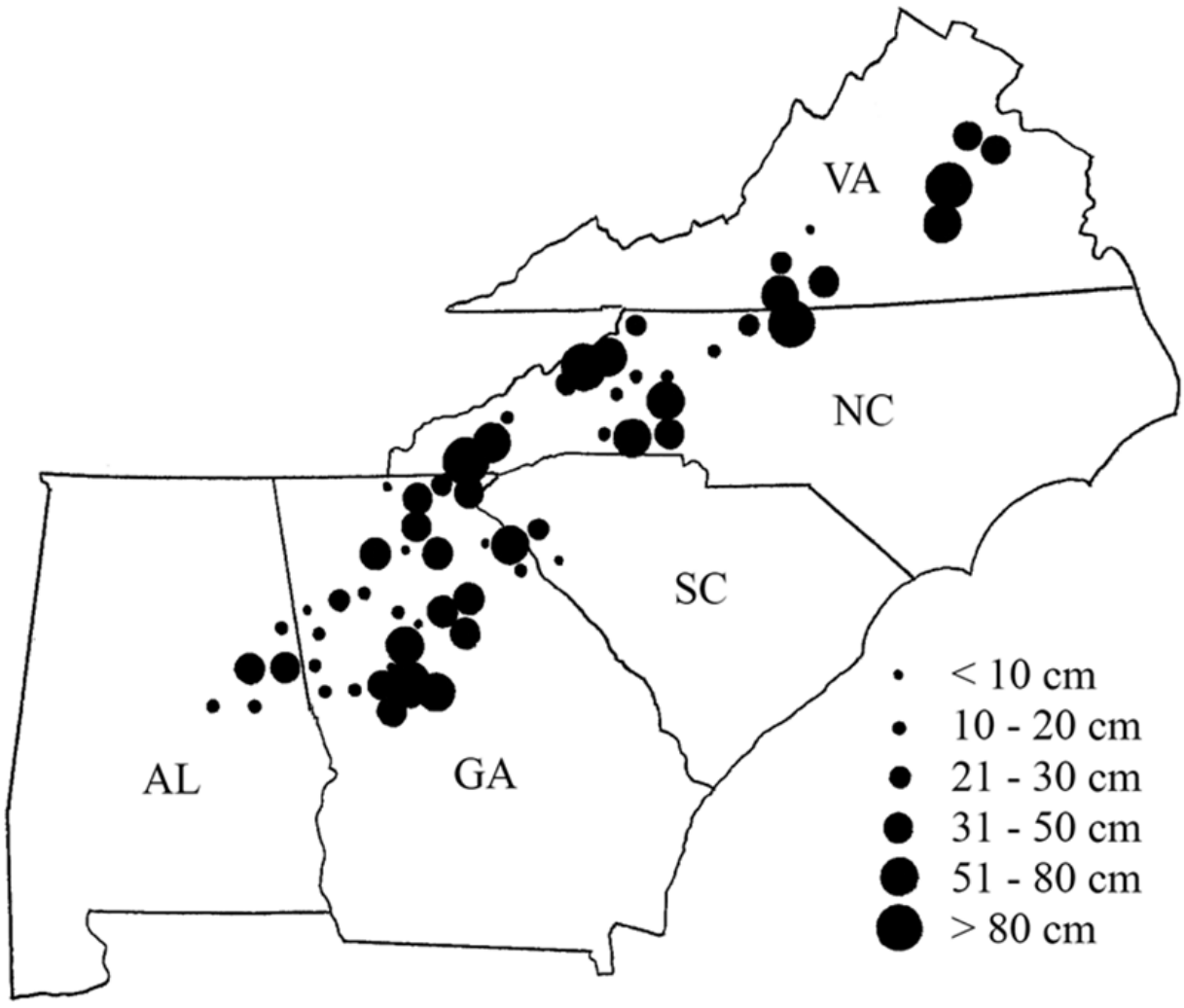

Figure 10: Size distribution southeastern pegmatitic muscovite. Sizes ranges correspond to the maximum recorded diameter (cm) of muscovite crystals observed or reported, by county.

Table 1: Muscovite size data. Maximum diameter (cm) of pegmatitic muscovite crystals, by county, in the southeastern United States. Data are compiled from Sterrett (1923), Furcron & Teague (1943), Lemke et al. (1952), Griffitts & Olson (1953a), Griffitts & Olson (1953b), Griffitts et al. (1953), Heinrich & Olson (1953) and Heinrich et al. (1953).

Mining District	State	County	Maximum diameter (cm)
Amelia	VA	Amelia	76
Anna River	VA	Spotsylvania, Caroline	38
Goochland-Powhatan	VA	Goochland, Powhatan	137
		Bedford	4
		Pittsylvania	41
		Franklin	30
		Henry	56
Ridgeway-Sandy Ridge	VA	Henry	61
	NC	Rockingham	96
		Stokes	25
Shelby-Hickory	NC	Alexander	15
		Caldwell	20
		Catawba	61
		Lincoln	36
		Gaston	46
		Cleveland	61
		Rutherford	20
Woodlawn	NC	Burke	10
Spruce Pine	NC	Mitchell	183
		Yancey	30
		Avery	51
Jefferson-Boone	NC	Ashe	30
outlying deposits	NC	Yadkin	15
Franklin-Sylva	NC	Haywood	13
		Jackson	51
		Macon	91
	GA	Rabun	38
Cherokee-Pickens	GA	Cherokee	46
		Pickens	46
Thomaston-Barnesville	GA	Lamar	180
		Monroe	51
		Upson	51
		Pike	30
North Georgia	GA	Lumpkin	46
		Union	46

Mining District	State	County	Maximum diameter (cm)
outlying deposits	GA	Carroll	15
		Cobb	15
		Dawson	8
		DeKalb	13
		Fannin	5
		Forsyth	9
		Franklin	5
		Hall	36
		Haralson	8
		Heard	15
		Henry	69
		Meriwether	15
		Morgan	36
		Oconee	46
		Paulding	30
		Rockdale	8
		Spaulding	3
		Towns	25
		Troup	20
		Walton	36
Hartwell	GA	Hart	71
		Elbert	20
	SC	Abbeville	3
		Anderson	30
Pyriton	AL	Clay	36
Lineville	AL	Clay	13
Pinetuckey	AL	Cleburne	20
		Randolph	41
Rockford	AL	Coosa	15
Dadeville	AL	Tallapoosa	20

individual pegmatite localities in Georgia and Alabama, see Appendix B. With reference to the Etowah mica artifacts observed and analyzed in this study (discussed in greater detail in following sections), it is found that the largest artifact (UWG-1019 2518, 7.7 cm in diameter) corresponds to the smallest size division presented in Figure 10. Table 1 precludes only 5 counties (Bedford in Virginia; Fannin, Franklin and Spaulding in Georgia; and Abbeville in South Carolina) of the 65 total counties from Virginia through Alabama from which size data are available. When the entire range of artifact sizes is considered, however, several artifacts measure less than 3 cm in diameter; none of the counties for which size data are available can be removed from consideration for these artifacts, as the smallest maximum diameter reported from any county is 3 cm. Size alone thus would not have been a limiting factor in the selection of muscovite sources among prehistoric Native Americans.

Cleavage and Related Properties

As the utility of mica for industrial purposes is ultimately controlled by properties either relating to or affecting cleavage, a number of terms are encountered in the historic literature with regard to cleavage irregularities within books of muscovite mica. *Perfect* cleavage in a fully developed muscovite crystal/book will be parallel to the basal plane and should allow the book to be split into sheets of equal thickness with plane surfaces. The cleavage planes should also form right angles with the six crystal faces. Incompletely developed crystals are termed *"A" mica* (also *housetop*, *fishtail*, *V-ridge*, or *spearhead*) and form where fine imperfections in the form of striations, shallow corrugations, or narrow folds (termed *reeves* or *cross grains*) lying within the plane of the cleavage intersect at approximately 60^{o} angles, resulting in uneven cleavage surfaces (Figures 11). In most cases, a single "A" structure will extend across an entire book of muscovite, with the apex of the "A" occurring close to one of the edges of the crystal. In such

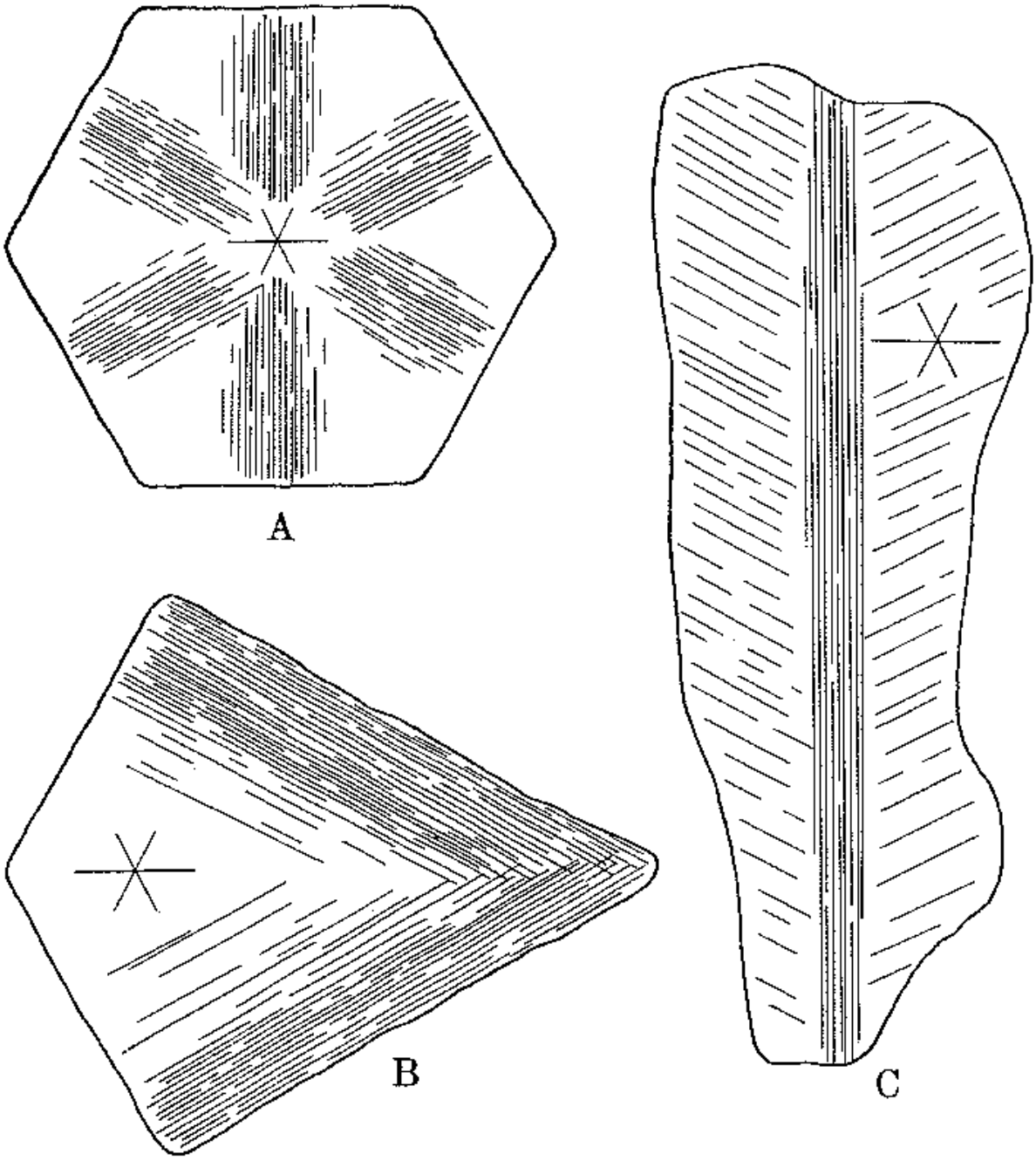

Figure 11: Relation of reeves to crystal directions in muscovite. A. Complete directional development of "A" reeves. B. Typical development of "A" reeves. C. Typical herringbone reeves. From Jahns & Lancaster (1950:9).

books, well-developed crystal faces are rarely displayed, with a single pair of "A" reeves corresponding to a highly distorted one-sixth of a crystal (Galpin 1915; Kesler & Olson 1942; Jahns & Lancaster 1950). Some books, however, contain multiple "A" structures; *double "A" mica* consists of two adjacent "A"-reeve structures sharing a common point and side. *Herringbone mica* (also *fishbone*, *fishback*, *feather*, or *horsetail*) consists of two reeve groups which intersect at about 120^{o}, with a central line, or strip, of reeves generally occurring perpendicular to the clinopinacoidal crystal faces and bisecting the angle formed by the edges of the "A" (Galpin 1915; Jahns & Lancaster 1950). In flat "A" mica, where reeves are spaced widely enough apart, sheets of commercial value could be recovered upon trimming away of the reeves, though most "A" mica will be reeved throughout the crystal, and the value of such mica was greatly diminished as a result (Kesler & Olson 1942; Jahns & Lancaster 1950). Reeves form in response to stress either during or after crystallization, or by discontinuities within incomplete sheets or laminae (Galpin 1915; Jahns & Lancaster 1950). With reeves, the "depth is a function of the number of missing laminae, and their spacing is a function of the distribution of discontinuities in the laminae" (Jahns & Lancaster 1950:8).

Not all books containing reeves are classified as "A" mica or herringbone mica; some books may contain a single set of reeves, and where sufficiently fine, the term *hair-lined* is applied (Jahns & Lancaster 1950). *Tanglesheet*, *gummy*, *locky*, *tangled*, and *tacky* are all terms which may be used to describe mica with cleavage planes that are not continuous throughout the book (Galpin 1915; Kesler & Olson 1942; Jahns & Lancaster 1950). Such discontinuity of cleavage has been attributed to internal distortions, partial intergrowths of books or laminae within the book, finely divided inclusions, or (rarely) twinning. In these books, the cause of the

discontinuity may not always visible, and books may not appear visibly different from *free splitting* books (Jahns & Lancaster 1950).

Wedge structures, or *wedging*, are terms frequently used to describe books with interlayered sheets of unequal size, in which incomplete laminae extend inward from the edge of the crystal and result in one edge of the book being markedly thicker than the other edges (Figure 12). It is particularly common in "A" and herringbone mica, leading to the term *wedge-"A" mica*; in such books, wedge angles may be in excess of 25^{o}. Small thickly-wedged "A" books are referred to as *chub-"A"* (Jahns & Lancaster 1950).

In mica that has been naturally distorted, books may be bent and possess curved cleavage planes or an induced secondary cleavage (*ruling*, or *parting*), the plane of which forms an approximately 60^{o} angle with the basal cleavage (Kesler & Olson 1942; Jahns & Lancaster 1950). A maximum of three sets of pressure-induced secondary cleavage planes may be present, and in the rare case where all three sets are present, the sheets are separated into triangular or hexagonal fragments. In books where ruling occurs in only two directions, the resulting fragmented shapes tend to be either rhombic or diamond-shaped, or straps/laths (Figures 13 & 14). *Ribbons* result from one well-developed set of ruling planes which separates the mica into strips, and where ruling is closely spaced, ribbons form accumulations of fine slivers called *hair mica* (Galpin 1915; Jahns & Lancaster 1950).

From an archaeological standpoint, it is important to appreciate the effects of ruling on the shape of natural mica crystals. In particular, where ruling imparts such highly geometric shapes as triangles, rhombs, diamonds, hexagons and strips with near-perfect parallel edges, these can be mistaken for "cut" pieces of mica. Catalog information on the Etowah micas from the Waring Lab references cut triangular mica artifacts and cut mica strips; while time

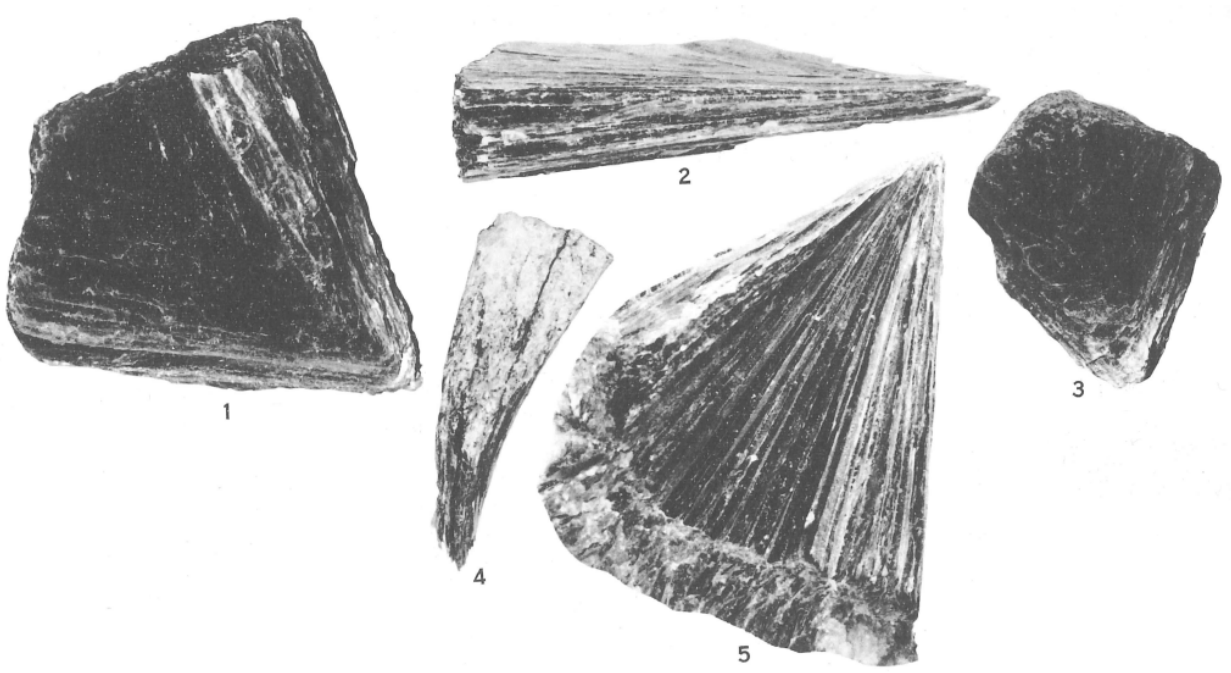

Figure 12: Cleavage defects in mica. 1. Wedge-“A” mica. 2. Edgewise view of (1). 3. Curved wedge-“A”. 4. Edgewise view of (3). 5. Chub-“A” mica. From Jahns & Lancaster (1950:Plate 3).

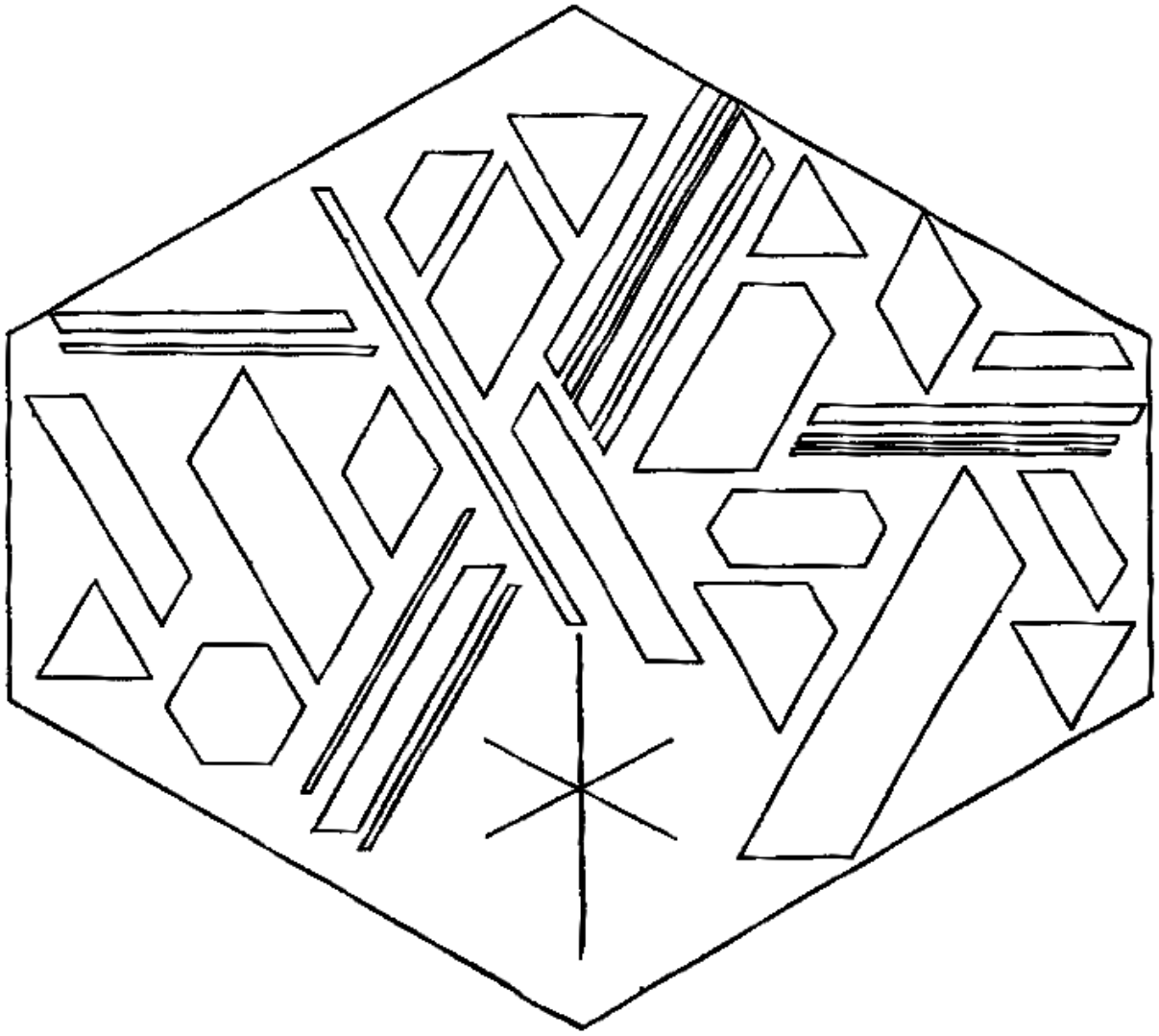

Figure 13: Fragments formed by breaking along parting or ruling planes in a muscovite crystal. Orientation is shown with respect to percussion-figure directions and crystal faces. From Jahns & Lancaster (1950:10).

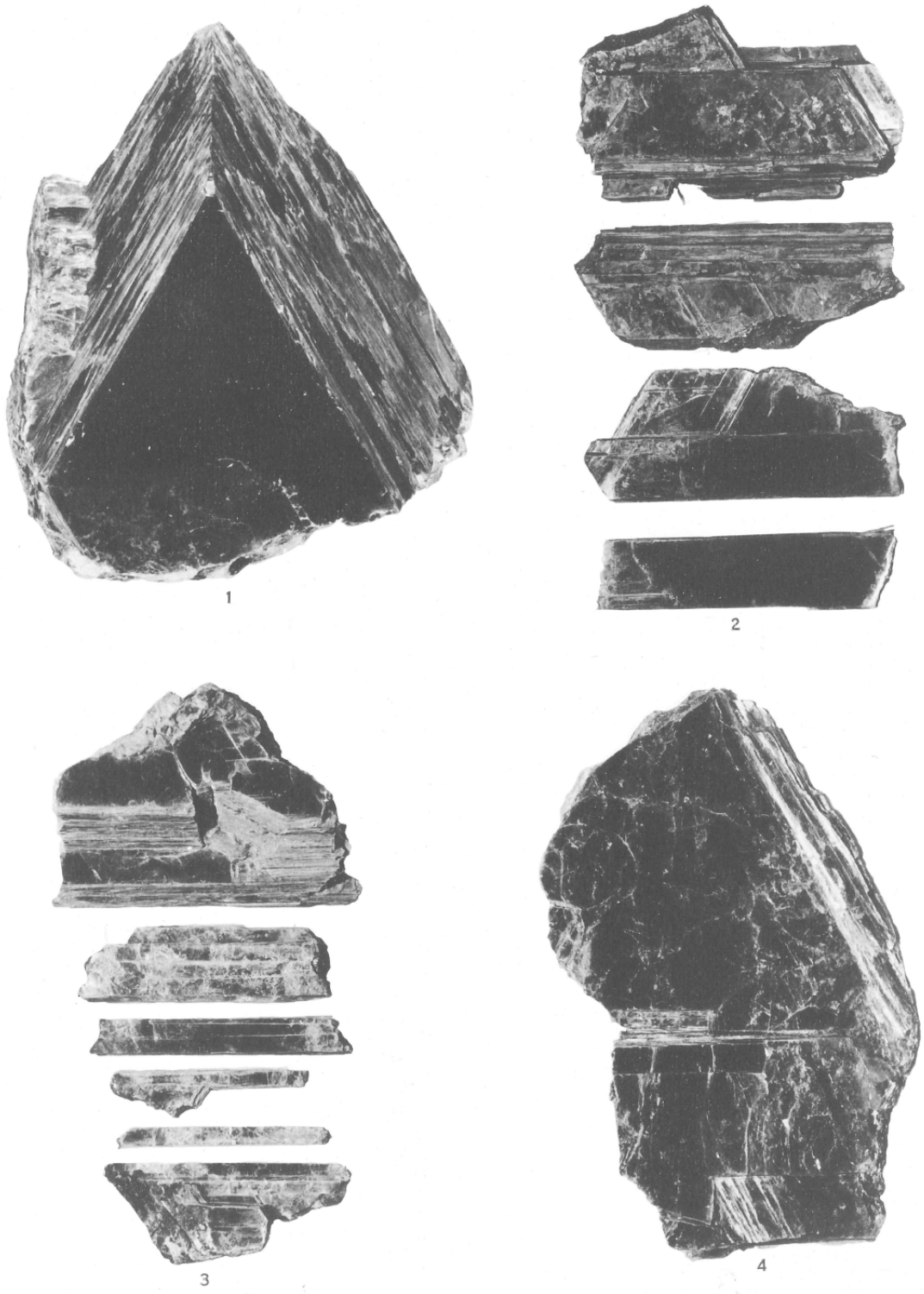

Figure 14: Ruling in mica. 1. Book bounded by two well-developed ruling planes. 2. Deeply ruled pieces of mica, with ribbon mica at bottom. 3. Deeply ruled and cracked mica from warped book. 4. Flat-"A" mica showing relation of ruling to reeve directions. From Jahns & Lancaster (1950:Plate 4).

constraints did not permit the inspection of all mica artifacts in the collections, it is likely that some of the artifacts identified as "cut" pieces are simply the result of natural or otherwise geologically-induced cleavage/ruling planes and are thus not worked artifacts. While common in "A" and herringbone mica, either in the same direction as the reeves or forming a crossbar to the "A" structure, ruling tends to be more common in unreeved books.

Ruling, along with rippling, warping, and buckling, is usually more pronounced in books from deposits near faults or slip joints. The waves, warps, and ridges of distorted mica (referred to as *wavy*, *warped*, *rippled*, *ribbed*, *ridged*, or *creped* mica) are the result of deformation occurring after crystallization. Varying degrees of deformation are implied by some of the terms: *wavy* mica is only slightly affected, whereas *buckled*, *warped*, or *cupped* mica is the most severe and occurs on the broadest scale (Figure 15). A phenomenon known as *cleavage stepping* occurs where sub-parallel flexures distort the cleavage faces, forming low, broad step-like features (Jahns & Lancaster 1950).

Mineral Inclusions

Inclusions in muscovite typically consist of the minerals actinolite, albite, allanite, apatite, beryl, biotite, epidote, fluorite, garnet, hematite, kyanite, magnetite, pyrite, quartz, rutile, tourmaline, vermiculite, zircon, and zoisite (Kesler & Olson 1942; Jahns & Lancaster 1950). Quartz and albite are typically found interlayered with the muscovite or intergrown with the edges of books. Quartz (Figure 16), along with apatite and tourmaline, may also form perpendicular to the cleavage surface of the sheets, effectively tying books together (Jahns & Lancaster 1950). Quartz grains have a tendency to appear rounded, perhaps as a result of resorbtion (Galpin 1915). Inclusions of apatite and zircon are characteristically associated with brown and buff-colored muscovite, occurring in much lesser abundance in green muscovite

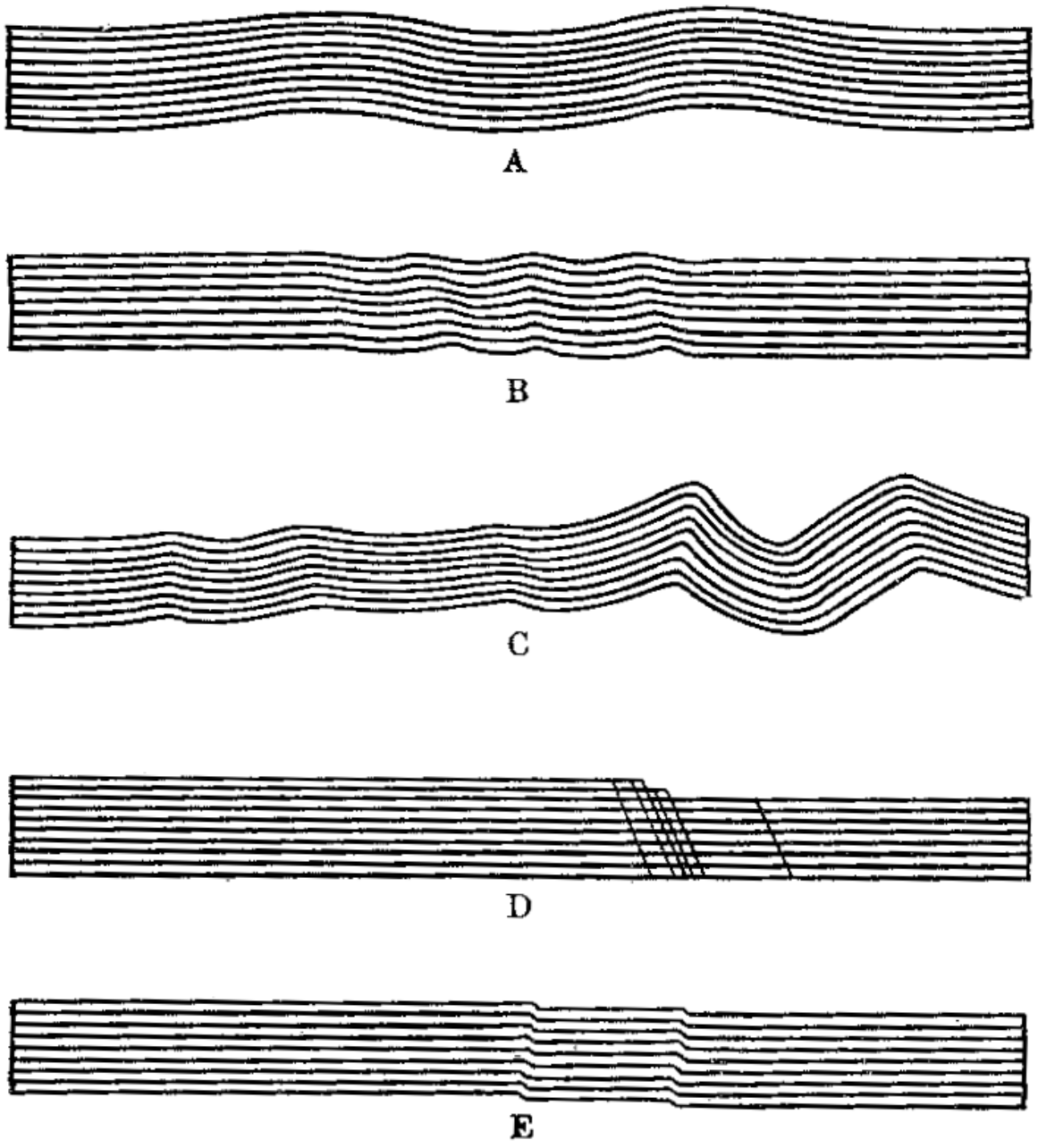

Figure 15: Warped mica (side view). A. Broadly warped (wavy) mica. B. Warped (rippled) mica. C. Warped mica grading into buckled (folded) mica. D. Mica cut by ruling (parting planes). E. Cleavage-stepped mica. From Jahns & Lancaster (1950:10).

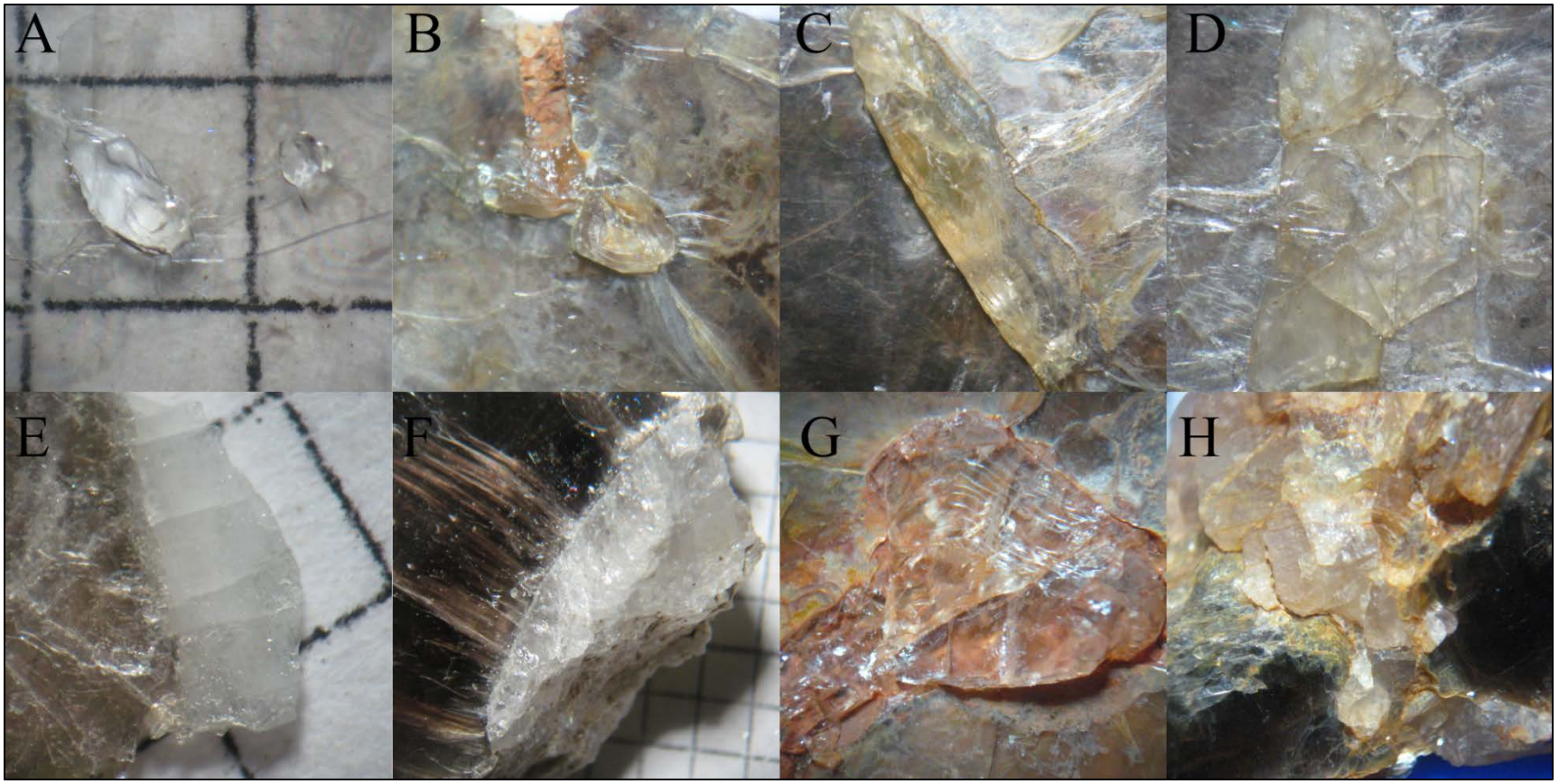

Figure 16: Quartz inclusions/intergrowths in pegmatitic muscovite (sample number, stereoscopic microscope magnification, field of view): A. LW7, 45X, 3.5 mm. B. LW24, 40X, 3.9 mm. C. LW26, 25X, 5.7 mm. D. LW30, 35X, 4.3 mm. E. UGA16, 45X, 3.5 mm. F. UGA23, 10.5X, 1.42 cm. G. VB11, 20X, 7.1 mm. H. VB18, 15X, 9.9 mm. *LW* = Lake Walton, Walton Co., GA; *UGA* = UGA parking lot W03, Clarke Co., GA; *VB* = Vaughn-Butler Rd., Monroe Co., GA. Where grid lines are visible, segments are 2 mm in length

Figure 17: Tourmaline inclusion in pegmatitic muscovite (artifact UWG-1019 308); 45X microscope magnification, <4X digital zoom, field of view < 3.5 mm.

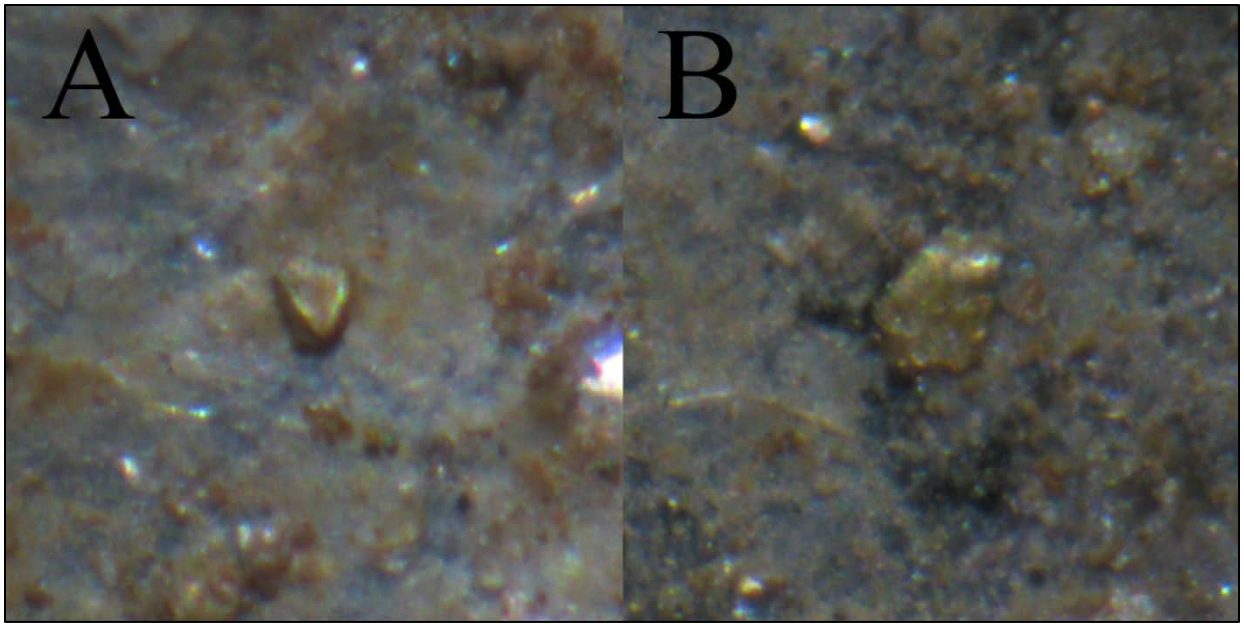

Figure 18: Pyrite inclusions in pegmatitic muscovite artifacts (45X microscope magnification, <4X digital zoom, field of view < 3.5 mm): A. Artifact UWG-1019 308-4. B. Artifact UWG-1019 308-5.

(Jahns & Lancaster 1950). Actinolite, allanite, beryl, kyanite, rutile, tourmaline, zoisite, and other elongate minerals tend to form parallel to the cleavage surfaces, and may reach lengths up to several centimeters. Equant fluorite, garnet, tourmaline (Figure 17), and pyrite (Figure 18) inclusions are typically flattened parallel to the cleavage plane of the muscovite (Galpin 1915; Jahns & Lancaster 1950). Where thicker, these inclusions may tie the sheets of muscovite together. While inclusions of garnet may show variability in size, most are less than 5 mm in diameter and less than 0.3 mm thick. Inclusions of garnet are characteristically associated with green muscovite. Pinholes, small holes extending only through a few laminae within a given book, may form when small inclusions of garnet, apatite, zircon, or other minerals "pop out" of the laminae (Figure 19). Biotite and vermiculite (as an alteration product of the biotite) are commonly intergrown with or included in the muscovite as well; cleavages are usually parallel to those of the sheets of muscovite, though occurrences where biotite books are oriented oblique to the cleavage plane of the muscovite have been documented. Inclusions of biotite (Figure 20) are generally well-developed euhedral crystals displaying pinacoid and prism faces, though some take on a pyramidal shape. These intergrowths are common in all colors of muscovite, though the coarse euhedral grains occur more prevalently in reddish muscovite and only rarely in green muscovite; they are rare in iron-stained muscovite. Rarely, other muscovite crystals can be found as inclusions within books or rimming the core of other books, but such occurrences are difficult to recognize (Jahns & Lancaster 1950). Where found as inclusions as opposed to mineral stains, hematite and magnetite usually occur as either small (<0.5 mm) or large (>1.5 mm) specks or spots. Magnetite inclusions typically display smooth regular edges, though they may also take on thin dendritic crystallization patterns parallel to the cleavage planes of the mica (Galpin 1915; Jahns & Lancaster 1950). Hematite tends to take on dendritic forms (Figure 21).

Neither hematite nor magnetite inclusions are particularly common in brown or buff-colored muscovite (Jahns & Lancaster 1950).

Stains

Stains result from the introduction of clays, limonite, and other weathered materials into splits in the muscovite crystals, typically via the movement of water (Galpin 1915). Primary mineral staining consists of black spots or specks of iron oxide (i.e., mineral inclusions), usually of magnetite which can then weather into either hematite or limonite (Kesler & Olson 1942). Hematite staining (Figure 22A) tends to affect the overall pattern of inclusions in the mica in that the outer portions of books stained by hematite, as well as the areas surrounding cracks, parting planes, and holes, are generally free of inclusions. Where biotite intergrowths are very thin and do not display distinct crystal outlines, they tend to be treated as mineral stains as well and impart a greenish or brownish color and "distinctly curdy" appearance to the muscovite. Goethite can occur as stains as well, though it can also form as *scales* displaying a wide range of colors (brown, red, orange, and yellow) within the sheets of muscovite or as pseudomorphs of different iron oxide minerals, typically altering from magnetite or hematite (Jahns & Lancaster 1950).

Most stains are of primary origin, though secondary clay mineral stains as well as secondary organic *vegetable* stains may also occur (Kesler & Olson 1942). Weathering and the percolation of meteoric waters can lead to the coating of the muscovite with clay minerals, hydrous iron oxides, manganese oxides, calcite, chalcedony, or other secondary minerals. The designation of mica as *clay-stained*, where used in the literature, can refer to staining from the clay minerals, silica/chalcedony, or calcite, and tends to be the most common form of staining (Figure 22A-D). *Iron-stained* is used to refer to staining by iron oxides (usually hematite) and

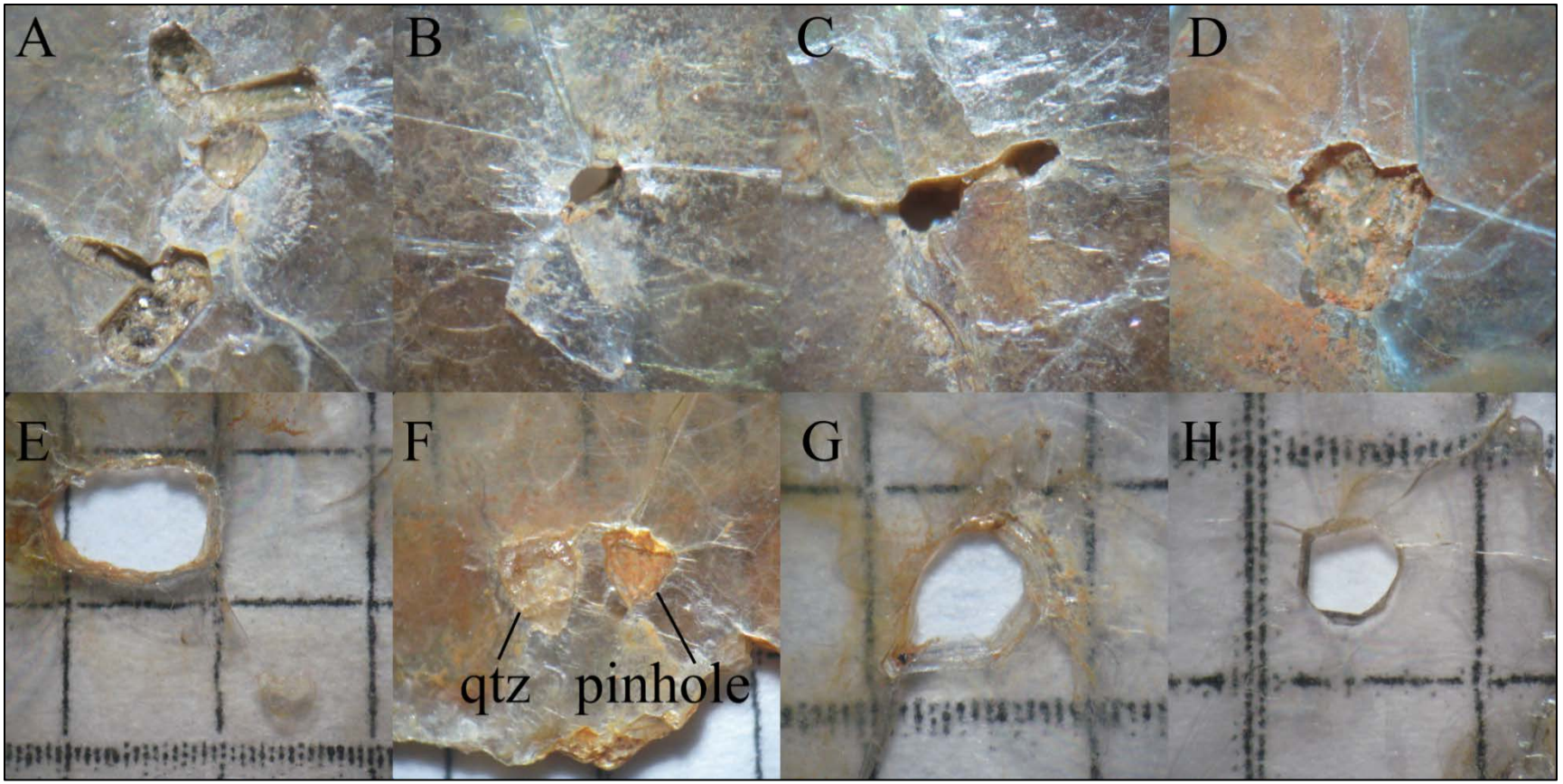

Figure 19: Pinholes in pegmatitic muscovite (sample number, stereoscopic microscope magnification, field of view): A. DM3, 45X, 3.5 mm. B. JDHP3, 45X, 3.5 mm. C. JDHP8, 45X, 3.5 mm. D. PM5, 35X, 4.3 mm. E. VB3, 30X, 5.0 mm. F. VB5, 30X, 5.0 mm (pinhole, next to qtz inclusion). G. VB17, 45X, 3.5 mm. H. VB18, 45X, 3.5 mm. *DM* = Dean Mine, Cherokee Co., GA; *JDHP* = J.D. Hillhouse prospect, Cherokee Co., GA; *PM* = Poole Mine, Pickens Co., GA; *VB* = Vaughn-Butler Rd., Monroe Co., GA. Where grid lines are visible (E, F, G & H), each side of the square is 2 mm.

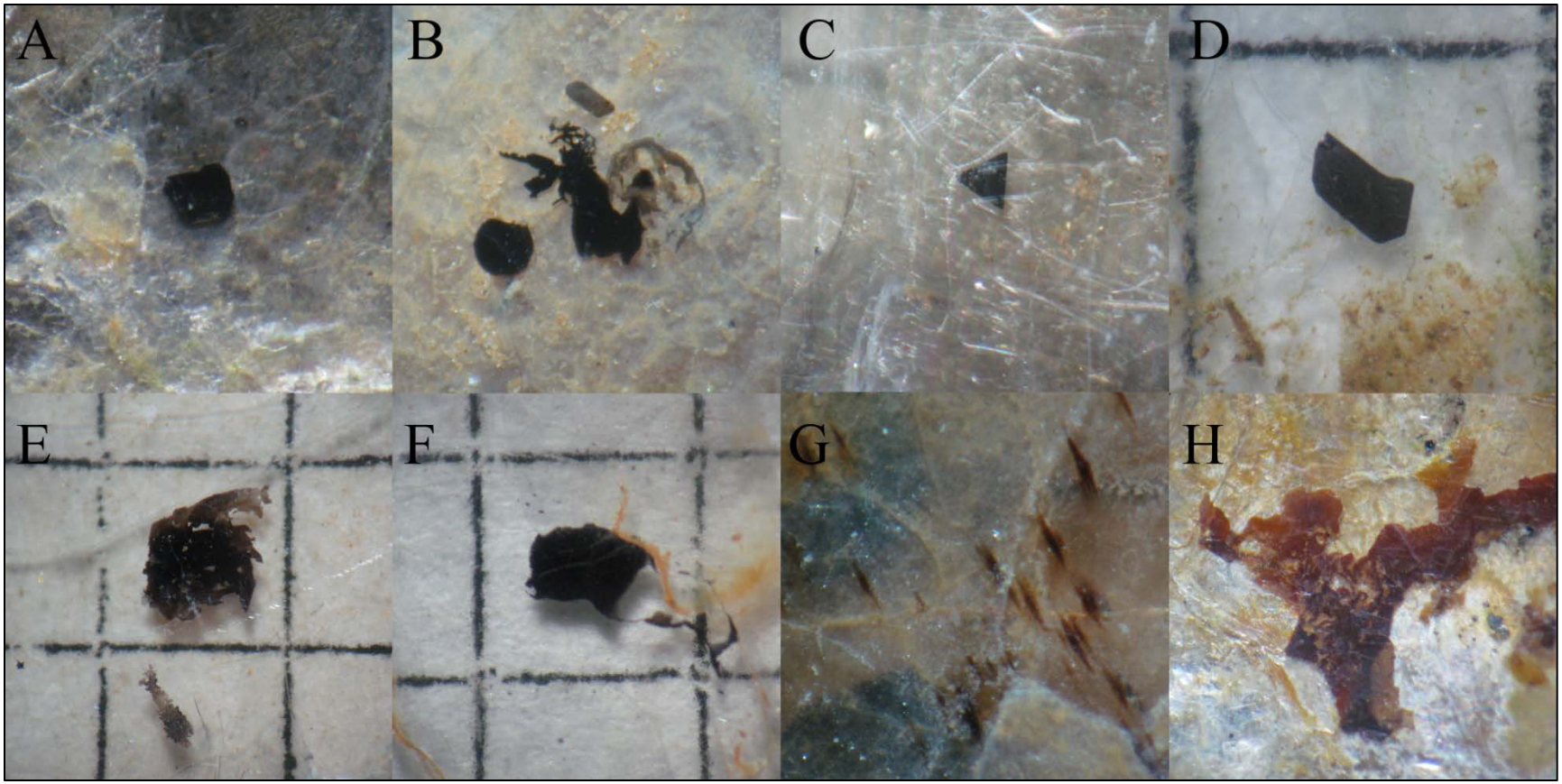

Figure 20: Biotite inclusions in pegmatitic muscovite (sample number, stereoscopic microscope magnification, digital zoom, field of view): A. DM17, 45X, < 4X digital zoom, < 3.5 mm. B. MMe2, 45X, < 4X digital zoom, < 3.5 mm. C. JDHM6, 45X, 3.5 mm. D. JDHP13, 45X, < 4X digital zoom, < 3.5 mm. E. KP4, 35X, 4.3 mm. F. PM6, 45X, < 4X digital zoom, < 3.5 mm. G. Biotite wisps, artifact UWG-1017 1027, 45X, < 4X digital zoom, < 3.5 mm. H. Artifact UWG-1017 1350, 45X, 3.5 mm. *DM* = Dean Mine, Cherokee Co., GA; *MMe* = Hillhouse prospect, Cherokee Co., GA; *JDHM* = J.D. Hillhouse mine, Cherokee Co., GA; *JDHP* = J.D. Hillhouse prospect, Cherokee Co., GA; *KP* = Kuykendell prospect, Cherokee Co., GA; *PM* = Poole Mine, Pickens Co., GA; *VB* = Vaughn-Butler Rd., Monroe Co., GA. Where grid lines are visible, each side of the square is approximately 2 mm in length.

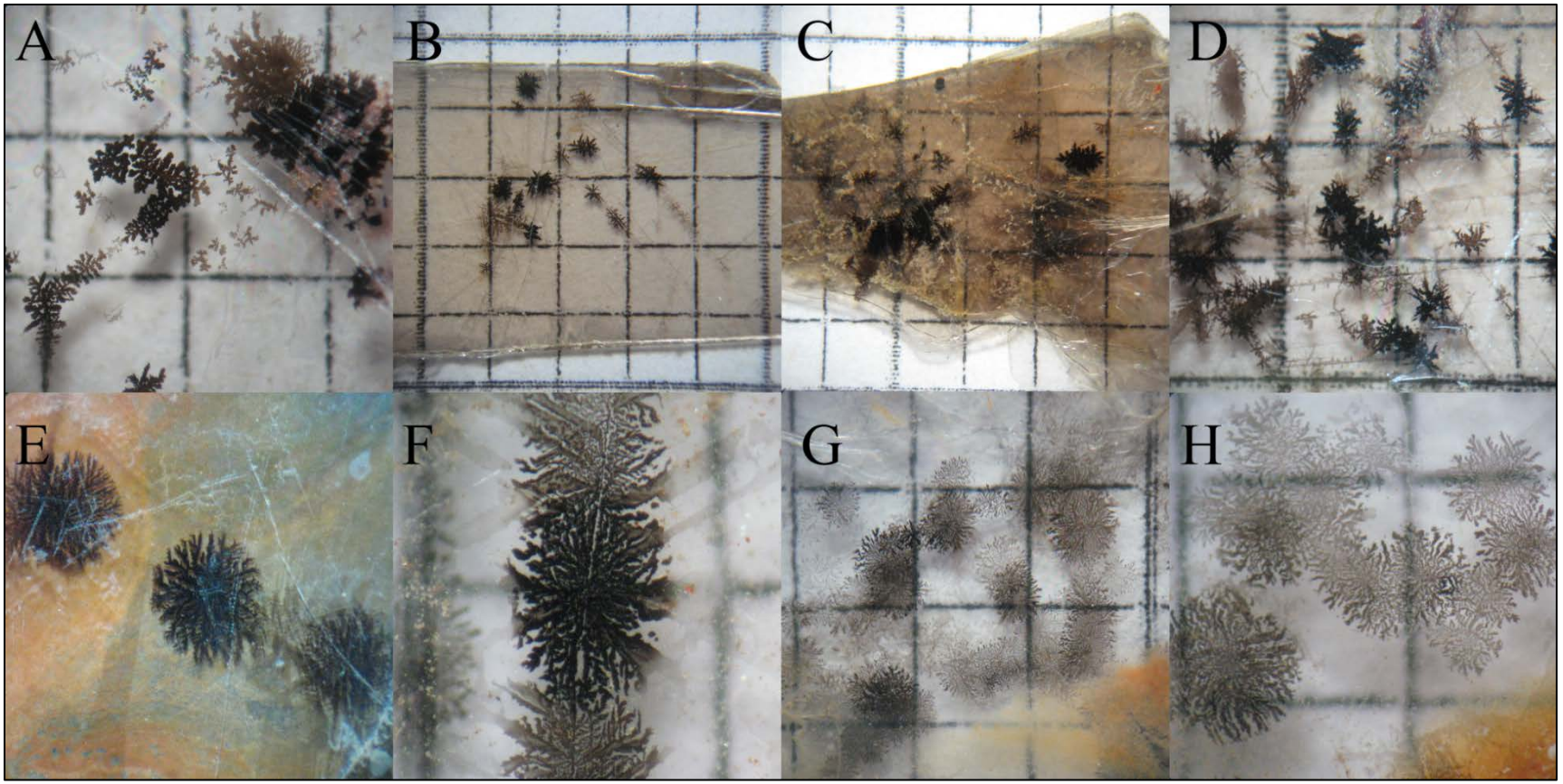

Figure 21: Hematite inclusions in pegmatitic muscovite (sample number, stereoscopic microscope magnification, field of view): A. JDHM7, 17X, 9.2 mm. B. LM7, 13.5X, 1.14 cm. C. LM17, 14X, 1.07 cm. D. LM18, 23X, 6.4 mm. E. PM1, 45X, 3.5 mm. F. PM1, 45X, < 4X digital zoom, < 3.5 mm. G. PM5, 22.5X, 6.7 mm. H. PM11, 45X, 3.5 mm. *JDHM* = J.D. Hillhouse mine, Cherokee Co., GA; *LM* = Ledford Mine, Cherokee Co., GA; *PM* = Poole Mine, Pickens Co., GA. Where grid lines are visible, the side of each square is 2 mm in length.

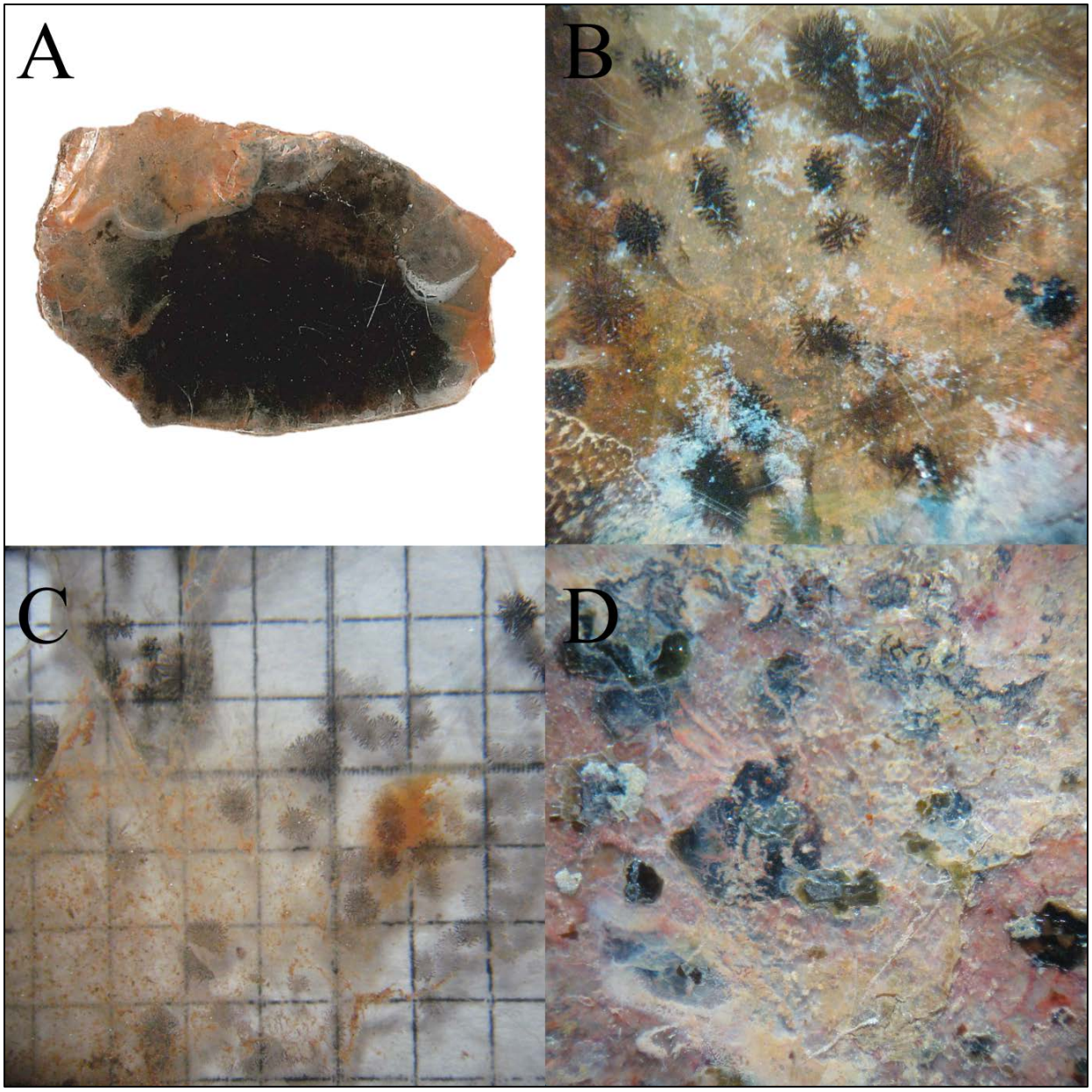

Figure 22: Primary and secondary staining in pegmatitic muscovite (sample number, microscope magnification, field of view): A. Poole mine, Pickens Co., GA (no magnification; hematite staining [darkened portion], clay staining around top-left and right edges). B. PM2, 15X, 9.9 mm (reddish-brown area around hematite inclusions). C. PM11, 10.5X, 1.42 cm (reddish-brown area around hematite inclusions). D. Artifact UWG-1017 1350-1, 20X, 7.1 mm (reddish area around dark green biotite inclusions). *PM* = Poole mine, Pickens Co., GA. Where grid lines are visible (C), the side of each square is approximately 2 mm in length.

results in a strong yellow, red, or brown color (Figure 23). *Manganese-stained* muscovite is that which has been stained by manganese oxides, and is the rarest of the secondary mineral stains. Organic vegetable stains are produced when plant material coats the outer surfaces and cleavage laminae of muscovite books (Figure 24). Characteristic of muscovite found within the weathered zone of deposits, vegetable staining usually occurs in association with heavy clay or iron staining. Secondary air staining (*air creep*) occurs when air is able to penetrate along cleavage planes within the books after entering through the edges, usually as a result of rough handling or trimming. These air pockets are usually connected to the edge of the sheet, and are in contrast to primary air staining, in which the bubbles or pockets of air are completely enclosed within the book (Jahns & Lancaster 1950).

Staining significantly raises the power factor of muscovite mica; defined as "[t]he loss of electrical energy in films of sheet mica used as the dielectric in condensers," lower power factors (0.04 percent or less) are "essential in any mica used for transmitter condensers" (Kesler & Olson 1942:18); thus, the degree of staining at mines/prospects is well noted.

Elasticity

Mica that is considered to be of good quality should have good flexibility and elasticity; it should be able to be distorted without breaking. Fine cracks may be present within the laminae of *haircracked* mica, which causes it to become brittle (Kesler & Olson 1942). Hair cracks are more abundant in the green mica than in brown and buff mica (ruby mica), and are very common in the yellowish olive books from the Spruce Pine district (Jahns & Lancaster 1950).

Color

While regarded as one of the white micas, muscovite occurs in a broad range of colors: gray, white, yellow, amber, brown, reddish brown (*rum*), red (*ruby*), and green (Figure 25,

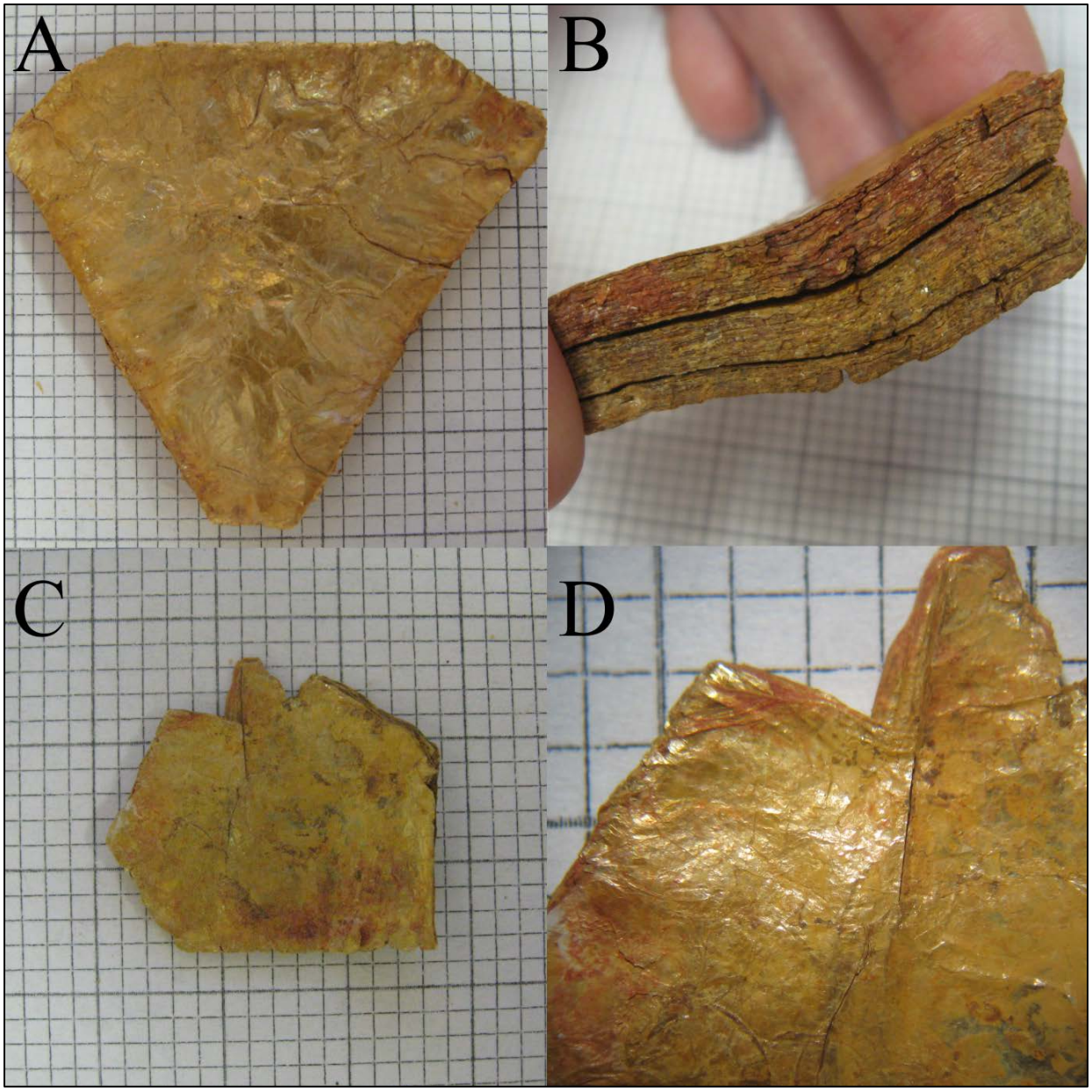

Figure 23: Heavily iron-stained muscovite from the J.A. Partridge mine, Upson Co., GA. A. JAPM17. B. JAPM17 (edgewise view). C. JAPM23. D. JAPM23, 10.5X microscope magnification, field of view approximately 1.42 cm. Where grid lines are visible, the side of each square is 2 mm in length.

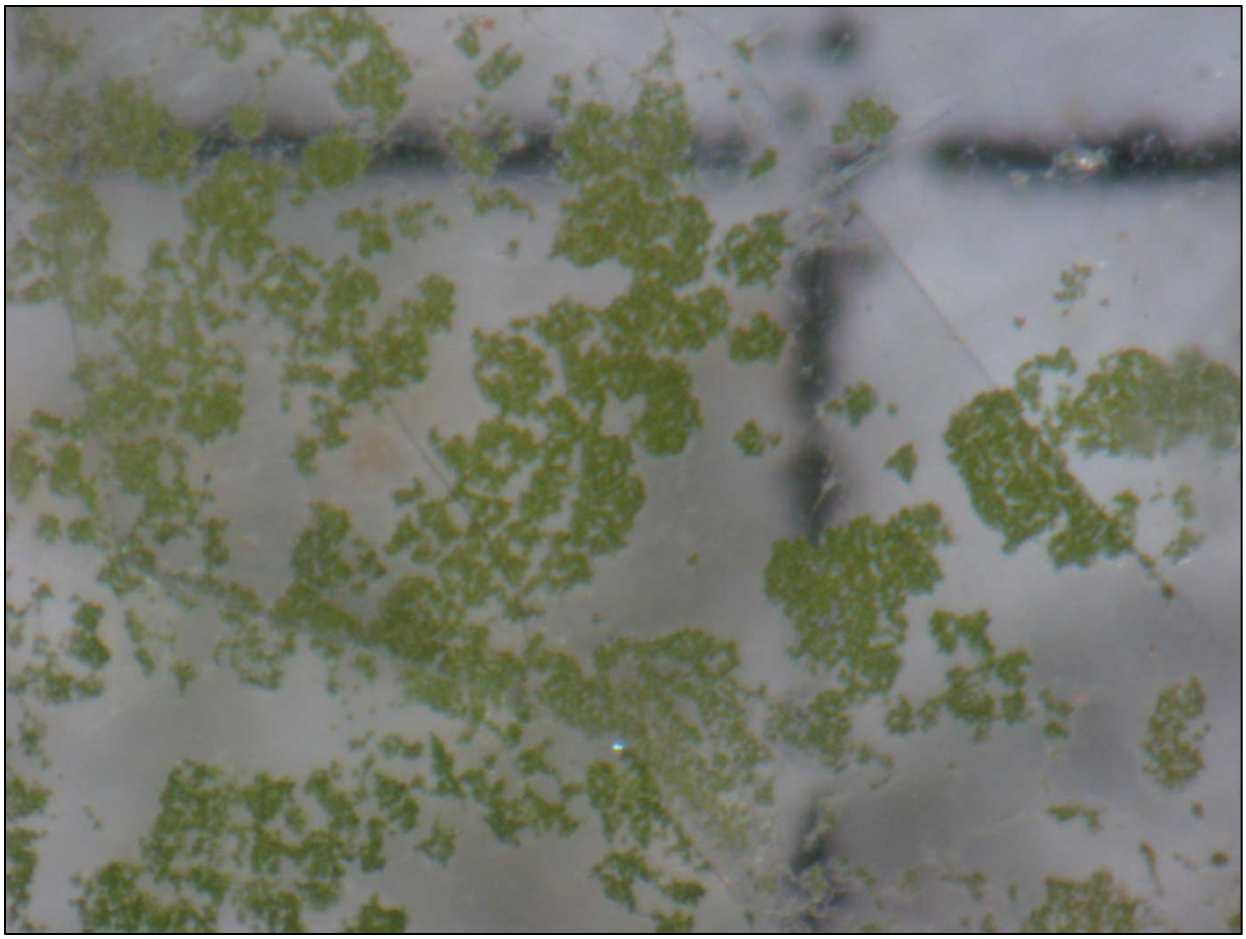

Figure 24: Organic “vegetable” stains in muscovite (JDHP12, 45X, < 4X digital zoom, field of view < 3.5 mm) from the J.D. Hillhouse prospect, Cherokee Co., GA.

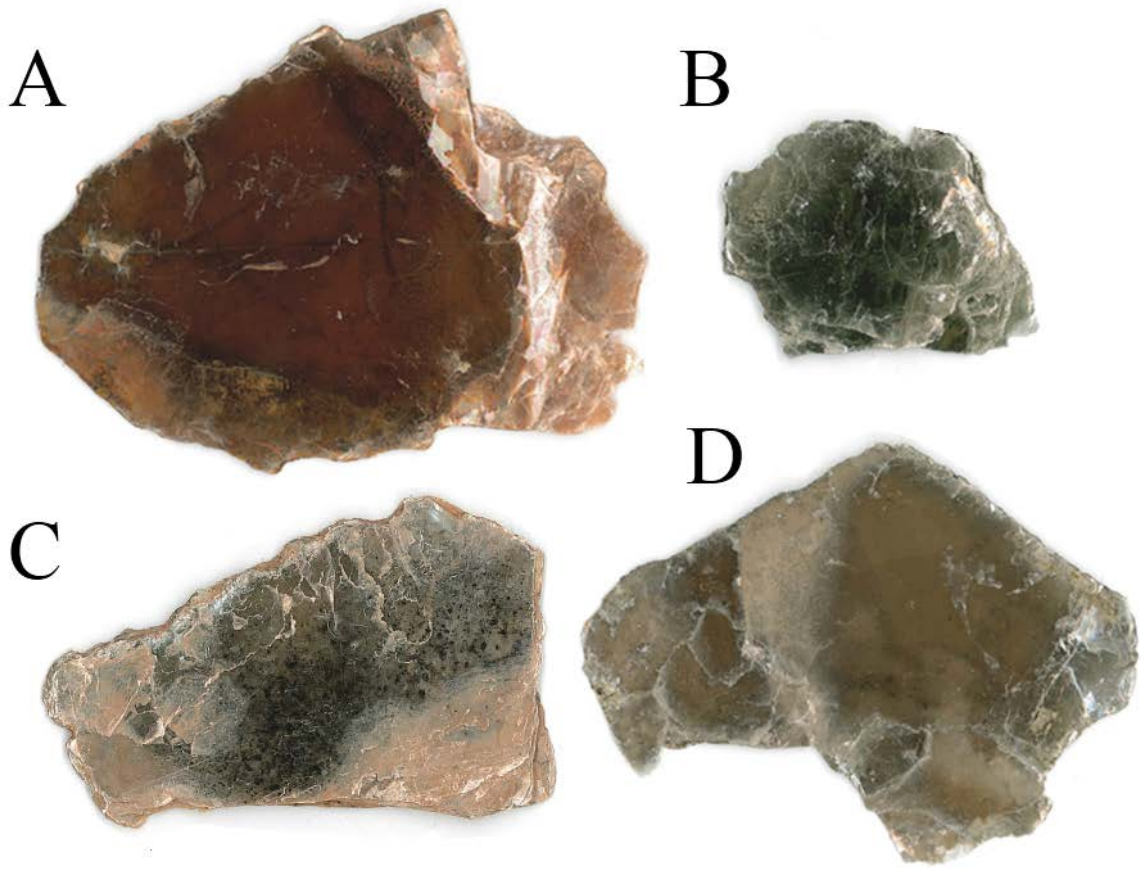

Figure 25: Color variation in pegmatitic muscovite: A. rum (MM32, Mauldin mine, Upson Co., GA). B. green (McK10, McKinney mine, Mitchell Co., NC). C. silver (WM92, Wacaster mine, Cherokee Co., GA). D. olive (DPM39, Deer Park mine, Mitchell Co., NC).

McCallie 1910; Whitlatch 1962; Nesse 2000; Klein 2002). Traditionally, the best mica was regarded as that which was flat and either ruby or rum colored; ruby mica was considered by the electrical industry to possess the highest dielectric properties (Kesler & Olson 1942; Margolin 2000). In this hierarchy, the most desirable muscovite was, in descending order: ruby (light pink to light brownish red), rum (light brown), white (any color possessing a very pale tone), greenish rum (light greenish brown), water-colored (deep greenish brown), and lastly, green (pale to deep bottle green) (Kesler & Olson 1942). Kesler & Olson (1942:11) point to the apparent "prejudice against clear green mica," but note that it is not well founded.

At the time much of the early data concerning the properties of mica was obtained, there were no formally accepted standards in place for the color designation of muscovite. Judd's (1945) study of the color of mica was the only such definitive study available. Inspectors in the mica trade were responsible for the classification of muscovite samples, taking into consideration not only the hue index of the samples, but also factors such as the thickness of the samples and the presence of inclusions and stained or cloudy areas. Despite this lack of a standard system, Judd concluded that the inspectors' classifications were reliable and consistent (Ruthberg et al. 1963).

A more methodological approach to the color designation of muscovite is based on the absorption spectra produced by samples. These spectra display weak absorption bands in the 0.3 μm to 1 μm wavelength region, the activities of which have been shown to be directly associated with the color of the mica (e.g., Ruthberg et al. 1963, Finch 1963):

> The main feature [of ruby mica] is the 0.47 to 0.6 μ[m] absorption structure which indicates the degree of pinkness. The other two are represented by the extreme curves of the greens, i.e., dark green… and by light green…. The attenuation of the pink correlated region of 0.47 to 0.6 μ[m] transforms pink ruby to green ruby category, and its superposition upon the green spectral types is associated with olives, ambers, etc. (Ruthberg et al. 1963:315).

Green micas possess a characteristic line at a wavelength of 0.44 μm. Prominent bands appear in the 1 μm to 8 μm region of the spectrum, in particular, the absorption multiplet at the wavelength region from 3 μm to 3.7 μm which is "strongly associated with the redness of specimens" of the color subgroups of the ruby-colored micas (Ruthberg et al. 1963:315-316). Ruthberg et al. (1963) conclude that all color variation in sheets of commercial muscovite can be attributed to the variation in the three spectral types associated with the deep absorption edge at 0.32 μm and the weak lines and absorption regions at its base.

The underlying chemistry is responsible for the behavior of the absorption spectra and the color variation in muscovite mica. Kesler & Olson (1942:8), in regards to the Spruce Pine district of North Carolina, observed that the character of the wall rock can influence the composition of pegmatites, and that pegmatites of similar composition contain muscovite of the same color; for example, they state that "pegmatite having kyanitic wall rock yields mica of ruby color almost exclusively, and that in alaskite contains mostly green and greenish-rum mica". While it is noted that muscovite color tends to be uniform within a given shoot, it may differ between multiple shoots within the same pegmatite. Wood (1996) tested samples of muscovite from the Spruce Pine region for variation in chemical composition on the basis of color, and concluded that higher concentrations of Fe_2O_3 are associated with green coloration in muscovite, whereas lower concentrations are associated with red muscovite. A spectroscopic study of muscovite of various colors by Finch et al. (1982) found that color variation was mainly the result of a charge transfer interaction between the ferric (Fe^{+3}) and ferrous (Fe^{+2}) cations. The absorption of light at different wavelengths resulted from the differing amounts of Fe^{+3} and Fe^{+2} within the muscovite, producing the observed variations in color. Green muscovite was found to

contain the largest amount of ferric iron, while red muscovite contained predominantly ferrous iron (Wood 1996).

Other studies point to the possibility of elements other than iron influencing the color of the mica. In the muscovites of northern New Mexico, the composition of red muscovite, in terms of most elements, does not differ significantly from that of other similarly-derived muscovites. The significant differences were found to be in the elevated levels of Mn, Cu, and Zn, and lower values for Cr, possessed by red muscovite relative to other samples. In this study, Mn^{+3} in distorted octahedral sites was identified as a possible chromophore in red muscovite (Gresens & Stensrud 1977).

CHAPTER 4

RESEARCH DESIGN

Materials

Georgia

Mines and prospects targeted for sampling were located on Google Earth satellite imagery by means of identifying roadways, railways, and other features (e.g., rivers) common to both the modern satellite images and the historical sketch maps. Furcron & Teague's (1943) maps of the Cherokee-Pickens and Thomaston-Barnesville districts were extensively utilized, and it was found throughout the course of the fieldwork that the positions of mines on the basis of these maps could generally be estimated to within tens of meters in the field; Cocker's (1992a) compilation of UTM coordinates for pegmatites in the Thomaston-Barnesville district, based on United States Geological Survey 7.5 minute quandrangle maps on file at the Georgia Geologic Survey, found a similar level of accuracy in locating mines/prospects in the field. Over 20 additional mines and prospects in the North Georgia district were mapped by Galpin (1915), but the lack of readily identifiable features in that map makes location with any confidence unlikely. Furcron & Teague (1943) present maps of the Cherokee-Pickens (35 mines/prospects) and Thomaston-Barnesville (75 mines/prospects) districts only.

Of the 110 separate occurrences identified from the maps, attempts were made to locate 27 (14 in the Cherokee-Pickens district and 13 in the Thomaston-Barnesville district) in the field for sampling. Mines/prospects selected for sampling were those that were either large and extensively mined in the past, or were deemed most likely to be accessible (e.g., those in open

fields, in the vicinity of accessible roads, or not located deep within wooded areas). Of the 27 targeted mines, only 11 were located in the field (9 in the Cherokee-Pickens district and 2 in the Thomaston-Barnesville district), with the remaining 16 being either inaccessible (e.g., on fenced-off private property or along roads with no access) or no longer showing traces of muscovite books at the surface. Three additional occurrences not referenced in the literature were also sampled. One will be discussed in the following section regarding the Thomaston-Barnesville district. The other two are outlying deposits in Clarke County and Walton County. The Clarke County samples (samples UGA1 – UGA42) were collected from parking lot W03 near the intersection of Baxter Street and Lumpkin Street on the University of Georgia's Athens campus. The Walton County samples (samples LW1 – LW30) were collected approximately two-tenths of a km southwest of the Liberty Hill Church at the southwest end of Liberty Hill Church Road, from the shores of the "Lake Walton" body of water between Walnut Grove and Monroe.

Cherokee-Pickens District

From the Cherokee-Pickens district, samples were collected from two distinct pegmatite fields (Holly Springs and Ball Ground, Figure 26); all pegmatites within this district are muscovite-class pegmatites, though those which are beryl-bearing "show a geochemical affinity to the rare-element class" (Gunow & Bonn 1989:1). The southwestern cluster (the Holly Springs pegmatite field) consists of 10 mines and prospects, the majority of which are located less than 1.5 km to the west of Interstate 575 between Holly Springs and Woodstock in southern Cherokee County. It is important to point out that 10 of the 11 mines comprising this cluster are an approximate straight-line distance of 22 to 28 km from the Etowah mounds, and are the closest identified occurrences of pegmatitic muscovite to the site; trending northeast along the banks of the Etowah River from the Etowah mounds (prior to the construction of Lake Allatoona) would

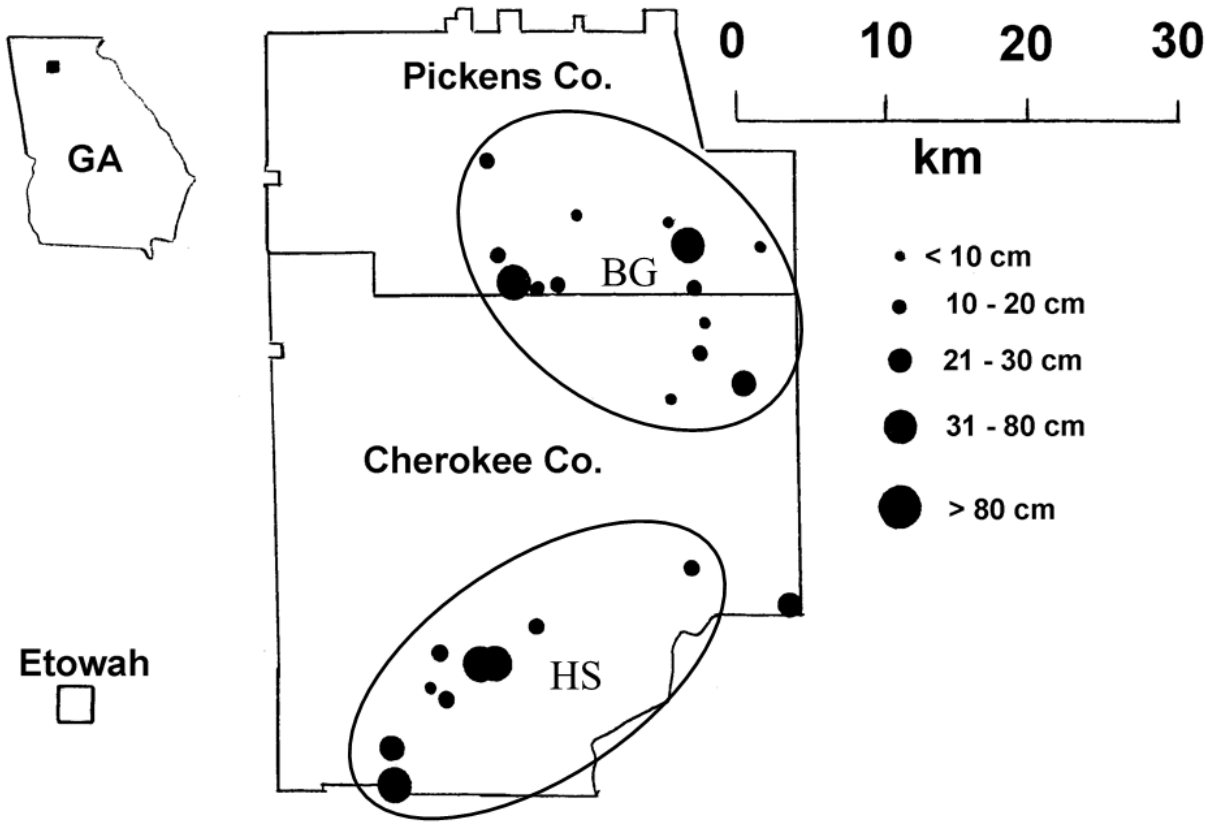

Figure 26: Map of the Cherokee-Pickens district (GA) pegmatite fields. *HS* = Holly Springs. *BG* = Ball Ground. Filled circles correspond to the maximum recorded diameter of muscovite crystals obtained from that locality. Location of the Etowah mounds are shown for reference.

lead one to within only a few kilometers of some of these muscovite deposits. Samples were collected from 7 of the mines/prospects in this area: the Dean mine (samples DM1 – DM35), Hillhouse prospect (samples MMe1 – Mme8, excluding MMe4 which was found to be a fragment of MMe3), J.D. Hillhouse mine (samples JDHM1 – JDHM59), J.D. Hillhouse prospect (samples JDHP1 – JDHP17), Kuykendell prospect (samples KP1-KP25), Ledford mine (samples LM1 – LM31), and Wacaster mine (samples WM1 – WM177). However, the Hillhouse prospect samples were recovered from a series of conical dirt and gravel piles that appeared to have been transported from elsewhere, but were the only muscovite crystals to be found in the immediate vicinity. Attempts at locating the Hause mine were unsuccessful. Regardless, this remains the most intensively sampled pegmatite field within this investigation.

The second pegmatite field, the Ball Ground pegmatite field, extends across both sides of the border between Cherokee County and Pickens County, extending clockwise in a west-to-southeast arc centered on Nelson in Pickens County. Of the 31 mines in this cluster, only the Poole mine (samples PM1 – PM10, excluding PM3 which was found to be a fragment of PM1) and Reynolds mine (samples RM1 – RM89) in the southeastern corner of Pickens County were sampled. The general area of the Bennett mine was inaccessible, and neither of the two Denson mines could be located in the field. All of the mines in this region are between approximately 42 and 58 km from Etowah. Again, the section of the Etowah River, prior to crossing the Cherokee-Forsyth border, runs a mere few kilometers south of the mines in northeastern Cherokee County.

Thomaston-Barnesville District

The Thomaston-Barnesville district mines form a longer, more continuous belt than those of the Cherokee-Pickens district. It extends from approximately 5 to 6 km south of Thomaston in Upson County northeast through parts of Lamar County and Monroe County before

terminating approximately 3 or 4 km from the northeastern border of Monroe County; the axis of this belt runs approximately 58 to 60 km in length, and the belt is approximately 21 km wide at its widest point perpendicular to the center of the long axis. Cocker (1992a) extends the district to include mines in Jasper, Pike, Crawford, and Talbot counties, and approximates the total area of the Thomaston-Barnesville pegmatite district to be 2,000 km^2.

Cocker (1992a) divides the Thomaston-Barnesville district into nine geographically-isolated pegmatite fields; these are the Indian Grave, Concord, Lighthouse, Blount, Juliette, Russellville, Yatesville, Waymanville, and Lazer Creek fields (Figure 27). Of the 75 mines and prospects identified from Furcron & Teague's (1943) maps of the district, 13 were targeted for sampling. However, only the J.A. Partridge mine (samples JAPM1 – JAPM24) from the Indian Grave field and the Mauldin mine (samples MM1 – MM94) from the Waymanville field were located and sampled. The Bennie Baron mine, Dick Fletcher mine, King and Thurston mine, Miles Brown mine, Short-Mitchell mine, and Stevens Rock mine were all inaccessible at the time, while the E.M. Thompson property, L.P. Goodwin mine, L.P. Phinazee mine, Owens prospect, and T.D. Thurman mine could not be located in the field. One additional occurrence in the Thomaston-Barnesville district was found by chance while attempting to locate the T.D. Thurman mine on Vaughn Road southwest of Forsyth in Monroe County (the eastern end of the Yatesville pegmatite field) and was subsequently sampled; this occurrence is located within approximately one-tenth of a kilometer north (following the road) of the intersection of Vaughn Road and Butler Road and will be referred to as the Vaughn-Butler Road occurrence (samples VB1 – VB19).

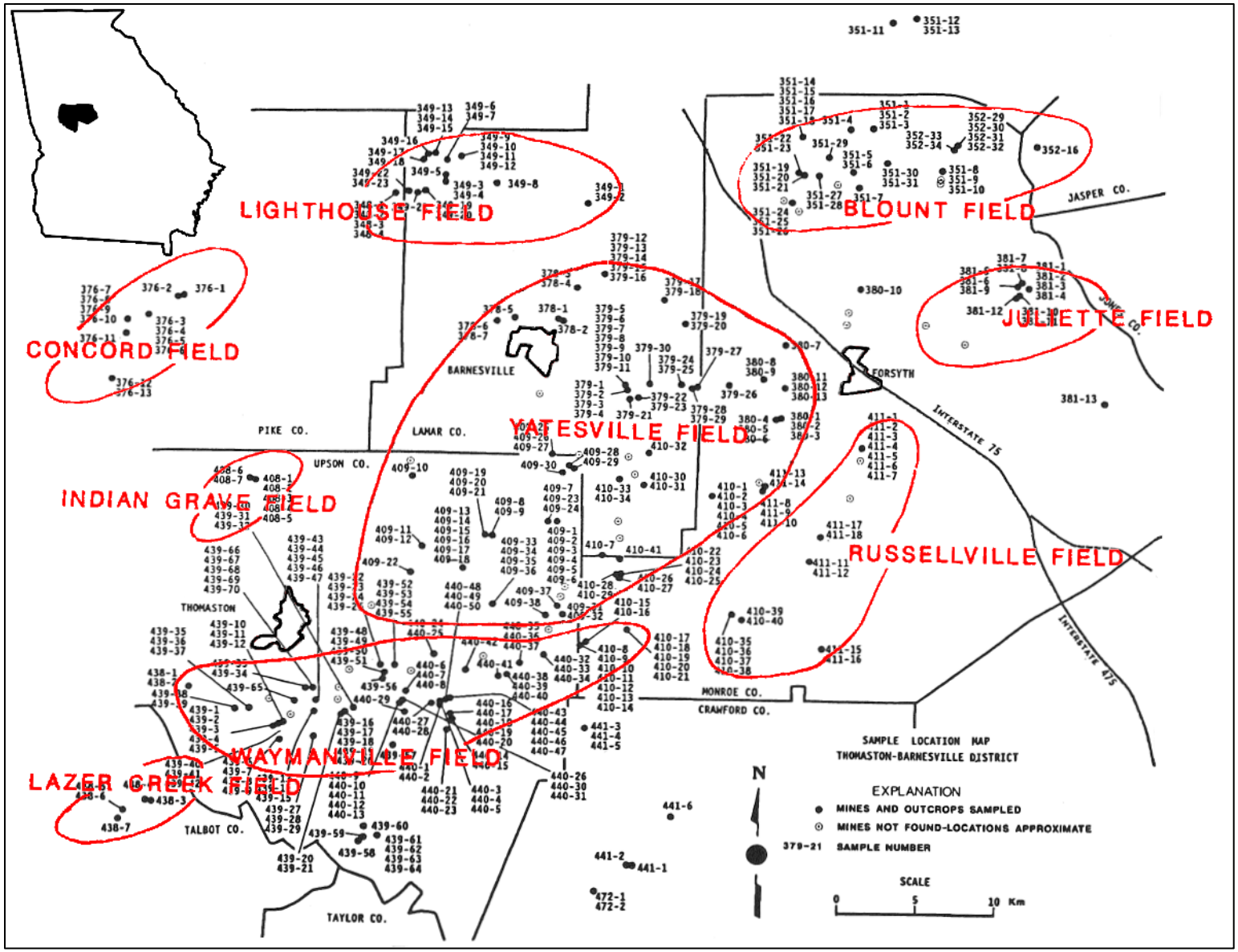

Figure 27: Map of Thomaston-Barnesville district pegmatite fields. Sample locations and numbers from Cocker (1992a).

North Carolina

While no field collection in North Carolina was undertaken as part of this research, trace element data on Spruce Pine muscovite is available in Wood's (1996) master's thesis. Additional samples of Spruce Pine muscovite from the University of Georgia's Department of Geology, collected as part of Veal's (2004) Master's thesis on the mineralogy of the Spruce Pine plutonic suite in North Carolina, have been made available for analysis. These samples are from Mitchell County's Deer Park mine (DPM1 – DPM41), Pink mine (Pink1 – Pink12), and McKinney mine (McK1 – McK15).

Sampling Strategy of Geological Samples for XRF Analysis

Not all samples which were collected were suitable for XRF analysis, and, due to timing constraints, not all samples deemed suitable for analysis were able to be analyzed. The sub-sampling strategy employed in the selection of samples to analyze was not random in that only those samples from each locality thought to yield the most reliable XRF readings of the muscovite itself were analyzed. Samples to be analyzed were thus selected on the basis of: (1) thickness (samples needed to be thick enough to ensure that the XRF instrument was taking readings of the mica only, and not of any background materials); (2) degree of staining and abundance of mineral inclusions (a large enough area [approximately 8 mm in diameter, the size of the opening for the X-ray beam] on the surface of the mica, free of stains or large proportions of mineral inclusions, was necessary to avoid "contaminating" the XRF readings of the mica with readings from the mineral inclusions or clay/iron stains); and (3) flatness of the sample (presenting a relatively uniform flat surface to the X-ray beam was preferred over uneven/curved surfaces).

Ideally, the same number of samples would be analyzed from each locality. However, as will be explained in following sections, successful discrimination among sources is more likely to be achieved on a district-scale basis as opposed to an individual pegmatite basis, and synthesis of these data with data presented in the published literature is desirable. As such, different numbers of samples were analyzed from individual localities, so that when these analyses are combined with the published datasets of varying sample size, districts will contain approximately equal sample sizes. A list of individual samples thus selected for analysis, given the selection criteria, is presented in Appendix C.

Etowah Muscovite Artifacts

Muscovite artifacts from Etowah are currently being stored at the Etowah Mounds Museum in Cartersville, Georgia, at the University of West Georgia's Antonio J. Waring, Jr. Archaeological Laboratory in Carrollton, Georgia, and at Panola Mountain State Park in Georgia; only those artifacts curated at the Waring Lab were analyzed during this investigation, as the availability of a rental pXRF instrument at the Waring Lab made this the most practical and least expensive course of action. Artifacts were accessed from two catalogs, UWG-1017 (artifacts 308-1, 308-2, 308-3, 308-4, 308-6, 308-7, 308-8, 308-9, 1027, 1311, 1332-1, 1350-1, 1350-2, 1567, and 1713) and UWG-1019 (artifacts 2014, 2430, 2445, 2518, 3236 and 3944). For a complete listing of artifact descriptions and images, see Appendix D. Artifacts will subsequently be referenced by their artifact number only, without the catalog number.

For the most part, these artifacts consist of unworked fragments and sheets of muscovite. Of those artifacts described and/or analyzed in the present study, only 1567 (a mica disc), 1713 (the mica "sun symbol"), 2014 (a tourmaline-muscovite schist gaming disc) and 3949 (a perforated mica disc) show any obvious evidence of having been worked. Additional artifacts

from the Waring Lab's special collections (mica discs, crosses and curved symbols), largely unavailable for analysis due to their fragile conditions as a result of weathering, also display obvious signs of having been worked. However, several of the artifacts observed in the present study display sharp linear ruling planes or portions of the euhedral hexagonal crystal outline not typically observed in (or associated with) most micas, and as a result, have been incorrectly labeled as cut (or possibly) cut artifacts (e.g., 308-1, 1350, 1027 and 3236).

Of special interest, despite not being included in the statistical treatment of the pXRF data, are artifacts 1713 (the mica "sun symbol") and 2014 (the schist gaming disc). The schist gaming disc was not analyzed with the pXRF, as it does not consist of a single crystal of pegmatitic muscovite. The mica sun symbol, while fashioned from pegmatitic muscovite, appears to have been purposely coated with a black pitch or similar material, and was thus not incorporated in the statistical analysis of the data. Though not included in the statistical treatment of the artifacts, 2430 was nevertheless analyzed with the pXRF, and it can be assumed that the large concentrations of Cu (38,483 ppm), Fe (47,816 ppm), Pb (92 ppm), Sr (210 ppm) and S (1,573 ppm) relative to any of the other artifacts or geological samples analyzed are concentrated within that coating substance.

As previously mentioned in association with the presented size data, none of the Etowah micas are particularly large. Maximum length dimensions of the artifacts observed in the present study range from 1.7 to 7.7 cm; thickness of the artifacts vary from fractions of a mm (with some artifacts, particularly the mica discs, consisting of only a few sheets) upwards to approximately 3 mm at most. As with the geological samples, not all of the Etowah muscovite artifacts were suitable for the pXRF analysis as a result of issues relating to thickness. Only the following were

determined to be of sufficient thickness for analysis and subsequent inclusion in the statistical treatment: 308-2, 308-4, 1027, 1311, 1332-1, 1350-1, 1350-2, 2430, 2518 and 3236.

Analytical Methods

Visual Examination/Physical Characteristics of Samples

Visual examination of both the geological and archaeological samples of muscovite was undertaken with a Leica Zoom 2000 stereoscopic microscope, with 12.5x – 45x magnification capabilities. The primary objective of visual examination was to identify mineral inclusions or intergrowths present within the muscovite as well as to record the color of the muscovite for inclusion as supplemental data to that which is presented in the published literature; such information has been synthesized into Appendix B. For the most part, however, such visual examination did not add much new information to that which was already observed at the localities sampled. The size of the muscovite books comprising the geological samples was not recorded; most (if not all) of the samples remaining at any given locality are mine scrap, having been discarded in favor of the larger books, and thus size of samples collected should not be used to characterize the deposits.

Portable X-ray Fluorescence (pXRF) Analysis of Samples

Both the geological and archaeological samples used in this investigation were analyzed at the Antonio J. Waring, Jr. Archaeological Laboratory with a Thermo Scientific Niton XL3t 600 handheld XRF analyzer using a preloaded soil testing routine. Elements were analyzed using three separate filters: *Main* filter elements (As, Au, Co, Cu, Fe, Hg, Mn, Mo, Ni, Pb, Rb, Se, Sr, Th, U, W, Zn and Zr) were analyzed first for 45.0 s, followed by the *Low* filter elements (Ca, Cr, K, S, Sc, Ti and V) for an additional 45.0 s, and lastly the *High* filter elements (Ag, Ba, Cd, Cs, Pd, Sb, Sn and Te) for 45.0 s.

To address the issue relating to sample thickness, samples were analyzed against an acid-free Hollinger box lid background (Figure 28). Throughout the course of performing the analyses, it was found that none of the samples of appreciable thickness contained any detectable amounts of Mo, whereas four replicate analyses of the Hollinger box lid detected Mo (22, 23, 25 and 25 ppm Mo). Therefore, where Mo was found in the analysis of thinner samples, it was assumed the XRF readings were being influenced by the background and the sample was deemed too thin to rely on the readings; such samples were removed from any following statistical treatment.

The clearest (i.e., free of appreciable staining or mineral inclusions) flattest surface present on a given sample, with an area of at least 8 mm in diameter (the size of the circular opening through which the X-ray beam is focused), was chosen as the site for analysis. All samples were analyzed only once, with the exception of three samples (MM93, WM124 and JDHM48) chosen as "working standards" on which to perform replicate analyses for purposes of determining analytical precision and standard deviations. The large number of samples to be analyzed (including replicate analyses of the working standards, $N \approx 290$, at over two minutes per analysis) in a limited amount of time (only three days were available to perform the analyses) precluded replicate analyses of individual samples other than the substandards. One standard was analyzed at arbitrary intervals on any given day of analytical work, and was used as the standard only for that day. The decision was made to sacrifice better estimates of precision associated with using a single substandard for all three days of analysis in favor of using multiple standards; as not every element is expected to be measured in detectable concentrations in a single standard, the use of multiple standards should thus allow for the calculation of precision estimates of a broader suite of elements. MM93 (9 replicate analyses) was used as the standard

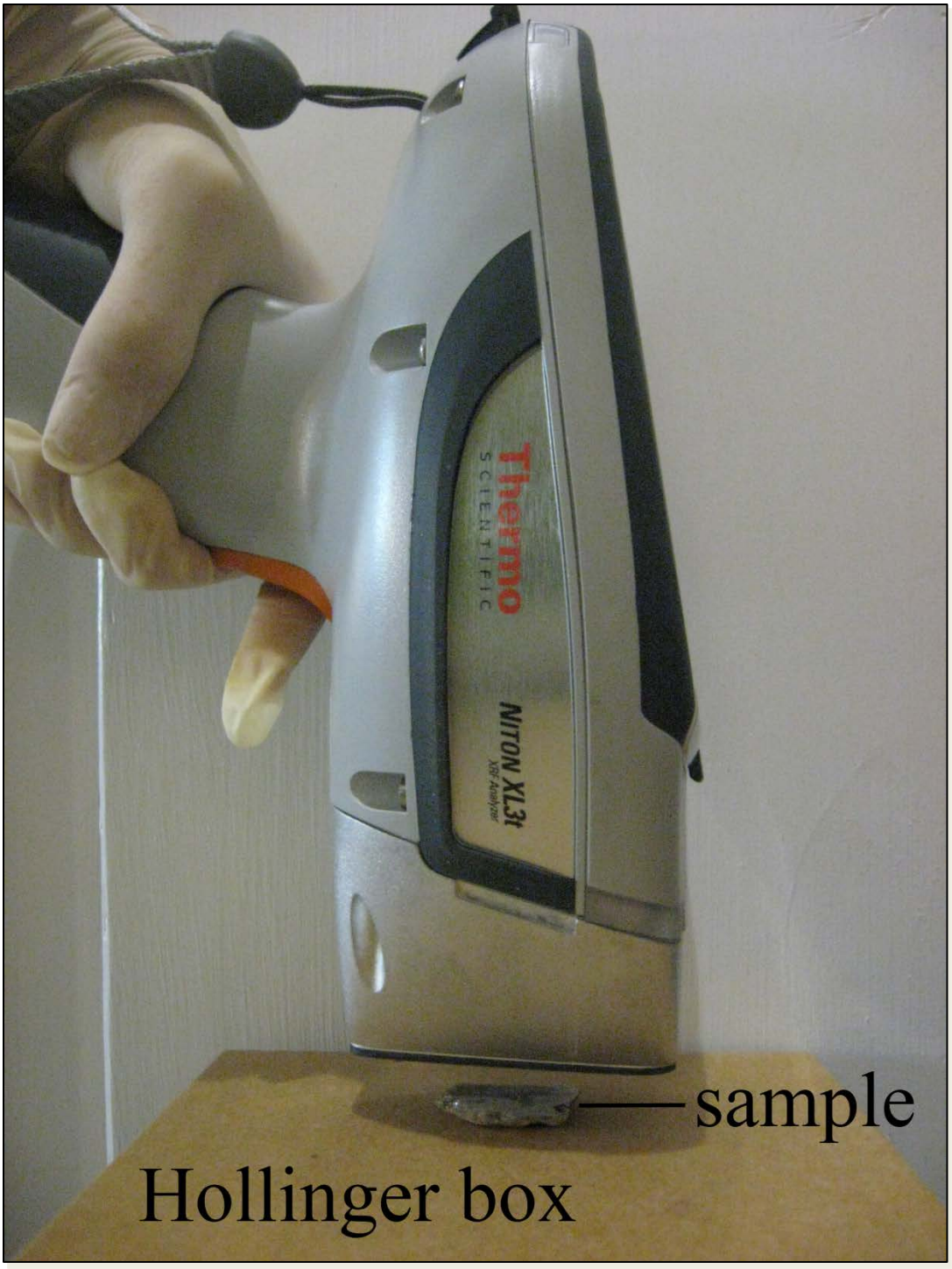

Figure 28: pXRF analytical setup. Samples were placed on an acid-free Hollinger box lid for analysis, with the Thermo Scientific Niton XL3t 600 handheld XRF analyzer operating in an upright position, as shown. The analyzer was held in direct contact with all samples during each analysis.

on the first day of analysis, WM124 (8 replicate analyses) on the second day, and JDHM48 (8 replicate analyses) on the third day. The pXRF results from analyses of these standards are presented in Table 2. These standards are currently in preparation for shipment to a commercial laboratory (Activation Laboratories Ltd., Ontario, Canada) for a more precise determination of their composition and to gauge the accuracy of the pXRF instrument.

The pXRF analyzer returns 2σ error limits along with the measured concentrations for each element in a given analysis. Where concentrations are below detectable limits, the 2σ error serves as the limit of detection (LOD) for that element in an individual analysis. Depending on the scan time (longer scans result in lower error limits) and concentrations of the given element (as shown in Table 2, higher concentrations of an element are associated with greater error limits), the 2σ error limits and LODs for that element vary from analysis to analysis. Given that 135.0 s scan times were utilized for each analysis, the concentration of a given element in a sample is likely the main contributing factor to variation in error limits. With respect to the reproducibility of results, it was found that for most elements in which concentrations above detectable limits were measured in the majority of replicate analyses for at least one of the standards (i.e., Ba, Cr, Cs, Fe, Mn, Rb, Sn, Sr, Ti and Zn), the standard deviation was either less than, or within reasonable proximity of, the average of the 2σ error limits provided for that element by the pXRF. This indicates that for these elements, variation in measured values between replicate analyses can be attributed primarily to error/precision limitations associated with the instrument. Additionally, Zr may be added to this list of elements, despite none of the standards yielding Zr concentrations above detectable limits in the majority of replicate analyses; where Zr was measured in 4 of 9 replicate analyses of MM93, the low 2σ errors/LODs (4 – 5 ppm) allow reasonable confidence to be placed in the measured values. The only element of

Table 2: pXRF data from replicate analyses of working standards (JDHM48, WM124 and MM93). All values are in ppm; *LOD* indicates concentrations below the limits of detection. Values in the first column under a given element are the measured concentrations; values in the second column represent the 2σ error limits displayed on the pXRF. Where concentrations are below the limits of the detection, the 2σ value represents the limit of detection. *mean* is the mean value of the measured concentrations, *sd* is the standard deviation of the measured concentrations, and *mean 2σ* is the mean value of all 2σ errors for which elements were present in detectable concentrations. Where all or most replicate analyses of the standard yield measured concentrations below detectable limits, *mean 2σ* is the average limit of detection. Means and standard deviations were calculated only on those replicate analyses measuring concentrations above detectable limits.

JDHM48	As ± 2σ		Ba ± 2σ		Ca ± 2σ		Cd ± 2σ		Co ± 2σ	
1	LOD	8	1586	55	LOD	417	LOD	10	LOD	152
2	LOD	9	1499	55	LOD	359	LOD	10	LOD	151
3	LOD	8	1488	55	LOD	369	LOD	10	LOD	156
4	LOD	8	1526	55	LOD	405	LOD	10	LOD	152
5	LOD	8	1399	52	LOD	419	LOD	10	LOD	152
6	LOD	9	1433	53	LOD	413	LOD	10	LOD	151
7	LOD	8	1617	56	LOD	393	LOD	11	LOD	152
8	LOD	8	1514	55	LOD	407	LOD	10	LOD	153
mean			**1508**							
sd			**72**							
mean 2σ	**8**		**55**		**398**		**10**		**152**	
JDHM48	**Cr ± 2σ**		**Cs ± 2σ**		**Cu ± 2σ**		**Fe ± 2σ**		**Hg ± 2σ**	
1	60	26	48	17	LOD	27	25457	427	LOD	10
2	LOD	31	42	18	LOD	30	23088	428	LOD	10
3	37	23	27	18	LOD	30	24842	433	LOD	10
4	69	26	33	17	LOD	28	25186	425	LOD	10
5	79	26	LOD	25	LOD	28	25630	430	LOD	10
6	77	26	27	17	LOD	27	25145	427	LOD	9
7	67	25	41	18	LOD	28	24164	421	LOD	10
8	121	27	33	17	LOD	29	25244	428	LOD	10
mean	**73**		**36**				**24845**			
sd	**25**		**8**				**837**			
mean 2σ	**26**		**17**		**28**		**427**		**10**	
JDHM48	**K ± 2σ**		**Mn ± 2σ**		**Pb ± 2σ**		**Rb ± 2σ**		**S ± 2σ**	
1	94911	1324	366	86	LOD	11	213	10	LOD	995
2	78595	1130	254	80	LOD	11	206	10	LOD	909
3	82115	1174	283	82	LOD	11	214	10	LOD	963
4	91232	1294	261	78	LOD	9	209	10	LOD	971
5	93579	1317	343	83	LOD	10	225	10	LOD	1079
6	91781	1303	277	80	LOD	12	220	10	LOD	980
7	86868	1239	259	79	LOD	10	209	10	LOD	931
8	91998	1296	341	85	LOD	11	218	10	LOD	944
mean	**88885**		**298**				**214**			
sd	**5821**		**45**				**6**			
mean 2σ	**1260**		**82**		**11**		**10**		**971**	

JDHM48	Sb ± 2σ		Sc ± 2σ		Se ± 2σ		Sn ± 2σ		Sr ± 2σ	
1	LOD	28	LOD	29	LOD	5	LOD	28	33	4
2	LOD	29	LOD	23	LOD	5	29	19	26	4
3	LOD	29	LOD	25	LOD	5	LOD	29	31	4
4	LOD	28	LOD	26	LOD	5	LOD	28	31	4
5	LOD	27	LOD	26	LOD	5	LOD	27	31	4
6	LOD	28	LOD	29	LOD	4	LOD	27	34	4
7	LOD	29	LOD	26	LOD	5	32	19	29	4
8	LOD	28	LOD	28	LOD	5	LOD	28	33	4
mean									**31**	
sd									**3**	
mean 2σ	**28**		**27**		**5**		**28**		**4**	
JDHM48	**Te ± 2σ**		**Ti ± 2σ**		**U ± 2σ**		**V ± 2σ**		**W ± 2σ**	
1	LOD	58	1985	168	LOD	17	LOD	71	LOD	62
2	LOD	60	1605	141	LOD	17	LOD	61	LOD	71
3	LOD	60	1730	149	LOD	18	LOD	64	LOD	73
4	LOD	59	2009	162	LOD	16	LOD	69	LOD	66
5	LOD	56	1848	167	LOD	17	LOD	71	LOD	64
6	LOD	57	1936	164	LOD	17	LOD	71	LOD	63
7	LOD	60	1901	156	LOD	17	LOD	66	LOD	66
8	LOD	58	1905	159	LOD	17	LOD	68	LOD	71
mean			**1865**							
sd			**136**							
mean 2σ	**59**		**158**		**17**		**68**		**67**	
JDHM48	**Zn ± 2σ**		**Zr ± 2σ**							
1	40	13	LOD	6						
2	23	12	7	4						
3	41	14	LOD	6						
4	45	13	LOD	6						
5	38	13	LOD	6						
6	44	13	LOD	6						
7	44	13	LOD	6						
8	33	13	LOD	6						
mean	**39**									
sd	**7**									
mean 2σ	**13**		**6**							

WM124	As ± 2σ		Ba ± 2σ		Ca ± 2σ		Cd ± 2σ		Co ± 2σ	
1	LOD	8	112	43	LOD	388	LOD	9	LOD	120
2	LOD	7	76	42	LOD	396	LOD	9	LOD	123
3	LOD	7	68	42	LOD	398	LOD	9	LOD	125
4	LOD	8	112	42	LOD	398	LOD	9	LOD	124
5	LOD	8	76	42	LOD	389	LOD	9	LOD	126
6	LOD	7	62	42	LOD	396	LOD	9	LOD	125
7	LOD	8	65	42	LOD	376	LOD	9	LOD	121
8	LOD	7	117	43	LOD	381	LOD	9	LOD	121
mean			**86**							
sd			**23**							
mean 2σ	**8**		**42**		**390**		**9**		**123**	
WM124	**Cr ± 2σ**		**Cs ± 2σ**		**Cu ± 2σ**		**Fe ± 2σ**		**Hg ± 2σ**	
1	139	24	LOD	23	LOD	26	16895	338	LOD	10
2	87	23	LOD	23	LOD	26	17323	343	LOD	10
3	108	24	LOD	23	LOD	27	17507	345	LOD	9
4	89	24	LOD	23	LOD	27	17662	348	LOD	9
5	100	24	LOD	23	LOD	27	17768	353	LOD	10
6	93	24	LOD	23	LOD	27	17572	347	LOD	10
7	67	22	LOD	23	LOD	29	16857	342	LOD	9
8	78	23	LOD	24	LOD	25	16982	340	LOD	9
mean	**95**						**17321**			
sd	**22**						**364**			
mean 2σ	**23**		**23**		**27**		**344**		**9**	
WM124	**K ± 2σ**		**Mn ± 2σ**		**Pb ± 2σ**		**Rb ± 2σ**		**S ± 2σ**	
1	95100	1234	91	58	LOD	9	305	11	LOD	949
2	96393	1255	168	66	LOD	9	311	12	LOD	936
3	96286	1261	174	66	LOD	9	324	12	LOD	972
4	96885	1266	170	67	LOD	11	310	12	LOD	977
5	94696	1238	180	68	LOD	11	327	12	LOD	908
6	96194	1260	195	68	LOD	10	325	12	LOD	987
7	91061	1187	222	70	LOD	10	300	11	LOD	927
8	92803	1217	161	64	LOD	9	306	11	LOD	992
mean	**94927**		**170**				**313**			
sd	**2035**		**37**				**10**			
mean 2σ	**1240**		**66**		**10**		**12**		**956**	

WM124	Sb ± 2σ		Sc ± 2σ		Se ± 2σ		Sn ± 2σ		Sr ± 2σ	
1	LOD	26	LOD	25	LOD	5	LOD	26	8	2
2	LOD	25	LOD	25	LOD	5	26	17	11	3
3	LOD	25	LOD	25	LOD	4	26	17	7	2
4	LOD	26	LOD	26	LOD	4	43	17	7	2
5	LOD	25	LOD	25	LOD	4	29	17	10	3
6	LOD	25	LOD	25	LOD	5	LOD	25	9	3
7	LOD	25	LOD	23	LOD	5	LOD	25	9	3
8	LOD	26	LOD	25	LOD	4	48	18	10	3
mean							**34**		**9**	
sd							**10**		**1**	
mean 2σ	**25**		**25**		**5**		**17**		**3**	
WM124	**Te ± 2σ**		**Ti ± 2σ**		**U ± 2σ**		**V ± 2σ**		**W ± 2σ**	
1	LOD	53	2789	127	LOD	18	LOD	49	LOD	62
2	LOD	52	2765	128	LOD	19	LOD	49	68	45
3	LOD	52	2752	132	LOD	19	LOD	51	LOD	62
4	LOD	53	2790	131	LOD	19	LOD	51	LOD	60
5	LOD	53	2601	130	LOD	19	LOD	50	LOD	63
6	LOD	52	2688	130	LOD	19	LOD	51	LOD	63
7	LOD	53	2592	123	LOD	19	LOD	48	LOD	65
8	LOD	54	2603	127	LOD	19	LOD	49	LOD	60
mean			**2697**							
sd			**88**							
mean 2σ	**52**		**129**		**19**		**50**		**62**	
WM124	**Zn ± 2σ**		**Zr ± 2σ**							
1	47	13	LOD	5						
2	34	12	LOD	5						
3	42	13	LOD	5						
4	44	13	6	4						
5	56	14	LOD	6						
6	36	12	LOD	5						
7	36	12	LOD	5						
8	44	13	LOD	5						
mean	**43**									
sd	**7**									
mean 2σ	**13**		**5**							

MM93	As ± 2σ		Ba ± 2σ		Ca ± 2σ		Cd ± 2σ		Co ± 2σ	
1	9	5	204	44	LOD	345	LOD	9	LOD	92
2	LOD	8	696	48	LOD	356	LOD	10	LOD	93
3	LOD	8	343	44	LOD	363	LOD	9	LOD	92
4	LOD	7	592	46	LOD	363	LOD	9	LOD	92
5	LOD	8	357	45	LOD	365	LOD	10	LOD	91
6	LOD	7	566	46	LOD	356	LOD	9	LOD	90
7	LOD	8	619	46	LOD	357	LOD	10	LOD	91
8	LOD	8	569	45	LOD	362	LOD	9	LOD	93
9	LOD	7	622	46	LOD	358	LOD	10	LOD	92
mean			**507**							
sd			**165**							
mean 2σ	**7**		**46**		**358**		**10**		**92**	
MM93	**Cr ± 2σ**		**Cs ± 2σ**		**Cu ± 2σ**		**Fe ± 2σ**		**Hg ± 2σ**	
1	104	21	LOD	24	LOD	25	10215	259	LOD	9
2	LOD	29	65	17	LOD	27	10148	256	LOD	10
3	86	21	LOD	24	LOD	25	10071	254	LOD	9
4	94	21	44	16	LOD	25	10099	256	LOD	9
5	71	21	LOD	24	LOD	25	10121	253	LOD	9
6	66	20	39	16	LOD	25	9851	253	LOD	9
7	57	20	52	16	LOD	27	9861	254	LOD	9
8	67	21	33	16	LOD	27	10118	255	LOD	9
9	79	21	41	16	LOD	26	9878	252	LOD	9
mean	**78**		**46**				**10040**			
sd	**16**		**11**				**138**			
mean 2σ	**21**		**16**		**26**		**255**		**9**	
MM93	**K ± 2σ**		**Mn ± 2σ**		**Pb ± 2σ**		**Rb ± 2σ**		**S ± 2σ**	
1	87849	1090	159	60	LOD	9	297	11	LOD	858
2	91956	1129	LOD	74	LOD	10	290	11	LOD	873
3	93546	1137	LOD	71	LOD	9	289	11	LOD	857
4	94047	1137	LOD	74	LOD	9	293	11	LOD	908
5	95383	1154	113	55	LOD	10	288	11	LOD	835
6	93808	1130	98	54	LOD	9	286	11	LOD	828
7	93890	1132	104	54	LOD	10	292	11	LOD	886
8	94586	1143	LOD	76	LOD	10	289	11	LOD	912
9	94282	1134	105	55	LOD	10	297	11	LOD	833
mean	**93261**		**116**				**291**			
sd	**2227**		**25**				**4**			
mean 2σ	**1132**		**56**		**10**		**11**		**866**	

MM93	Sb ± 2σ		Sc ± 2σ		Se ± 2σ		Sn ± 2σ		Sr ± 2σ	
1	LOD	26	LOD	21	LOD	4	LOD	26	12	3
2	LOD	28	LOD	22	LOD	4	52	18	14	3
3	LOD	26	LOD	22	LOD	4	LOD	25	13	3
4	LOD	26	LOD	22	LOD	4	30	17	14	3
5	LOD	26	LOD	22	LOD	5	LOD	26	13	3
6	LOD	27	LOD	22	LOD	5	27	17	13	3
7	LOD	27	LOD	23	LOD	5	48	18	14	3
8	LOD	26	LOD	22	LOD	4	LOD	26	14	3
9	LOD	27	LOD	22	LOD	4	54	18	14	3
mean							**42**		**14**	
sd							**12**		**1**	
mean 2σ	**26**		**22**		**4**		**18**		**3**	
MM93	**Te ± 2σ**		**Ti ± 2σ**		**U ± 2σ**		**V ± 2σ**		**W ± 2σ**	
1	LOD	54	3256	129	LOD	18	LOD	51	LOD	53
2	72	38	3593	136	LOD	18	LOD	54	LOD	63
3	LOD	53	3161	131	LOD	18	LOD	51	LOD	59
4	LOD	54	3563	137	LOD	18	LOD	53	LOD	57
5	LOD	54	3473	140	LOD	18	LOD	54	LOD	60
6	LOD	55	3643	136	LOD	18	LOD	52	LOD	58
7	LOD	55	3571	140	LOD	18	LOD	55	LOD	62
8	LOD	54	3623	137	LOD	18	LOD	53	LOD	59
9	LOD	55	3699	141	LOD	18	LOD	54	LOD	59
mean			**3509**							
sd			**183**							
mean 2σ	**54**		**136**		**18**		**53**		**59**	
MM93	**Zn ± 2σ**		**Zr ± 2σ**							
1	48	12	LOD	5						
2	54	13	9	4						
3	37	12	8	4						
4	57	13	LOD	5						
5	45	12	20	4						
6	40	12	LOD	5						
7	35	12	LOD	5						
8	51	13	6	4						
9	45	12	LOD	5						
mean	**46**		**11**							
sd	**8**		**6**							
mean 2σ	**12**		**4**							

concern with regard to this discrepancy between the calculated standard deviation and the 2σ error limit provided by the pXRF is K, where standard deviations for all standards are appreciably greater than the average of their 2σ error limits. None of the standards contained detectable concentrations of As, Ca, Cd, Co, Cu, Hg, Mo, Pb, S, Sb, Sc, Se, Te, U, V or W in more than one replicate analysis; thus, average concentrations and standard deviations could not be calculated for these elements. Lastly, the elements Ag, Au, Mo, Ni, Pd and Th were not measured in any of the standard or non-standard samples analyzed, and thus were not included in the estimation of analytical precision.

CHAPTER 5

STATISTICAL TREATMENT OF MULTIVARIATE COMPOSITIONAL DATA

Overview of the Application of Multivariate Statistical Techniques to Archaeometric Provenancing

Modern archaeometric data analysis commonly utilizes the application of multivariate statistical techniques (Beier & Mommsen 1994; Baxter 2006). As per Baxter (1994:659), multivariate statistical techniques, as applied to archaeometry, serve three primary functions: (1) "to provide a basis for provenancing specimens whose chemical composition, but not provenance, is known"; (2) "to identify those elements which are most useful in discriminating between groups"; and (3) "to display graphically the chemical distinction between groups". However, the application of such techniques to archaeological characterization/provenance studies is only a relatively recent phenomenon. While the "developmental phase" of the marriage of modern mathematics and statistics with archaeology has its roots in the 1950s and 1960s, the "explosion of interest" did not come about until the 1970s (Baxter 2008:968). The utilization of multivariate techniques in the archaeological literature on a frequent basis began in the mid-1970s (Baxter et al. 2008), in coincidence with the advent of "modern" computers with statistical packages capable of handling extensive data sets (Vitali & Franklin 1986:196). Owing to the availability of modern statistical packages (e.g., BMDP, CLUSTAN, CODA, MINITAB, Parvus, R, S-Plus, SPSS-X, STATISTICA, SYSTAT, etc.) and the ease with which they allow such statistical analyses to be performed, however, Baxter & Freestone (2006:511) argue that "[m]ost archaeological scientists who undertake such analyses on a routine basis probably do so without giving much thought to the statistical theory underpinning the methods they use"; Baxter

(2008:970) references many early publications on the use of multivariate statistics in archaeometry in which either a statistical software program or treatment was applied whether it was appropriate or not, and "with little or no explanation of why". As such, a brief survey of the literature concerning the use of multivariate techniques in archaeometry, chiefly those of principal component analysis (PCA), discriminant function analysis (DFA), and cluster analysis (CA), will follow. Such information is necessary to establish the basis for the selection of the multivariate statistical routine utilized in the present study, particularly with respect to the selection of sample sizes and variables, the application of data transformations to the raw data, the selection of discriminatory modeling techniques, methods of validating the appropriateness of the discriminant model, and general cautionary notes pertaining to the interpretation of such models given these (and other) factors.

The circumstances associated with the analysis of pegmatitic muscovite in particular lend themselves to treatment with multivariate techniques. While many provenance studies make effective use of bivariate or ternary diagrams of selected major, minor and/or trace elements or isotopic ratios to discriminate among sources, the materials at the focus of these investigations are typically more traditional archaeological materials than muscovite (e.g., chert, obsidian, marble, volcanic extrusives, etc.), and owing to the attention such materials have received in the literature, investigators have some prior knowledge of the important discriminating variables. Pegmatitic muscovite, however, has not received much, if any, attention in the archaeological literature; where muscovite geochemical data are presented in the context of archaeological provenancing, it is usually in the form of accessory mineral data within marble (e.g., Capedri & Venturelli 2004; Borghi et al. 2009) or as a component of clay sources at the center of ceramic studies. Few studies in the geological literature present any extensive datasets on southeastern

pegmatitic muscovite geochemistry, and even where such data is presented (e.g., Wood 1996), too few samples have been analyzed from individual localities to allow for any compelling determination of potential discriminating variables. As such, those elements serving as the best discriminators of pegmatitic muscovite have not been established. Multivariate techniques with the potential to assess structure in highly dimensional data in an exploratory fashion (in particular, PCA) are thus the obvious analytical choice for this type of investigation.

Principal Components Analysis (PCA)

Baxter (1989:45-46) provides a concise overview of PCA:

> Assume p commensurable variables [elements] are measured on each of n objects [samples] and that the [squared Euclidean] distance between objects i and k, d_{ik} say, is given by
>
> $$d_{ik}{}^2 = \sum_{j=1}^{p} (y_{ij} - y_{kj})^2$$
>
> where y_{ij} is the value of the jth variable on the ith object. The objects can be represented as n points in p-dimensional Euclidean space with inter-object distance d_{ik}. We are interested in identifying clusters of points in this space but cannot easily do so graphically if $p > 3$.
>
> In PCA the data are transformed to p new variables or components for which a similar geometric representation is possible. Sometimes only the first two or three components are important. In this case component plots based on the first two or three components may reveal much of the structure in the data in the sense that clusters and inter-object distances in p dimensions are approximately reproduced in two or three dimensions and can be visually identified.
>
> If V is the variance matrix of the data, the sum of the eigenvalues of V provides a measure of the variability of the data. If the sum of the leading two or three eigenvalues, associated with the most important components, accounts for most of the variability then the geometric approach described should be successful.

In other words, PCA serves to reduce the dimensionality of the data (the number of "important" components p) from the original number of variables to a smaller set of variables which are

responsible for some arbitrary amount of variance in the data (Alden et al. 2006:578; Erdem et al. 2008:2487). The first principal component is thus some linear combination of the original variables that displays the maximum variance, while the second principal component is the linear combination of variables (uncorrelated to the first principal component) that displays the second maximum variance, and so forth (Baxter 1999; Baxter & Freestone 2006:514; Erdem et al. 2008). Where the first few components account for the majority of the observed variation in the data, the assumption can be made "that the proximity of each sample in three or four dimensions reflects the structure of the data in [*p*] dimensions" (Kennett et al. 2004:40); according to Grave et al. (2005:892), the first four components in highly structured data sets should account for more than 70% of the total variation. Plots based on some combination of at least two of these principal components (generally the first two or three components) are usually sufficient to identify groups within multivariate data (Baxter & Freestone 2006:514; Erdem et al. 2008; Papachristodoulou et al. 2010).

In PCA terminology, the sums of the linear combinations of variables are referred to as *scores*, while the coefficients of the variables in the linear combinations are called *loadings* (Catalano et al. 2007). Loadings are thus "the proportion of variance of a variable that is accounted for by a particular data point" (Neff 1994:116). Often, it is of interest to plot both the component scores and loadings on the same bivariate diagram (e.g., Neff 1994; Sharratt et al. 2009) "to understand the chemical basis of group separation" (Neff 1994:115). Where bivariate plots of the loadings of the principal components are given, the length of the vector from the origin to the plotted variable point is a measure of the proportion of variance of that variable, while the angle between any two loading vectors visualizes the sign and magnitude of the correlation between those elements: small angles are indicative of high positive correlations,

right angles suggest little or no correlation, and angles approaching 180^{o} indicate high negative correlations (Neff 1994). Neff (1994) references issues relating to differences in the range of coordinate values between the object scores and variable loadings as obstacles to the graphical presentation of both on the same diagram; such issues relate primarily to object scores being more dispersed about the origin of the plot than the loading scores. While Neff (1994) presents ways of circumventing this problem (e.g., plotting subsets of the original data or zooming in on select areas within the plot), scaling the loading vector lengths by a constant amount provides a simpler (and easily implemented) solution, as the lengths of the loading vectors relative to one another, as well as the angles between them, will remain unchanged.

PCA can be viewed as an exploratory technique for identifying structure (i.e., groups) in data where there is no prior knowledge of the structure (Baxter 1989; Neff 1994; Baxter 2006; Montana et al. 2009). As such, it is an ideal technique for investigations where no prior assumptions regarding the major sources of variation in the data can be made, and is typically utilized in modern provenance studies (e.g., Mirti et al. 1990; Neff 1994; Rotunno et al. 1997; Bartlett et al. 2000; Papageorgiou et al. 2001; Hall 2004; Kennett et al. 2004; Zhu et al. 2004; Grave et al. 2005; Alden et al. 2006; Catalano et al. 2007; Papageorgiou & Liritzis 2007; Baxter et al. 2008; Erdem et al. 2008; Tschegg et al. 2008; Montana et al. 2009; Seelenfreund et al. 2009; Sharratt et al. 2009; Goren et al. 2010; Mills et al. 2010; Papachristodoulou et al. 2010; Teodor et al. 2010).

Discriminant Function Analysis (DFA)

Discriminant function analysis (DFA; also simply discriminant analysis [DA], or canonical discriminant analysis [CDA]) functions similarly to PCA, and is also widely used in archaeometric studies (Baxter 1994; Attanasio et al. 2005). Attanasio et al. (2003:557; see also

Goren et al. 2010) define DFA as "a statistical technique that uses variable transformation to obtain proper linear combinations of the original variables (discriminant functions) capable of maximizing the distances between the various groups"; a simplified mathematical overview of this theory is provided by Baxter (1994:660). Unlike PCA, DFA is considered a *supervised learning* or *supervised pattern recognition* technique; it is possible to train a model to a subset of the data (usually quarry samples of known source), and then predict group classifications of the remaining data or additional data (usually artifacts being investigated for provenance) on the basis of that model (Mello et al. 1988; Heidke and Miksa 2000; Baxter 2006). The performance of a particular model (commonly referred to as the *classification rule*) can be assessed by looking at the percentage of samples of known source (i.e., the geological samples) that are correctly reassigned to their original grouping on the basis of the classification rule (Attanasio et al. 2003). Despite having obvious implications for provenance studies in allowing a model to be trained on the basis of the geological source data and then subsequently applied to the artifact data, Baxter (2006) states that such predictive applications (i.e., supervised learning techniques) are not particularly common in archaeometry. Examples of the utilization and/or discussion of DFA in provenance studies can be found in Bimson et al. (1982); Craddock et al. (1983); Vitali & Franklin (1986); Baxter (1994); Holmes et al. (1994); Schmid et al. (1999); Attanasio et al. (2000); Bartlett et al. (2000); Attanasio et al. (2003); Hein et al. (2004); Attanasio et al. (2005); Iñañez et al. (2008); Montana et al. (2008); Goren et al. (2010); Teodor et al. (2010); and Yavuz et al. (2010).

The two forms of DFA commonly encountered are linear discriminant analysis (LDA) and quadratic discriminant analysis (QDA). According to Baxter (1994:659), LDA is utilized in "the vast majority of published applications". With LDA, two discriminant functions consisting

of linear combinations of the original variables are determined, and samples are assigned to the nearest group centroid (Baxter 2006). LDA assumes identical covariance matrices in sample groupings, and is thus more appropriate than QDA in cases where covariances are equal. However, such homoscedasticity cannot always be assumed for geological trace element data (Vitali & Franklin 1986). When such covariances are not equal, the use of QDA is supported (Wahl & Kronmal 1977). In other words, QDA "takes into account the different variability of the… predefined groups [samples associated with particular source occurrences] and uses this property as additional information for obtaining improved classification performance" (Attanasio et al. 2000:264, after Gnanadesikan 1997; similar sentiments are echoed by Attanasio et al. 2005). As the name implies, the discriminant functions obtained by QDA consist of quadratic rather than linear combinations of the variables (Baxter 2006). While it is not necessary with DFA to imply normality of the data, there are particular cases in which transformations which improve normality are known to yield better results and allow for additional statistical treatments (Attanasio et al. 2000; Attanasio et al. 2003; Attanasio et al. 2005). LDA, however, is less sensitive than QDA with respect to deviations from normality.

The decision of whether LDA or QDA is the more appropriate technique in a given situation can be further complicated by sample size in relation to the number of variables measured. In general, where the number of variables and covariance differences are large, QDA will perform better than LDA "*provided* the sample size is sufficient" (Wahl & Kronmal 1977:483). Sufficient sample sizes experimentally determined by Wahl & Kronmal (1977:484) are approximately 25 data points per group where p (the number of variables) = 4, 50 per group where p = 6, 75 per group where p = 8, and 100 per group where p = 10; QDA is generally favored in cases where more than 100 data points have been collected from each group. With

QDA in particular, it is important to consider this relation between "the number of experimental data points necessary for adequate group classification" and the number of variables analyzed (Attanasio et al. 2000:267). If this ratio is too small, a problem referred to as *data overfitting*, in which the model works very well at reproducing groups within the experimental data set "but gives substantially poorer results when applied to the classification of real unknowns", becomes a legitimate concern (Attanasio et al. 2000:267). In general, the number of data points required increases rapidly with an increase in the number of variables measured (Attanasio et al. 2000, after Leese 1988). Baxter (2006), in testing a variety of supervised and unsupervised learning techniques, does argue that LDA tends to perform as well or better than most other techniques, except in cases involving very large or complex data sets.

Often, the selection of a *best* subset of variables which explain most of the variation in the data is advised (e.g., Baxter 1994; Attanasio et al. 2000; Attanasio et al. 2005; Baxter 2006; Iñañez et al. 2008; Goren et al. 2010), as the "inclusions of poorly discriminating variables may worsen the classification results" (Attanasio et al. 2005:314). Forward selection and stepwise discriminant analyses are frequently utilized in the selection of this subset (Baxter 1994). In stepwise selection, a multiple regression model can be used to obtain an equivalent of the discriminant function, with the coefficient of determination and measure of goodness of fit (R^2) being monotonically related to the measure of group separation (D^2) produced from the DFA (Baxter 1994:660). The variable selection process then proceeds as follows:

> The variable giving the largest R^2 for a single variable model is determined and the model tested for statistical significance. If significant, a second variable that most improves R^2 is added and tested, followed by a third if significant. …[O]nce a third variable is entered, variables already in the model are tested for significance and, at any stage, the least significant is deleted if not significant (Baxter 1994:660).

However, in cases with more than two groups, "the mathematical analogy between discriminant and regression analysis breaks down" (Baxter 1994:661). Baxter (1994:660) further cautions that "it is often misleading to attempt to select a single 'best' set of discriminating variables" because of the potential interchangeability of variables with little effect on the fit, and that "even if a 'best' set exists in some useful sense, stepwise methods are not guaranteed to find it". Baxter (1994:664) concludes in relation to the use of variable subsets that:

> (a) whatever the size of variable subset selected by an automatic selection procedure it will often be the case that other subsets of similar size can be found that perform as well or better;
> (b) in terms of performance at allocation it is often the case that a much smaller subset will perform as well or better than one selected in a stepwise fashion, and such subsets need not be discovered en route to a final model;

Regardless of the selection method, multivariate analyses based on subsets of the data, as opposed to the entire set, generally perform better, *except* where the discriminant function is used to provenance new samples from groups outside those used to derive the function. In such cases, it may not be possible to differentiate the new groups from the original groups, especially where the variables that might potentially discriminate between the new group sets were not incorporated into the original discriminant function; under such circumstances, the use of the entire set of variables is advised (Baxter 1994). Where discriminating variables are not known in advance, it is generally better to incorporate as many variables as possible in the analysis (Baxter 1999).

Success Rates and the Validation of Classification Rules

The *success* of the classification rule obtained through DFA is a measure of the ability of the function to allocate the scores of individuals to the centroid of the nearest group (Baxter 1994). It is possible to estimate the success rate, or discriminating capability, of a particular model or method on the basis of the percentage of test samples of known provenance (which

Leese and Main [1994] term *known-group items*) correctly reassigned to their known original source when treated as unknowns (Leese & Main 1994; Attanasio et al. 2003). There are a number of methods used to accomplish this, with each differing primarily in the selection of subsets; the subset on which the model is trained is termed the *training set*, and is subsequently used to allocate/classify cases belonging to the remaining *test set*. Among the commonly employed validation techniques are resubstitution, *k*-fold cross validation, jackknifing and various bootstrapping methods.

Resubstitution (R_OO) is one of the simpler validation techniques (see Attanasio et al. [2005] for an example of its application in provenance investigations). In resubstitution, the same samples/cases on which the discriminant function is modeled are reassigned using that model (Baxter 1994; Leese & Main 1994; Attanasio et al. 2005). In other words, the training set and test set consist of the same samples. However, due to the influence that each sample has on the form of the function, the resubstitution approach can yield illusory inflated (i.e., biased) rates of success (Craddock et al. 1983; Baxter 1994; Leese & Main 1994; Attanasio et al. 2005).

Cross validation, regarded as a more-or-less unbiased estimator of prediction error, is suggested as a better method for the estimation of error rates than resubstitution (Baxter 1994; Leese and Main 1994; Attanasio et al. 2000; Heidke & Miksa 2000; Wehrens et al. 2000; Wehrens 2011). In *k*-fold cross validation, the original number of samples *n* is divided into *k* approximately equal-sized subsets, $k - 1$ of which are used to train the discriminant model to then be applied to the remaining subset. The process is repeated so that "each [subset] is allocated on the basis of discriminant functions that are calculated omitting it" (Baxter 1994:662). *Leave-one-out* cross validation is the special case of *k*-fold cross validation where $k = n$; that is, all but one sample comprise the training subset of the data used to obtain the model,

which is then tested on the final sample. Leave-one-out cross-validation is particularly susceptible to large amounts of variance in error rates in small sample sizes (Leese and Main 1994; Wehrens et al. 2000; Wehrens 2011).

With respect to the validation of classification rules and the estimation of error rates, however, the alternate technique of bootstrapping is regarded as one of "the most flexible and powerful validation tool[s] available" despite being traditionally "largely overlooked in the archaeometrical literature" in favor of more popular methods such as cross-validation or the similar jackknife (Attanasio et al. 2005:312). Originally introduced by Efron (1979), the bootstrap resampling technique has only relatively recently begun to replace the jackknife in archaeometric/chemometric applications (Wehrens 2011). Simply put, bootstrapping uses random sampling *with replacement* to generate new or replicate datasets from the original dataset (Attanasio et al. 2005; Wehrens et al. 2000). In the words of Wehrens et al. (2000:37), in "performing this resampling scheme many times, a good estimate can be obtained of the distribution of the statistics of interest," and "[t]hese distributions can be seen as approximations to the true distributions of the estimators, and therefore statistics of interest such as bias, standard deviation, and confidence intervals can be derived from them in the usual manner".

There are several ways in which bootstrapping may be implemented in the validation of classification rules. The following descriptions focus on the use of *nonparametric bootstrapping* (which requires no assumptions with respect to the distribution of the data in generating the bootstrap samples), though once samples have been generated, there is no difference in subsequent analytical procedure between the parametric and nonparametric forms (Wehrens 2011). In the first bootstrapping validation method, a new data set of the same size as the original data set is randomly selected, with replacement (i.e., samples may appear more than

once in the bootstrapped sample set). The discriminant function is calculated on the bootstrapped sample set, and only that bootstrapped sample set is reassigned on the basis of the model. In this method ($R_{Bi}B_i$), which amounts to the resubstitution rate of the *i*-th bootstrap replica (R_{Bi}) used to reassign that same *i*-th bootstrap replica (B_i), the standard deviation of the bootstrapped resubstitution rates over *i* iterations is equal to the resubstitution error, or bias (Attanasio et al. 2005:316). Similar to resubstitution, however, this method is an overly optimistic estimator of the misclassification rate, as the testing set includes the same samples on which the model was trained. Likewise, reassigning the entire original data set on the model produced from the bootstrapped sample ($R_{Bi}O$) will also utilize some of the samples that went into the model. Both of these methods can be used to calculate an *optimism* value to improve the classification (Attanasio et al. 2005); for the *i*-th bootstrap replica, the bootstrapped resubstitution rate on the original sample set ($R_{Bi}O$) is subtracted from the bootstrap resubstitution rate ($R_{Bi}B_i$) (i.e., optimism = $R_{Bi}B_i$ - $R_{Bi}O$), and the average of this optimism over *i* bootstrap replicas is equal to the bootstrapped resubstitution error/bias (Attanasio et al. 2005:316). This optimism is then subtracted from the original non-bootstrapped resubstitution rate (R_OO) to obtain "the corrected performance of the [classification] rule" (Attanasio et al. 2005:317).

A third method of bootstrapping again randomly selects a new data set, with replacement, from the original data, but this time only applies the resultant discrimination model to those samples which were not included in the model ($R_{Bi}[-B_i]$), in which $[-B_i]$ represents those samples not included in the *i*-th bootstrap replica. This method, however, is biased in being too pessimistic. The popular .632 bootstrap estimate is a compromise between these positively and negatively biased bootstrapping methods (Wehrens et al. 2000; Wehrens 2011). The name is

drawn from the experimentally-derived 63.2% probability any one sample has of appearing at least once in any bootstrap replica set (Wehrens et al. 2000; Wehrens 2011); approximately 36.8% of the original samples will be replaced by duplicate data points in the bootstrapped sets, averaged over a large enough number of bootstrap replicas (Attanasio et al. 2005; Wehrens 2011). The .632 bootstrap weights the resultant error rates according to these percentages: $error^{.632} = 0.368(R_{Bi}B_i) + 0.632(R_{Bi}[-B_i])$. The .632 estimator has been found to perform slightly better than (and is preferred over) the optimism method (Attanasio et al. 2005). Wehrens et al. (2000) found the .632 bootstrap error estimates to be in good agreement with the unbiased leave-one-out estimates as applied to a large enough data set. A *corrected* form of the .632 bootstrap estimator, the .632+ estimator, exists, but the difference between the two methods tends to be small (Wehrens 2011).

The number of bootstrapped sample sets *B* to generate is more or less arbitrary. Attanasio et al. (2005:316) cites suggestions of *B* between 200 and 1,000, depending on the particular application, while Wehrens et al. (2000:46-47) cite authors suggesting the value of *B* to be between 100 and 500, or 40*n*, where *n* is the number of samples. In theory, the bootstrapped approximation of the distribution of errors is the sum of the independent errors associated with the bootstrap itself and the Monte Carlo simulation (i.e., repeated random sampling to obtain results); whereas "[t]he bootstrap error is unavoidable and is independent of *B*", the Monte Carlo error can be influenced by changing *B* (Wehrens et al. 2000:46). As such, *B* should be chosen "in such a way that the Monte Carlo error is no larger (and preferably a lot smaller) than the bootstrap error" (Wehrens et al. 2000:46). Wehrens et al. (2000:47) argue that for $B = 100{,}000$, the Monte Carlo error is almost negligible, but is "acceptably small" for $B = 1{,}000$. Thus, the selection of *B* between $B = 1{,}000$ and $B = 100{,}000$ is dependent primarily on

how much computing time the analyst is willing to spend. Increasing *B* will increase computing time, but will lead to a better approximation of the *theoretical bootstrap standard error* as defined by Wehrens et al. (2000).

Cautionary Notes on Discriminant Analysis

It should be cautioned that DFA "is based on the assumption that the unknowns to be assigned belong… to one of the selected groups" (Attanasio et al. 2005:317). In cases where all possible sources are known and included in the analysis, this has little negative implication to the resultant classification. However, in the present study, only a small number of the possible sources have been sampled for analysis; the resultant classifications of artifacts should thus *not* be considered final, as it merely assigns artifacts to the *most likely* (closest) source present in the dataset (Attanasio et al. 2005).

In cases where the composition of an artifact does not fall within the range of potential source samples, then it *can* be argued that the artifact comes from some unsampled source. The terms *posterior probability* and *typicality* are frequently encountered in relation to this predicament. The former "indicates the most probable group, under the assumption that the unknown sample must belong to one of the selected groups", with the latter measuring "the absolute probability that the unknown sample belongs to that group or… how typical it is of the chosen group" (Attanasio et al. 2003:558; see also Attanasio et al. 2005).

Data Transformation

Baxter (1989:46; 2006) identifies a "practical problem" arising from the use of PCA or DFA on compositional data as the need for prior standardization of the data (to zero mean and unit variance) so that the data will have similar variability, as different scales of measurement (e.g., weight percent versus parts per million in the major/minor and trace elements, respectively)

can produce different results (see also Beier & Mommsen 1994). Those variables displaying the greatest variances are likely to dominate the first few principal components in a PCA, even where all variables have been measured in similar units (Baxter 1989; Baxter & Freestone 2006:514). Baxter (1989, 1992) suggests a two-stage approach to analysis, i.e., analyzing subsets (e.g., major and minor elements, or those elements with abundances greater than 1.5% and those less than 1.5%) of the data separately, with these subsets acting primarily to identify subgroups or cross-cutting groups that might otherwise be masked by an all-encompassing analysis. While Baxter (1992) asserts that there is little concern regarding the closure problem when dealing strictly with trace element data, scaling the variables to have unit variance prior to performing the analysis is generally advised (R Development Core Team 2010). Wehrens (2011) cautions that standardization should be carried out on the training set only, and then applied to the test set; division of the data into training and test sets after the entire dataset has been scaled is viewed as "cheating" and can lead to underestimates of prediction error, and thus overestimates of success (Wehrens 2011).

Another issue stems from the discrepancy between the nature of elemental or compositional data and the assumptions that are required to perform these multivariate techniques. Unfortunately, such issues are often overlooked or ignored in the literature (Attanasio et al. 2005:313). As per Baxter (1989:48), Aitchison (1986) argues that the assumption "that objects can be validly represented as points in *p*-dimensional Euclidean space… is invalid for compositional data and that standard statistical analyses of the raw data are consequently inappropriate". This assertion hinges on the fact that major and minor elements expressed as oxide weight percentages will be constrained to sum to 100 (barring measurement error, loss of volatiles, alkali mobility during analysis, etc.), a constraint that "induces

relationships among the variables that invalidates the usual interpretation of correlations and covariances etc. and of statistical methods [DFA and PCA] based on them" (Baxter 1989:48; Baxter 1992); this is commonly referred to as the *element sum constraint*, or the *closure problem* (Baxter 1992; Baxter 2008).

The assumption of multivariate normality is often a requisite for multivariate analytical methods (Baxter 2008). However, most real compositional data does not follow a normal distribution (Attanasio et al. 2005). While Pollard (1986), in reference to ceramic compositions, argues for a normal distribution among the major elements, trace elements tend to follow a lognormal distribution. Data transformations on those variables that are not normally distributed are commonly adopted to bring the distributions closer to normality (Attanasio et al. 2005). The most commonly employed transformation with regard to compositional data in modern provenance studies utilizing multivariate analytical techniques is some variant of a logarithmic (typically the common logarithm, log_{10}) transformation (e.g., Craddock et al. 1983; Mello et al. 1988; Baxter 1989, 1992; Beier & Mommsen 1994; Neff 1994; Baxter 1999; Attanasio et al. 2000; Papageorgiou et al. 2001; Bartlett et al. 2000; Heidke & Miksa 2000; Hall 2004; Attanasio et al. 2005; Baxter 2006; Iñañez et al. 2008; Sharratt et al. 2009; Papachristodoulou et al. 2010). Log transformations tend to impart a greater degree of symmetry to variables displaying long-tailed distributions and convert variables to similar orders of magnitude, making variances more similar and helping to avoid the problem previously discussed in which those variables with the largest variances will strongly dominate the principal components (Baxter & Freestone 2006).

Some studies argue for the use of log-ratio transformed data, citing Aitchison et al.'s (2002) assessment that the nature of compositional data as relative rather than absolute values necessitates characterization by ratios, with the logarithms of these ratios being simpler to

interpret statistically than the raw data (e.g., Heidke & Miksa 2000; Baxter & Freestone 2006; Iñañez et al. 2008; Papachristodoulou et al. 2010). Log-ratio transformations are the ratios of logarithms resulting from dividing each chemical component in the data set by the component which introduces the least amount of variability (Iñañez et al. 2008:431; Papachristodoulou et al. 2010).

However, despite being the *de facto* transformation standard, it has been suggested that a log-transformation is "not particularly effective and, sometimes, strongly worsens the classification performance" (Attanasio et al. 2000:266). Log-ratio transformed data in particular, due to the focus on relative variation, have been experimentally shown through both real and artificial examples to mask useful and interpretable absolute differences in composition which "are readily detected using standardized raw data" (Baxter & Freestone 2006:516); ratio data in general, whether transformed or not, is likely to influence clustering in undesirable ways (Baxter 1989).

In comparing the results of different multivariate techniques using both standardized and log-transformed data, however, Baxter (2006:687) concluded that neither method consistently performed better than the other, and even where one method did perform better, the difference in performance was usually not significant. In particular, both methods will perform similarly well and lead to similar conclusions when there are no outliers present in the data (Baxter 1999). The applicability of log-transformed data as opposed to standardized data is, therefore, something which needs to be evaluated on a case-by-case basis. It is to this end that the multivariate statistical analyses undertaken in the present investigation will be carried out using each of the three methods of data transformation previously discussed, with the success rates from the validation of the DFA classification rule providing quantitative measures of the effectiveness of

each transformation. Additional references for the arguments for or against the use of standardized, log-transformed and log-ratio transformed data can be found in Baxter (2008).

Treatment of Statistical Outliers

Arguments are made for the removal of statistical outliers prior to analysis of the data, as the presence of such outliers can negatively affect the interpretability of the analysis and the identification of distinct subsets (e.g., Baxter 1999; Baxter et al. 2008); Baxter (1999) is particularly effective at illustrating the impact that a single outlier can have on an analysis (in this case, PCA). Baxter (1999:323) gives a working definition of an outlier as a data point that is not close, in terms of Euclidean (or, alternately, Mahalanobis) distance, to any particular group, and raises concerns regarding the applicability of using either distance measure for the detection of outliers; Euclidean distance does not allow for the correlation between variables to be considered, and the use of Mahalanobis distance requires a stable estimate of the covariance matrix, which requires a large sample size per group of over three to five times the number of variables analyzed. In either case, the presence of outliers will affect the distances between all groups (Baxter 1999).

With PCA in particular it is easy to identify such outliers. Baxter (1999:326) states that "[c]ases that are gross outliers with respect to one or more variables can be expected to have a strong influence on the first few components and be evident on plots based on them". PCA is also able to identify outliers where other approaches might not (Baxter 1999). Where outliers have been identified in PCA plots, reanalysis omitting those points may be necessary (Baxter 1999). However, the treatment of outliers is also dependent on the context of the research; Baxter (1999:334-335), referencing Scaife et al. (1996), states that:

> if the aim of the analysis is to detect or present broad patterns in a data set, it will often be sensible to identify and delete outliers before a final analysis. If the aim

> is to depict the full range of compositional variation possible in material from a source, for example, and the 'outliers' are genuine and unaffected by measurement error and so on, then their retention is equally sensible.

Additional Considerations Regarding the Interpretation of PCA and DFA

Where only a small fraction of the potential sources have been sampled (as in the present study), definitive statements regarding sources should be avoided. Unless it is certain that every potential source has been sampled (a highly unlikely scenario), PCA or DFA can identify, at best, (1) the *most likely* source *among those tested* and/or (2) sources to which the artifact does *not* belong. The possible existence of an untested source having an indistinguishable chemical signature from the *potential* artifact source cannot be ruled out. The possibility that additional sources may have been completely mined or quarried out in antiquity needs to be given consideration as well (Leese & Main 1994), though given the scale of prehistoric mica mining operations, it is unlikely that this presents any legitimate concern.

Cluster Analysis

Cluster analysis (CA), one of the better-known statistical techniques, has commonly been utilized for quantitative archaeological applications over the past 40 years (Baxter 2009); Baxter (2008:972) describes it as "the most widely applied multivariate technique in archaeometry". While CA has not been utilized in the present investigation (for reasons presented later in this section, PCA yields more "compelling" representations of structure in data and is less likely to impose structure on the data where no structure is present), CA at least deserves mention as an alternative technique in comparison to both PCA and DFA.

Similar to PCA, many methods of CA also define clusters on the basis of the inter-object distances, d_{ik} (Baxter 1989). As with DFA, there are several variations of CA from which to choose, with the most common methods for archaeometric analysis being hierarchical clustering,

k-means clustering, fuzzy clustering, and model-based clustering performed on standardized or transformed data (Baxter 2006). The simpler (and more common) methods will be discussed in brief in the subsequent paragraphs; readers are referred to Baxter (2006) and Baxter (2009) for discussions of fuzzy clustering, and to Baxter (2006) and Papageorgiou et al. (2001) for information on model-based clustering.

Average linkage clustering is one of the most commonly utilized of the hierarchical agglomerative clustering techniques and will be the focus of the discussion regarding hierarchical clustering (Baxter 2006). Such techniques treat each sample as an individual cluster initially, and successively merge clusters together on the basis of the dissimilarity measure (Euclidean distance) until only one remains. Baxter (2006:675-676) raises concerns with hierarchical clustering techniques, chiefly that the clustering produced "may be less than 'optimal'" as a result of hierarchical clustering being unable to revise a decision to merge or split clusters once that decision has been made. *k*-means clustering algorithms are viewed as more appropriate techniques, having the ability to improve the clustering "by moving cases between clusters" (Baxter 2006:676).

k-means clustering operates on the *nearest neighbor* principle of assigning samples to the least distant among the *k* pre-defined cluster centroids, or *prototypes*; after each sample assignment, the centroids are recalculated and the process repeated until none of the samples are reassigned to new clusters (Baxter 2006:676). Baxter (2006:675) suggests using clustering results as labels on PCA plots as a validation "that the clustering is sensible".

Depending on the dimensionality (the number of important components *p*) of the data, the benefit to using PCA as opposed to CA may be more or less apparent; according to Baxter (1989:46):

> It follows that if there is real clustering in the data and a low dimensional PCA is possible then PCA and CA should produce similar results, with PCA giving the more compelling representation.

It is often cautioned that CA tends to produce clusters even where no real structure exists in the data, especially in cases of low dimensionality (Baxter 1989, 2009); the complementary use of PCA in addition to CA is suggested as a "guard against over interpretation" (Baxter 1989:46). When dimensionality is higher (e.g., $p \geq 4$), the drawbacks associated with CA relative to PCA become less obvious (Baxter 1989). Regardless, PCA is generally regarded as "a visually more appealing method" for displaying structure in data (Baxter & Freestone 2006:512); where PCA is able to "show clearly the degree of separation between the different groups and also the presence of unusual specimens", similar information will be less evident in CA dendrograms (Baxter 1989:46). Baxter (1992) suggests the use of cluster analyses using Ward's method on the PCA scores, rather than the compositional data, as an interpretive aid. While a multi-method approach is commonly employed in provenance studies (e.g., CA or DFA following PCA), with additional methods serving as means with which to validate the groupings suggested by the initial method, Baxter (1994) questions such a procedure. Examples of the utilization and/or discussion of cluster analysis in relation to provenance studies can be found in: Vitali & Franklin 1986; Mirti et al. 1990; Rotunno et al. 1997; Bartlett et al. 2000; Hall 2004; Kennett et al. 2004; Zhu et al. 2004; Papageorgiou & Liritzis 2007; Iñañez et al. 2008; Baxter 2009; and Seelenfreund et al. 2009.

As with PCA and DFA, outliers present problems for CA as well (Pollard 1986; Baxter 1999). Baxter (1999) cautions that many researches identify and treat outliers as a byproduct of the clustering procedure, which is problematic in that such outliers likely influenced the procedure used to obtain other clusters. The implementation of multiple techniques to identify

outliers, such as single linkage and average linkage clustering, can be helpful in identifying the outliers that need to be considered prior to any form of a *final* analysis (Baxter 1999). Where outliers are present, they will be manifested as small groupings within the dendrogram (Baxter 1999).

Proposed Statistical Routine, Using R

All statistical analyses presented in this thesis have been carried out using the statistical analysis freeware R (R Development Core Team 2010). PCA will be carried out using the *vegan* package's *prcomp( )* function (Oksanen et al. 2010) to assess structure in the data and to preliminarily identify the major discriminating variables. Results of the PCA will be compared against those produced by LDA, utilizing the *MASS* package's *lda( )* function (Venables & Ripley 2002). Success rates of the LDA will be assessed through simple resubstitution, leave-one-out cross-validation, bootstrap resubstitution, bootstrap cross-validation, the optimism method and the .632 bootstrap applied separately to each of the standardized, log-transformed, and log-ratio transformed datasets to determine which transformation technique, if any, produces better discrimination amongst pegmatitic muscovite sources. While functions for the estimation of prediction error/success rates associated with DFA packages are available within additional libraries/packages for R (e.g., the *errorest( )* function within the *ipred* package [Peters & Hothorn 2011]), the author's own command codes have been written and utilized (see Appendix E for the command codes used to perform the validation of the discriminant function analysis). Such code may be implemented by sourcing the function (*lda.reclass*) into R and executing the command *lda.reclass(DATA, REP, MIN.N)*, where *DATA* is replaced with the name of the dataset in question (arranged as an *n* x *p* matrix, with the first column containing sample names, the second column containing the source grouping information, and subsequent columns the

measured variables), *REP* is the defined number of bootstrap replicates *B* to be utilized in the procedure, and *MIN.N* is the sample size *n* of the smallest group (i.e., if group A consists of 10 samples and group B consists of 8 samples, *MIN.N* = 8).

With R, it is also possible to construct iso-probability ellipsoids corresponding to user-defined confidence levels around the centroids of the principal component scores or discriminant function scores for each group of data using the *ordiellipse( )* function contained within the *vegan* package (Oksanen et al. 2010). This is convenient in that, "[i]n archaeometric applications, it is often to be expected that clusters are ellipsoidal" rather than spherical (Baxter 2006:677). For the present study, a 95% confidence level was chosen using the *conf = .95* argument within the function. While constructed with different statistical software, confidence/probability ellipsoids of PCA and DFA scores, as well as elemental concentrations, have commonly been utilized in archaeological provenance studies (e.g., Beier & Mommsen 1994; Heidke & Miksa 2000; Hall 2004; Hein et al. 2004; Kennett et al. 2004; Catalano et al. 2007; Montana et al. 2008; Sharratt et al. 2009; Papachristodoulou et al. 2010; Yavuz et al. 2010). Owing to the concerns addressed in the previous sections, it is important to stress that discretion must be utilized in the interpretation of artifact scores with relation to such ellipsoids. While samples plotting outside the confidence ellipsoids of a particular group should not be confidently assigned to that group (Kennett et al. 2004), artifact scores plotting within the ellipsoid can only be said to belong to that group at the associated confidence level if all potential sources have been sampled and incorporated into the function.

CHAPTER 6

REVIEW AND ANALYSIS OF THE PUBLISHED DATA

Review of Published Literature on Trace Element Compositions of Pegmatitic Muscovite

For obvious reasons relating to economic potential, the overwhelming majority of the published literature regarding trace element geochemistry of pegmatitic muscovite has been focused on the rare-element pegmatites, particularly those in the Black Hills of South Dakota (e.g., Shearer et al. 1986; Walker et al. 1986; Jolliff et al. 1987; Laul & Lepel 1987; Jolliff et al. 1992). There has been little previous research conducted on southeastern pegmatitic muscovite geochemistry, let alone comparable analyses of muscovite artifacts; Černỳ & Burt (1984:257) admit that pegmatitic micas in general "have not been examined in as detailed and systematic a fashion as the micas of plutonic and metamorphic rocks".

Geological Society of America abstracts by Gunow (1987) and Cocker (1991, 1992b, 1992c, 1994) present limited information on muscovite trace-element data from Georgia's Cherokee-Pickens (Gunow 1987, Cocker 1992b), Thomaston-Barnesville (Cocker 1991, 1992b, 1992c), Jasper (Cocker 1992b) and Troup (Cocker 1992b, 1994) pegmatite districts. Gunow (1987) identifies contrasting geochemical trends among muscovite from the feldspar-quartz-muscovite pegmatites of the Holly-Springs pegmatite field (Li < 50 ppm, F < 2,000 ppm, Be < 7 ppm, Nb < 100 ppm and Rb[ppm]/K[%] < 50) and the feldspar, quartz, muscovite, tourmaline ± beryl pegmatites of the Ball Ground field (Be > 24 ppm, Nb > 200 ppm and Rb[ppm]/K[%] > 100), attributing the differences to varying degrees of fractionation/differentiation from a presumed parental source rock, with the incompatible-element enriched beryl-bearing pegmatites

displaying greater amounts of fractionation relative to the beryl-poor pegmatites. Cocker (1992b) identifies similar trends of incompatible-element enrichment associated with more highly fractionated beryl-bearing (or in the immediate vicinity of beryl-bearing) pegmatites in the Cherokee-Pickens, Thomaston-Barnesville, Jasper and Troup districts. The more highly fractionated pegmatites constitute between 42 and 48% of the pegmatites sampled from each district, with the exception of the Thomaston-Barnesville district (7%), and display mean values of 1118 – 1732 ppm Rb, 1867 – 3083 ppm F, 91 – 278 ppm Li, 7.7 – 31 ppm Be, 122 – 147 ppm Ga, 122 – 315 ppm Nb, 137 – 254 ppm Zn, 19 – 234 ppm Ba, with Ba/Rb ratios between 0.01 and 0.21 and Rb/K_2O ratios between 129 and 177; the less fractionated pegmatites display mean values of 381 – 675 ppm Rb, 748 – 1622 ppm F, 33 – 221 ppm Li, 4.8 – 20.6 ppm Be, 56 – 80 ppm Ga, 32 – 152 ppm Nb, 59 – 113 ppm Zn, 218 – 857 ppm Ba, with Ba/Rb ratios between 0.44 and 2.83 and Rb/K_2O ratios between 39 and 76 (Cocker 1992b). Cocker (1992c) expands on the list of elements for the Thomaston-Barnesville district indicative of stronger amounts of fractionation, including Sn up to 265 ppm and Ta up to 251 ppm. Within the Thomaston-Barnesville district, beryl- and tourmaline-bearing pegmatites contain 58 – 330 ppm Li, 2,000 – 7,076 ppm F, 102 – 334 ppm Nb, 76 – 189 ppm Ta, 545 – 1,234 ppm Rb and 58 – 167 ppm Ba, while beryl- and tourmaline-absent pegmatites contain 9 – 38 ppm Li, 426 – 1,458 ppm F, 38 – 97 ppm Nb, <1 – 66 ppm Ta, 292 – 500 ppm Rb and 272 – 1,1456 ppm Ba (Cocker 1991). The more strongly fractionated pegmatites of the Troup County pegmatite district (relative to other districts) display 283 – 2,200 ppm Rb (mean = 1,187), 2 – 46 ppm Sr (mean = 8.1), 24 – 716 ppm Li (mean = 248.6), 337 – 3,444 ppm F (mean = 1,741), 2.6 – 154.3 ppm Be (mean = 18.9), 6 – 1,420 ppm Ba (mean = 141.5), 36 – 169 ppm Ga (mean = 113), 10 – 686 ppm Sn (mean =

132), 55 – 590 ppm Nb (mean = 231) and 28-375 ppm Zn (mean = 123), with mean Ba/Rb ratios of 0.248 and Rb/K_2O of 131.

Cocker (1992a) provides one of the few extensive published trace element datasets of pegmatitic muscovite from Georgia (in the Thomaston-Barnesville district), analyzing for 24 trace elements (As, Ba, Be, Bi, Cd, Ce, Co, Cr, Cu, Ga, La, Mo, Nb, Ni, Pb, Rb, Sc, Sn, Sr, Ta, V, Y, Zn and Zr) with a number of analytical techniques (including ICP-MS, AAS and XRF, among others). Unfortunately, the limited number of analyses carried out on samples from any one particular mining locality is less than ideal for characterization studies requiring relatively larger sample sizes from individual localities. Similarly, Wood's (1996) dataset is the only existing extensive dataset regarding North Carolina's (Spruce Pine district) pegmatitic muscovite, and is of a nature similar to that of Cocker's (1992a) data in terms of the trace elements analyzed (As, Ba, Ce, Co, Cr, Cs, Cu, Ga, Nb, Ni, Pb, Rb, Sn, Sr, Ta, Tl, V, W, Y, Zn and Zr) and number of analyses per mine; Veal's (2004) data on pegmatitic muscovite geochemistry from Spruce Pine is limited to the major elements only. Gunow & Bonn (1989) present geochemical analyses of pegmatitic muscovite from Georgia's Cherokee-Pickens district; while this dataset contains analyses of multiple samples per mine for several mines, the differing suite of elements analyzed (owing to the main focus of the study in investigating economic potential in association with the rare-element enriched muscovite-class pegmatites of the beryl-bearing Ball Ground pegmatites) does not make it readily comparable to the datasets of either Cocker (1992a) or Wood (1996) in that only three trace elements (Ba, Nb and Rb) are common to all three datasets.

The author is not aware of any prior geochemical provenance investigations of North American muscovite artifacts. Reece (2006:102) alludes to provenance studies of thick layers of

mica found at Teotihuacán's Pyramid of the Sun in Mexico in which the mica was found to have a local source, in contrast to the extremely distant Brazilian source referenced by Childress (2007). Unfortunately, neither camp references any published data or reports by their "experts". A local Alabama source for the Moundville micas has been surmised by Scarry (1998:75), though it is mentioned only in passing with reference to the overall stone assemblage found at the site. With respect to the Etowah mounds in particular, King (2001:4) notes that "prehistorically important minerals like galena, ochre, mica, and graphite" are found in Georgia's Piedmont "[j]ust a few kilometers up the Etowah River from the Etowah site", but the issue is not addressed in any further detail. As such, this will be a pioneering study in both a geological and archaeological context, and the methods that follow will establish the protocol for future archaeometric investigations of pegmatitic muscovite.

Muscovite compositions within the muscovite-class pegmatites "reflect the primitive geochemical features of their parent pegmatites" as well as those of associated granites and surrounding gneissic rocks (Černỳ & Burt 1984:284). Černỳ & Burt (1984:279) reference several studies in Russian (e.g., Manuylova et al. 1966; Shmakin 1973, 1975; Gordiyenko 1975; Gordiyenko & Leonova 1976) which present trace element data on muscovite from muscovite-class pegmatites. These investigations identify a general geochemical signature displaying: (1) an enrichment in Ba, Ti (with a general range of 600 – 9,000 ppm), Sc (5 – 90 ppm), and V (<5 – 220 ppm); (2) moderate concentrations of Ni (10 – 30 ppm); and very low concentrations of Li, Rb, Cs, Be, Zn, Ga and Sn. Again referencing Gordiyenko (1975) and Gordiyenko & Leonova (1976), Černỳ & Burt (1984:279) note geochemical trends "[w]ithin the 3-dimensional configuration of pegmatite groups and fields". Where pegmatite fields are associated with fractionation from a magmatic core, the concentrations of the trace elements Ba, Ni, Co, Sc, V,

Cr and Ba/Rb should decrease in an outward and upward direction, while the concentrations of Li, Rb, Cs, Tl, Be and Sn should increase; the amount of Sr should not display a trend (Gordiyenko 1975; Gordiyenko & Leonova 1976).

Wood (1996) analyzed the trace element chemistry of 53 samples of muscovite from 35 locations within the Spruce Pine pegmatite district (Figure 29A-B). Wood (1996) speculated that muscovite within pegmatites forming from a later-phase magma derived from the crystallization of the core of the pluton should display fractionation patterns among the trace elements. The muscovite was analyzed for systematic regional variation in the major and trace elements using a Cameca SX-50 electron microprobe and a Philips Model PW1480 X-ray fluorescence spectrometer. While data are presented on the concentrations of 21 trace elements, Wood's (1996) interpretation of the data concentrates primarily on Tl, Nb, Ga, Zn, Ba and Rb (reported as the ratio of K/Rb) and the ratio of Al/Ga, with the following two trends being observed: (1) Ga, Tl, Nb and Zn were found in high concentrations in muscovite from the immediate vicinity of the town of Spruce Pine, decreased with distance outward, then increased again toward the western margin of the study area; and (2) Ba and the ratios of K/Rb and Al/Ga were found at low concentrations in the immediate vicinity of the town of Spruce Pine, increased in concentration moving outward, then decreased again at the western margin of the study area. In observing that all of these elements display a trend opposite of that which is expected according to Černỳ & Burt (1984), Wood (1996) attributes this to the possibility that the actual plutonic core may not be exposed and suggests that if the center of magmatic activity was located where those chemical trends divide, then those trends would display as expected.

Laul & Lepel (1987) also identified fractionation patterns in rare earth elements (REEs) in muscovite from the Etta pegmatite in the Black Hills of South Dakota. Noting that muscovite

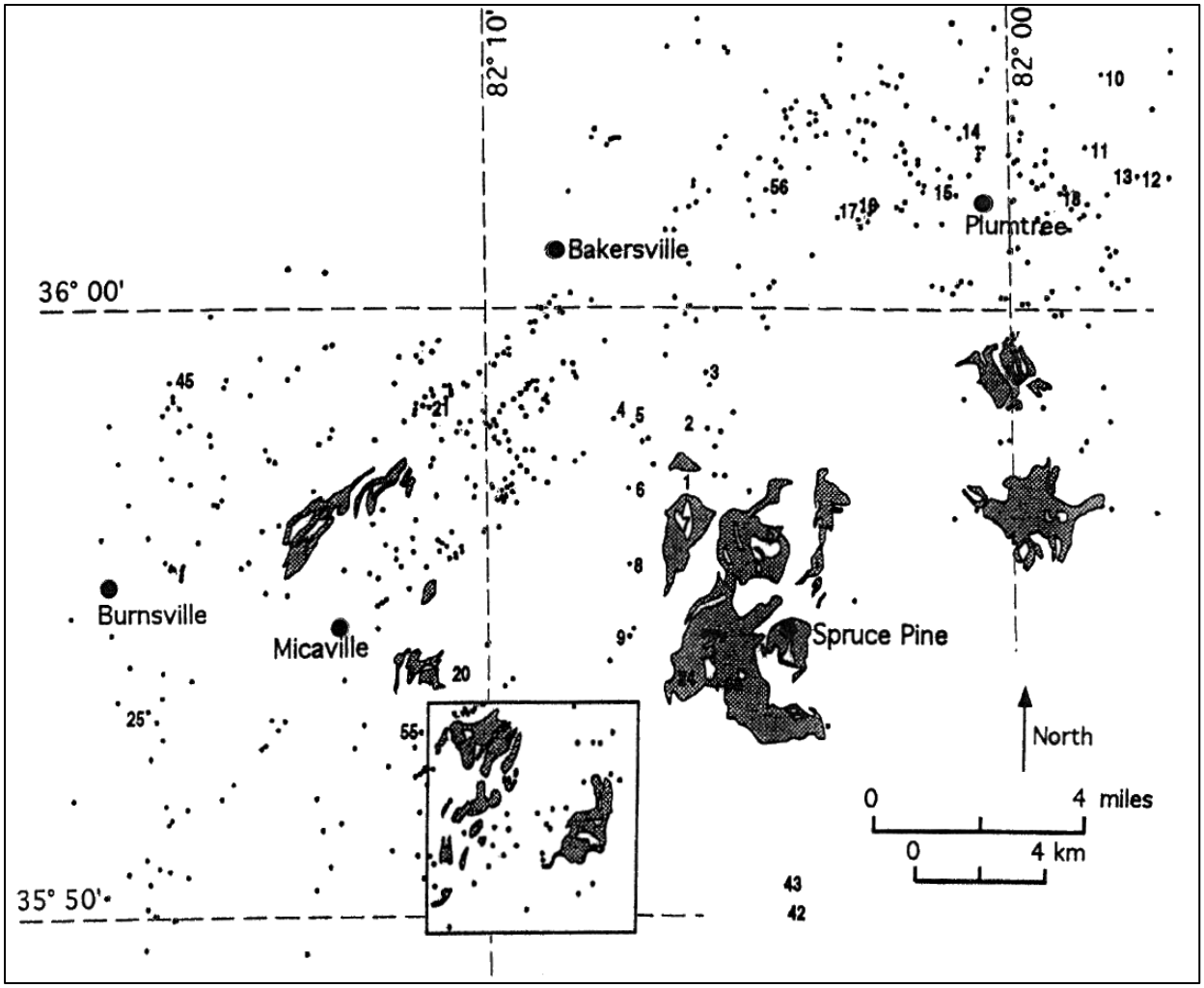

Figure 29A: Map of Wood's (1996) sampling locations from the Spruce Pine district, NC. Reproduced from Wood (1996:Figures 3 & 6. A.).

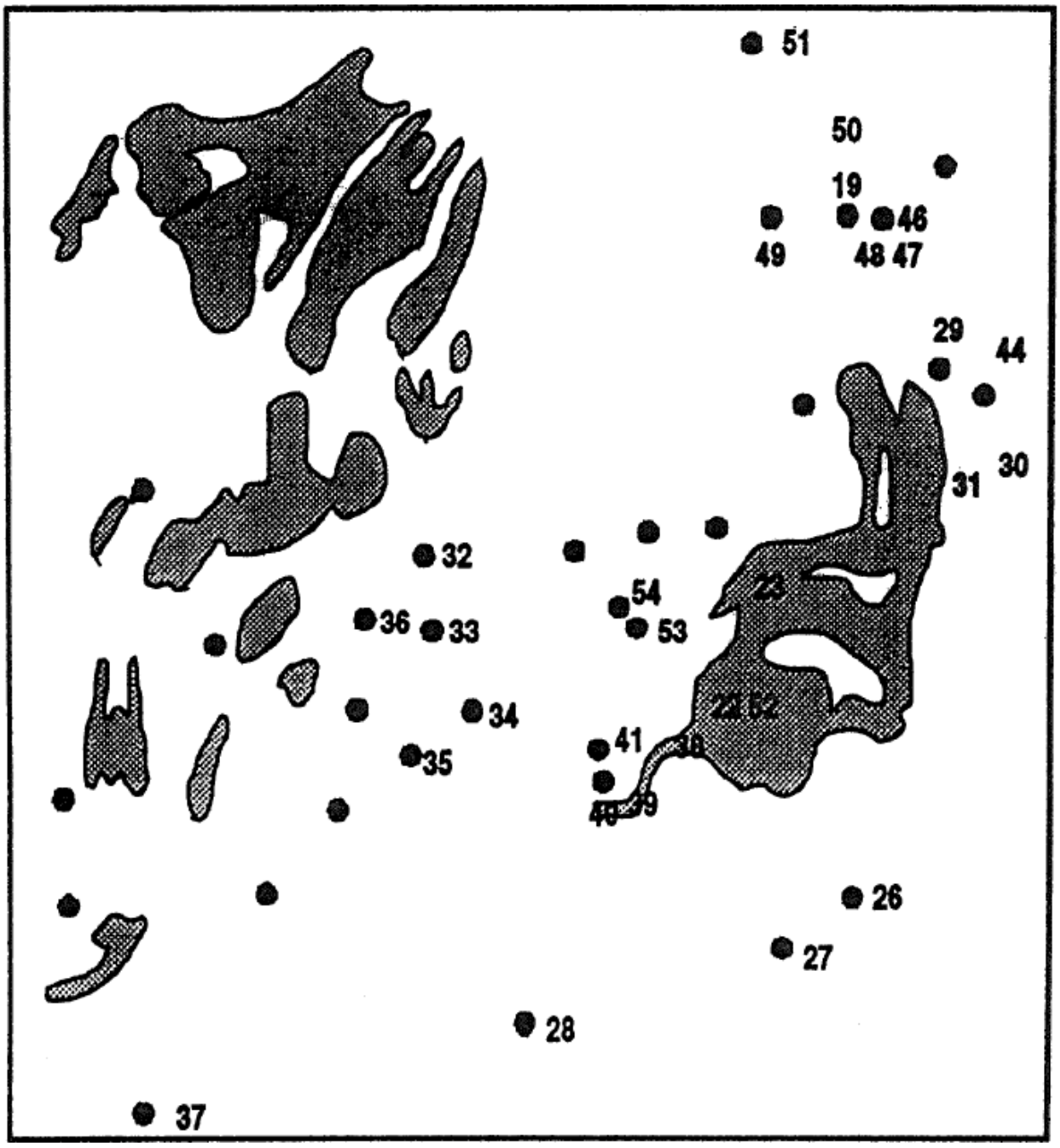

Figure 29B: Map of Wood's (1996) sampling locations from within the boxed area of Figure 38a within the Spruce Pine district, NC. Reproduced from Wood (1996:Figure 6. B.).

typically contains high concentrations of the REEs, Rb, Cs and Ta, high amounts of fractionation were discerned from the light REEs to the heavy REEs, with that fractionation increasing with distance away from the pegmatite contact (Laul & Lepel 1987). However, as previously noted, the southern Black Hills pegmatite field is classified as a rare-element pegmatite field (Černỳ 1982); micas of muscovite-class pegmatites display "a poorly fractionated spectrum of trace elements" relative to the rare-element pegmatites (Černỳ & Burt 1984:284). In general, muscovite from rare-element pegmatites will display differing geochemical signatures from muscovite of muscovite-class pegmatites, particularly with respect to the ratio of K/Rb plotted versus the concentrations of Li, Cs, Tl, Ba, Be, Zn, Ga and Sn (Černỳ & Burt 1984:282). Different pegmatite types within the rare-element class, however, tend to display largely overlapping geochemical signatures (Černỳ & Burt 1984:282).

Černỳ & Burt (1984:283) caution, at least with respect to the rare-element pegmatites, that generalized summaries of the geochemical signatures of the classes of pegmatites can "obscure smaller-scale differences that are commonly encountered among individual pegmatites and pegmatite groups, even on a local scale of genetically related bodies". The geochemical trends observed by Gordiyenko (1975), Gordiyenko & Leonova (1976), Cocker (1992a) and Wood (1996) suggest the same may be true of the muscovite-class pegmatites. Thus, some degree of geochemical variation within pegmatite groupings may be discernable at sub-district or sub-field levels, allowing for more precise determinations of provenance.

Preliminary Statistical Analysis of Published Data

Published trace element data for southeastern pegmatitic muscovite has been analyzed via PCA as a preliminary means of assessing the potential to successfully discriminate amongst pegmatitic muscovite sources on the basis of both (1) *pegmatite districts* and (2) *pegmatite fields*

within a single district. Test data consist of Cocker's (1992a) muscovite data from the Thomaston-Barnesville district of Georgia and Wood's (1992) Spruce Pine data. Due to issues previously discussed regarding the compatibility (in terms of the elements analyzed) of Gunow & Bonn's (1989) Cherokee-Pickens district data with that of Cocker (1992a) and Wood (1996), it will not be utilized in the principal components and discriminant function analyses that follow. The use of DFA in the preliminary data analysis is precluded by large differences in sample size between both datasets, as well as large differences in sample size between Cocker's (1992a) individual pegmatite fields.

Prior to performing the PCA, pretreatment of each dataset was necessary. The statistical routine utilized in R is unable to handle non-numeric values, such as those preceded by a *less than* operator (e.g., *<1* ppm) or those resulting from the base-10 logarithmic transformation of concentrations of *0* ppm, as $log_{10}(0)$ is returned as *–Inf.* This problem requires (1) the removal of all samples containing *less than* or *0 ppm* concentrations for any element, (2) the exclusion of all elements from the PCA for which any sample contains a *less than* or *0 ppm* concentration, or (3) modification of these values so that the statistical routine can handle them appropriately. In order to incorporate as many samples and variables in the PCA as is justifiable, the decision was made to halve all *less than* values (i.e., *<1* ppm was entered as *0.5* ppm, *<5* ppm as *2.5* ppm, etc.). Since most *less than* values common to the two datasets typically range in magnitude from *<1* ppm to *<5* ppm, a maximum possible difference of 2.5 ppm between any actual value and the assumed value is considered trivial. The only exception is found within Sn concentrations from Cocker (1992a), which are commonly reported as *<20 ppm*; regardless, these data are modified in the same manner. Prior to performing the logarithmic transformations, all *0 ppm* values were converted to *0.1 ppm* for all elements, following Aitchison's (1986:268-269) recommendation of

replacing *0 ppm* values "with positive values smaller than the smallest recordable value" (Heidke & Miksa 2000:284). Given the transformation of *<1 ppm* values to *0.5 ppm*, all *0 ppm* values would thus need to be converted to values less than 0.5 ppm; since Cocker (1992a) measured several variables to the tenths place (e.g., As, Be, Co and Zr), 0.1 was chosen as a logical substitute.

Testing Discrimination on a Sub-District Scale

Cocker's (1992a) dataset divides the Thomaston-Barnesville district into nine geographically-isolated pegmatite fields: Indian Grave, Concord, Lighthouse, Blount, Juliette, Russellville, Yatesville, Waymanville, and Lazer Creek. As such, Cocker's (1992a) data may be utilized to assess the ability to resolve pegmatite field groupings within a district (thus, on a sub-district scale) on a principal components plot.

Those elements analyzed on a ppm scale by Cocker (1992a) include: As, Ba, Be, Ce, Co, Cr, Cu, F, Ga, K, Li, Nb, Ni, Pb, Rb, Sn, Sr, Ta, V, Y, Zn and Zr. However, not all of these 22 elements were analyzed in every sample, creating a situation in which either the sample (which is missing any number of elemental concentrations) or the element (which has not been analyzed in any number of samples) must be removed prior to performing the PCA. Removing only samples which were not analyzed for every element would result in the removal of 31 samples from the dataset (n = 123), which would account for over 25% of the dataset. Likewise, removing only those variables which were not recorded in every sample would leave only four variables (Be, Sn, Sr and Ta) on which to perform the PCA. In order to preserve the maximum number of both samples and variables, the following method was utilized in making the decision to remove either the sample or the variable:

(1) The data were arranged in an *n* x *p* matrix, with *n* samples (rows) containing measurements on *p* elements/variables (columns). Blank cells within this matrix represent elements that have not been analyzed in a given sample, and the total number of blank cells in a given column was counted.

(2) Starting with the column with the lowest total number of blank cells (in this case F, with one blank cell), those samples which were not analyzed for F were removed from the analysis.

(3) The "blank cell" totals were recalculated for each of the columns, and the process repeated until the number of samples which would need to be removed either equaled or exceeded the total change in blank-cell sums of the remaining columns. For example, at the step where As presents the lowest blank-cell sum of 7, eliminating those samples lacking As measurements would also reduce the blank-cell sums for 10 additional variables (Ce, Co, Cr, Cu, Nb, Ni, Pb, V, Y and Zr) by 7 apiece, for a total change in blank-cell sums of 70. Since 70 > 7, the procedure would continue to the next element/column with the lowest blank-cell sum.

(4) At the step where the number of samples which would need to be removed equals or exceeds the total change in blank-cell sums of the remaining columns, all columns with blank-cell sums greater than 0 are removed. Thus, at the step where Y presents the lowest blank-cell sum of 8, eliminating those samples lacking Y measurements would only reduce the blank-cell sum of the remaining Ce column by 8; at this point, the Ce and Y columns are removed from the matrix and not entered into the PCA.

In proceeding in such a manner, only 14 of Cocker's (1992a) samples (378-01, 379-03, 379-3, 379-04, 379-05, 379-06, 379-08, 379-8, 379-10, 409-9, 409-37, 410-33, 410-35 and 441-3) and

two variables (Ce and Y) needed to be removed so that there were no missing values remaining in the matrix.

The resulting PCA was thus carried out on n = 109 samples (10 from Blount, 4 from Concord, 3 from Indian Grave, 4 from Juliette, 2 from Lazer Creek, 11 from Lighthouse, 5 from Russellville, 36 from Waymanville, 32 from Yatesville, and 2 samples not belonging to any of the recognized pegmatite fields), using 20 variables. PCA, unlike DFA, is not subject to restrictions on the number of variables in relation to sample sizes per group, since PCA does not take into consideration any groupings assigned to the data points prior to performing the analysis. As such, data overfitting is only a concern where the *total* number of samples N is small relative to the number of variables p entered into the analysis. For the PCA of Cocker's (1992a) data, this is not a concern, as $N > 5p$.

Plots of the first two principal components of the Thomaston-Barnesville district data (Figure 30A-C) show that, regardless of the method of data transformation applied to the data, individual muscovite-class pegmatite fields within a given district are largely indistinguishable from one another on the basis of muscovite geochemistry, with the possible exception of muscovite from the Indian Grave pegmatite field.

While not analyzed as part of the present study, figures from Gunow & Bonn's (1989) Cherokee-Pickens district (Georgia; Figure 31A-B) data present a similar prospect of discriminating between pegmatitic muscovite sources at the sub-district scale, showing a high degree of overlap of muscovite from the Holly Springs pegmatite field with that of the beryl-poor Ball Ground pegmatite field. Possible exceptions to this generalization appear to be where districts contain either rare-element-enriched muscovite-class pegmatite fields (e.g., the beryl-bearing pegmatites of the Ball Ground field) or where the muscovite can be shown to trend in

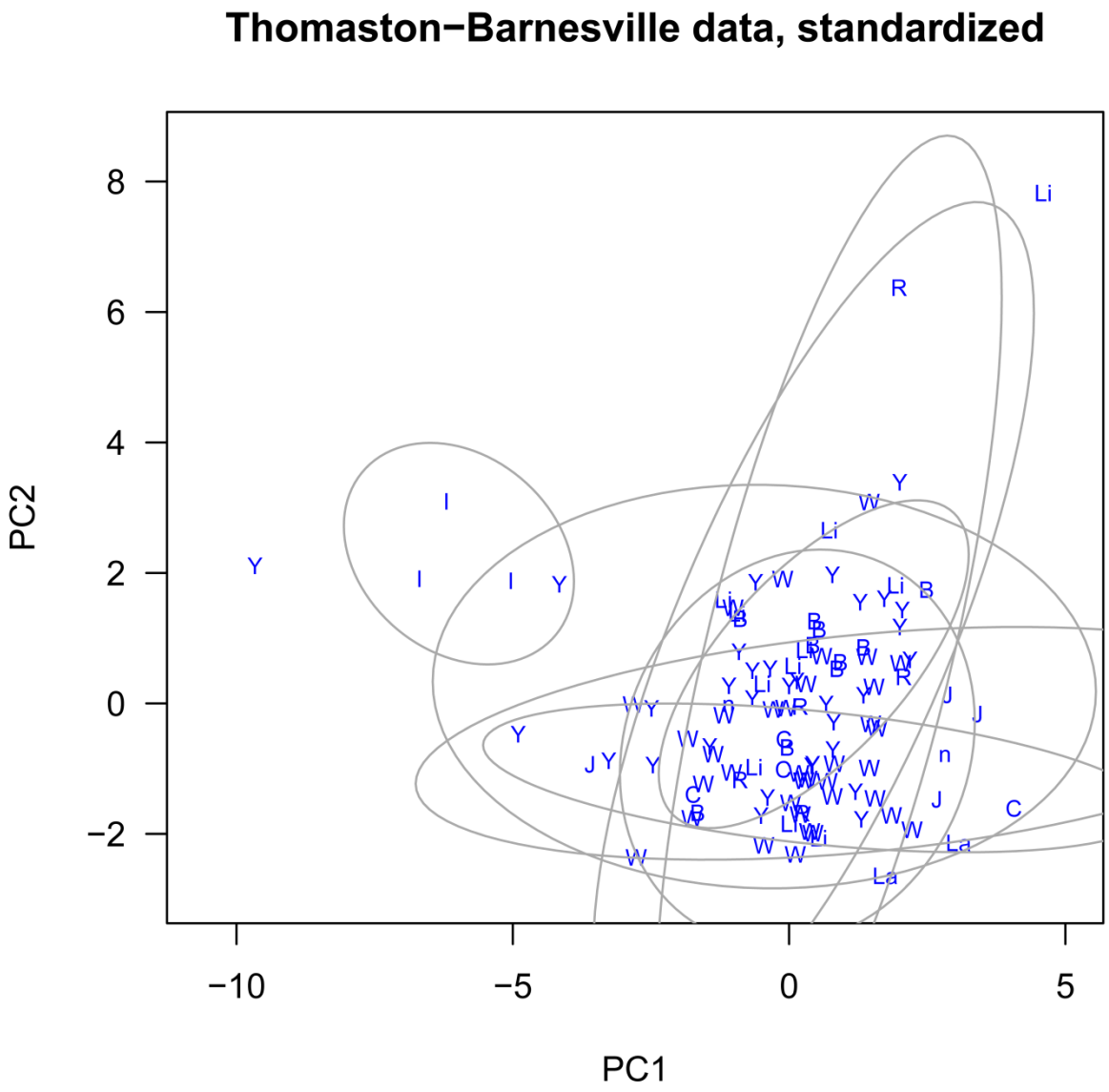

Figure 30A: PCA of Cocker's (1992a) Thomaston-Barnesville district data. Data (standardized) are grouped on the basis of pegmatite fields: B = Blount, C = Concord, I = Indian Grave, J = Juliette, La = Lazer Creek, Li = Lighthouse, R = Russellville, W = Waymanville, Y = Yatesville and n = pegmatites not belonging to any field. 95% confidence ellipsoids have been constructed around the centroids of group data points, with the exception of fields containing less than three data points (Lazer Creek and the pegmatites not belonging to any field).

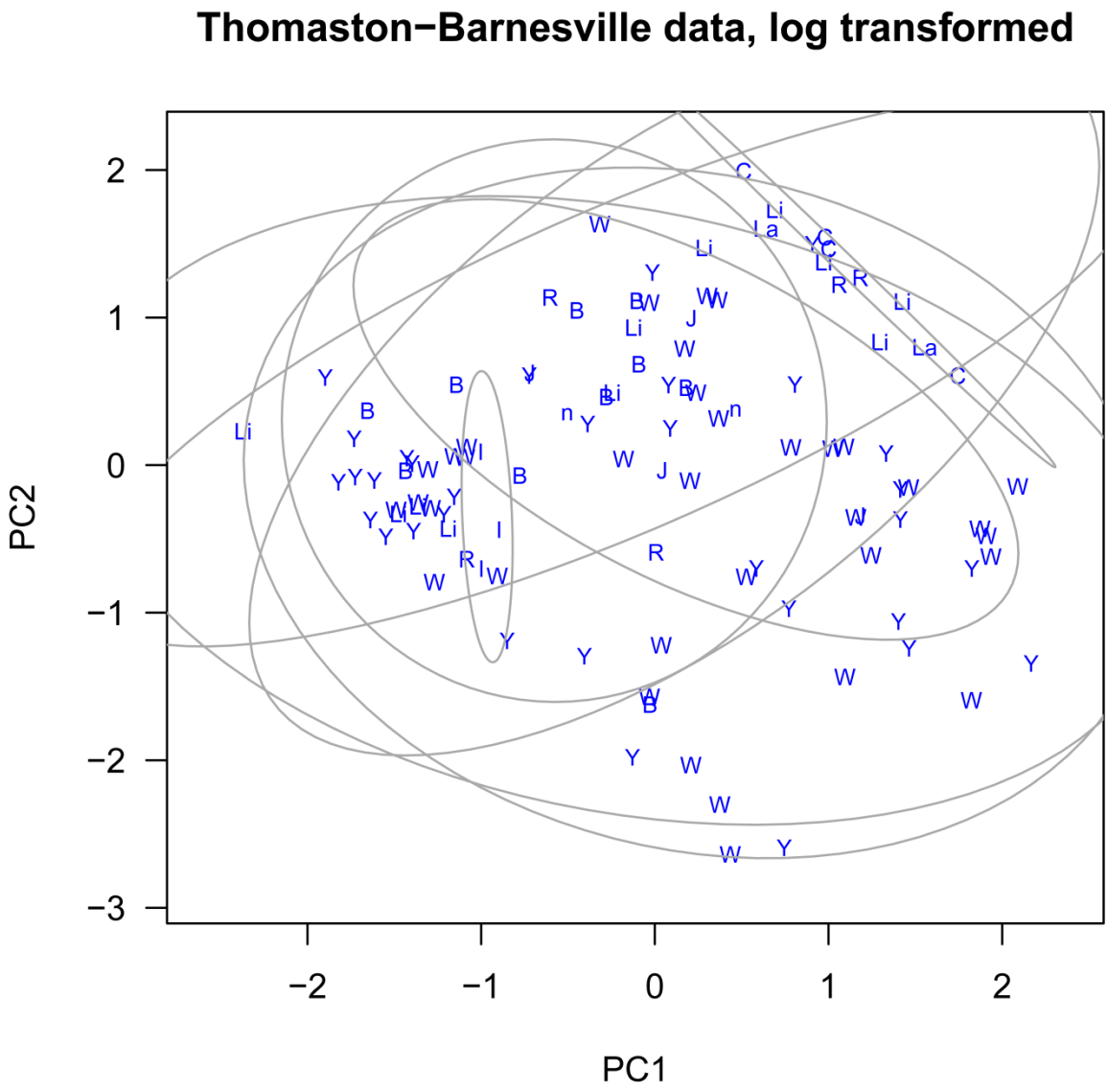

Figure 30B: PCA of Cocker's (1992a) Thomaston-Barnesville district data. Data (log transformed) are grouped on the basis of pegmatite fields: B = Blount, C = Concord, I = Indian Grave, J = Juliette, La = Lazer Creek, Li = Lighthouse, R = Russellville, W = Waymanville, Y = Yatesville and n = pegmatites not belonging to any field. 95% confidence ellipsoids have been constructed around the centroids of group data points, with the exception of fields containing less than three data points (Lazer Creek and the pegmatites not belonging to any field).

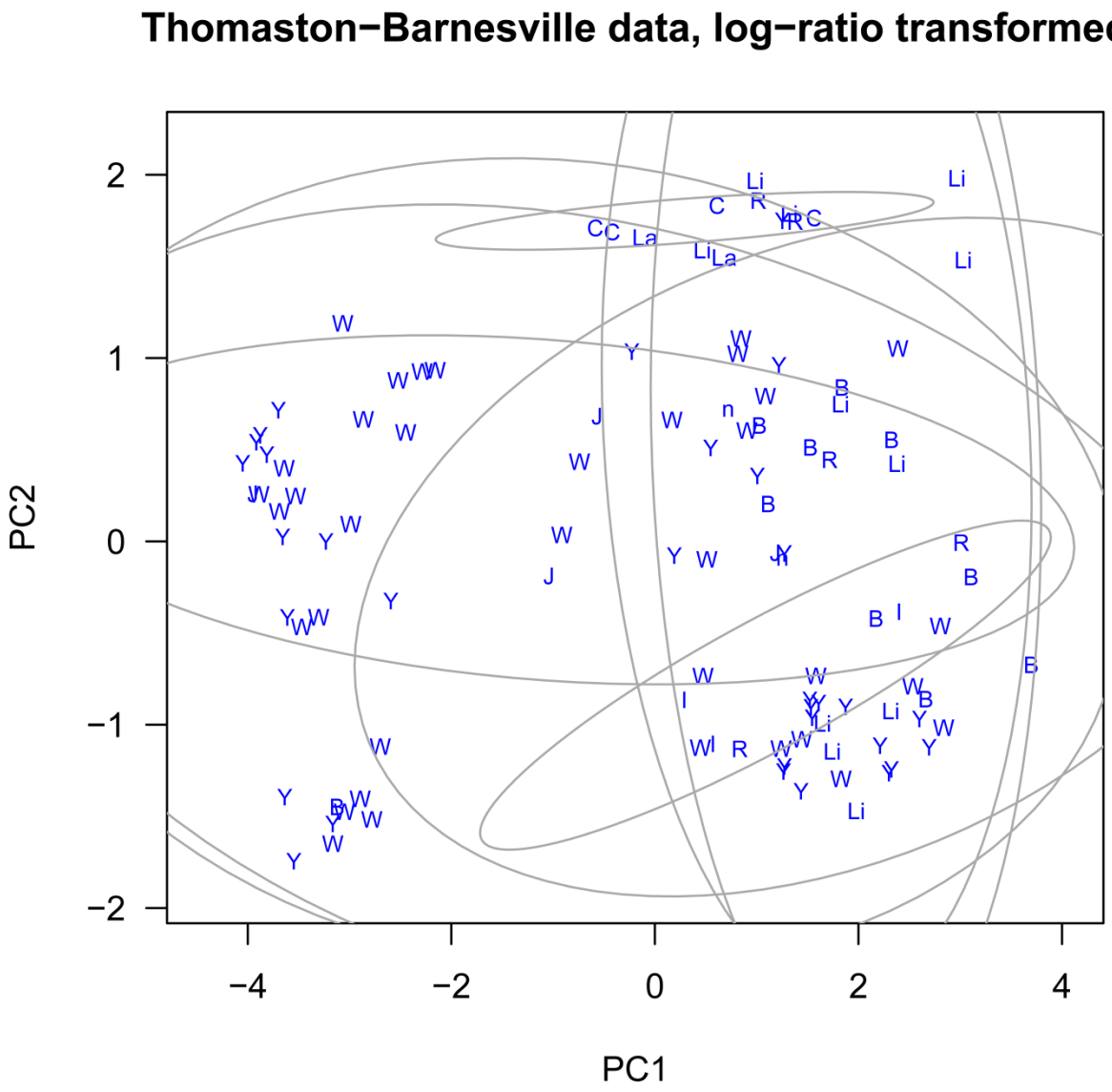

Figure 30C: PCA of Cocker's (1992a) Thomaston-Barnesville district data. Data (log-ratio transformed) are grouped on the basis of pegmatite fields: B = Blount, C = Concord, I = Indian Grave, J = Juliette, La = Lazer Creek, Li = Lighthouse, R = Russellville, W = Waymanville, Y = Yatesville and n = pegmatites not belonging to any field. 95% confidence ellipsoids have been constructed around the centroids of group data points, with the exception of fields containing less than three data points (Lazer Creek and the pegmatites not belonging to any field).

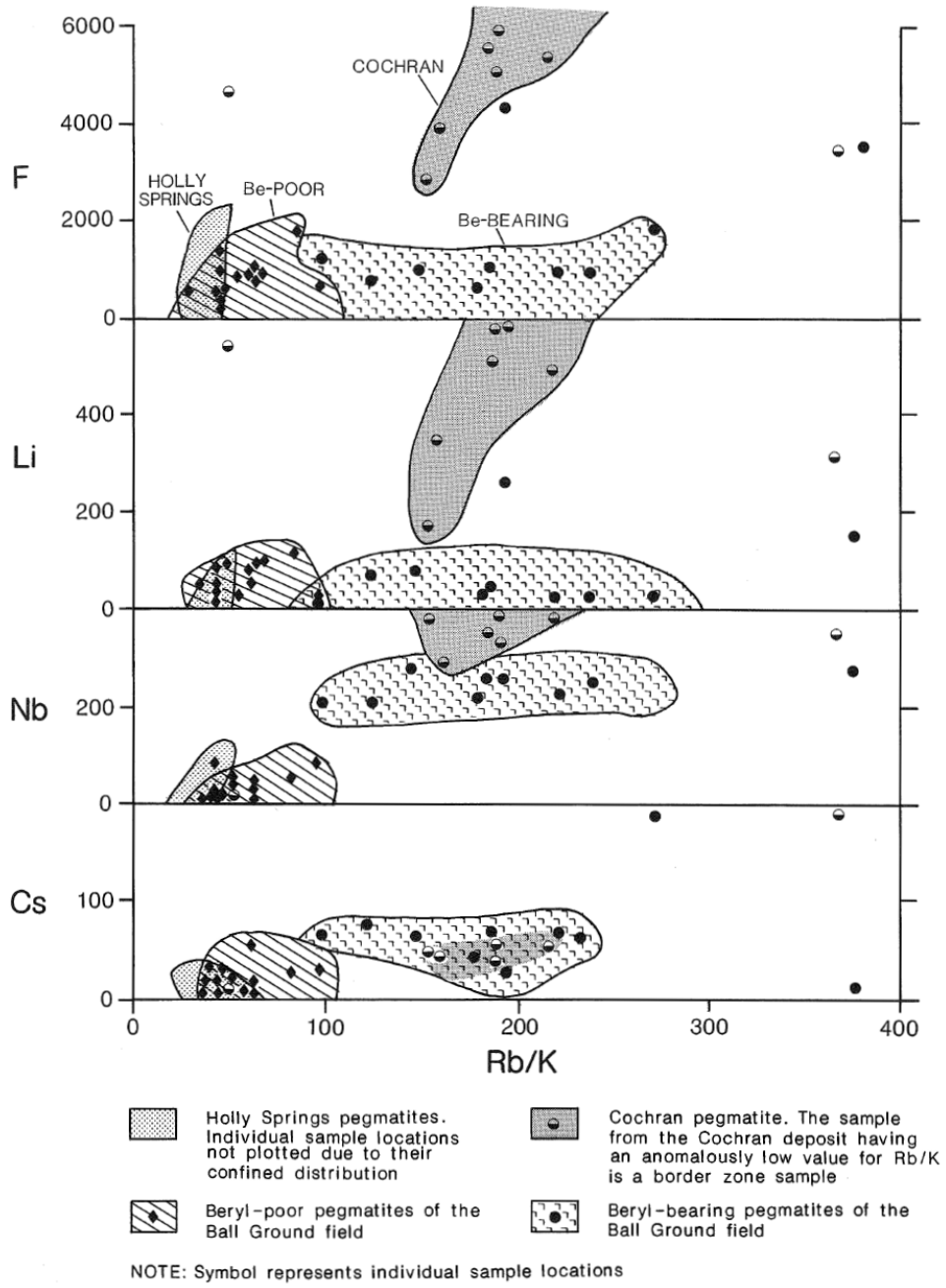

Figure 31A: Plot of selected trace elements as a function of Rb(ppm)/K(%) for pegmatitic muscovite. Muscovite from the Holly Springs field (HS) exhibits consistently low values for incompatible trace elements. Muscovite from the Cochran deposit exhibits significant enrichment in incompatible elements. The beryl-bearing pegmatites typically show enrichment in several trace elements relative to beryl-poor pegmatites. Reproduced from Gunow & Bonn (1989:Figure 5).

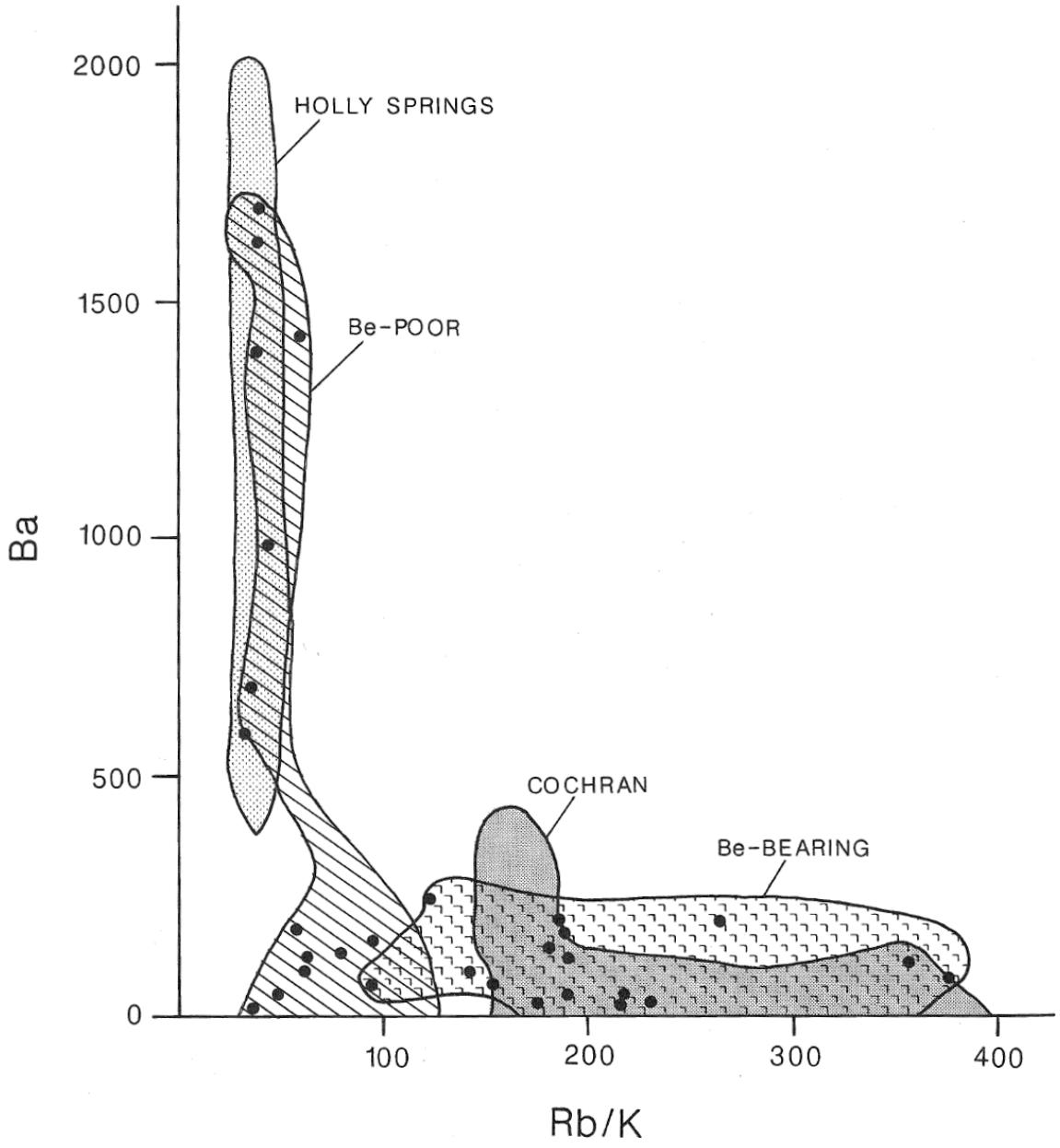

Figure 31B: Correlative plot of barium (ppm) as a function of Rb(ppm)/K(%) for pegmatitic muscovite. Muscovite from the Holly Springs field and muscovite from the Be-poor pegmatites of the Ball Ground field exhibit a large range in Ba values. Muscovite from the Be-bearing pegmatites and the Cochran pegmatite exhibit uniformly low Ba values (< 300 ppm). The non-linear distribution shown in this diagram can be attributed to the mutual competition of Ba and Rb for the same K ion site, and suggests that Ba is preferentially incorporated into the mica structure (less incompatible than Rb) during relatively early stages of pegmatite differentiation. Reproduced from Gunow & Bonn (1989:Figure 6).

composition toward rare-element enrichment, typically on the basis of enrichment in one or more of the trace elements Sn, Rb and Zn (e.g., certain beryl-poor pegmatites of the Ball Ground field, or pegmatites of the Indian Grave pegmatite field in the Thomaston-Barnesville district).

Testing Discrimination on a District Scale

The PCA of Cocker's (1992a) dataset suggests that pegmatitic muscovite from most pegmatite fields within a given district will be geochemically indistinguishable from one another. However, it also suggests that those same samples, when grouped on a district-scale basis, should produce relatively tight clusters. It follows that if distinguishable geochemical variation exists between muscovite from different pegmatite districts, then discrimination amongst more generalized sources (e.g., Spruce Pine versus Thomaston-Barnesville or Cherokee-Pickens) should be possible.

To test this assumption, Cocker's (1992a) Thomaston-Barnesville district data (n = 109) was entered into a PCA along with Wood's (1996) Spruce Pine data (n = 53). The following 18 elements measured in ppm quantities are common to both datasets: As, Ba, Co, Cr, Cu, Ga, K, Nb, Ni, Pb, Rb, Sn, Sr, Ta, V, Y, Zn and Zr. However, as previously discussed, the removal of Y from Cocker's (1992a) data was necessary to eliminate missing values from the data matrix; it was necessary to remove K from Wood's (1996) dataset in a similar manner. Thus, p = 16 variables were entered into the PCA, with $N > 10p$. No *less than* values were present in Wood's (1996) dataset, and *0 ppm* values were again replaced with *0.1 ppm*.

Plots of the first two principal components of the Thomaston-Barnesville and Spruce Pine district muscovite data (Figure 32A-C) show that while there is not complete separation of the two fields as defined by the data points, there is a greater degree of separation associated with the geochemical signatures of muscovite across two pegmatite districts than is associated with

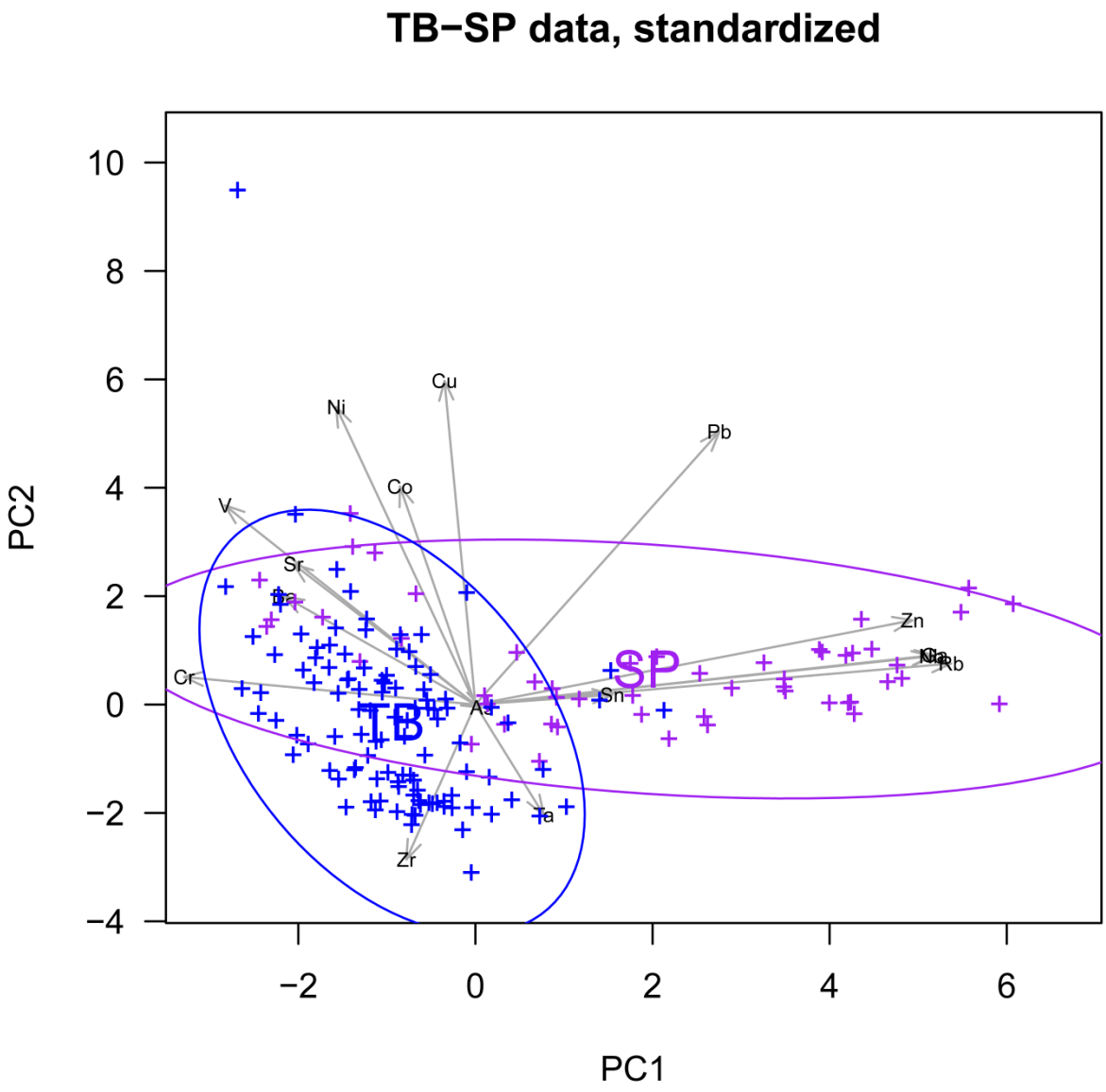

Figure 32A: PCA of published Thomaston-Barnesville and Spruce Pine data (standardized). Cocker's (1992a) Thomaston-Barnesville district data (TB, blue) and Wood's (1996) Spruce Pine data (SP, purple), grouped on the basis of pegmatite districts. Labeled 95% confidence ellipsoids have been constructed around the centroids of group data points. Loading vectors shown as gray arrows with black text.

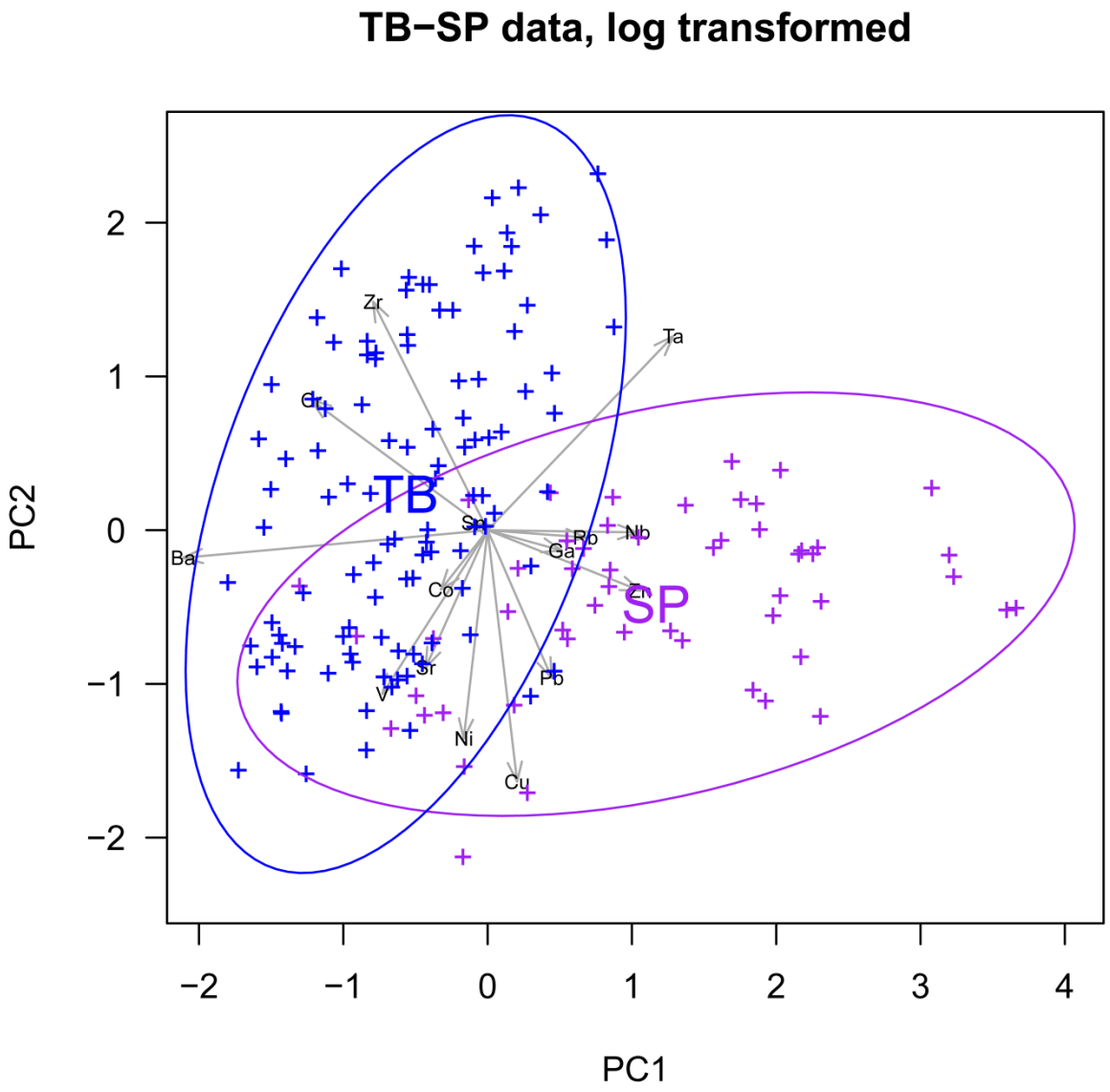

Figure 32B: PCA of published Thomaston-Barnesville and Spruce Pine data (log transformed). Cocker's (1992a) Thomaston-Barnesville district data (TB, blue) and Wood's (1996) Spruce Pine data (SP, purple), grouped on the basis of pegmatite districts. Labeled 95% confidence ellipsoids have been constructed around the centroids of group data points. Loading vectors shown as gray arrows with black text.

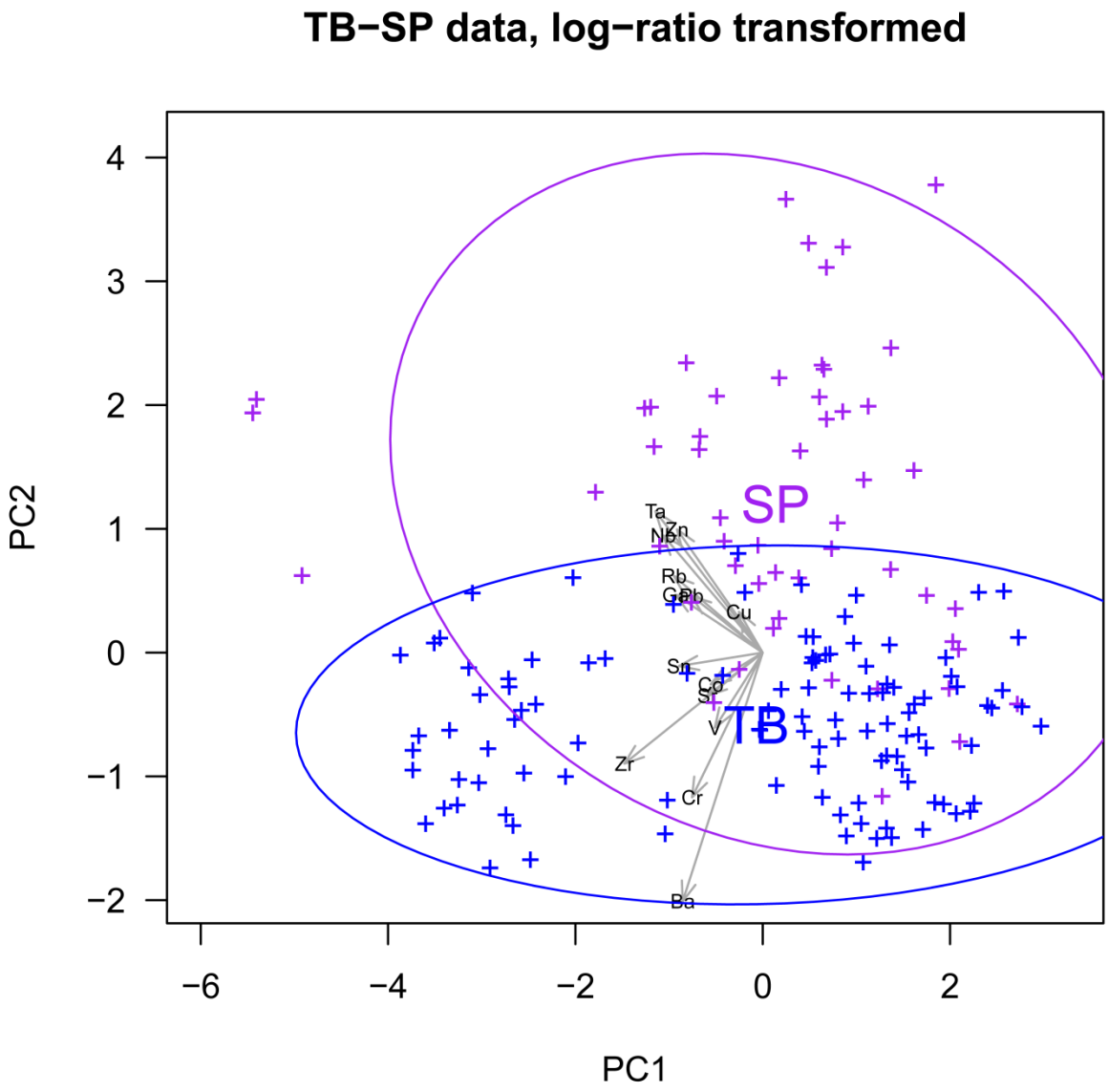

Figure 32C: PCA of published Thomaston-Barnesville and Spruce Pine data (log-ratio transformed). Cocker's (1992a) Thomaston-Barnesville district data (TB, blue) and Wood's (1996) Spruce Pine data (SP, purple), grouped on the basis of pegmatite districts. Labeled 95% confidence ellipsoids have been constructed around the centroids of group data points. Loading vectors shown as gray arrows with black text.

geochemical signatures across pegmatite fields within districts. The principal component plots, particularly those utilizing the standardized and log-transformed data, show an appreciable portion of the Spruce Pine muscovite to be separable from the Thomaston-Barnesville muscovite on the basis of increased concentrations of one or more of the elements Ga, Nb, Pb, Rb and Zn, and relatively lower concentrations of Cr and/or Zn. Such trends are less obvious in the PCA based on log-ratio transformed data. Nevertheless, these principal component plots suggest the possibility that muscovite compositions, when considered at the district scale, *may* occupy regions of principal-component space in which there is little ambiguity in terms of the district of origin (i.e., where data points clearly plot outside areas of overlap).

CHAPTER 7

PXRF DATA COLLECTED IN THE PRESENT INVESTIGATION

Synthesis of New Data with the Published Literature

PCA Justification for Combining Datasets

Several factors hinder a straightforward comparison of the new data obtained with the Thermo Scientific Niton pXRF and data presented by Cocker (1992a) or Wood (1996). The first and main issue is whether or not the dataset generated by the present pXRF study is compatible with the published datasets, given the use of different instruments in each investigation. To assess whether combining the datasets can be justified, principal components analyses were performed on the Spruce Pine data (both the present study and Wood [1996]) and on the Thomaston-Barnesville data (present study and Cocker [1992a]).

Compatibility of Thomaston-Barnesville Data

Cocker's (1992a) Thomaston-Barnesville data were compared against data collected from the Thomaston-Barnesville samples (MM, JAPM and VB) in the present investigation on the basis of the following 12 elements: As, Ba, Cr, Cu, K, Pb, Rb, Sn, Sr, V, Zn and Zr. While Mo had been analyzed for in both datasets, the fact that it was not detectable in any samples utilized in the present study precluded its inclusion in the analysis. Before direct comparisons between the datasets could be made, however, two issues must be addressed.

Firstly, the replicate analyses of the MM93 substandard must be combined into a single analysis, as replicate analyses were not taken of any of the remaining samples. This does not present problems for most elements in that all replicate analyses of the standard either measured detectable concentrations of most elements or measured concentrations below the limits of

detection for most elements. In the former scenario, the average concentration of the given element over all replicate analyses will substitute as the singular concentration of that element in the standard; in the latter case, it will suffice to say that the concentration of that particular element in the standard is below the average limit of detection over all replicate analyses. However, detectable concentrations of certain elements were not measured in every replicate analysis of MM93. Where some replicate analyses for a given element measured detectable concentrations and others did not, the decision was made to substitute the average limit of detection over all replicate analyses as the concentration for those replicate analyses in which detectable concentrations were not measured. The reasoning for this approach is as follows: for detectable concentrations to be measurable in some replicates and not others, it is assumed that the actual concentration must be reasonably close to the upper threshold of the limit of detection so that given the range of analytical precision associated with each element, some replicate analyses from the same sample may display concentrations above the limit of detection, while others will display below it.

The second issue again relates to limits of detection, specifically the differences in limits of detection across datasets resulting from differences in the sensitivity of the instruments used in each study. In many cases, Cocker (1992a) was able to measure elemental concentrations much less than the values obtained by halving the limits of detection associated with the Thermo Scientific Niton pXRF. To work around this issue, it was decided to first establish limits of detection on the basis of the least sensitive instrument (in this case, the Thermo Scientific Niton pXRF, with the exception of Sn measurements), and then to reassign a single same numeric value to all concentrations measuring below this limit of detection, regardless of whether that concentration may have been detectable by the methods employed by Cocker (1992a). For

example, limits of detection for Zn across all pXRF analyses ranged from *15 – 18 ppm*; even though Cocker (1992a) was able to accurately measure Zn in single-digit concentrations, those concentrations less than *15 ppm* were still reassigned a numeric value based on the lower limit of detection as defined by the pXRF (in this case, *15 ppm*). In doing so, concentrations of elements associated with a high degree of uncertainty (i.e., those in concentrations below limits of detection) with respect to any of the analytical instruments will be depicted as having little to no variance across groups in the resulting principal component or discriminant function plots. As a result, the principal component and discriminant function analyses of the muscovite data will represent a "worst-case scenario" which is biased against using those elements as a basis for producing separation between samples and/or source groups. It follows that if separation is possible under conditions biased against producing group separation, then it can be assumed that that separation is a real geochemical feature and not simply an artifact resulting from analytical uncertainties.

In reassigning such singular values to those samples measuring concentrations of a given element below these established limits of detection, it was found that none of the concentrations of Co measured by Cocker (1992a) were greater than the lower limit of detection for Co measured by the pXRF; thus, Co was excluded from further analysis. The lower limit of detection for Sn associated with the pXRF (16 ppm) was lower than the limit of detection for Sn (20 ppm) reported by Cocker (1992a), leading to the decision to assign a value of 20 ppm to all samples with low or uncertain Sn concentrations. The values thus reassigned to low and uncertain concentrations were: As – 6 ppm; Ba – 44 ppm; Cr – 19 ppm; Cu – 24 ppm; Pb – 9 ppm; Sn – 20 ppm; Sr – 3 ppm; V – 22 ppm; Zn – 15 ppm; Zr – 5 ppm. Reassignment of values

was not necessary for the elements K and Rb, as all samples analyzed contained detectable concentrations of these elements.

The PCA of the Thomaston-Barnesville muscovite data (Figure 33A-C) shows that the majority of the samples analyzed in the present study plot within the data field defined for the Thomaston-Barnesville district by Cocker's (1992a) broader range of sampling localities; thus, it can be assumed that the two datasets are compatible with one another, and the data can be justifiably combined. PCA also identifies an interesting trend in that, regardless of the method of data transformation applied to the raw data, samples from the J.A. Partridge Mine (from the present study, samples JAPM2, JAPM8, JAPM9, JAPM10, JAPM15 and JAPM17, and from Cocker [1992a], sample 408-6) and the Thompson prospect (from Cocker [1992a], samples 408-1 and 408-4), both belonging to the Indian Grave pegmatite field, consistently plot together at the extreme periphery of, or entirely outside of, the main cluster of data points for the Thomaston-Barnesville district and the 95% confidence ellipse constructed about the centroid of all the data points. These samples display (on the basis of the PCA loading vectors) an enrichment in, and strong positive correlation between, the elements Rb, Sn and Zn, similar to trends observed among more highly fractionated pegmatites (Gunow 1987; Cocker 1991, 1992b, 1992c). The appearance of these geochemical trends, regardless of which method of data transformation is applied to the raw data, suggests that they are real features and not simply artifacts resulting from any one particular transformation. Thus, where Cocker (1992a) identifies nine *geographic* pegmatite fields within Georgia's Thomaston-Barnesville district, there may be only two distinct *geochemical* pegmatite fields, one of which (the Indian Grave pegmatite field) may approach pegmatite compositions typical of the rare-element-enriched muscovite-class of pegmatites.

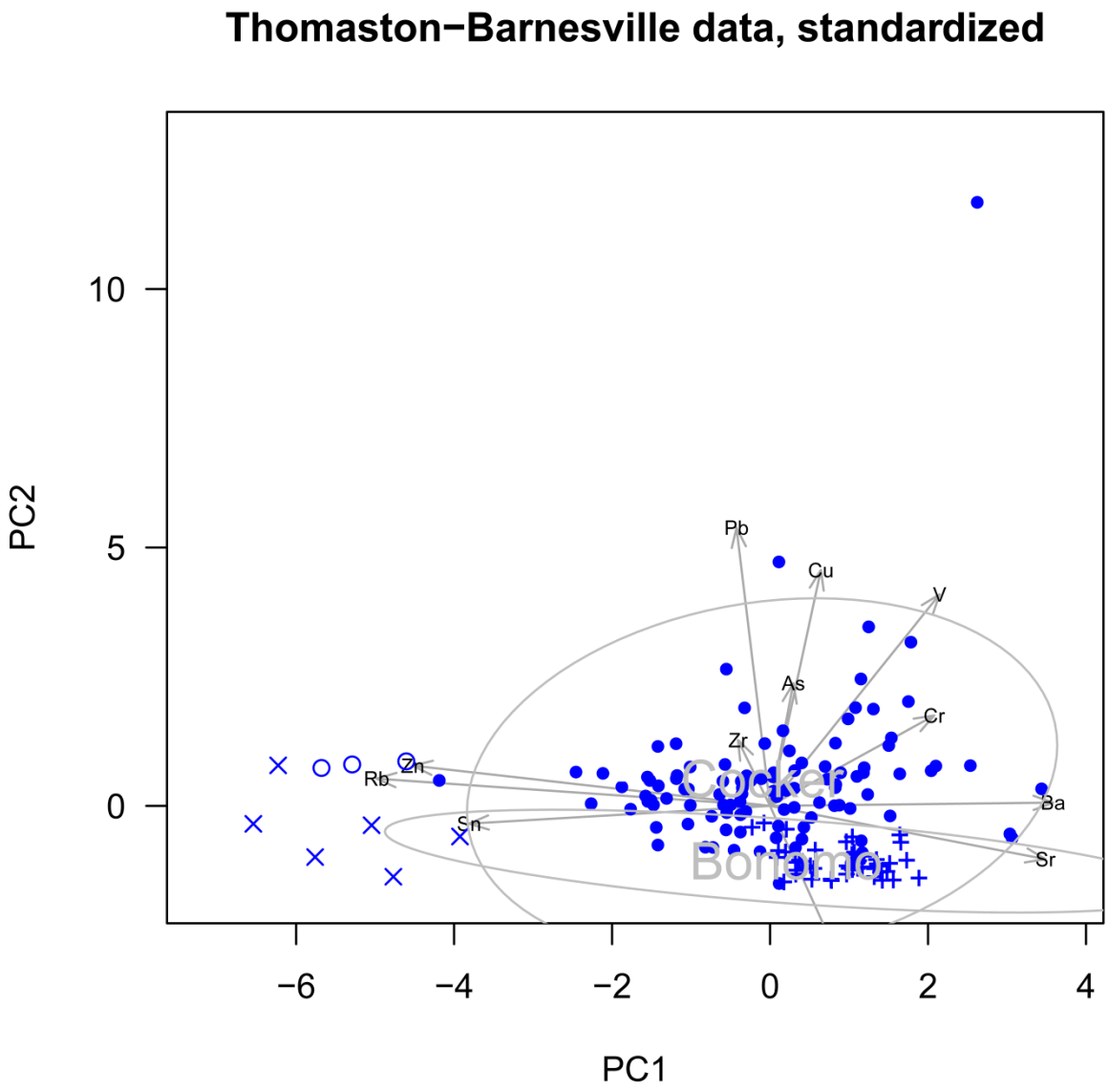

Figure 33A: PCA compatibility test of Thomaston-Barnesville district data (standardized). Data from Cocker (1992a, filled and open circles, “Cocker” at centroid of 95% confidence ellipsoid) and the present study (crosses and exes, “Bonomo” at centroid of 95% confidence ellipsoid). Samples belonging to the Indian Grave pegmatite field plot as open circles and exes. Loading vectors are shown by gray arrows with black text.

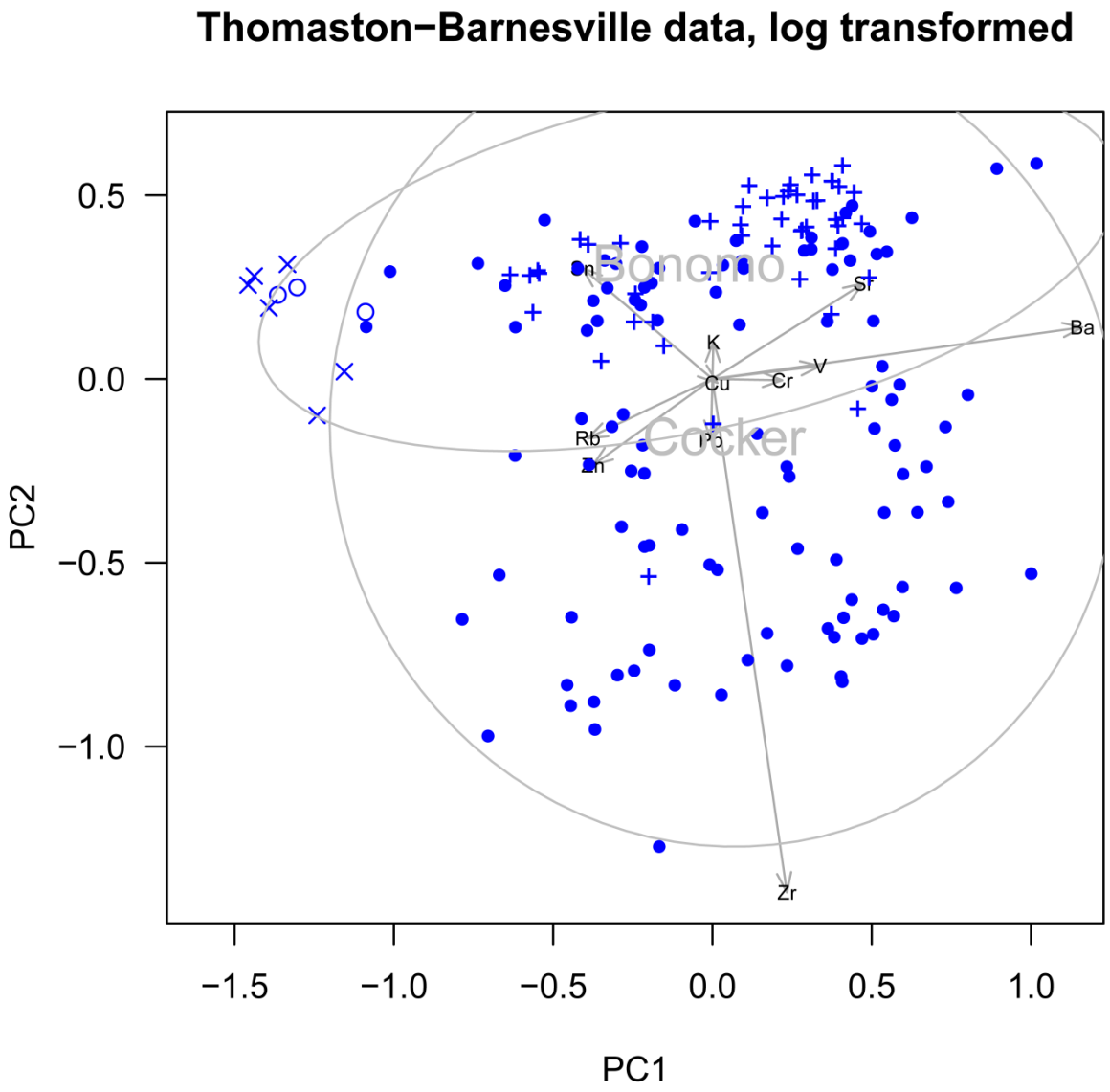

Figure 33B: PCA compatibility test of Thomaston-Barnesville district data (log transformed). Data from Cocker (1992a, filled and open circles, “Cocker” at centroid of 95% confidence ellipsoid) and the present study (crosses and exes, “Bonomo” at centroid of 95% confidence ellipsoid). Samples belonging to the Indian Grave pegmatite field plot as open circles and exes. Loading vectors are shown by gray arrows with black text.

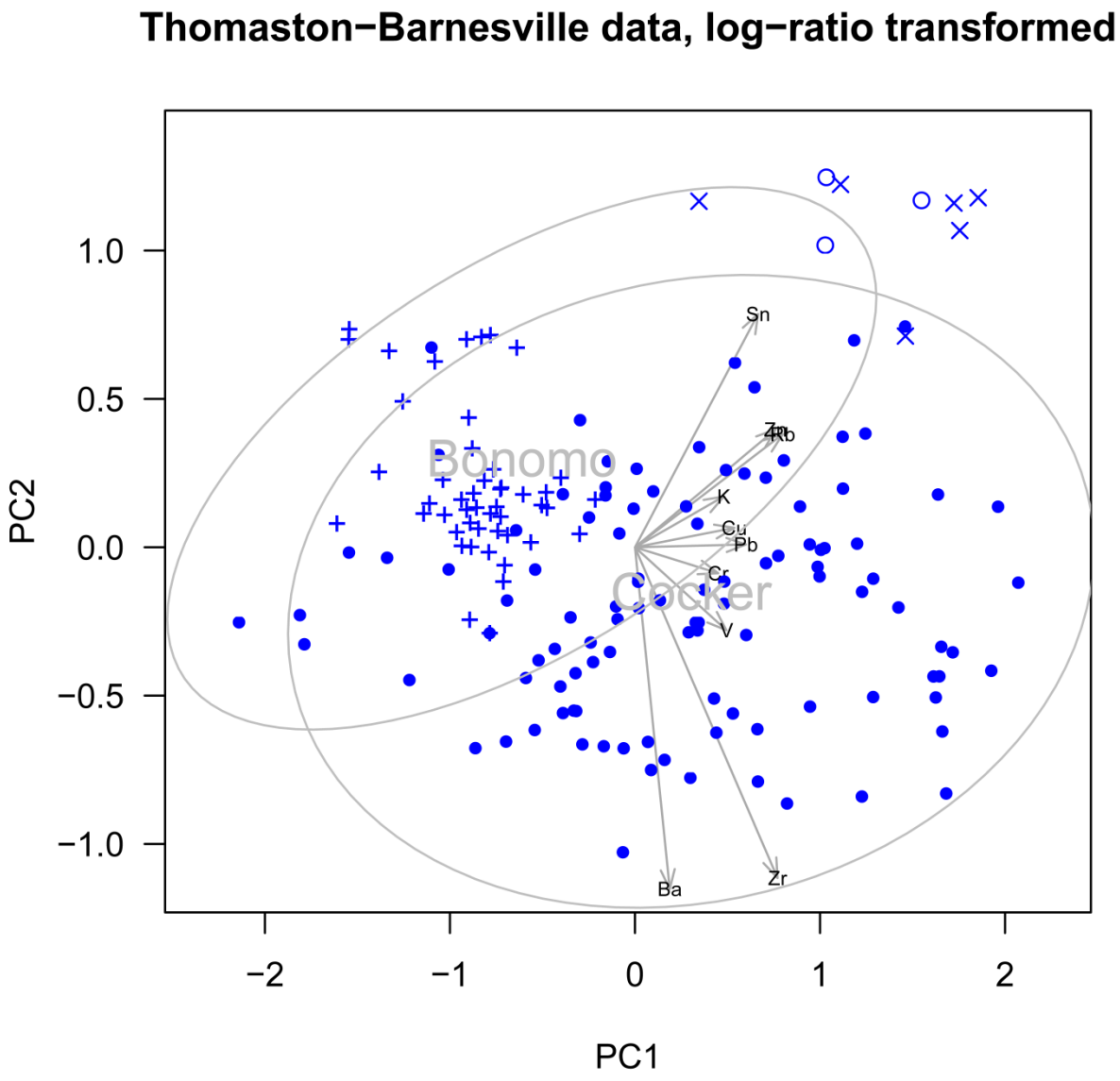

Figure 33C: PCA compatibility test of Thomaston-Barnesville district data (log-ratio transformed). Data from Cocker (1992a, filled and open circles, “Cocker” at centroid of 95% confidence ellipsoid) and the present study (crosses and exes, “Bonomo” at centroid of 95% confidence ellipsoid). Samples belonging to the Indian Grave pegmatite field plot as open circles and exes. Loading vectors are shown by gray arrows with black text.

Compatibility of Spruce Pine Data

Wood's (1996) Spruce Pine data was compared against data collected from the Spruce Pine samples (DPM, McK and Pink) from the present investigation on the basis of the following 12 elements: As, Ba, Cr, Cu, K, Pb, Rb, Sn, Sr, V, Zn and Zr. While Cs was also analyzed by both datasets, it has been excluded from this analysis; Cs is not a variable measured in Cocker's (1992a) dataset, and thus cannot be incorporated in analyses of the database as a whole. Concentrations of K, while excluded from the previous PCA performed using Wood's (1996) data, have been included in the current PCA. The removal of six samples from the dataset (byard-m-1, mead-m-1, hoot-m-1, sink-m-1, poll-m-1 and wsb-m-1) was required so that there were no missing values within the data matrix. In doing so, PCA of the Spruce Pine muscovite data can be performed on the same suite of elements as were utilized in the PCA of the Thomaston-Barnesville muscovite data. The same procedures and values for low or uncertain elemental concentrations as were utilized in the pre-treatment of the Thomaston-Barnesville district data were used in preparing the Spruce Pine data for PCA.

PCA of the Spruce Pine muscovite data (Figure 34A-C) shows that the majority of the pXRF data collected in the present study, with the possible exception of the log-ratio transformed data, fall within the 95% confidence ellipse representing the broader spread of Spruce Pine data defined by Wood's (1996) greater number of sampling localities, again providing justification for the combination of the presently collected pXRF dataset with those appearing in the published literature.

As with the PCA of the Thomaston-Barnesville district data, PCA of the Spruce Pine data also reveals an additional trend in that there appears to be a greater number of distinctive clusters formed by Wood's (1996) data from Spruce Pine than were formed by Cocker's (1992a) data

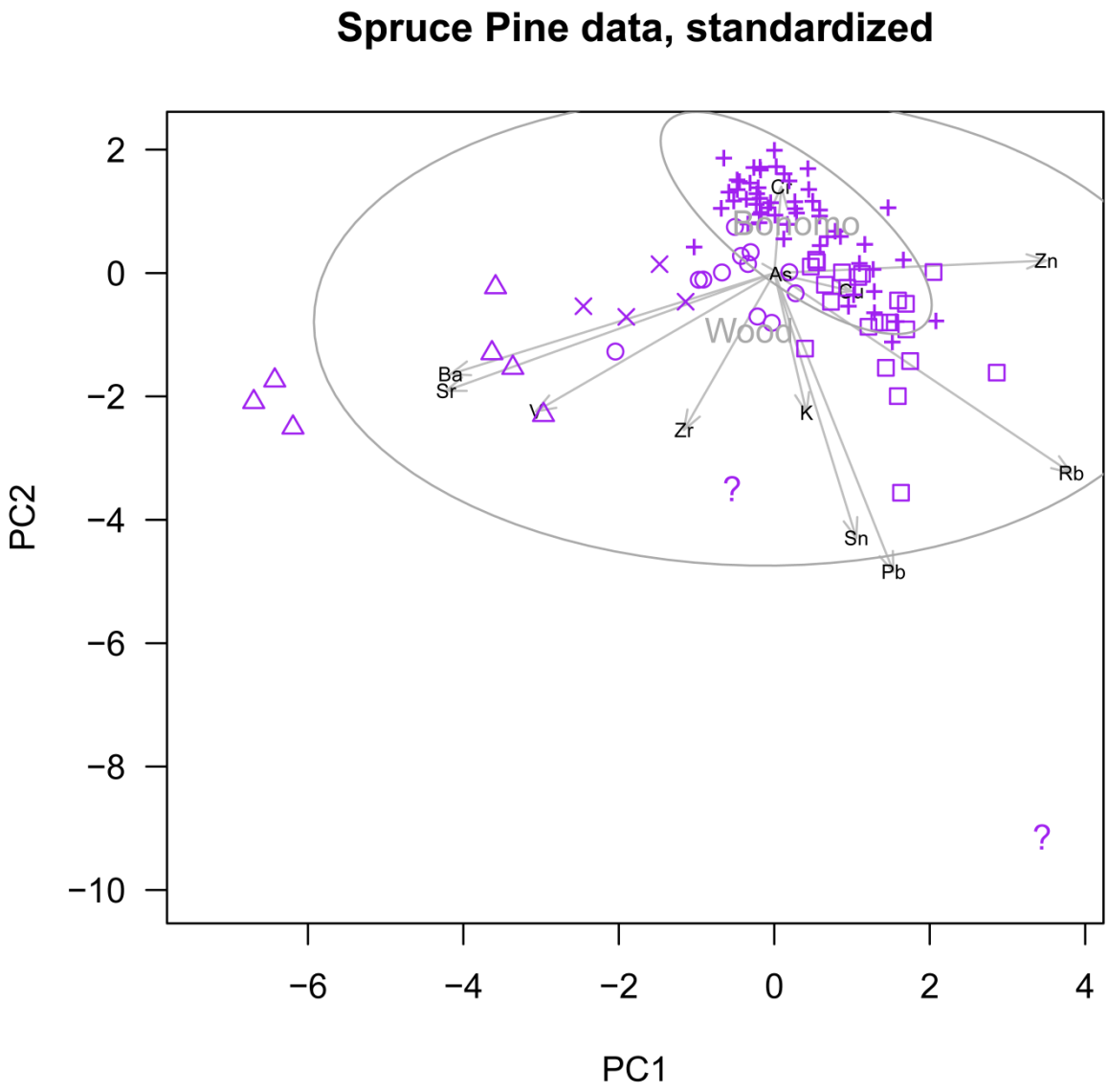

Figure 34A: PCA compatibility test of Spruce Pine data (standardized). Data from Wood (1996, "Wood" at centroid of 95% confidence ellipsoid) and the present study ("Bonomo" at centroid of 95% confidence ellipsoid). Samples belonging to the geochemical clusters identified in Wood's (1996) data are as follows: Group 1 (open squares); Group 2 (open circles); Group 3 (x's); Group 4 (open triangles). Two data points ("?") do not appear to correspond with any particular group. Loading vectors are shown as gray arrows with black text. *Geochemical groupings do not correspond to any well-defined geographic clusters within the Spruce Pine district.

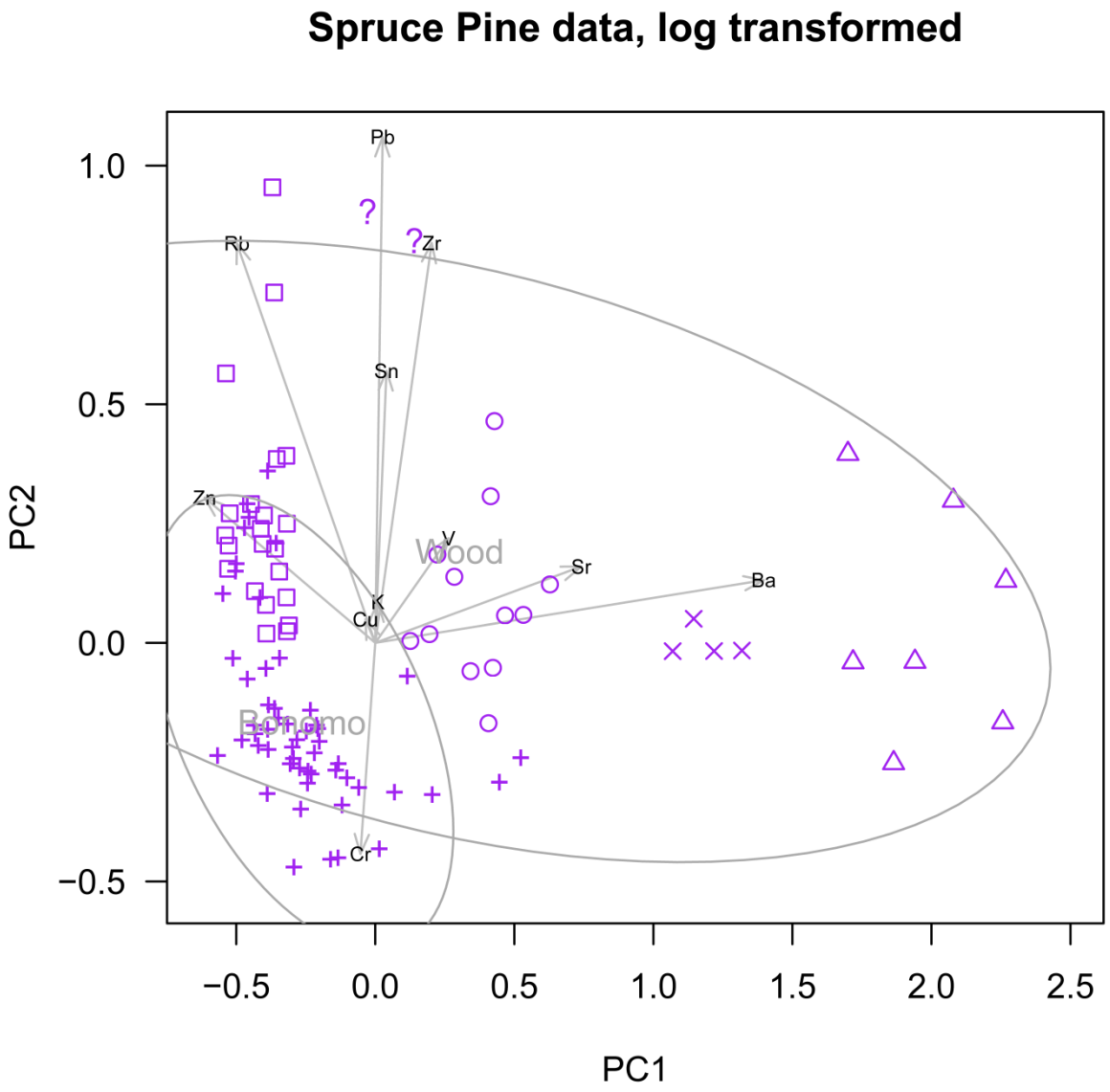

Figure 34B: PCA compatibility test of Spruce Pine data (log transformed). Data from Wood (1996, "Wood" at centroid of 95% confidence ellipsoid) and the present study ("Bonomo" at centroid of 95% confidence ellipsoid). Samples belonging to the geochemical clusters identified in Wood's (1996) data are as follows: Group 1 (open squares); Group 2 (open circles); Group 3 (x's); Group 4 (open triangles). Two data points ("?") do not appear to correspond with any particular group. Loading vectors are shown as gray arrows with black text. *Geochemical groupings do not correspond to any well-defined geographic clusters within the Spruce Pine district.

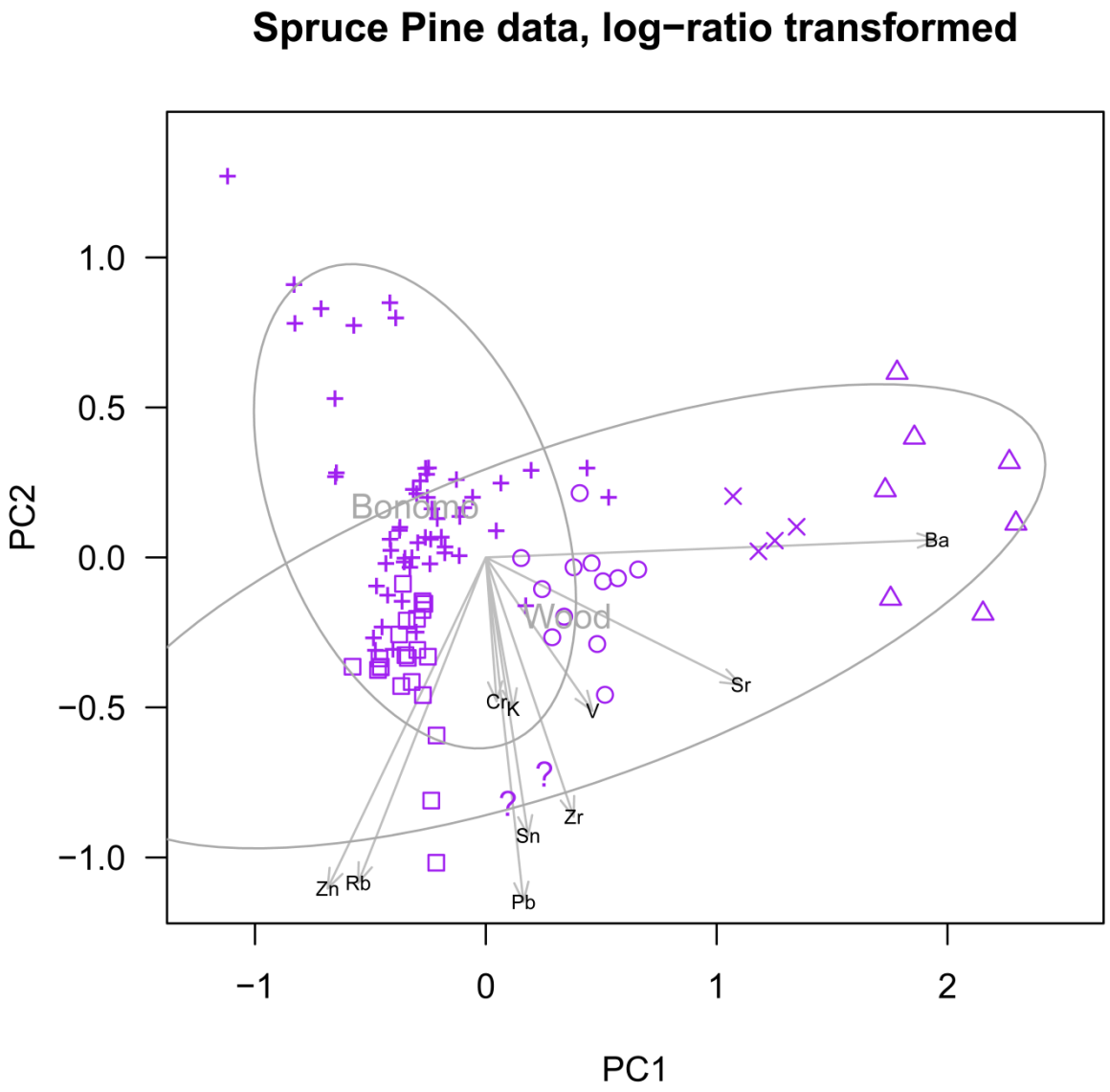

Figure 34C: PCA compatibility test of Spruce Pine data (log-ratio transformed). Data from Wood (1996, "Wood" at centroid of 95% confidence ellipsoid) and the present study ("Bonomo" at centroid of 95% confidence ellipsoid). Samples belonging to the geochemical clusters identified in Wood's (1996) data are as follows: Group 1 (open squares); Group 2 (open circles); Group 3 (x's); Group 4 (open triangles). Two data points ("?") do not appear to correspond with any particular group. Loading vectors are shown as gray arrows with black text. *Geochemical groupings do not correspond to any well-defined geographic clusters within the Spruce Pine district.

from the Thomaston-Barnesville district. Four distinct clusters of data are evident within the overall field of data bounded by the 95% confidence ellipse, with the same clusters emerging when each of the three methods of data transformation are applied: Group 1 samples display enrichment in Rb, Sn and/or Zn, indicating greater amounts of fractionation relative to the other groups, and consist of samples polly-m-3, ray-m-7, ray-m-1, ray-m-1acid, pros30-m-1, 22-m-1a, murph-m-3, hoot-m-1-2, goph-m-1, 22-m-1b, hopsw-m-1, JD-m-1, WSB-m-1b, 707-m-1, field-m-1, mck-m-3, wild-m-1, pros44-m-1, chalk-m-4, ray-m-8, cmtn-m-1 and chalk-m-1; Group 2, consisting of samples cmc20-m-2, wild-m-3, WSB-m-2, graph-m-2, JY-m-1, cmc3-m-2, bear-m-1, graph-m-4, grind1-m-1, bart-m-1, H&B-m-3 and byard-m-2; Group 3, consisting of samples pros1-m-1, pros1-m-2, hawk-m-1, hawk-m-2, frank-m-1, arvin-m-1, poll-m-2; and Group 4, consisting of samples sink-m-2, 43-m-1, FV-m-1 and 16-m-1. Samples ray-m-10 and polly-m-3 do not show strong affinity toward any particular one of these subgroups.

When these groupings are plotted according to Wood's (1996) sampling locations, it is found that there is no obvious geographic correlation among samples belonging to the same geochemical group, with the possible exceptions of Group 1 and Group 2 samples tending to plot primarily 8 – 10 km southwest of the modern town of Spruce Pine. However, this may simply be an artifact resulting from that area southwest of Spruce Pine being the most densely sampled portion of Wood's (1996) study area. The opposite relationship between geographic and geochemical clusters should be true as well: if pegmatite fields within Spruce Pine are defined on the basis of geographic clusters, then the geochemical signatures of those fields should overlap significantly, supporting the notion that there is little chance of distinguishing spatially-related pegmatite fields within a single district from one another on a geochemical basis. The Spruce Pine and Thomaston-Barnesville data suggest that the division of pegmatite districts into

pegmatite fields should only be warranted where those fields form distinct geographic *and* geochemical clusters.

PCA of Cherokee-Pickens Data from the Present Study

Given that the principal components analyses performed in the preceding sections demonstrate the compatibility of muscovite trace element data collected in the present study with data presented in the published literature, it is possible to analyze and interpret the Cherokee-Pickens district data collected in the present study in a similar manner. While the PCA of the standardized data (Figure 35A) shows fairly distinct clustering among samples from the Holly Springs pegmatite field (samples from the Dean mine, J.D. Hillhouse mine, J.D. Hillhouse prospect, Kuykendell prospect, Ledford mine and Wacaster mine in Cherokee Co.) and Ball Ground pegmatite field (samples from the Reynolds mine and Poole mine in Pickens Co.), such clustering is less evident in principal component plots using log-transformed (Figure 35B) and log-ratio transformed (Figure 35C) data. This may be attributable to differences in the number of localities sampled within each field (six from Holly Springs versus only two from Ball Ground), and the possibility exists that given a greater range of sampling localities from the Ball Ground field, clustering with respect to the Holly Springs field may become more or less evident in plots applying different transformations to the raw data.

Figures 38A-B suggest that the ability to resolve pegmatite fields within the Cherokee-Pickens district from one another on the basis of muscovite geochemistry is largely dependent on the individual pegmatite in question; on the basis of several bivariate geochemical plots (Gunow & Bonn's [1989] Figures 5 & 6), it appears that there is significant overlap in terms of geochemical signature of the Holly Springs muscovite with muscovite from some of the beryl-poor Ball Ground fields. However, some of the pegmatitic muscovite from the Ball Ground field

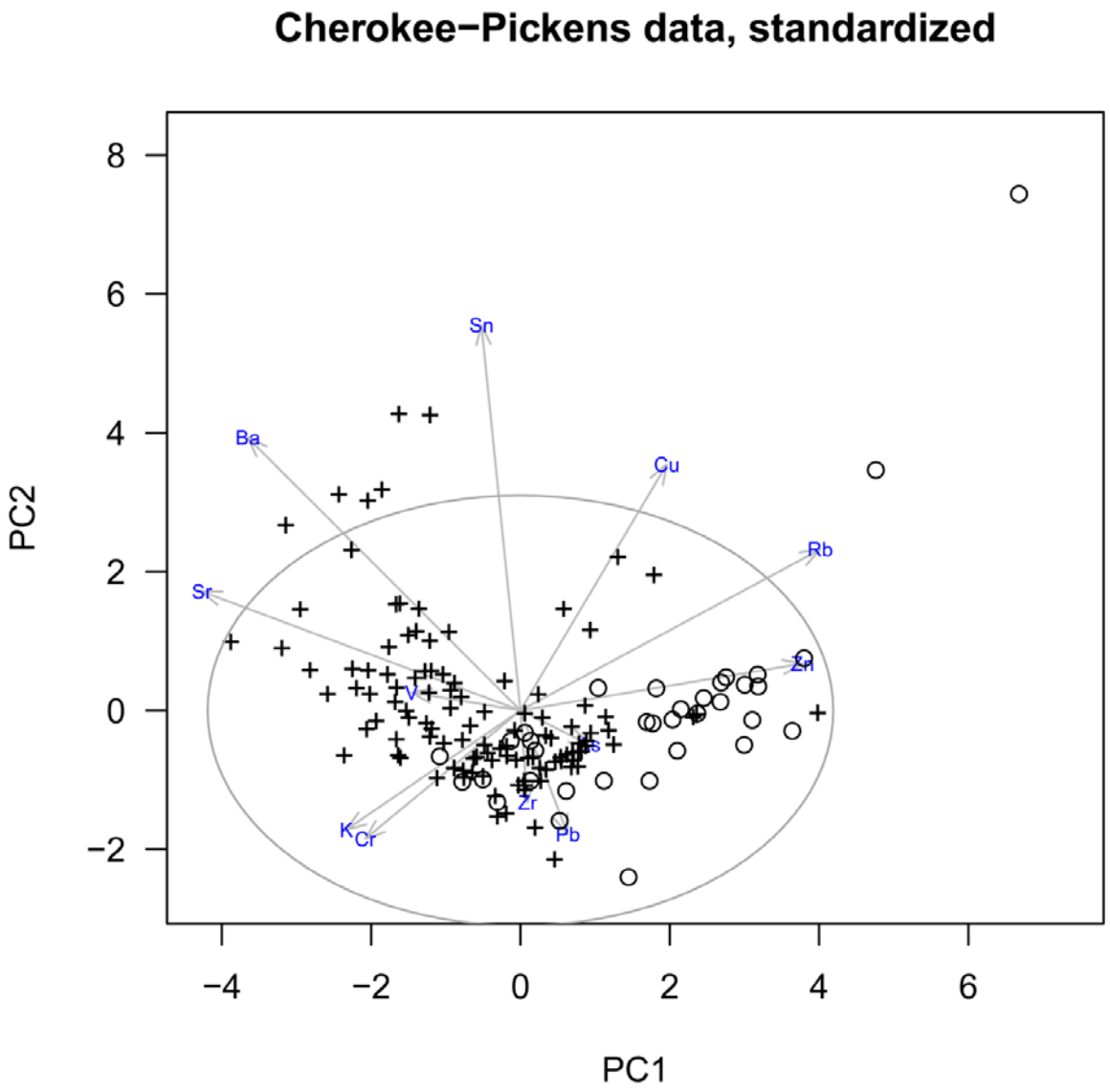

Figure 35A: PCA of Cherokee-Pickens district data. Data are from the Holly Springs pegmatite field (Cherokee Co., crosses) and the beryl-poor Ball Ground field (Pickens Co., open circles). Loading vectors are shown as gray arrows with blue text.

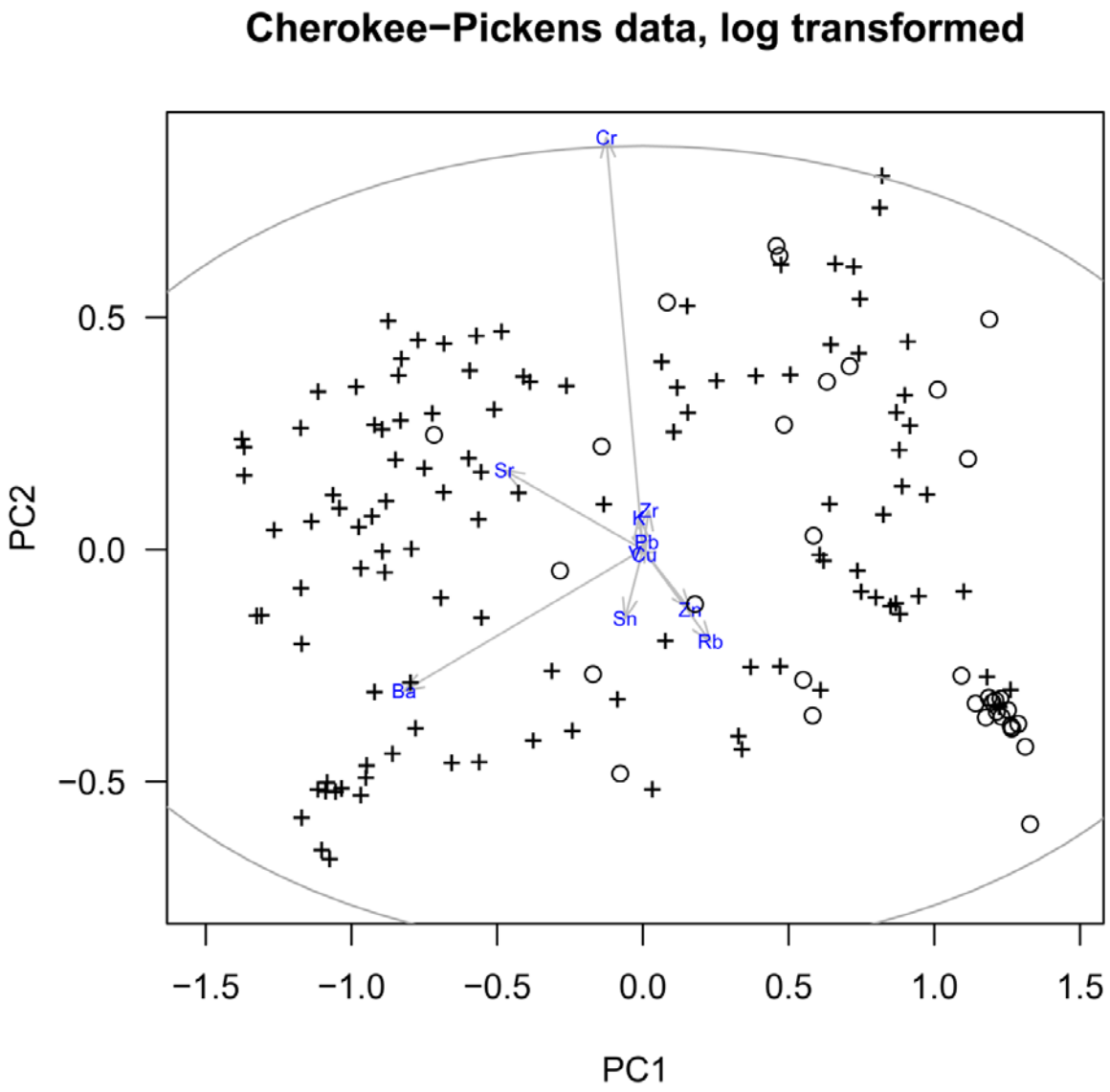

Figure 35B: PCA of Cherokee-Pickens district data. Data are from the Holly Springs pegmatite field (Cherokee Co., crosses) and the beryl-poor Ball Ground field (Pickens Co., open circles). Loading vectors are shown as gray arrows with blue text.

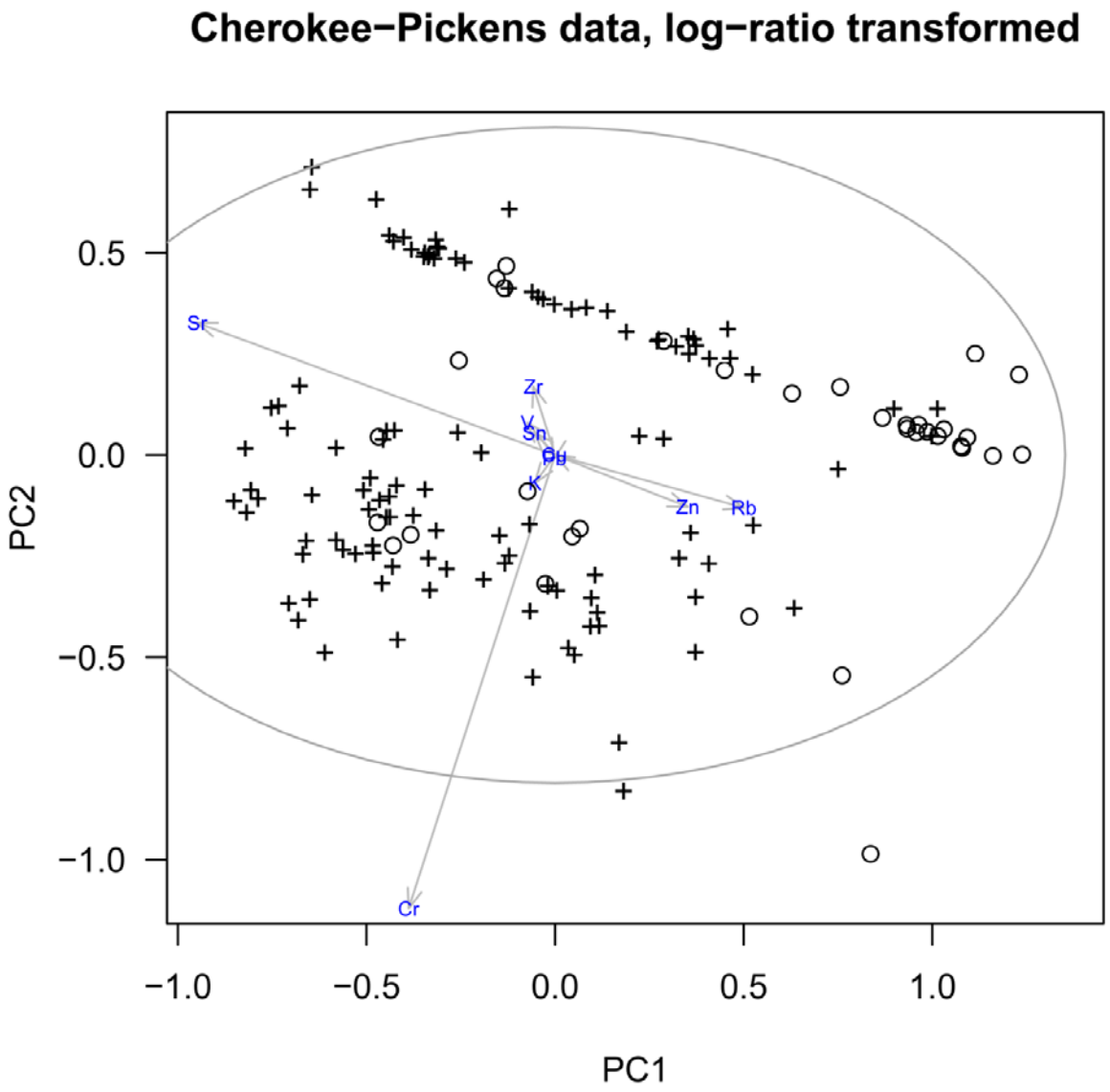

Figure 35C: PCA of Cherokee-Pickens district data. Data are from the Holly Springs pegmatite field (Cherokee Co., crosses) and the beryl-poor Ball Ground field (Pickens Co., open circles). Loading vectors are shown as gray arrows with blue text.

appears to occupy its own region of geochemical space between this area of overlap with the Holly Springs field and the area defined by the geochemically distinct muscovite from the rare-element enriched beryl-bearing pegmatites of the Ball Ground field. Thus, the portion of the field defined by muscovite from the beryl-poor Ball Ground pegmatites, where they trend toward geochemical signatures displayed by muscovite from the rare-element enriched beryl-bearing pegmatites, should be clearly resolvable from the Holly Springs field in principal component plots.

PCA of the Combined Datasets

PCA has been performed on the entire compiled body of southeastern pegmatitic muscovite data; Figures 36A-C display individual sample points on the principal component plots, while Figures 36D-F display only the 95% confidence ellipses constructed about the centroids of those data points for visual simplification. Data are grouped on the basis of geochemically and geographically distinct pegmatite fields within districts, as identified in the principal component analyses performed in the preceding sections. For the Spruce Pine district, there were no such geochemically and geographically distinct pegmatite fields and the data were treated as a single group (*SP*). For the Thomaston-Barnesville district (*TB*), the majority of geographic pegmatite fields do not display distinct geochemical signatures with respect to one another, with the exception of the Indian Grave pegmatite field; thus, the Thomaston-Barnesville muscovite data is divided into two groups, one for the majority of the district (*TB*) and one for the Indian Grave field (*IG*). Lastly, data from the Cherokee-Pickens district are divided into a Holly Springs (*HS*) group and a Ball Ground (*BG*) group. PCA was performed on the 12 elements common to all three original datasets (As, Ba, Cr, Cu, K, Pb, Rb, Sn, Sr, V, Zn and Zr).

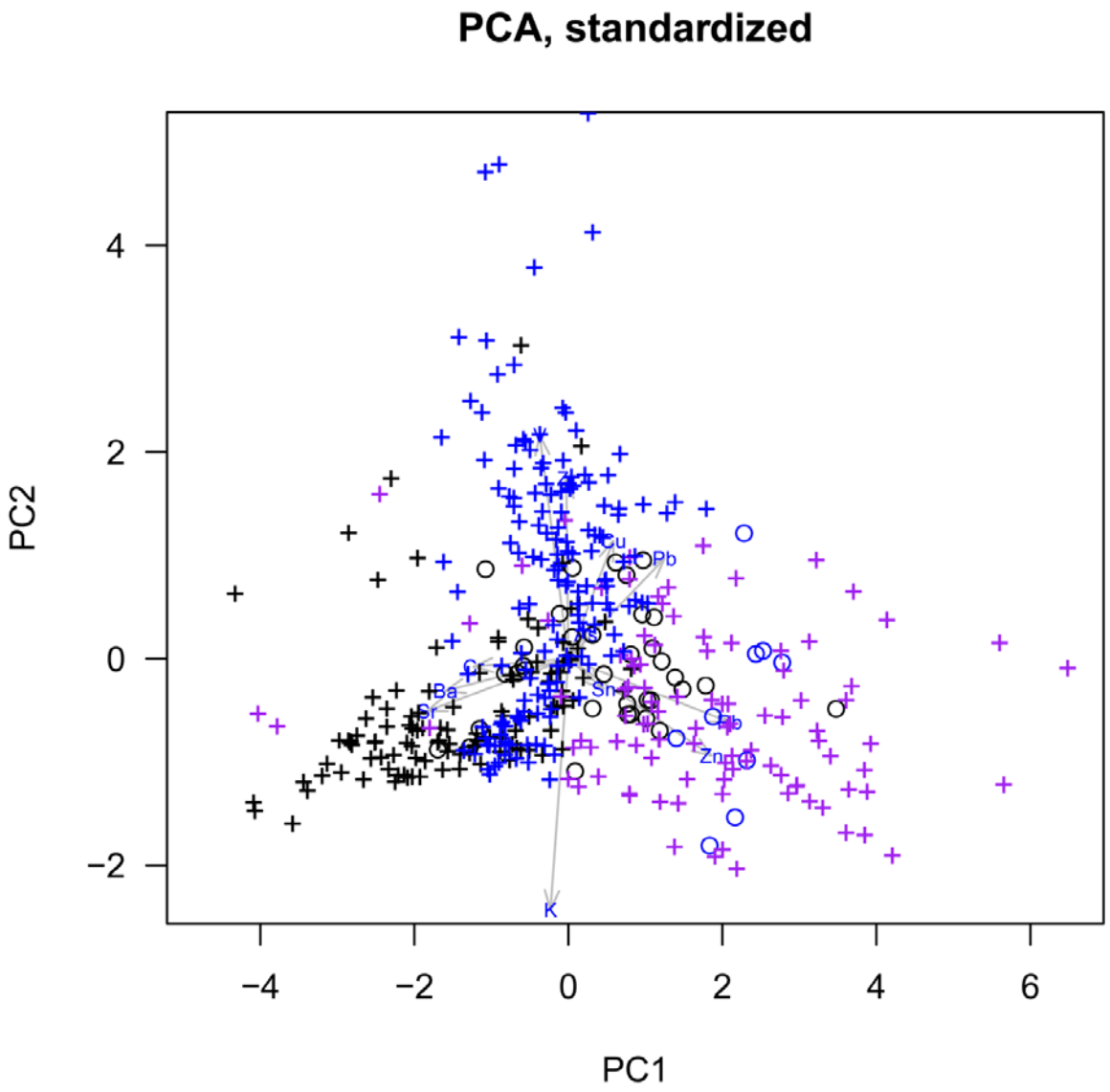

Figure 36A: PCA of southeastern pegmatitic muscovite database using standardized data compiled from the present study, Cocker (1992a) and Wood (1996). Black data points correspond to Cherokee-Pickens district data (crosses for the Holly Springs pegmatite field, *HS*, and open circles for Ball Ground, *BG*); blue data points correspond to Thomaston-Barnesville district data (crosses for the main grouping of data, *TB*, and open circles for the Indian Grave pegmatite field, *IG*); purple data points correspond to Spruce Pine data. Loading vectors are shown as gray arrows with blue text. Note that axes have been truncated to obtain better resolution of the data, and that only one data point, 349-8 from the *TB* field, plots outside this range.

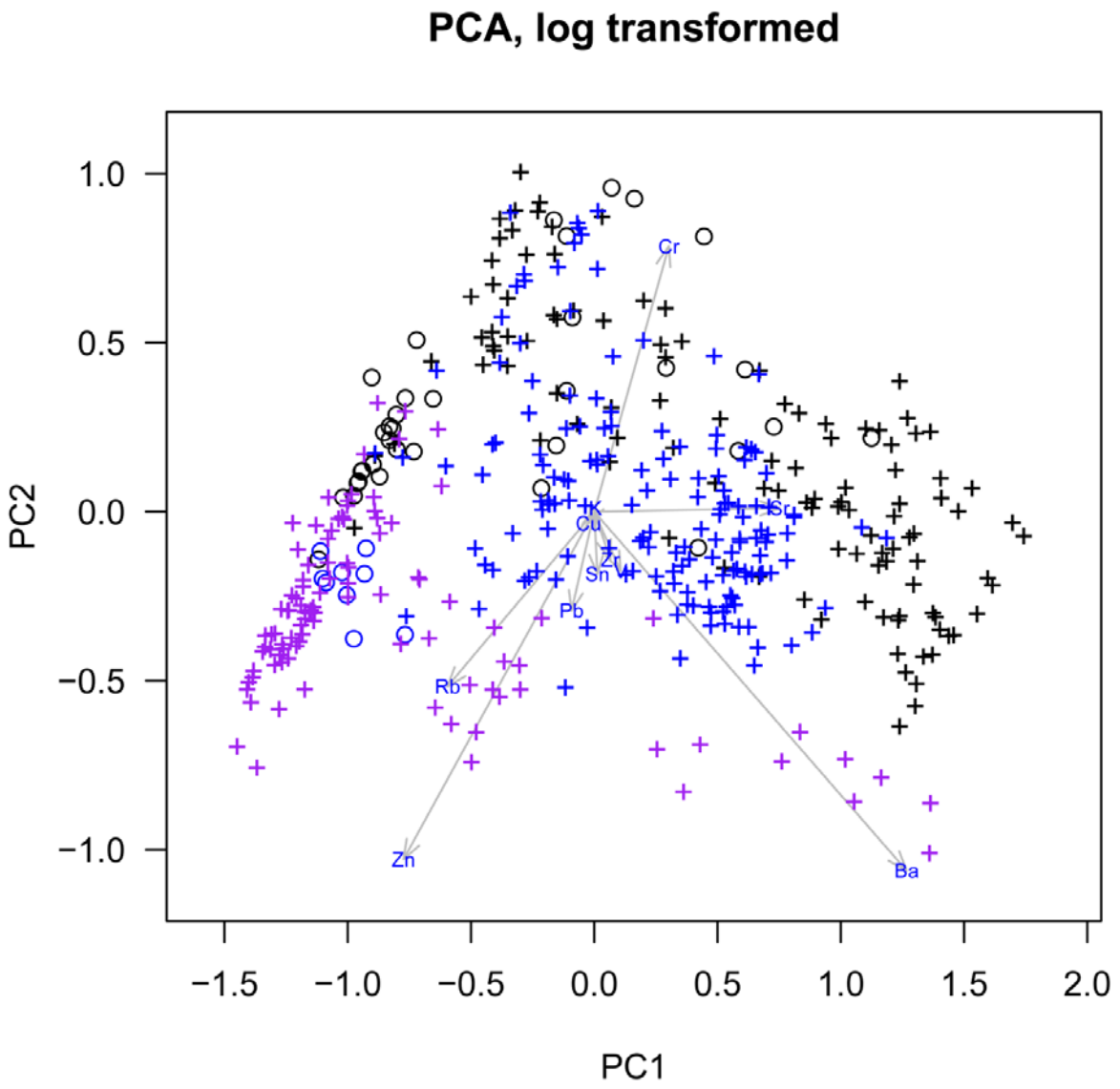

Figure 36B: PCA of southeastern pegmatitic muscovite database using log-transformed data compiled from the present study, Cocker (1992a) and Wood (1996). Black data points correspond to Cherokee-Pickens district data (crosses for the Holly Springs pegmatite field, *HS*, and open circles for Ball Ground, *BG*); blue data points correspond to Thomaston-Barnesville district data (crosses for the main grouping of data, *TB*, and open circles for the Indian Grave pegmatite field, *IG*); purple data points correspond to Spruce Pine data. Loading vectors are shown as gray arrows with blue text.

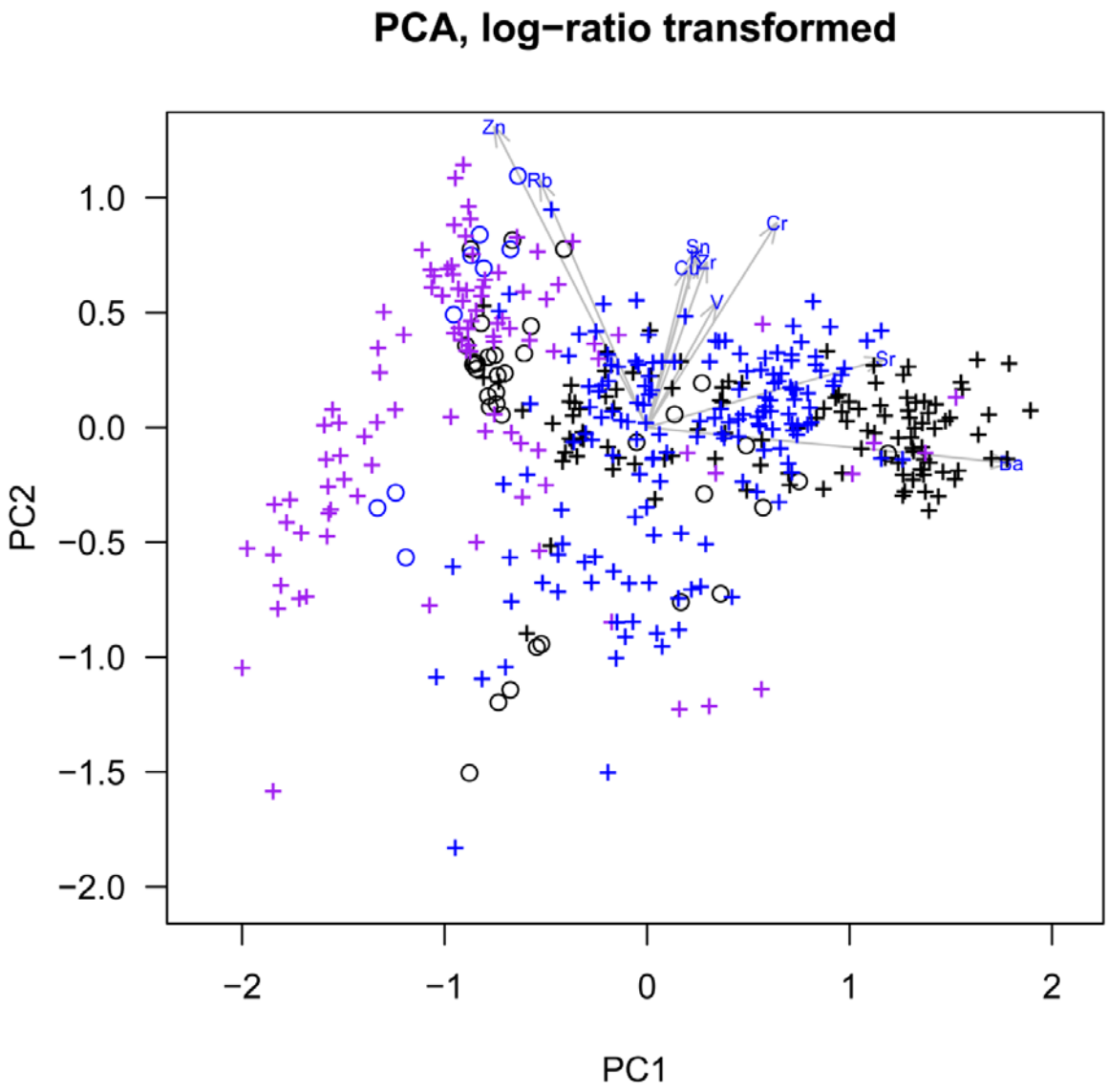

Figure 36C: PCA of southeastern pegmatitic muscovite database using log-ratio transformed data compiled from the present study, Cocker (1992a) and Wood (1996). Black data points correspond to Cherokee-Pickens district data (crosses for the Holly Springs pegmatite field, *HS*, and open circles for Ball Ground, *BG*); blue data points correspond to Thomaston-Barnesville district data (crosses for the main grouping of data, *TB*, and open circles for the Indian Grave pegmatite field, *IG*); purple data points correspond to Spruce Pine data. Loading vectors are shown as gray arrows with blue text.

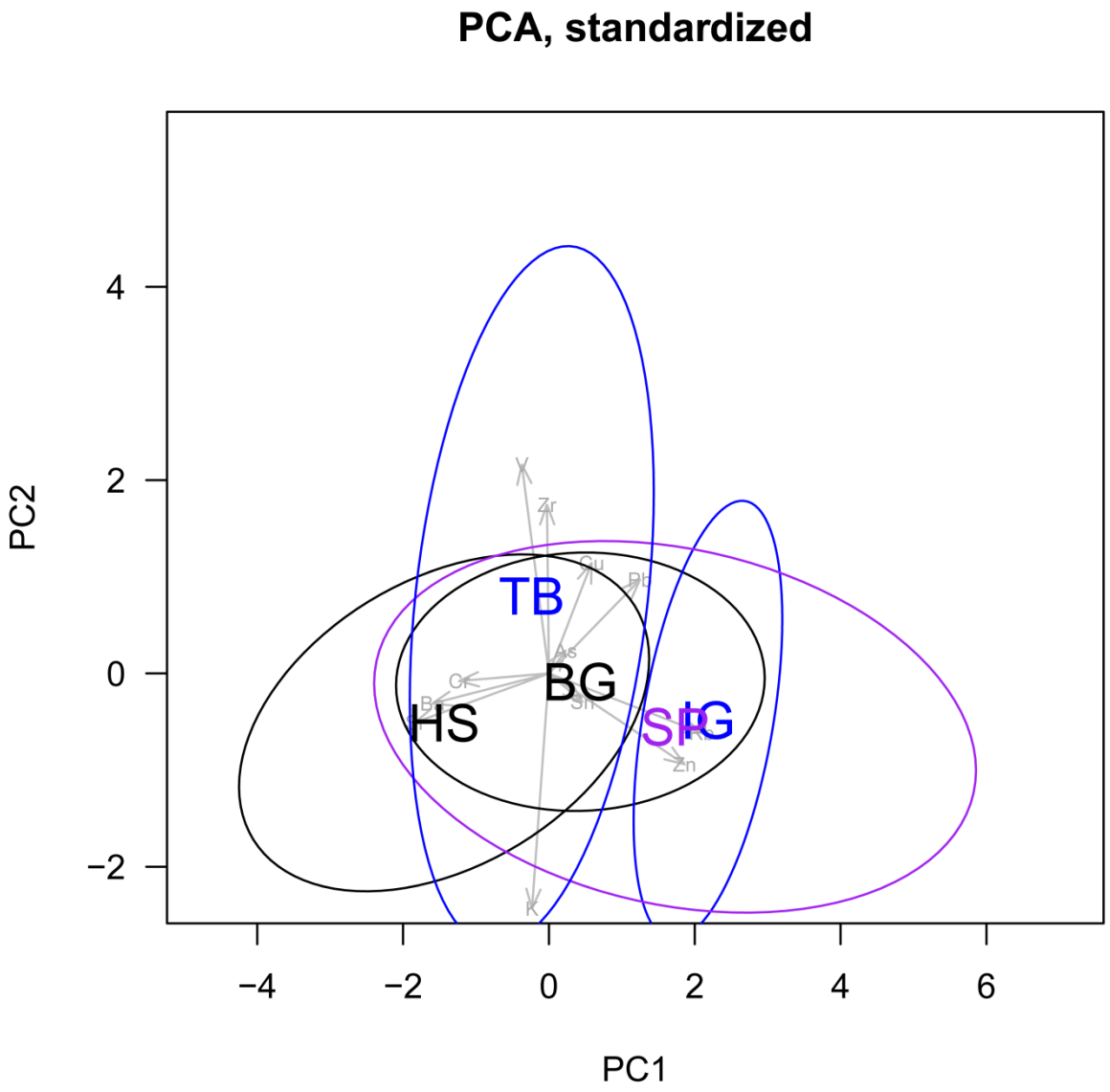

Figure 36D: PCA of southeastern pegmatitic muscovite database using standardized data compiled from the present study, Cocker (1992a) and Wood (1996); 95% confidence ellipses have been constructed around the centroids of the data presented in Figure 45A for the Cherokee-Pickens district (Holly Springs pegmatite field, *HS*, and Ball Ground, *BG*), Thomaston-Barnesville district (main grouping of data, *TB*, and the Indian Grave pegmatite field, *IG*), and Spruce Pine. Loading vectors are shown as gray arrows. Note that axes have been truncated to obtain better resolution of the data, and that only one data point, 349-8 from the *TB* field, plots outside this range.

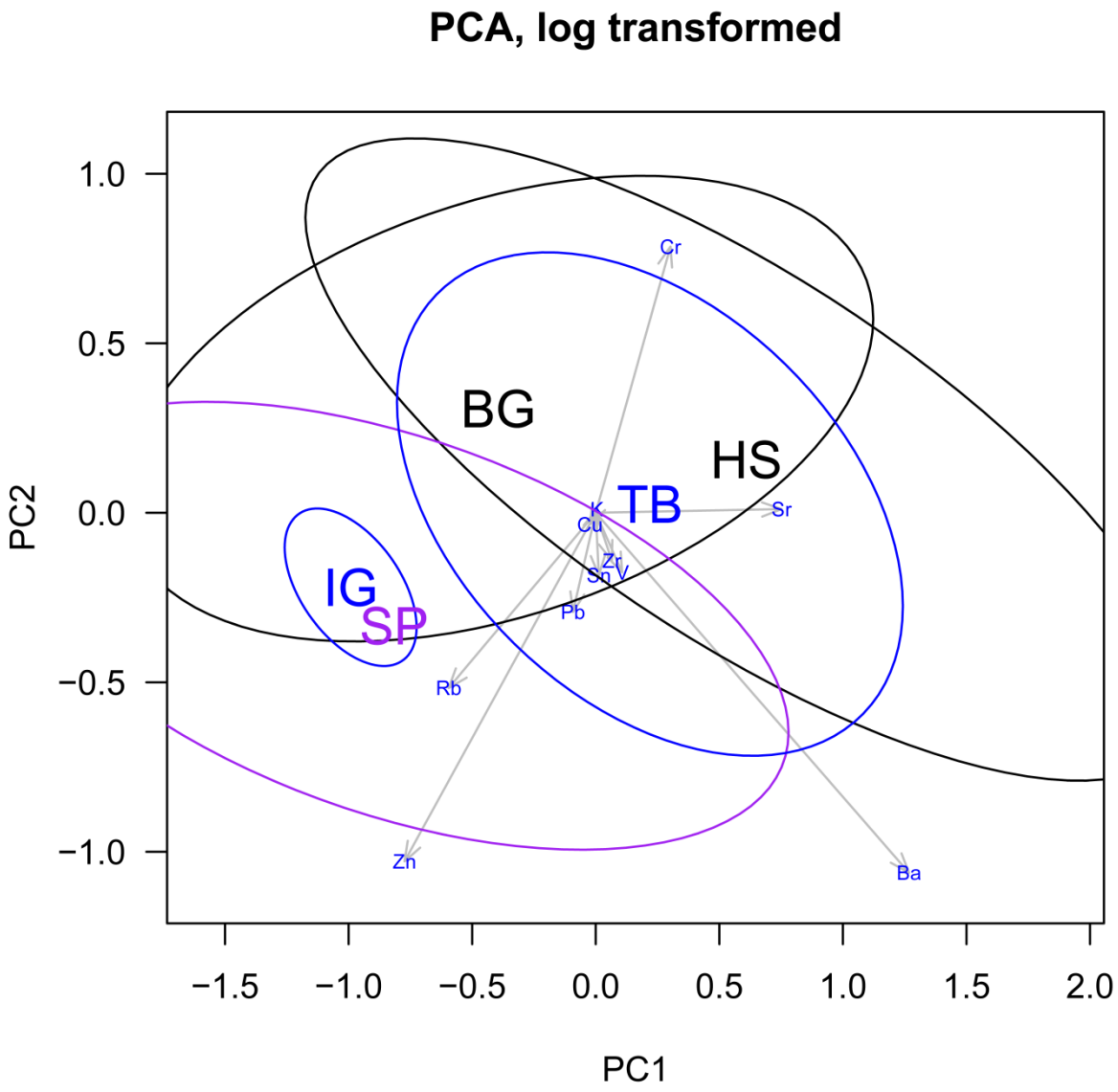

Figure 36E: PCA of southeastern pegmatitic muscovite database using log-transformed data compiled from the present study, Cocker (1992a) and Wood (1996); 95% confidence ellipses have been constructed around the centroids of the data presented in Figure 45A for the Cherokee-Pickens district (Holly Springs pegmatite field, *HS*, and Ball Ground, *BG*), Thomaston-Barnesville district (main grouping of data, *TB*, and the Indian Grave pegmatite field, *IG*), and Spruce Pine. Loading vectors are shown as gray arrows.

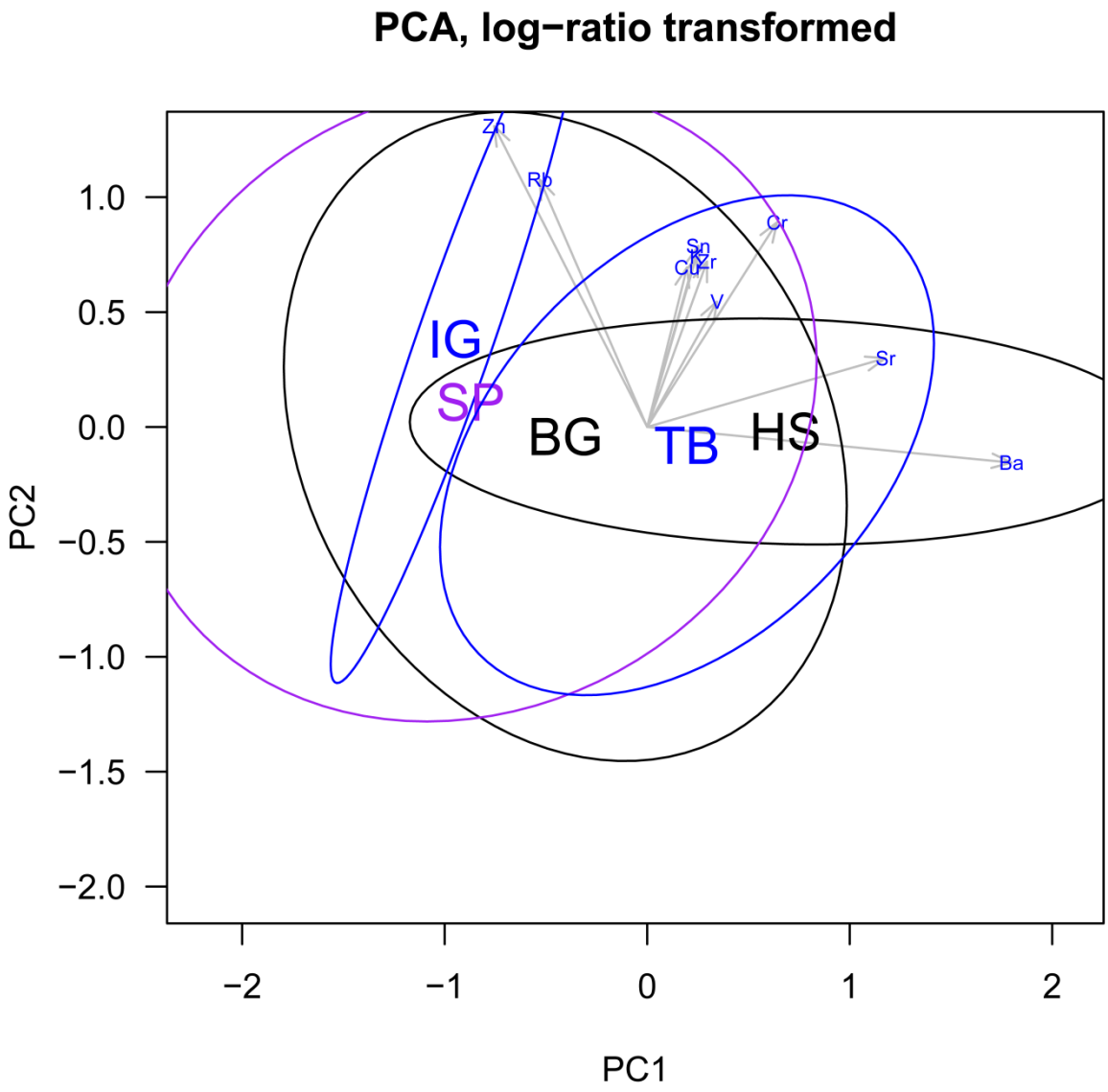

Figure 36F: PCA of southeastern pegmatitic muscovite database using log-ratio transformed data compiled from the present study, Cocker (1992a) and Wood (1996); 95% confidence ellipses have been constructed around the centroids of the data presented in Figure 45A for the Cherokee-Pickens district (Holly Springs pegmatite field, *HS*, and Ball Ground, *BG*), Thomaston-Barnesville district (main grouping of data, *TB*, and the Indian Grave pegmatite field, *IG*), and Spruce Pine. Loading vectors are shown as gray arrows.

With any plot of principal components, it is hoped that the first few principal components will account for a high proportion of the total variance in the dataset. In assessing the proportion of variance accounted for by each principal component in the southeastern muscovite dataset, the first four principal components for the standardized data account for only 56.83% of the total variance, with only 35.76% accounted for in the first two principal components. These numbers are far from the 70% threshold for the first four principal components that Grave et al. (2005) suggest for highly structured data. The lack of structuring in the standardized southeastern muscovite data is evident in the high degree of overlap displayed in the principal component plots (Figures 43A,D). However, in performing PCA on the same data to which both logarithmic and log-ratio transformations had been applied, the proportions of variance accounted for by the first four principal components rise to 84.20% and 86.11% (with the first two principal components accounting for 67.17% and 68.48% of the variance), respectively. Thus, the principal component plots based on the first two principal components for the log-transformed (Figure 43B,E) and log-ratio transformed (Figure 43C,F) data should display more readily interpretable structure in the data for provenancing purposes.

DFA of Muscovite Database

Prior to plotting the Etowah muscovite artifact scores in relation to the geological source data, it is first necessary to assess the discriminating capabilities of a model on the basis of that data through DFA. The principal components analyses of the muscovite data show that the published datasets are compatible with the pXRF data from this study. This is significant for one main reason: the combination of the data collected during the present investigation with that presented in the published literature is necessary to help eliminate any large discrepancies in sample size *n* between data groups, as the estimation of success rates of DFA is highly

susceptible to being influenced by large differences in sample size across groups. In combining datasets, the total number of samples *n* per group are thus *n* = 148 for the Cherokee-Pickens district, *n* = 163 for the Thomaston-Barnesville district, and *n* = 101 for Spruce Pine. If only the data from the present study were utilized, group sample sizes would be *n* = 148 for the Cherokee-Pickens district, *n* = 62 for the Thomaston-Barnesville district, and *n* = 54 for Spruce Pine. Combining datasets also eases additional concerns relating to the fact that, if only data from the present study are considered, only three localities were sampled in each of the Thomaston-Barnesville and Spruce Pine districts as opposed to eight localities from the Cherokee-Pickens district. Thus, combining datasets also serves to increase the number of sampling localities per district, making the data fields defined by PCA or DFA more representative of any given district as a whole.

While differences in sample size still exist after the combination of the datasets, they are much less pronounced. In order to eliminate sample-size differences completely, the DFA routine provided in Appendix E has incorporated random sampling of the larger Cherokee-Pickens and Thomaston-Barnesville datasets to select only *n* = 101 samples (i.e., the size of the smallest dataset, the Spruce Pine dataset) from each of the larger datasets. For similar reasons relating to sample size per group, the Indian Grave pegmatite field (*n* = 9) of the Thomaston-Barnesville district and the Ball Ground field (*n* = 35) of the Cherokee-Pickens district could not be treated as separate groups in the DFA as they had been in the PCA.

Discriminant function analysis was performed using the *MASS* package's built-in *lda( )* function (Venables & Ripley 2002). While sample sizes per group ($n > 100$) in relation to the number of variables ($p = 12$) reasonably justify the use of QDA, issues relating to its greater sensitivity to deviations from multivariate normality of the data than, and minimal increase in

performance over, LDA have led to the decision to use LDA exclusively. For the log-ratio transformations, the element introducing the least variability to the dataset was identified as that element with the lowest standard deviation across the entire dataset (in this case, Pb, with σ = 7.14); after the ratio of each element to that with the least variability was calculated for each sample (i.e., the concentration of Rb in sample *i* divided by the concentration of Pb in sample *i*, repeated for all elements in all samples) and the base-10 logarithm calculated for each ratio, the element introducing the least variability was removed from the dataset and thus was not incorporated in the log-ratio DFA. The success rates of each analysis were calculated from the average of B = 10,000 randomly generated replicate datasets using resubstitution, leave-one-out cross-validation, bootstrap resubstitution, bootstrap cross-validation, the optimism method, and the .632 bootstrap method.

The discriminant functions obtained from the log-transformed southeastern muscovite data (which will be shown in the following paragraph to yield better discrimination than other transformations) are:

$$\begin{aligned} LD1 = {} & -0.06160117*[\text{As}] + 0.24373202*[\text{Ba}] + -0.88412216*[\text{Cr}] + \\ & 0.97033889*[\text{Cu}] + 3.06651152*[\text{K}] + 0.32407299*[\text{Pb}] + \\ & 0.33220099*[\text{Rb}] + -0.98595934*[\text{Sn}] + 0.70973454*[\text{Sr}] + \\ & 0.86295477*[\text{V}] + 4.22648537*[\text{Zn}] + -0.50822560*[\text{Zr}] \\ LD2 = {} & 1.5209052*[\text{As}] + 0.6805542*[\text{Ba}] + 0.4427993*[\text{Cr}] + \\ & -1.4258074*[\text{Cu}] + -1.1320000*[\text{K}] + 0.8906544*[\text{Pb}] + \\ & -1.5707757*[\text{Rb}] + 1.9610182*[\text{Sn}] + -2.5323694*[\text{Sr}] + \\ & 2.1242154*[\text{V}] + 0.7522955*[\text{Zn}] + 1.6559571*[\text{Zr}] \end{aligned}$$

with *LD1* accounting for 83.00% of the total variation in the data (note that only two linear discriminant functions are calculated in DFA, as opposed to the greater number of principal components calculated in PCA). Figures 37A-C display individual sample points plotted according to the discriminant functions; Figures 37D-F display only the 95% confidence ellipses constructed about the centroids of those data points for visual simplification.

Table 3 lists the success rates of the DFA model on the basis of known-group muscovite samples, which when treated as unknowns, are reassigned to their correct source. Based on these success rates associated with known-group samples, it is shown that the application of a logarithmic or log-ratio transformation will, on average, yield better discrimination amongst sources compared to standardization of the raw data. It can also be shown that a logarithmic transformation will yield slightly better results relative to a log-ratio transformation, at least where trace elements in pegmatitic muscovite are concerned. The unbiased estimators of success (cross-validation, optimism and the .632 bootstrap) for the log-transformed data are fairly consistent, ranging from 82.63% to 84.00%; thus between 250 and 255 samples (on average) were correctly reassigned by the discriminant model after a log-transformation was applied to the raw data, compared to 246 – 253 following a log-ratio transformation and 225 – 233 following standardization.

From the discriminant function plots, it is easy to see why both the log-transformed and log-ratio transformed data yielded higher rates of successful reclassification than the standardized data. The discriminant functions calculated on the log-transformed and log-ratio transformed data were more successful at separating the Spruce Pine samples from the Cherokee-Pickens and Thomaston-Barnesville samples. Given the relatively higher degree of overlap associated with muscovite from the Cherokee-Pickens and Thomaston-Barnesville

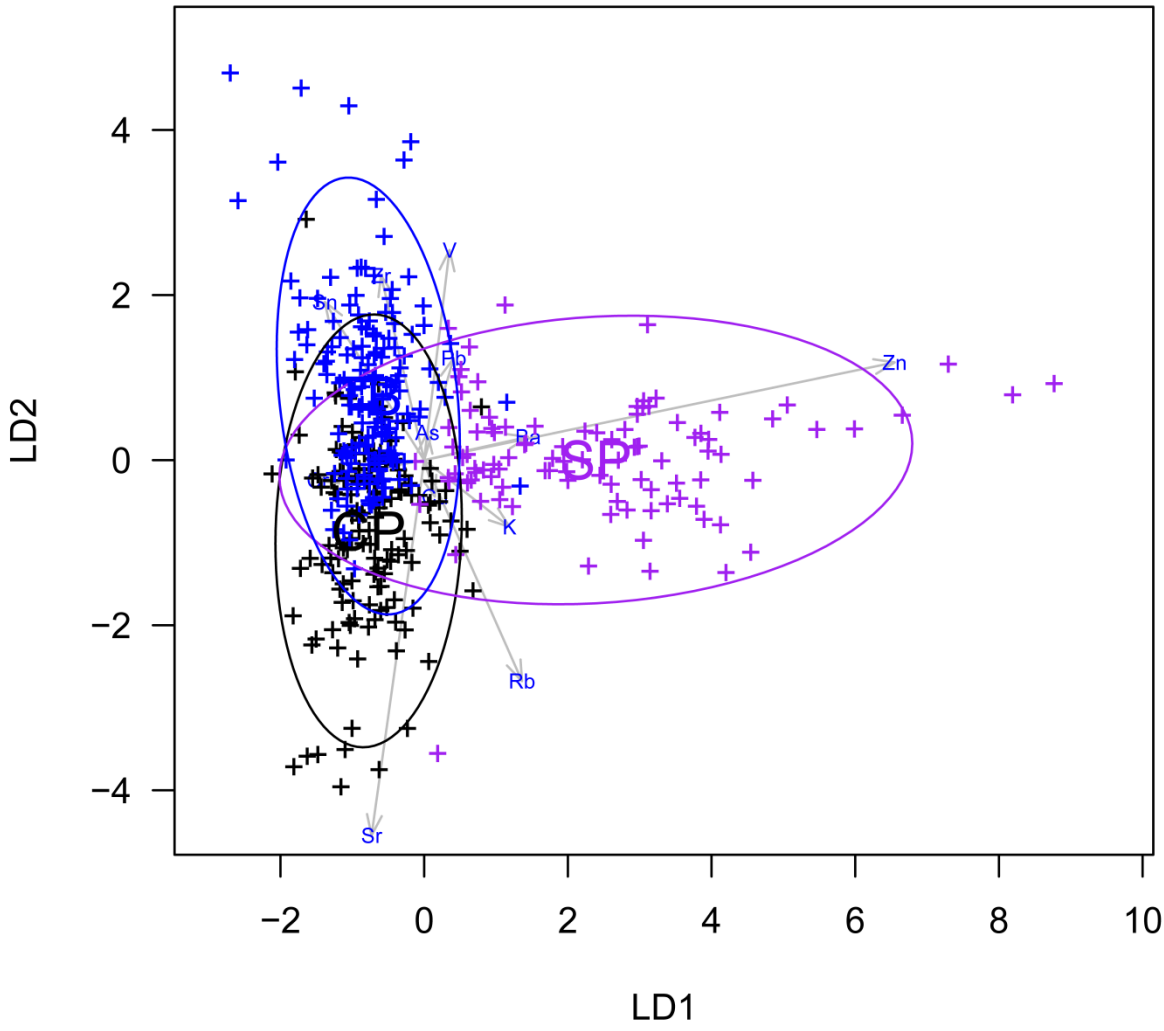

Figure 37A: LDA of southeastern muscovite database, using standardized data compiled from the present study, Cocker (1992a) and Wood (1996). Black data points correspond to Cherokee-Pickens district data (*CP* at centroid of 95% confidence ellipse), blue data points correspond to Thomaston-Barnesville district data (*TB* at centroid of 95% confidence ellipse) and purple data points correspond to Spruce Pine data (*SP* at centroid of 95% confidence ellipse). Loading vectors are shown as gray arrows with blue text.

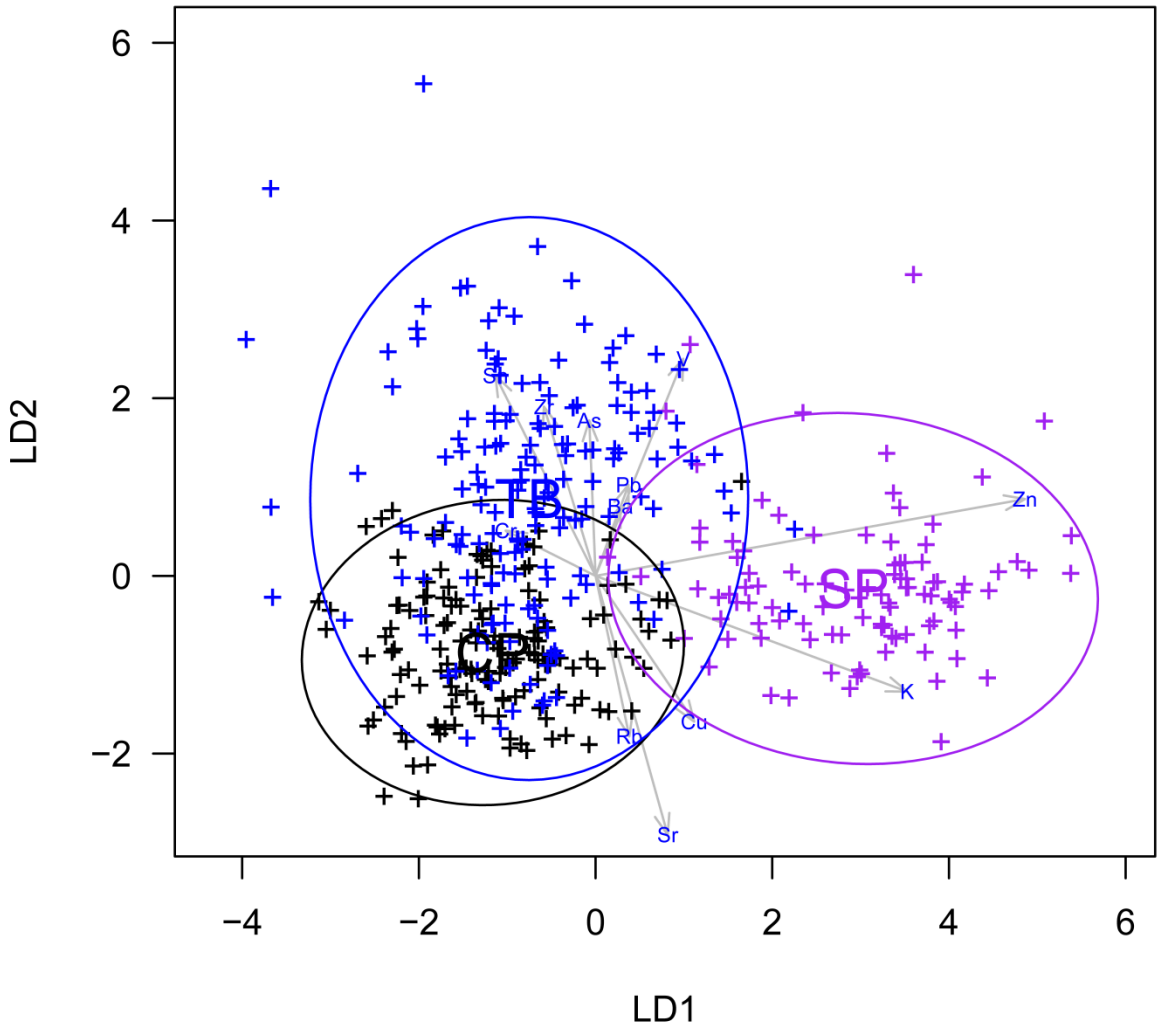

Figure 37B: LDA of southeastern muscovite database, using log-transformed data compiled from the present study, Cocker (1992a) and Wood (1996). Black data points correspond to Cherokee-Pickens district data (*CP* at centroid of 95% confidence ellipse), blue data points correspond to Thomaston-Barnesville district data (*TB* at centroid of 95% confidence ellipse) and purple data points correspond to Spruce Pine data (*SP* at centroid of 95% confidence ellipse). Loading vectors are shown as gray arrows with blue text.

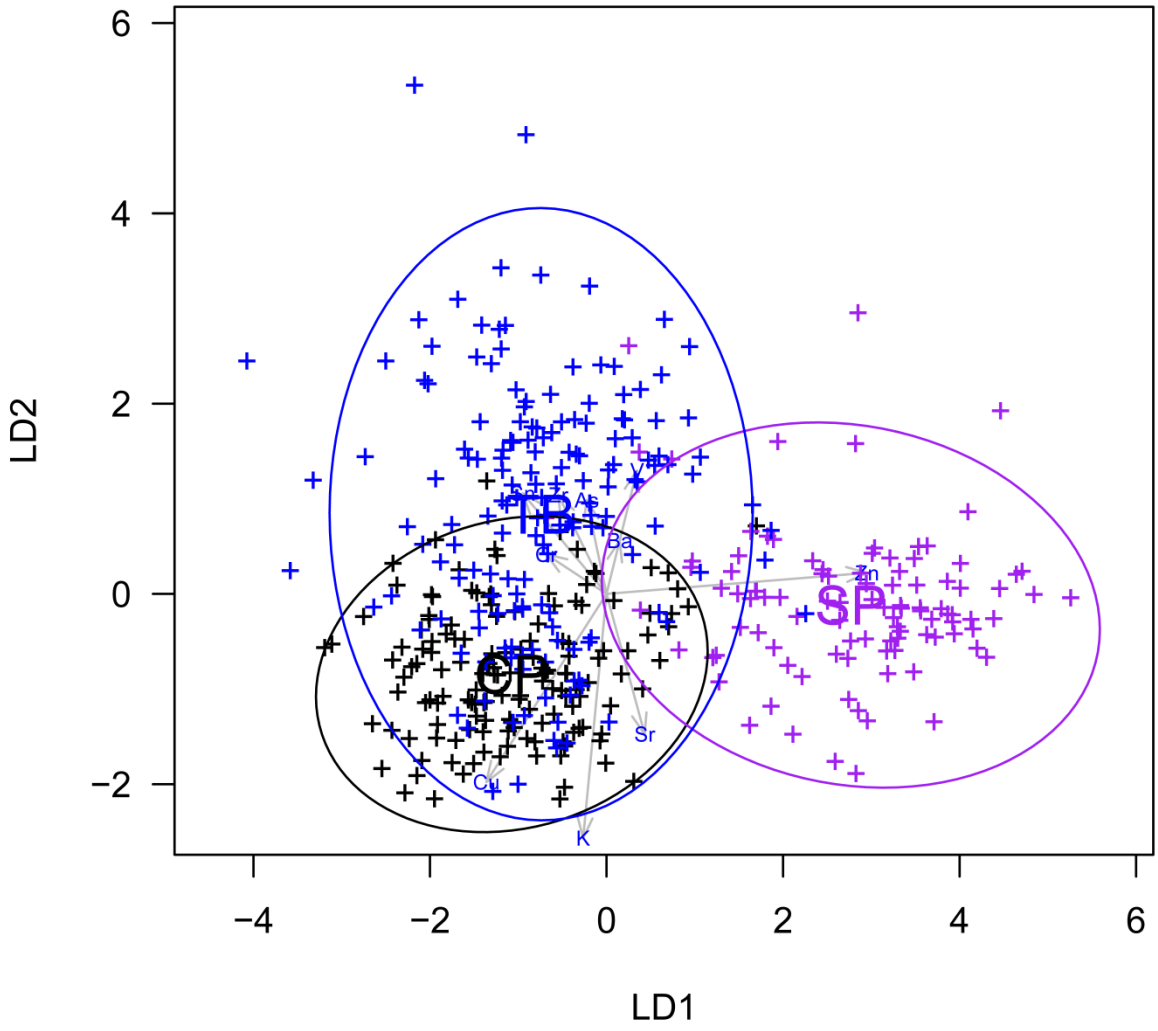

Figure 37C: LDA of southeastern muscovite database, using log-ratio transformed data compiled from the present study, Cocker (1992a) and Wood (1996). Black data points correspond to Cherokee-Pickens district data (*CP* at centroid of 95% confidence ellipse), blue data points correspond to Thomaston-Barnesville district data (*TB* at centroid of 95% confidence ellipse) and purple data points correspond to Spruce Pine data (*SP* at centroid of 95% confidence ellipse). Loading vectors are shown as gray arrows with blue text.

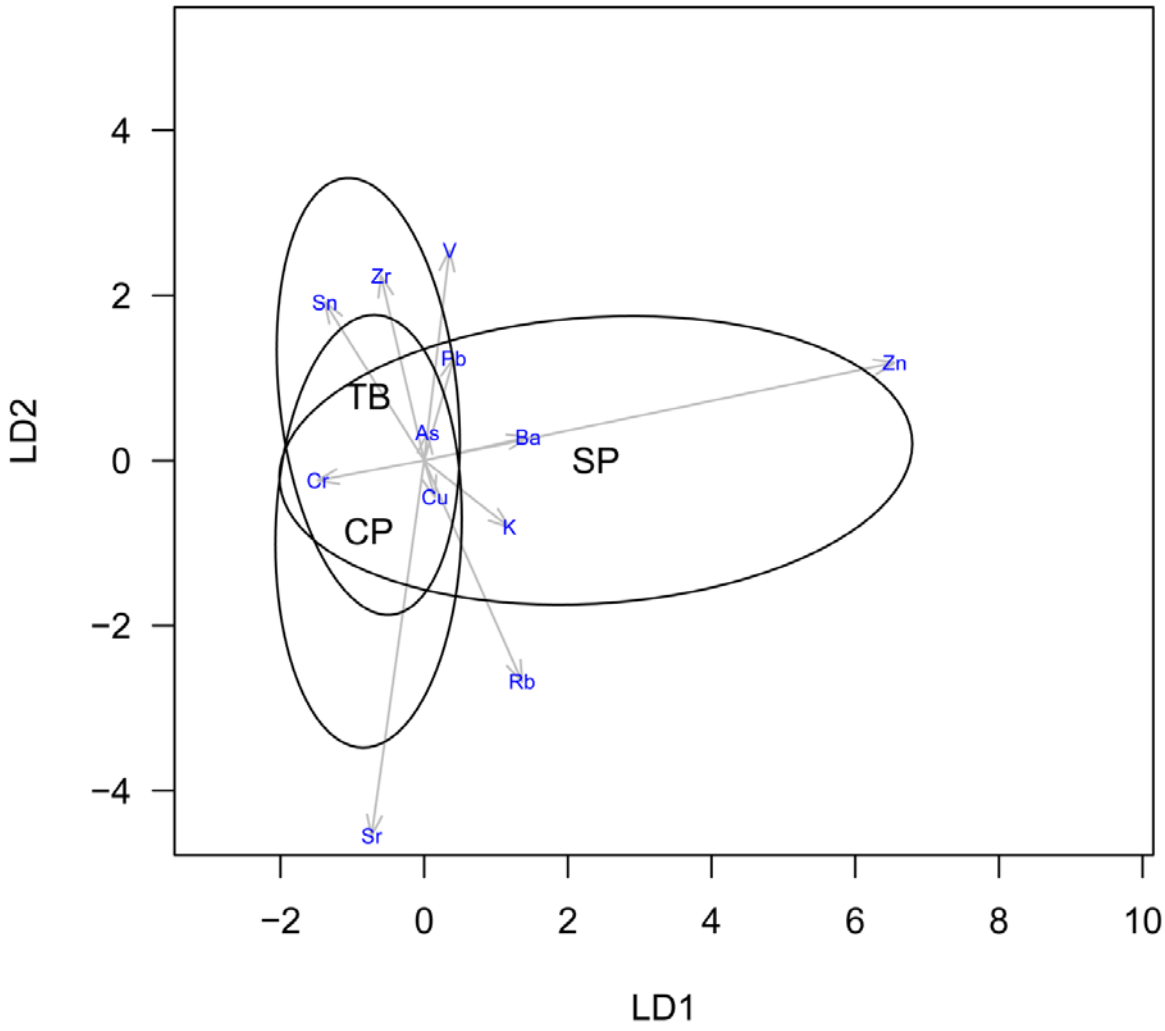

Figure 37D: LDA of southeastern muscovite database, using standardized data compiled from the present study, Cocker (1992a) and Wood (1996). 95% confidence ellipses are constructed around the centroids of the Cherokee-Pickens district data (*CP*), Thomaston-Barnesville district data (*TB*) and Spruce Pine data (*SP*). Loading vectors are represented by gray arrows.

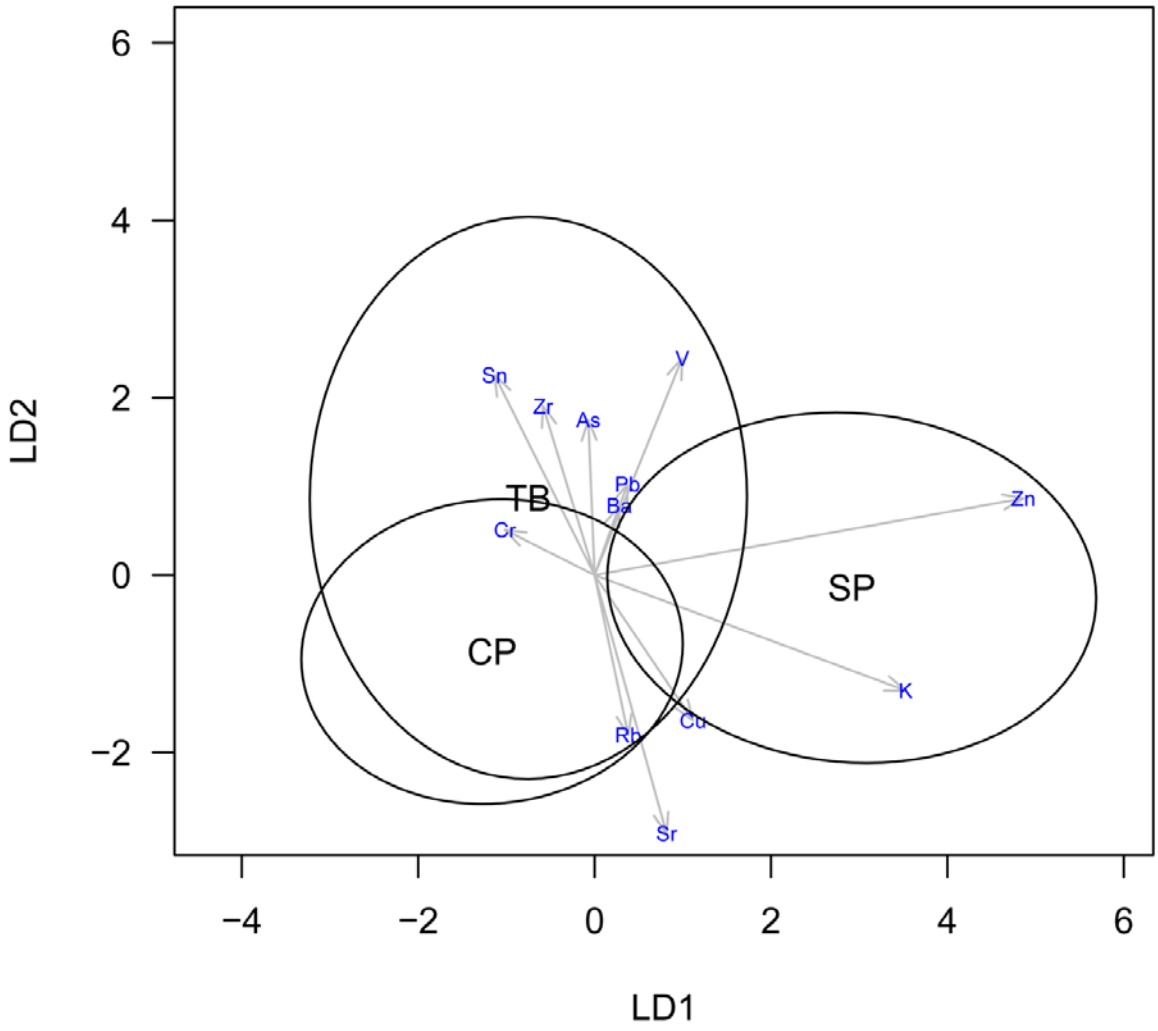

Figure 37E: LDA of southeastern muscovite database, using log-transformed data compiled from the present study, Cocker (1992a) and Wood (1996). 95% confidence ellipses are constructed around the centroids of the Cherokee-Pickens district data (*CP*), Thomaston-Barnesville district data (*TB*) and Spruce Pine data (*SP*). Loading vectors are represented by gray arrows.

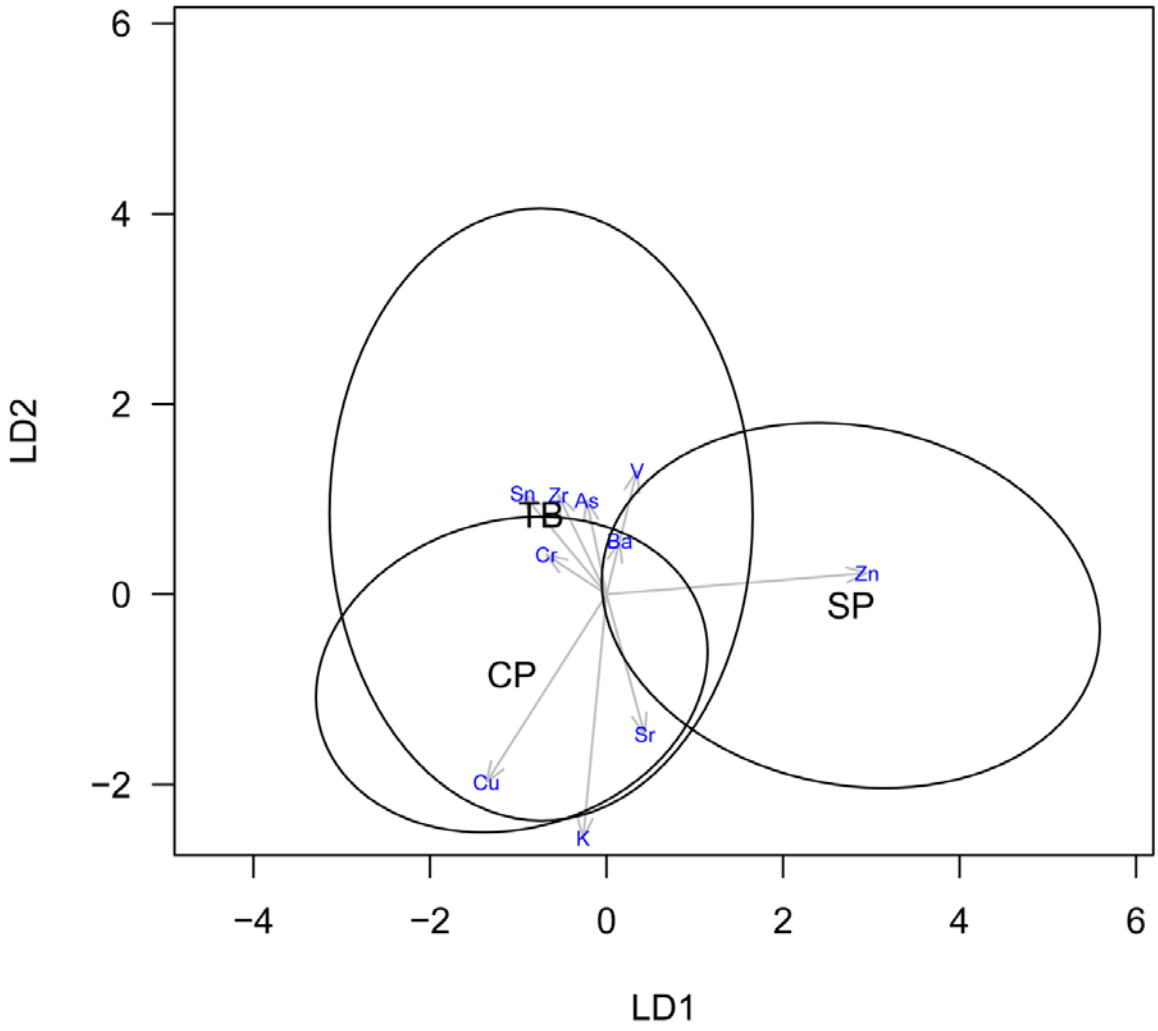

Figure 37F: LDA of southeastern muscovite database, using log-ratio transformed data compiled from the present study, Cocker (1992a) and Wood (1996). 95% confidence ellipses are constructed around the centroids of the Cherokee-Pickens district data (*CP*), Thomaston-Barnesville district data (*TB*) and Spruce Pine data (*SP*). Loading vectors are represented by gray arrows.

Table 3: DFA (LDA) success rates of muscovite source samples. DFA performed using standardized (std), log-transformed (log) and log-ratio transformed (log-r) data, with success determined by the validation techniques of resubstitution I, leave-one-out cross-validation (LOOCV), bootstrap resubstitution (BR), bootstrap cross-validation (BCV), optimism (O) and the .632 bootstrap (.632). All percentages represent the average success rate of 10,000 randomly-generated subsets of the data, with each group of data (*CP*, *TB* and *SP*) containing an equal number of samples, $n = 101$, for a total sample size of $N = 303$. Thus, using the .632 bootstrap validation method of the log-transformed data as an example, an average of approximately 252 of 303 samples were correctly reassigned to their known source when treated as unknowns.

	R	**LOOCV**	**BR**	**BCV**	**O**	**.632**
std	78.26	75.80	80.18	77.70	74.42	76.90
log	84.85	82.63	85.97	83.83	84.00	83.16
log-r	83.68	81.41	84.64	82.61	83.45	81.95

districts, most errors in reclassification likely stem from the model being unable to resolve the overlap between these two data fields. There should be less confusion associated with the reclassification of samples from the Spruce Pine data field, as the majority of the Spruce Pine data points plot away from those belonging to other data fields.

CHAPTER 8

PROPOSED SOURCE OF ETOWAH MUSCOVITE ARTIFACTS

Results of DFA and PCA of the Etowah Micas

Given the success rates for the discriminant function analysis (consistently in excess of 81% for the log-transformed and log-ratio transformed data), it can be argued that the discriminant model trained on the muscovite source data, while not perfect, is able to discriminate amongst district-scale sources fairly successfully. A relatively confident allocation of the Etowah muscovite artifact samples to proposed sources on the basis of that model alone should be possible, provided that the muscovite was acquired from one of those sources. However, the assumption that the artifacts must have come from a pegmatite within the Cherokee-Pickens, Thomaston-Barnesville, or Spruce Pine district cannot be verified given the number of districts and individual pegmatites for which the geochemical signatures of muscovite are simply not known. For example, an artifact plotting in the Spruce Pine data field is not necessarily indicative of a Spruce Pine source, as an unsampled Georgia district may possess a similar geochemical signature. It *is* reasonable to conclude that an artifact plotting *outside* the Spruce Pine data field is indicative of a non-Spruce Pine source, despite any inability to suggest an alternative source. However, additional considerations in the case of the Etowah mica artifacts (as will be discussed later) may allow for a reasonable suggestion of likely provenance.

The Etowah muscovite artifacts of sufficient thickness analyzed in the present investigation (from catalogue UWG-1017: 1027, 1311, 1332-1, 1350-1, 1350-2, 308-2, 308-4 and 308-5; from catalogue UWG-1019: 2430, 2518 and 3236) were thus allocated to potential sources on the basis of the discriminant model trained on the source samples; only the log-

transformed data has been utilized with respect to the Etowah artifacts, as discrimination using log-transformed data has been shown to yield the "correct" reclassification (stressing that the term "correct" is used only in relation to the geological samples of known source) more often than is obtained with other methods of data transformation. Figure 38A displays the predicted discriminant function scores (as calculated from the discriminant functions) for the Etowah mica artifacts plotted on the same axes as the source data from Figure 37B; Figure 38B removes the source data from the plot for visual simplification, displaying only the 95% confidence ellipses constructed about the centroids of the source data.

From the linear discriminant plots, it is apparent that a Spruce Pine source can be confidently ruled out for all but one of the Etowah mica artifacts (2430) which were analyzed. The predicted sources for the artifacts on the basis of the discriminant model, along with posterior probabilities, are listed in Table 4. All artifacts, with the exception of 2430, have been assigned to a Cherokee-Pickens district source by the model. Furthermore, these artifacts plot well within the 95% confidence ellipse constructed about the centroid of the Cherokee-Pickens district data, a trend also observed in PCA of the log-transformed artifact data (Figure 39). While the same artifacts assigned to a Cherokee-Pickens source also plot within the 95% confidence ellipse constructed about the centroid of the Thomaston-Barnesville district data, central limit theorem argues that the even dispersion about, and proximity to, the centroid of the Cherokee-Pickens data field is more indicative of a Cherokee-Pickens source, assuming that the artifacts come from the same single source.

Single Source Versus Multiple Sources?

Before more will be said about a potential source for the Etowah artifacts, it should be ascertained whether the data are consistent with a single source (i.e., a single pegmatite district,

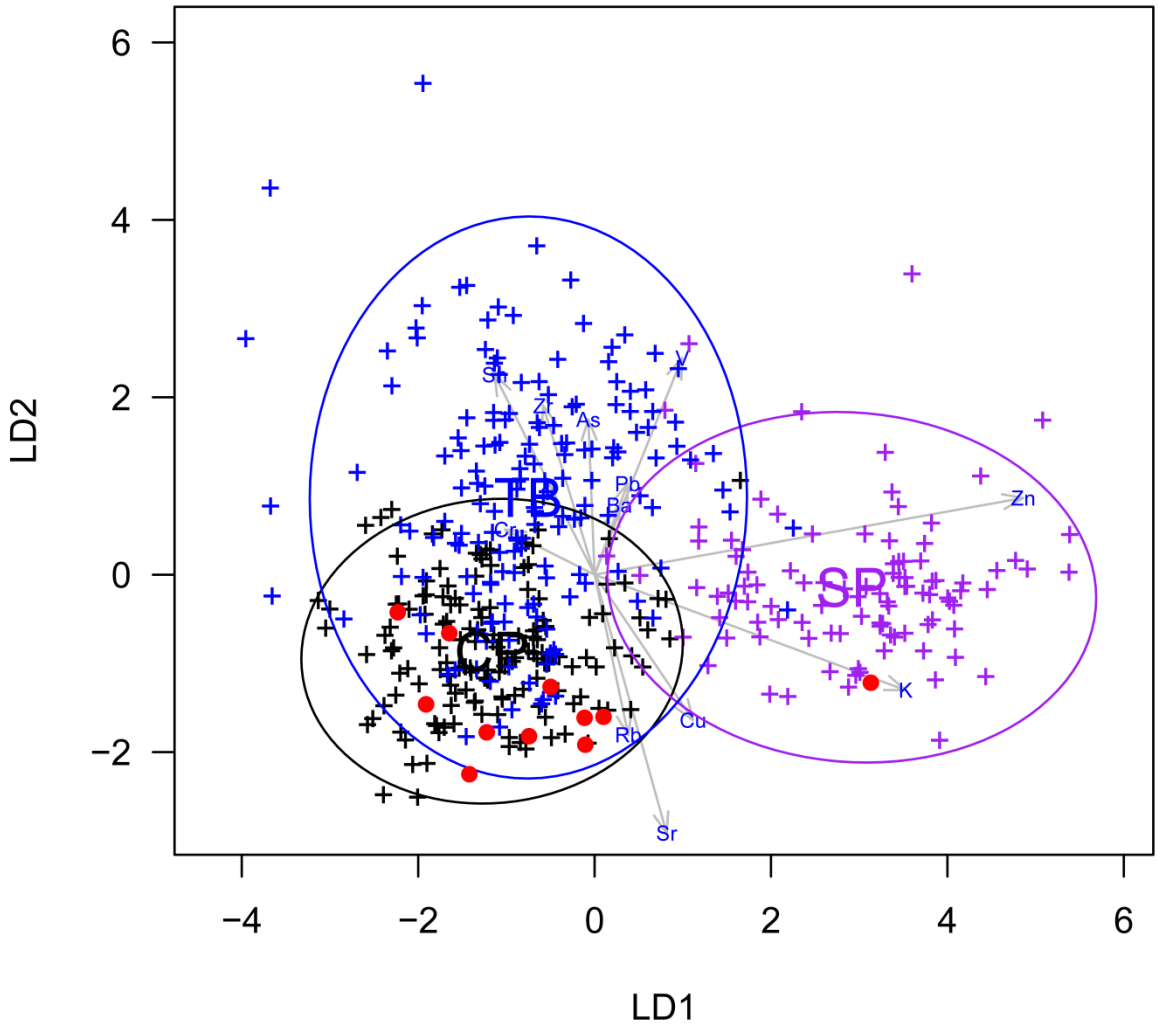

Figure 38A: LDA of southeastern muscovite database and Etowah artifacts, using log-transformed data compiled from the present study, Cocker (1992a) and Wood (1996). Black data points correspond to Cherokee-Pickens district data (*CP* at centroid of 95% confidence ellipse), blue data points correspond to Thomaston-Barnesville district data (*TB* at centroid of 95% confidence ellipse) and purple data points correspond to Spruce Pine data (*SP* at centroid of 95% confidence ellipse). Red data points represent muscovite artifact scores for the Etowah micas, as predicted by the discriminant functions calculated on the source data. Loading vectors are shown as gray arrows with blue text.

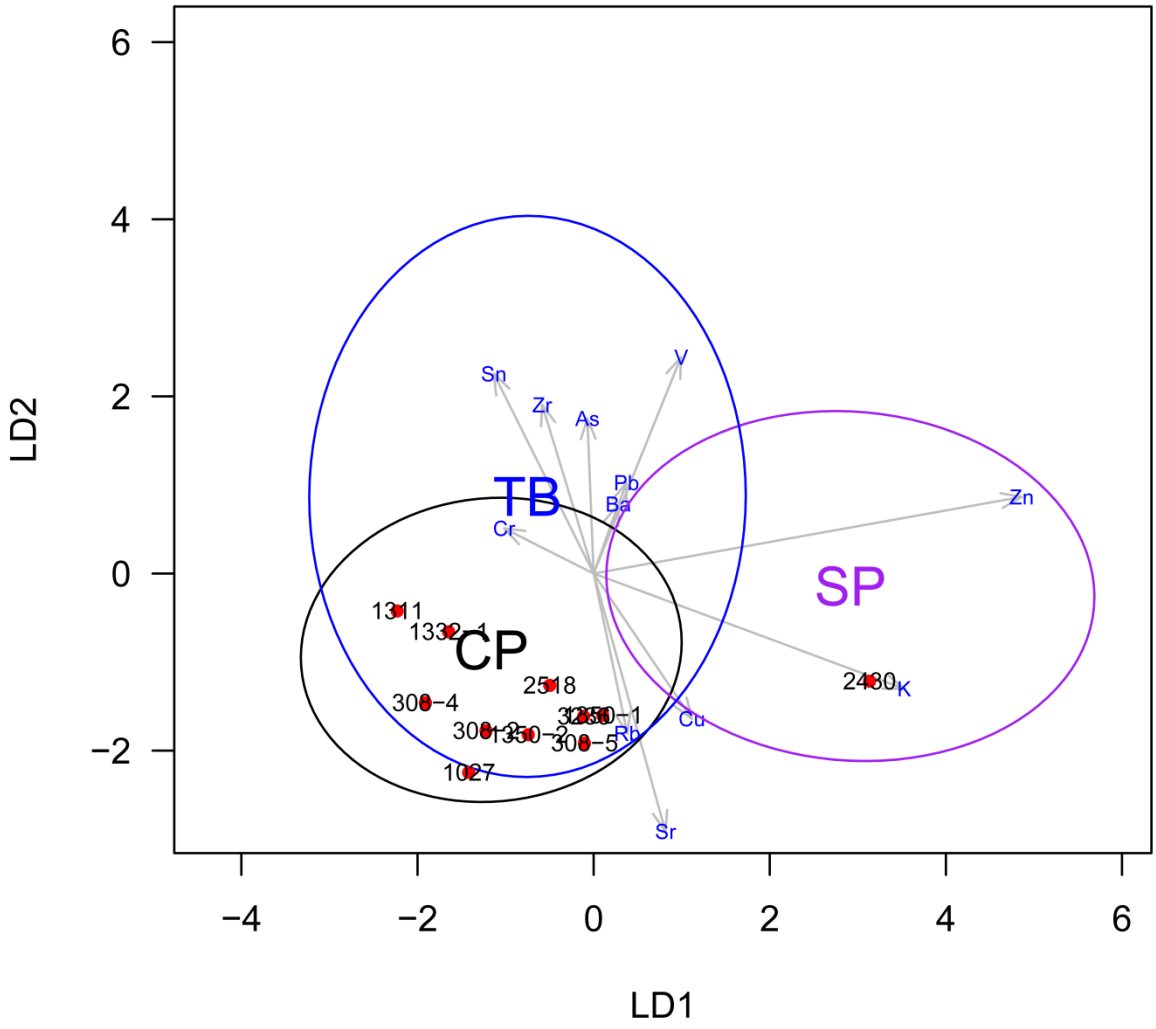

Figure 38B: Plot of the first two discriminant functions (LD1 and LD2) of muscovite data presented using log-transformed data compiled from the present study, Cocker (1992a) and Wood (1996). 95% confidence ellipses are constructed around the centroids of the Cherokee-Pickens district data (*CP*), Thomaston-Barnesville district data (*TB*) and Spruce Pine data (*SP*). Red data points represent muscovite artifact scores for the Etowah micas (labeled), as predicted by the discriminant functions calculated on the source data. Loading vectors are represented by gray arrows. Loading vectors are shown as gray arrows with blue text.

Table 4: Predicted source and posterior probabilities for the Etowah muscovite artifacts. Posterior probabilities should approach 1.00 with increasing likelihood that an artifact belongs to a given source group (Cherokee-Pickens, *CP*, Spruce Pine, *SP*, or Thomaston-Barnesville, *TB*), provided the artifact must belong to one of the specified groups.

Artifact		**Predicted**	**Posterior Probabilities (%)**		
Cat. #	Art. #	**Source**	CP	SP	TB
1017	1027	CP	98.19	< 0.01	1.81
1017	1311	CP	76.25	< 0.01	23.75
1019	2430	SP	0.02	99.96	0.02
1019	2518	CP	87.00	0.13	12.87
1019	3236	CP	90.89	0.49	8.62
1017	1332-1	CP	79.16	< 0.01	20.84
1017	1350-1	CP	89.38	1.18	9.44
1017	1350-2	CP	95.11	0.04	4.85
1017	308-2	CP	95.67	0.01	4.32
1017	308-4	CP	94.44	< 0.01	5.56
1017	308-5	CP	94.28	0.42	5.30

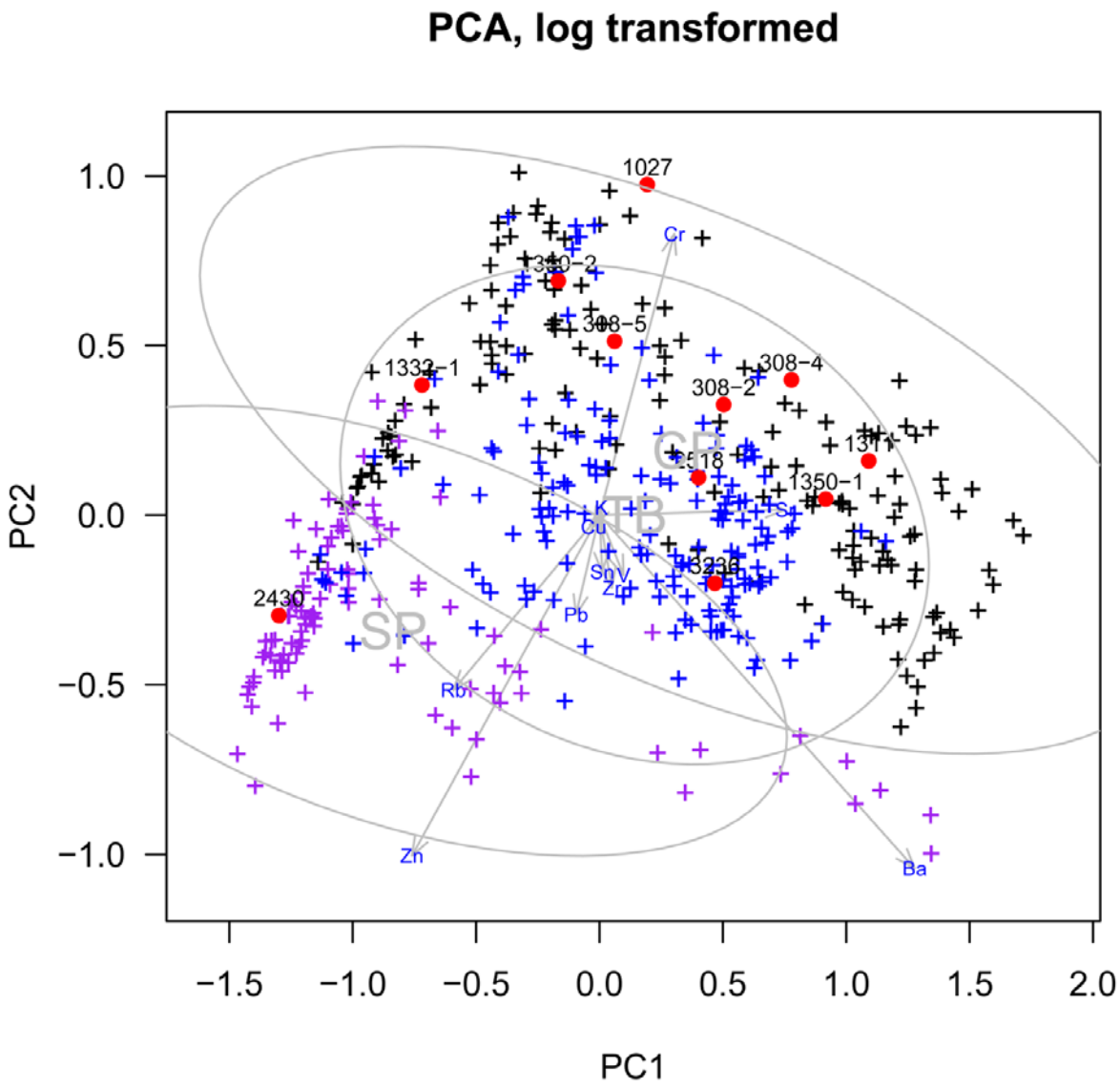

Figure 39: PCA of southeastern muscovite database and Etowah artifacts, using log-transformed data compiled from the present study, Cocker (1992a) and Wood (1996). Black data points correspond to Cherokee-Pickens district data (*CP* at centroid of 95% confidence ellipse), blue data points correspond to Thomaston-Barnesville district data (*TB* at centroid of 95% confidence ellipse) and purple data points correspond to Spruce Pine data (*SP* at centroid of 95% confidence ellipse). Red data points represent muscovite artifact scores for the Etowah micas.

or even a single pegmatite) or multiple sources. The fairly tight clustering of all artifact scores (with the exception of 2430) within Figure 38 and Figure 39 suggest that a single-district source is entirely possible for that cluster of artifacts. Similar visual descriptions (see Appendix D) of all artifacts within that cluster also support the possibility of a single source; all artifacts display the same typical silver coloration, with light-brown discoloration of the sheets resulting from staining by dirt/soil of a similar nature with or without an additional reddish-brown clay stain (most obvious in artifacts 1350-1, 2518 and 3236). Most of these artifacts, with the exception of 308 and 1350-1, lack any "black spots" (typically Fe-oxides) commonly referenced in the literature. Differences in the degree of staining or spotting of muscovite books within a single pegmatite, however, are frequently encountered in the historic literature; not all samples collected from a single pegmatite will be stained, and not all books will contain spots. Thus, a single source for these geochemically similar artifacts is not only possible, but fairly likely, at least on the district scale.

Artifact 2430, the lone "outlier" identified on a geochemical basis in the discriminant function and principal component plots, also differs visually from the previously discussed main grouping of artifacts. Unlike the other artifacts, 2430 displays a fairly strong green coloration. Given that muscovite color tends to be uniform within a pegmatite (unless there are multiple shoots within the pegmatite), it is very unlikely that artifact 2430 represents muscovite taken from the same locality as any of the other artifacts. The extreme geochemical difference between this artifact and the others makes the possibility that 2430 may have come from a separate shoot within the same pegmatite as the others unlikely as well.

While differences in coloration and geochemical signature effectively preclude the possibility that artifact 2430 may be sourced to the same pegmatite as any of the other Etowah

micas, it is not definitive proof that it comes from a different district. While 2430 apparently plots in the Spruce Pine field, far from the other artifacts in either the Cherokee-Pickens or Thomaston-Barnesville district, it must be remembered how these fields were defined. For DFA, it was necessary to combine the separate geochemical Holly Springs and Ball Ground fields into a single Cherokee-Pickens field, and the Indian Grave field and main Thomaston-Barnesville field into a single Thomaston-Barnesville field. By nature of displaying distinctly different geochemical trends approaching those of rare-element enrichment, some of the Ball Ground pegmatites and all of the Indian Grave pegmatites would plot outside the 95% confidence ellipses drawn about the centroids of their respective districts as a whole, since data from within the Cherokee-Pickens and Thomaston-Barnesville districts tend to be dominated by samples which do not display this enrichment. When the 95% confidence ellipses about the centroid of the district data from the PCA in Figure 39 are reconstructed on the basis of separate geochemical fields within the districts (Figure 40), it is found that the more highly fractionated Indian Grave pegmatite samples and Ball Ground samples enriched in Rb and Zn plot well within the data field defined by the Spruce Pine samples (which tend to be more highly fractionated than pegmatites from the other districts, on the basis of enrichment in Rb, Sn and Zn), and in close proximity to artifact 2430. Thus, artifact 2430 may originate from one of these (potentially) highly-fractionated rare-element enriched pegmatites within either the Cherokee-Pickens or Thomaston-Barnesville districts. It should be noted that there are two such pegmatites (the Cochran mine and J.L. Mullinax prospect) in the rare-element enriched beryl-bearing pegmatites of the Ball Ground field from which green mica has been observed.

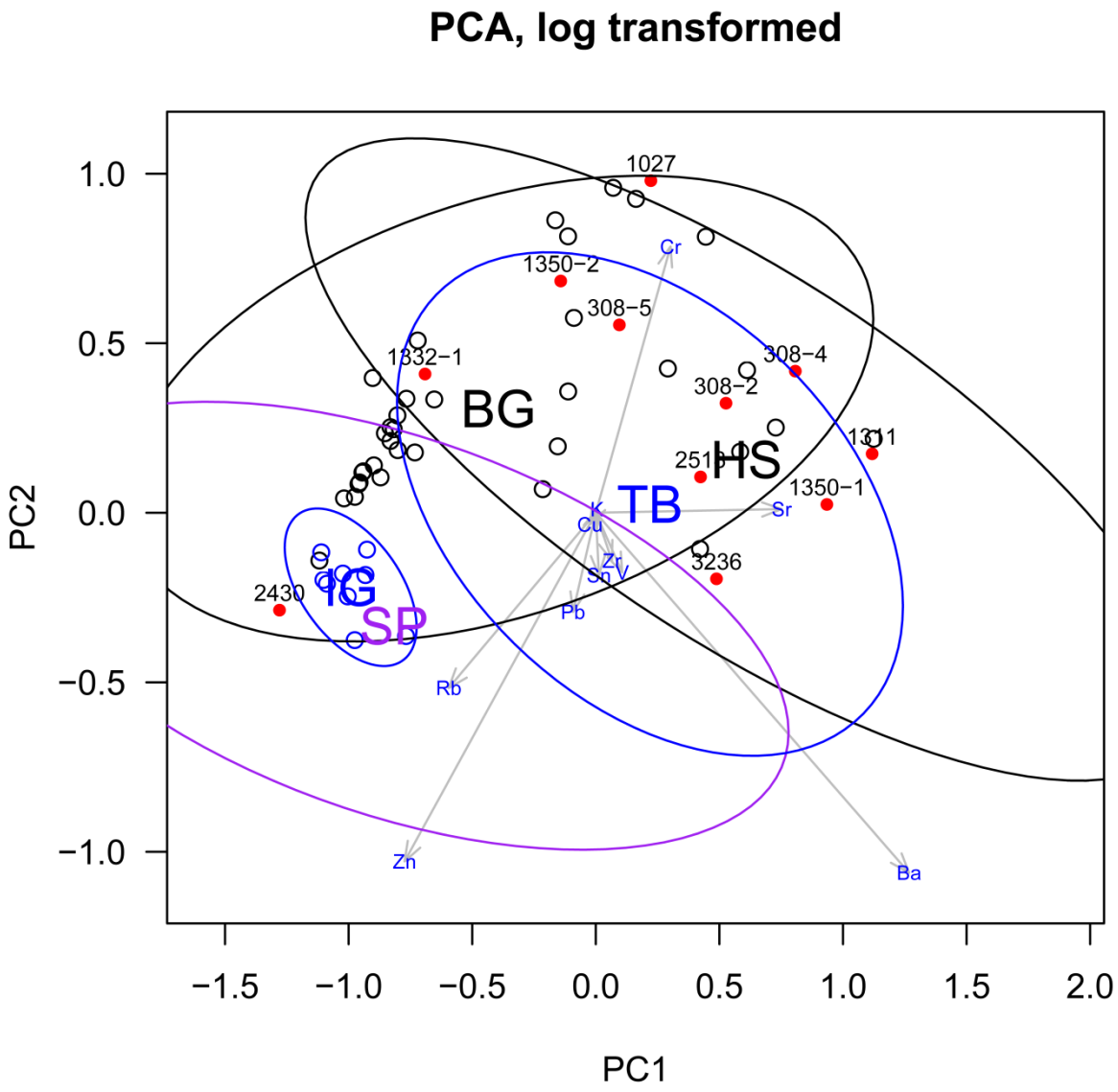

Figure 40: PCA of southeastern muscovite database and Etowah artifacts, using log-transformed data compiled from the present study, Cocker (1992a) and Wood (1996). Black data fields correspond to Cherokee-Pickens district data (open circles for Ball Ground, *BG*), blue data fields correspond to Thomaston-Barnesville district data (open circles for the Indian Grave field, *IG*) and the purple data field corresponds to Spruce Pine data (*SP*). Red data points represent muscovite artifact scores for the Etowah micas.

Georgia's Cherokee-Pickens Pegmatite District as a Potential Source

With this information, the possibility arises that *all* of the Etowah muscovite artifacts (including artifact 2430) may originate from within a single district. However, the geochemical data alone is insufficient for making a definitive provenance determination; while the data appear to more closely resemble that of a Cherokee-Pickens source, a Thomaston-Barnesville source cannot be entirely ruled out. The suite of mineral inclusions identified in the Etowah micas (biotite, tourmaline, pyrite and possibly magnetite) act as additional discriminating variables. In comparing mineral inclusion data from the historic literature (Appendix B) with the suite of inclusions identified in the Etowah micas, it is found that biotite and magnetite tend to be very common inclusions and are thus not particularly helpful discriminators; tourmaline and pyrite, however, tend to be found much less frequently as inclusions within muscovite. Tourmaline inclusions in muscovite were not observed in any of the 37 mines (0%) within the Thomaston-Barnesville district for which inclusion data are available, and were only identified as accessory pegmatite minerals in seven of the 53 pegmatites (~13%) for which accessory mineral information was available; pyrite inclusions were found at only two (~5%) of these locations as mineral inclusions, and not as an accessory pegmatite mineral (0%). In the Cherokee-Pickens district, tourmaline inclusions have been identified at four of the 33 mines (~12%) for which mineral inclusion data are available, and as an accessory mineral in 26 of 30 pegmatites (~87%) for which information pertaining to accessory pegmatite minerals was available. While pyrite was not mentioned specifically as an inclusion within the muscovite at any of these locations, it is observed as an accessory mineral within at least one pegmatite in both the Holly Springs and Ball Ground fields.

The geochemical data, along with the mineral inclusion data, suggest the possibility that the muscovite artifacts originated from within a single, potentially local, district. It is often difficult to confidently propose an origin when a large number of potential sources have yet to be characterized in sufficient detail. At the very least, recognizing that there is much future work remaining to be done, a new logical working hypothesis can be established to guide future investigations. In the case of the Etowah muscovite artifacts, this new hypothesis would replace the Spruce Pine assumption of source with an assumed local Cherokee-Pickens source, the validity of which would then need to be assessed through sampling from any of the presently unsampled districts. The local-source hypothesis is based on the following arguments:

(1) The Cherokee-Pickens pegmatite district, where pegmatites of the Holly Springs field occur within approximately 20 – 30 km of the Etowah mounds, is closer to the site than any other significant described occurrence of pegmatitic muscovite. The location of the Holly Springs field pegmatites within only a few kilometers of the banks of the Etowah River would have required Native Americans simply to follow the river to the northeast in search of muscovite, ultimately leading them to the pegmatites of the Ball Ground field as well. In addition, while no evidence of prehistoric mica mining has survived (if it existed to begin with) from the Cherokee-Pickens district, Thomas (1891) (and also Ferguson [1974], though Ferguson [1974] has incorrectly placed the mine in Gordon Co.) reference at least one prehistoric mica mine in Gilmer Co. from the area between Georgia's Cherokee-Pickens and North Georgia pegmatite districts. Prehistoric Native Americans may have had a familiarity with the Cherokee-Pickens district mica deposits as well, as they were actively mining at least one pegmatite in the surrounding area.

(2) The Etowah artifacts display a strong geochemical affiliation with muscovite from the Cherokee-Pickens district; all but one of the artifacts analyzed plot fairly uniformly about, and within close proximity of, the centroid of the Cherokee-Pickens data at the district scale.

(3) The single green mica artifact (2430) which does not plot within the Cherokee-Pickens data field at the district scale does plot within the rare-element enriched Ball Ground field when data are grouped at the sub-district scale; green muscovite has also been observed in at least two of the rare-element enriched beryl-bearing pegmatites within the Ball Ground field.

(4) None of the Etowah artifacts display coloration or contain mineral inclusions inconsistent with a Cherokee-Pickens source.

CHAPTER 9

CONCLUSION

Summary of Results

Occurrences of pegmatitic muscovite are both numerous and widespread throughout the southeastern United States. A Spruce Pine source for archaeological pegmatitic muscovite is often assumed, despite the lack of any focused attempts at testing such a hypothesis or consideration for the exploitation of more local resources. The lack of archaeometric provenance investigations with respect to mica artifacts may in part be a result of the lack of availability of geochemical data for an overwhelming majority of pegmatitic muscovite sources, as muscovite-class pegmatites have until only recently been largely ignored in the geological literature in favor of the relatively few occurrences of rare-element pegmatites of economic interest.

Principal components analysis and discriminant function analysis of the geochemical data compiled from the only available sources of trace element compositions of southeastern pegmatitic muscovite (Gunow & Bonn [1989], Cocker [1992a], Wood [1996] and the present study) suggest that, despite geochemical similarities between muscovite from similarly fractionated or derived pegmatite fields within districts (i.e., muscovite-class versus rare-element-enriched muscovite class), the prospect of obtaining inter-district discrimination on the basis of trace elements shows considerable promise.

Conclusive statements regarding provenance should be avoided where such a small percentage of possible sources have been tested. The information presented in this investigation suggests that (1) a distant Spruce Pine source cannot be supported for the muscovite artifacts

from the Etowah mounds in Cartersville, Georgia, and (2) that a local Cherokee-Pickens source cannot be excluded on either a geochemical or mineral-inclusion basis. The proximity of the Etowah mounds to the Cherokee-Pickens pegmatite district, the strong geochemical similarity of these artifacts to muscovite samples collected from both the Holly Springs and Ball Ground pegmatite fields within the district, and the prevalence of Cherokee-Pickens muscovite which displays similar suites of mineral inclusions and coloration, may be used to justify a new working hypothesis of the utilization of local pegmatitic muscovite resources during Etowah's Mississippian period occupation. It is this hypothesis that future investigations should aim to test in favor of the Spruce Pine hypothesis.

Future Work

Much work remains to be done regarding adequate characterization of the muscovite-class pegmatites with respect to more aspects than simply muscovite geochemistry or archaeometry, though several recent studies (e.g., Gunow & Bonn 1989, Cocker 1992a, Wood 1996, and the present investigation) showcase the use of muscovite geochemistry in assessing the rare-element potential of pegmatites. Of particular appeal for future research is the applicability of muscovite geochemical data as a viable means for assessing the economic potential of subsurface pegmatites; Cocker (1992a:20) asserts that "[o]f the common minerals present in a typical pegmatite, muscovite is the only mineral structurally favorable to include a variety of the incompatible trace elements as substitutions in its structure" and is often the only surface indicator of an unexposed mica-bearing pegmatite (be it muscovite-class or rare-element-class) due to its general resistance to weathering. Thus, the generation of more geochemical data on pegmatitic muscovite has the potential to benefit multiple seemingly unrelated fields.

Focusing on the archaeological aspects of such characterization, the Etowah site is only one of several Mississippian period sites in the southeastern United States in which muscovite artifacts have been found. Provenance investigations of artifacts from the Moundville site in Alabama, as well as smaller sites throughout the Carolinas, may argue for the utilization of local resources as well. There may also be applicability of the southeastern data to studies of the Ohio Valley micas, as the southern Appalachians represent the closest sources of pegmatitic muscovite to the Ohio Valley.

REFERENCES

Aitchison, J. (1986). The statistical analysis of compositional data. London: Chapman & Hall.

Aitchison, J., Barceló-Vidal, C., Pawlowsky-Glahn, V. (2002). Some comments on compositional data analysis in archaeometry, in particular the fallacies in Tangri and Wright's dismissal of logratio analysis. Archaeometry, 44, 295-304.

Alden, J.R., Minc, L., Lynch, T.F. (2006). Identifying the sources of Inka period ceramics from northern Chile: results of a neutron activation study. Journal of Archaeological Science, 33, 575-594.

Attanasio, D., Armiento, G., Brilli, M., Emanuele, M.C., Platania, R., Turi, B. (2000). Multi-method marble provenance determinations: the Carrara marbles as a case study for the combined use of isotopic, electron spin resonance and petrographic data. Archaeometry, 42(2), 257-272.

Attanasio, D., De Marinis, G., Pallecchi, P., Platania, R., Rocchi, P. (2003). An EPR and isotopic study of the marbles of the Trajan's arch at Ancona: an example of alleged Hymettian provenance. Archaeometry, 45(4), 553-568.

Attanasio, D., Platania, R., Rocchi, P. (2005). White marbles in Roman architecture: electron paramagnetic resonance identification and bootstrap assessment of the results. Journal of Archaeological Science, 32, 311-319.

Baby, R.S., Langlois, S.M. (1979). Seip Mound State Memorial: Nonmortuary Aspects of Hopewell. In D.S. Brose & N. Greber (Eds.), Hopewell Archaeology: The Chillicothe Conference (pp.16-18). Kent, Ohio: Kent State University Press.

Bartlett, M.L., Neff, H., McAnany, P.A. (2000). Differentiation of Clay Resources on a Limestone Plain: The Analysis of Clay Utilization during the Maya Formative at K'axob Belize. Geoarchaeology, 15(2), 95-133.

Baxter, M.J. (1989). Multivariate analysis of data on glass compositions: a methodological note. Archaeometry, 31(1), 45-53.

Baxter, M.J. (1992). Statistical analysis of chemical compositional data and the comparison of analyses. Archaeometry, 34(2), 267-277.

Baxter, M.J. (1994). Stepwise Discriminant Analysis in Archaeometry: a Critique. Journal of Archaeological Science, 21, 659-666.

Baxter, M.J. (1999). Detecting multivariate outliers in artifact compositional data. Archaeometry, 41(2), 321-338.

Baxter, M.J. (2006). A review of supervised and unsupervised pattern recognition in archaeometry. Archaeometry, 48(4), 671-694.

Baxter, M.J. (2008). Mathematics, statistics and archaeometry: the past 50 years or so. Archaeometry, 50(6), 968-982.

Baxter, M.J. (2009). Archaeological data analysis and fuzzy clustering. Archaeometry, 51(6), 1035-1054.

Baxter, M.J., Freestone, I.C. (2006). Log-ratio compositional data analysis in archaeometry. Archaeometry, 48(3), 511-531.

Baxter, M.J., Beardah, C.C., Papageorgiou, I., Cau, M.A., Day, P.M., Kilikoglou, V. (2008). Archaeometry, 50(1), 142-157.

Beier, T., Mommsen, H. (1994). Modified Mahalanobis filters for grouping pottery by chemical composition. Archaeometry, 36(2), 287-306.

Bimson, M., La Neice, S., Leese, M. (1982). The characterisation of mounted garnets. Archaeometry, 24(1), 51-58.

Borghi, A., Vaggelli, G., Marcon, C., Fiora, L. (2009). The Piedmont white marbles used in antiquity: an archaeometric distinction inferred by a miner-petrographic and C-O stable isotope study. Archaeometry, 51(6), 913-931.

Cameron, E.N., Jahns, R.H., McNair, A.H., Page, L.R. (1949). Internal Structure of Granitic Pegmatites. Monograph 2, Economic Geology. Urbana, Illinois: Economic Geology Publishing Co.

Capedri, S., Venturelli, G. (2004). Accessory minerals as tracers in the provenancing of archaeological marbles, used in combination with isotopic and petrographic data. Archaeometry, 46(4), 517-536.

Catalano, I.M., Genga, A., Laganara, C., Laviano, R., Mangone, A., Marano, D., Traini, A. (2007). Lapis lazuli usage for blue decoration of polychrome painted glazed pottery: a recurrent technology during the Middle Ages in Apulia (Southern Italy). Journal of Archaeological Science, 34, 503-511.

Černỳ, P. (1982). Anatomy and classification of granitic pegmatites. In P. Černỳ (Ed.), Granitic Pegmatites in Science and Industry, Mineralogical Association of Canada, Short Course Handbook, vol. 8 (pp.1-39).

Černỳ, P., Burt, D.M. (1984). Paragenesis, crystallochemical characteristics, and geochemical evolution of micas in granite pegmatites. In S.W. Bailey (Ed.), Reviews in Mineralogy, vol. 13: Micas (pp.257-297). Mineralogical Society of America.

Childress, D.H. (2007). The Mystery of the Olmecs. Kempton, Illinois: Adventures Unlimited Press.

Cocker, M.D. (1991). Geochemical zoning in muscovites from the Thomaston-Barnesville pegmatite district, Georgia. Geological Society of America Abstracts with Programs, 23(1), 17.

___ (1992a). Geochemistry and economic potential of pegmatites in the Thomaston-Barnesville district, Geologic Report 7. Atlanta: Georgia Geologic Survey.

___ (1992b). Enrichment of trace elements in rare-metal bearing pegmatites of the muscovite class: examples from the Jasper, Thomaston-Barnesville, Troup and Cherokee-Pickens districts in Georgia. Geological Society of America Abstracts with Programs, 24(7), 216.

___ (1992c). Muscovite geochemistry and rare-metal potential of pegmatites in the Thomaston-Barnesville pegmatite district, Georgia. Geological Society of America Abstracts with Programs, 24(2), 9.

___ (1994). Muscovite geochemistry and rare-metal potential of pegmatites in the Troup County pegmatite district, Georgia. Geological Society of America Abstracts with Programs, 26(4), 8.

Craddock, P.T., Cowell, M.R., Leese, M.N., Hughes, M.J. (1983). The trace element composition of polished flint axes as an indicator of source. Archaeometry, 25(2), 135-163.

Dickens, R.S. Jr. (1976). Cherokee Prehistory: The Pisgah Phase in the Appalachian Summit Region. Knoxville: University of Tennessee Press.

Efron, B. (1979). Bootstrap Methods: Another Look at the Jackknife. Annals of Statistics, 7, 1-26.

Erdem, A., Çilingiroğlu, A., Giakoumaki, A., Castanys, M., Kartsonaki, E., Fotakis, C., Anglos, D. (2008). Characterization of Iron age pottery from eastern Turkey by laser-induced breakdown spectroscopy (LIBS). Journal of Archaeological Science, 35, 2486-2494.

Ferguson, L.G. (1974). Prehistoric Mica Mines in the Southern Appalachians. South Carolina Antiquities, 6(2), 211-7.

Finch, J. (1963). A colorimetric classification of Australian pegmatitic muscovite. American Mineralogist, 48, 525-554.

Finch, J., Gainsforn, A.R., Tennant, W.C. (1982). Polarized optical absorption and ^{57}Fe Mossbauer study of pegmatitic muscovite. American Mineralogist, 67, 59-68.

Franz, G., Morteani, G. (1984). The Formation of Chrysoberyl in Metamorphosed Pegmatites. Journal of Petrology, 25(1), 27-52.

Furcron, A.S., Munyan, A.C., Peyton, G., Smith, R.W. (1938). Mineral Resources of Georgia. Georgia: Division of Mines, Mining and Geology.

Furcron, A.S., Teague, K.H. (1943). Mica-Bearing Pegmatites of Georgia. The Geological Survey, Bulletin No. 48. Atlanta: Department of Mines, Mining and Geology.

Galpin, S.L. (1915). A Preliminary Report on the Feldspar and Mica Deposits of Georgia. Bulletin No. 30. Atlanta: Geological Survey of Georgia.

The Geological Survey (1941). Directory of Georgia Mineral Producers. Atlanta: Georgia Department of Mines, Mining and Geology.

___ (1943). Directory of Georgia Mineral Producers. Atlanta: Georgia Department of Mines, Mining and Geology.

___ (1950). Directory of Georgia Mineral Producers (6th Edition). Atlanta: Georgia Department of Mines, Mining and Geology.

___ (1954). Directory of Georgia Mineral Producers (8th Edition). Atlanta: Georgia Department of Mines, Mining and Geology.

___ (1956). Directory of Georgia Mineral Producers (9th Edition). Atlanta: Georgia Department of Mines, Mining and Geology.

___ (1961). Directory of Georgia Mineral Producers (11th Edition). Atlanta: Georgia Department of Mines, Mining and Geology.

___ (1963). Directory of Georgia Mineral Producers (12th Edition). Atlanta: Georgia Department of Mines, Mining and Geology.

___ (1968). Directory of Georgia Mineral Producers (15th Edition). Atlanta: Georgia Department of Mines, Mining and Geology.

Gnanadesikan, R. (1997). Methods for statistical data analysis of multivariate observations. New York: Wiley-Interscience.

Gordiyenko, V.V. (1975). Geochemistry of the processes of pegmatite formation and muscovite generation. In Muscovite Pegmatites of the U.S.S.R. (pp.107-117). Leningrad: Nauka.

Gordiyenko, V.V., Leonova, V.A. (Eds.) (1976). Mica-bearing Pegmatites of Northern Karelia. Leningrad: Nedra.

Goren, Y., Mommsen, H., Klinger, J. (2010). Nondestructive Provenance Study of Cuneiform Tablets using Portable X-Ray Fluorescence (pXRF). Journal of Archaeological Science, in press.

Grave, P., Lisle, L., Maccheroni, M. (2005). Multivariate comparison of ICP-OES and PIXE/PIGE analysis of east Asian storage jars. Journal of Archaeological Science, 32, 885-896.
Gresens, R.L., Stensrud, H.L. (1977). More data on red muscovite. American Mineralogist, 62, 1245-1251.

Griffitts, W.R., Olson, J.C. (1953a). Mica Deposits of the Southeastern Piedmont. Part 5. Shelby-Hickory District of North Carolina; Part 6. Outlying Deposits in North Carolina. United States Geological Survey Professional Paper 248 – D. Washington: United States Government Printing Office.

Griffitts, W.R., Olson, J.C. (1953b). Mica Deposits of the Southeastern Piedmont. Part 7. Hartwell District, Georgia and South Carolina; Part 8. Outlying Deposits in South Carolina. United States Geological Survey Professional Paper 248 – E. Washington: United States Government Printing Office.

Griffitts, W.R., Jahns, R.H., Lemke, R.W. (1953). Mica Deposits of the Southeastern Piedmont. Part 3. Ridgeway-Sandy Ridge District, Virginia and North Carolina; Part 4. Outlying Deposits in Virginia. United States Geological Survey Professional Paper 248 – C. Washington: United States Government Printing Office.

Gunow, A.J. (1987). The nature and origin of trace element variation in pegmatites, Cherokee-Pickens district, Georgia. Geological Society of America Abstracts with Programs, 19(2), 87-88.

Gunow, A.J, Bonn, G.N. (1989). The geochemistry and origin of pegmatites, Cherokee-Pickens district, Georgia. Bulletin 103. Atlanta: Georgia Geologic Survey.

Hall, M.E. (2004). Pottery production during the Late Jomon period: insights from the chemical analyses of Kasori B pottery. Journal of Archaeological Science, 31, 1439-1450.

Hally, D.J., Langford, J.B. Jr. (1988). Mississippi Period Archaeology of the Georgia Valley and Ridge Province. University of Georgia Laboratory of Archaeology Series Report No. 25, Georgia Archaeological Research Design Paper, No. 4.

Heidke, J.M., Miksa, E.J. (2000). Correspondence and discriminant analyses of sand and sand temper compositions, Tonto Basin, Arizona. Archaeometry, 42(2), 273-299.

Hein, A., Day, P.M., Quinn, P.S., Kilikoglou, V. (2004). The geochemical diversity of neogene clay deposits in Crete and its implications for provenance studies of Minoan pottery. Archaaeometry, 46(3), 357-384.

Heinrich, E. Wm., Olson, J.C. (1953). Mica Deposits of the Southeastern Piedmont. Part 11. Alabama District. Geological Survey Professional Paper 248 – G. Washington: United States Government Printing Office.

Heinrich, E. Wm., Klepper, M.R., Jahns, R.H. (1953). Mica Deposits of the Southeastern Piedmont. Part 9. Thomaston-Barnesville District, Georgia; Part 10. Outlying Deposits in

Georgia. United States Geological Survey Professional Paper 248 – F. Washington: United States Government Printing Office.
Holmes, L.L., Harbottle, G., Blanc, A. (1994). Compositional characterization of French limestone: a new tool for art historians. Archaeometry, 36(1), 25-39.

Holmes, W.H. (1919). Mica Mines. In Handbook of Aboriginal American Antiquities, Part I: Introductory, the Lithic Industries (pp.241-252). Bureau of American Ethnology, Bulletin 60. Washington, D.C.: Smithsonian Institution.

Iñañez, J.G., Speakman, R.J., Buxeda i Garrigós, J., Glascock, M.D. (2008). Chemical characterization of majolica from 14th – 18th century production centers on the Iberian Peninsula: a preliminary neutron activation study. Journal of Archaeological Science, 35, 425-440.

Jahns, R.H., Lancaster, F.W. (1950). Physical Characteristics of Commercial Sheet Muscovite in the Southeastern United States. Geological Survey Professional Paper 225. Washington: United States Government Printing Office.

Jahns, R.H., Griffitts, W.R., Heinrich, E.W. (1952). Mica Deposits of the Southeastern Piedmont. Part 1. General Features. Geological Survey Professional Paper 248 – A. Washington: United States Government Printing Office.

Jolliff, B.L., Papike, J.J., Shearer, C.K. (1987). Fractionation trends in mica and tourmaline as indicators of pegmatite internal evolution: Bob Ingersoll pegmatite, Black Hills, South Dakota. Geochimica et Cosmochimica Acta, 51, 519-534.

___ (1992). Petrogenetic relationships between pegmatite and granite based on geochemistry of muscovite in pegmatite wall zones, Black Hills, South Dakota, USA. Geochimica et Cosmochimica Acta, 56, 1915-1939.

Judd, D.B. (1945). Journal of Research of the National Bureau of Standards, 35, 245.

Keel, B.C. (1967). Garden Creek Mound, HW^{O}2, Haywood County, North Carolina. Abstracts of Papers, Society for American Archaeology. The University of Michigan, Ann Arbor.

Kennett, D.J., Anderson, A.J., Cruz, M.J., Clark, G.R., Summerhayes, G.R. (2004). Geochemical characterization of Lapita pottery via inductively coupled plasma-mass spectrometry (ICP-MS). Archaeometry, 46(1), 35-46.

Kerr, W.C. (1875). Report of the Geological Survey of North Carolina: Physical Geography, resumé, economical geology. North Carolina Geological Survey, 1, 325 pp.

Kerr, W.C. (1880). The mica veins of North Carolina. Transactions of the American Institute of Mining Engineers, 8, 457-462.

Kesler, T.L., Olson, J.C. (1942). Muscovite in the Spruce Pine District, North Carolina. Strategic Minerals Investigations, 1942, Bulletin 936-A. Washington: United States Government Printing Office.

King, A. (2001). Excavations at Mound B, Etowah: 1954 – 1958. University of Georgia Laboratory of Archaeology Series Report No. 37.

King, A. (2003). Etowah: The Political History of a Chiefdom Capital. Tuscaloosa: The University of Alabama Press.

Klein, C. (2002). Manual of Mineral Science (22nd Edition). United States: John Wiley & Sons, Inc.

Kretz, R. (1983). Symbols of rock-forming minerals. American Mineralogist, 68, 277-279.

Larson, L.H. Jr. (1971). Archaeological Implications of Social Stratification of the Etowah Site, Georgia. In J.A. Brown (Ed.), Approaches to the Social Dimensions of Mortuary Practices, pp. 58-67. Society for American Archaeology, Memoir 25.

Laul, J.C., Lepel, E.A. (1987). Rare Earth Element Patterns in Biotite, Muscovite and Tourmaline Minerals. Journal of Radioanalytical and Nuclear Chemistry, 112(2), 461-471.
Leese, M.N. (1988). Statistical treatment of stable isotope data. In N. Herz & M. Waelkens (Eds.), Classical marble: geochemistry, technology, trade. NATO ASI. E, 153. Dordrecht: Kluwer Academic Publishers.

Leese, M.N., Main, P.L. (1994). The efficient computation of unbiased Mahalanobis distances and their interpretation in archaeometry. Archaeometry, 36(2), 307-316.

Lester, J.G. (1946). Inclusions in Muscovite from Mitchell Creek Mine, Upson County, Georgia. American Mineralogist, 31, 77-81.

Lemke, R.W., Jahns, R.H., Griffitts, W.R. (1952). Mica Deposits of the Southeastern Piedmont. Part 2. Amelia District, Virginia. United States Geological Survey Professional Paper 248 – B. Washington: United States Government Printing Office.

London, D. (2008). Pegmatites. The Canadian Mineralogist, Special Publication 10. Mineralogical Association of Canada.

Long, S. (1971). Mines and Prospects of the Chattahoochee-Flint Area, Georgia. Athens: The University of Georgia Institute of Community and Area Development.

Manuylova, M.M., Petrov, L.L., Rybakova, M.M., Sokolov, Yu.M., Shmakin, B.M. (1966). Distribution of alkali metals and beryllium in pegmatite minerals from the North Baikalian pegmatite belt. Geokhimiya, 410-432.

Margolin, P.R. (2000). The Sink Hole at Bandana: An Historic Blue Ridge Mica Mine Reveals its Past. North Carolina Archaeology, 49, 43-58.

McCallie, S.W. (1910). A Preliminary Report on the Mineral Resources of Georgia. Bulletin No. 23. Atlanta: Geological Survey of Georgia.
Mello, E., Monna, D., Oddone, M. (1988). Discriminating sources of Mediterranean marbles: a pattern recognition approach. Archaeometry, 30(1), 102-108.

Mills, P.R., Lundblad, S.P., Field, J.S., Carpenter, A.B., McElroy, W.K., Rossi, P. (2010). Geochemical sourcing of basalt artifacts from Kaua'I, Hawaiian Islands. Journal of Archaeological Science, 37, 3385-3393.

Mills, W.C. (1922). Exploration of the Mound City Group. Ohio Archaeological and Historical Society Quarterly, 31, 423-584.

Mirti, P., Zelano, V., Aruga, R., Ferrara, E., Appolonia, L. (1990). Roman pottery from *Augusta Praetoria* (Aosta, Italy): a provenance study. Archaeometry, 32(2), 163-175.

Montana, N., Iliopoulos, I., Tardo, V., Greco, C. (2009). Petrographic and Geochemical Characterization of Archaic-Hellenistic Tableware Production at Solunto, Sicily. Geoarchaeology, 24(1), 86-110.

Moorehead, W.K. (1932). Exploration of the Etowah site in Georgia. In W.K. Moorehead (Ed.), The Etowah Papers. New Haven: Yale University Press.

Neff, H. (1994). RQ-mode principal components analysis of ceramic compositional data. Archaeometry, 36(1), 115-130.

Nesse, W.D. (2000). Introduction to Mineralogy. New York: Oxford University Press, Inc.

Oksanen, J., Blanchet, F.G., Kindt, R., Legendre, P., O'Hara, R.B., Simpson, G.L., Solymos, P., Stevens, M.H.H., Wagner, H. (2010). vegan: Community Ecology Package. R package version 1.17-4. http://CRAN.R-project.org/package=vegan.

Papachristodoulou, C., Gravani, K., Oikonomou, A., Ioannides, K. (2010). On the provenance and manufacture of red-slipped fine ware from ancient Cassope (NW Greece): evidence by X-ray analytical methods. Journal of Archaeological Science, 37, 2146-2154.

Papageorgiou, I., Liritzis, I. (2007). Multivariate mixture of normal with unknown number of components: an application to cluster Neolithic ceramics from Aegean and Asia Minor using portable XRF. Archaeometry, 49(4), 795-813.

Papageorgiou, I., Baxter, M.J., Cau, M.A. (2001). Model-based cluster analysis of artifact compositional data. Archaeometry, 43(4), 571-588.

Peters, A., Hothorn, T. (2011). ipred: Improved Predictors. R package version 0.8-11. http://CRAN.R-project.org/package=ipred.

Pollard, A.M. (1986). Data Analysis. In R.E. Jones (Ed.), Greek and Cypriot Pottery: a review of scientific studies, Fitch Laboratory Occasional Paper 1 (pp.56-83). Athens: British School at Athens.

Prufer, O.H. (1965). The McGraw Site: A Study in Hopewellian Dynamics. Scientific Publications of the Cleveland Museum of Natural History, New Series, 4(1).

R Development Core Team (2010). R: a language and environment for statistical computing. R Foundation for Statistical Computing, Vienna, Austria. ISBN 3-900051-07-0. http://www.R-project.org/.

Reece, K. (2006). Memoirs of a true believer. In G.G. Fagan (Ed.), Archaeological Fantasies: How pseudoarchaeology misrepresents the past and misleads the public (pp.96-106). New York: Routledge.

Rotunno, T., Sabbatini, L., Corrente, M. (1997). A provenance study of pottery from archaeological sites near Canosa, Puglia (Italy). Archaeometry, 39(2), 343-354.

Ruthberg, S., Barnes, M.W., Noyce, R.H. (1963). Correlation of Muscovite Sheet Mica on the Basis of Color, Apparent Optic Angle, and Absorption Spectrum. Journal of Research of the National Bureau of Standards, 67A(4), 309-324.

Scaife, B., Budd, P., McDonnell, J.G., Pollard, A.M., Thomas, R.G. (1996). A reappraisal of statistical techniques used in lead isotope analysis. In S. Demirci, A.M. Ozer & G.D. Summers (Eds.), Archaeometry ’94: proceedings of the 29th international symposium on archaeometry (pp.301-307). Ankara.

Scarry, C.M. (1998). Domestic Life on the Northwest Riverbank at Moundville. In V.J. Knight, Jr., & V.P. Steponaitis (Eds.), Archaeology of the Moundville Chiefdom (pp.63-101). Tuscaloosa: The University of Alabama Press.

Schmid, J., Ambühl, M., Decrouez, D., Müller, S., Ramseyer, K. (1999). A quantitative fabric analysis approach to the discrimination of white marbles. Archaeometry, 41(2), 239-252.

Seelenfreund, A., Fonseca, E., Llona, F., Lera, L., Sinclaire, C., Rees, C. (2009). Geochemical analysis of vitreous rocks exploited during the Formative period in the Atacama region, northern Chile. Archaeometry, 51(1), 1-25.

Sharratt, N., Golitko, M., Williams, P.R., Dussubieux, L. (2009). Ceramic Production During the Middle Horizon: Wari and Tiwanaku Clay Procurement in the Moquegua Valley, Peru. Geoarchaeology, 24(6), 792-820.

Shearer, C.K., Papike, J.J., Simon, S.B., Laul, J.C. (1986). Pegmatite-wallrock interactions, Black Hills, South Dakota: Interaction between pegmatite-derived fluids and quartz-mica schist wallrock. American Mineralogist, 71, 518-539.

Shmakin, B.M. (1973). Geochemical specialization of Indian Precambrian pegmatites in relation to alkali and ore-element contents of the minerals. Geochemistry, 890-899.

Shmakin, B.M. (1975). Geochemical model of the formation of muscovite pegmatites. In Yu.M. Sokolov (Ed.), Muscovite Pegmatites of the U.S.S.R. (pp.98-106). Leningrad: Nauka.

Silverberg, R. (1968). Mound Builders of Ancient America: The Archaeology of a Myth. Greenwich: New York Graphic Society Ltd.

Smith, C.D. (1877). Ancient Mica Mines in North Carolina. Annual Report of the Board of Regents of the Smithsonian Institution, Showing the Operations, Expenditures, and Condition of the Institution for the Year 1876. Washington: Government Printing Office.

Steele, W.M., O'Connor, B.J. (1987). Mining Directory of Georgia (19th Edition), Circular 2. Atlanta: Georgia Department of Natural Resources.
Sterrett, D.B. (1923). Mica Deposits of the United States. U.S. Geological Survey Bulletin 740.

Stuckey, J.L. (1965). North Carolina: Its Geology and Mineral Resources. Raleigh: North Carolina Department of Conservation and Development.

Teodor, E.S., Teodor, E.D., Virgolici, M., Manea, M.M., Truică, G., Liţescu, S.C. (2010). Non-destructive analysis of amber artefacts from the prehistoric Cioclovina hoard (Romania). Journal of Archaeological Science, 37, 2386-2396.

Thomas, C. (1891). Catalogue of prehistoric works east of the Rocky Mountains. Bulletin 12. Washington: United States Bureau of American Ethnology.

Thomas, C. (1894). Report on the Mound Explorations of the Bureau of Ethnology. Smithsonian Institution, Bureau of Ethnology, Twelfth Annual Report. Washington, D.C.

Townsend, R.F. (Ed.) (2004). Hero, Hawk and Open Hand: American Indian Art of the Ancient Midwest and South. New Haven: Yale University Press.

Tschegg, C., Hein, I., Ntaflos, Th. (2008). State of the art multi-analytical geoscientific approach to identify Cypriot Bichrome Wheelmade Ware reproduction in the Eastern Nile delta (Egypt). Journal of Archaeological Science, 35, 1134-1147.

Veal, W.B. (2004). Mineralogy of the Peraluminous Spruce Pine Plutonic Suite, Mitchell, Avery, and Yancey Counties, North Carolina. Unpublished master's thesis, The University of Georgia, Athens.

Venables, W.N., Ripley, B.D. (2002). Modern Applied Statistics with S (4th Edition). New York: Springer. ISBN 0-387-95457-0.

Vitali, V., Franklin, U.M. (1986). An Approach to the Use of Packaged Statistical Programs for Cluster, Classification, and Discriminant Analysis of Trace Element Data. Geoarchaeology, 1(2), 195-201.

Wahl, P.W., Kronmal, R.A. (1977). Discriminant Functions when Covariances are Unequal and Sample Sizes are Moderate. Biometrics, 33(3), 479-484.

Walker, R.J., Hanson, G.N., Papike, J.J., O'Neil, J.R., Laul, J.C. (1986). Internal evolution of the Tin Mountain pegmatite, Black Hills, South Dakota. American Mineralogist, 71, 440-459.

Wehrens, R. (2011). Chemometrics with R: Multivariate Data Analysis in the Natural Sciences and Life Sciences. Use R! New York: Springer

Wehrens, R., Putter, H., Buydens, L.M.C. (2000). The bootstrap: a tutorial. Chemometrics and Intelligent Laboratory Systems, 54, 35-52.

Welch, P.D. (1991). Moundville's Economy. Tuscaloosa: The University of Alabama Press.
Whitlatch, George I. (Ed.) (1962). Georgia's Mineral Resources: A Summary of Available Data on Their Past, Present and Future Status. Atlanta: Georgia Institute of Technology.

Wilson, H.H. (1986). Burials from the Warren Wilson Site: Some Biological and Behavioral Considerations. In D.G. Moore (Ed.), The Conference on Cherokee Prehistory (pp.42-72). Swannanoa, North Carolina: Warren Wilson College.

Wood, P.A. (1996). Petrogenesis of the Spruce Pine Pegmatites, North Carolina. Master's thesis, Virginia Polytechnic Institute, Blacksburg.

Yavuz, A.B., Bruno, M., Attanasio, D. (2010). An updated, multi-method database of Ephesos marbles, including white, *Greco Scritto* and *Bigio* varieties. Archaeometry, in press.

Zhu, J., Shan, J., Qiu, P., Qin, Y., Wang, C., He, D., Sun, B., Tong, P., Wu, S. (2004). The multivariate statistical analysis and XRD analysis of pottery at Xigongqiao site. Journal of Archaeological Science, 31, 1685-1691.

APPENDIX A

ANNOTATED LIST OF PREHISTORIC MICA MINES IN THE SOUTHERN APPALACHIANS

after Ferguson (1974)

Alabama

1. Clay County. "Ancient mica quarry in Sec. 26, T. 19 S., R. 7E. Described by William Gesner, Smithsonian Report, 1879, p. 382." (Thomas 1891:12)
2. Randolph County. The Curley Mine. "The Curley mine is 1 3/4 miles north by east of Pinetucky. Remnants of ancient pits and dumps were found near the modern workings made by Horner and Phillips." (Sterrett 1923:34)
3. Randolph County. Miller Mines. "Several deposits have been tested or worked on the Miller place, 2½ miles north by west of Pinetuckey. One of these deposits was worked by the aboriginals, though remains of more recent work is seen around it. The ancient work consists of an open cut 75 feet long in a northeasterly direction 40 feet wide and 10 feet deep, with 8 feet of waste reported in the bottom. The dumps are piled around the edge of the cut, and trees of considerable age are growing in them. In one place an oak tree 2½ feet thick is rooted in the dump." (Sterrett 1923:35)
4. Randolph County. Mines of the Great Southern Mica Co. #5. "Mine No. 5 of the Great Southern Mica Co. is 2 miles N. 35^{o} E. of Pinetuckey. Here the aboriginals dug a large irregular-shaped pit or open cut more than 60 feet across and 5 to 12 feet deep, around the mouth of which they piled the waste rock." (Sterrett 1923:32)
5. Talladega County. "Ancient mica quarry in Sec. 12, T. 20 S., R. 6. E. William Gesner, Smithsonian Report 1879, p. 382; also p. 433." (Thomas 1891:15)

Georgia

1. Gilmer County. "Old mining excavation at Whitepath." (Thomas 1891:49)
2. Hall County. "A mica quarry in this county is mentioned by T. K. Harris, Smithsonian Report 1879, p. 443." (Thomas 1891:51)

North Carolina

1. Ashe County. Little Phoenix Mine. "The Little Phoenix Mine, now owned (1923) by W. H. Witherspoon, is 2¼ miles N. 60^{o} E. of Jefferson, on the east side of Little Phoenix Mountain. The mine is on a rather steep hillside and has good facilities for opening and draining. The mass of pegmatite worked was mined by the aboriginals along its outcrop, which follows the outcrop of a ledge of massive white quartz up the slope of the hill." (Sterrett 1923:172-173)
2. Ashe County. Walnut Knob Mine. "The Walnut Knob mine is 2 miles N. 40^{o} W. of Elk Crossroads and three-quarters of a mile south of Black Mountain. The mine has been operated at different times, and the remains of prehistoric working can be seen around it." (Sterrett 1923:176)
3. Buncomb County. W. H. Burnett Mine. "The Connally mine is 4 miles north of Black Mountain Station, on the east side of the North Fork of Swannanoa River." (Sterrett 1923:186) "The Burnett Mine is 200 yards north of the Conally Mine…. It is said there were prehistoric working at this mine." (Sterrett 1923:199)
4. Cherokee County. "Ancient mining excavations on farm of Mercer Fain, near Colnard's Creek, on north side of Valley River, 5 miles above Murphy. Other old mining indications in the same county. Reported by James Mooney." (Thomas 1891:153)

5. Jackson County. Ocher Hill Mine. "The Ocher Hill mine is 1 3/4 miles east of Beta on Ocher Creek…. It is reported that the deposit was worked by aboriginals but has never been worked by white people." (Sterrett 1923:199)
6. Macon County. "Ancient mica mine in which iron tools and windlass (Spanish) was found, on Iola Creek, about 5 miles below Franklin. Other ancient mica workings also around Franklin. Reported by James Mooney." (Thomas 1891:156)
7. Macon County. Smith or Baird Mine. "The deposit at the Smith or Baird mine, which is about a mile west of Franklin was worked on a large scale by the aborigines." (Sterrett 1923:224) See also Smith (1876:442) and Thomas (1891:156)
8. Macon County. Winecoff Mine. "The Winecoff or Old Jacobs mine is 2½ miles northwest of Franklin…. At 1 Figure 66 remains of ancient working were found." (Sterrett 1923:236)
9. Macon County. N. L. Barnard Mines. "Two 'veins' of mica were opened on the N. L. Barnard place, 3¼ miles N. 60° W. of Franklin during 1905 and 1906…. Indications of ancient workings were found in one of the shafts." (Sterrett 1923:237)
10. Mitchell County. Clarissa Mine. "The Clarissa mine is 2½ miles due east of Bakersville, on the west side of a small cove about 200 yards north of Cane Creek…. Remains of prehistoric workings were found around the Clarissa mine. These workings consisted of a large amphitheatral cut in the northeast side of the ridge. Large trees were found in this cut and in the dumps. In 1896 a chestnut tree that measured 12 feet in circumference 3 feet above the ground was still in the dump." (Sterrett 1923:247) See also Thomas (1891:157)
11. Mitchell County. Buchannan Mine. "The Buchannan mine is on the south slope of a small mountain 1 1/3 miles N. 25° W. of Ledger…. There are two or more 'veins' and on one of them pits were made by the aborigines…. Stone implements used by the prehistoric miners have been found around these old works, and fragments of them were still to be seen at the mine when it was visited in 1904. The work by white men has been done principally on 'veins' east of that worked by the aborigines." (Sterrett 1923:249)
12. Mitchell County. Sink Hole Mine. "The Sink Hole mine is near Bandana. It is one of the old mines of Mitchell County and was first worked by the aborigines…. The ancient workings are said to have been extensive and to have included small tunnels and shafts where the formations were soft." (Sterrett 1923:250) See also Thomas (1891:157)
13. Mitchell County. "Ancient mica mines at Little Yellow Mountain. Reported by Charles M. Yates and Arthur P. Davis." (Thomas 1891:157)
14. Yancey County. Hensley Mine. "The Hensley mine is on Pigpen Creek, about 2 miles south by west of Green Mountain…. It is said that there were ancient workings at this mine, which was also worked before 1906 by white people." (Sterrett 1923:276)
15. Yancey County. "Ancient mica works, on Hurricane Mountain (part of Bowlen's Pyramid) a spur of the Black Mountain, 3 miles southeast of Burnsville, on a small headwater of Bowlen's Creek." (Thomas 1891:159)
16. Yancey County. "Ancient mica mines, 1½ miles east of Burnsville on the north bank of Crabtree Creek." (Thomas 1891:159)
17. Yancey County. "Ancient mica mine, on a small head branch of Crabtree Creek, about 1 mile north of the creek, and 5 miles northeast of Burnsville. Reported by James Mooney." (Thomas 1891:159)

APPENDIX B

LIST OF PEGMATITIC MUSCOVITE OCCURRENCES IN THE STATE OF GEORGIA

Compiled from Galpin (1915), The Geological Survey (1941, 1943, 1950, 1954, 1956, 1961, 1963, 1968), Furcron & Teague (1943); Jahns & Lancaster (1950); Heinrich et al. (1953); Long (1971); Steele & O'Connor (1987); Gunow & Bonn (1989), and Cocker (1992). Mineral abbreviations follow Kretz (1983).

CHEROKEE-PICKENS DISTRICT, GEORGIA						
Mine/Prospect	Field	County	Accessory Pegmatite Minerals	Max. Size (cm)	Color	Inclusions
Bennett mine	Ball Ground	Cherokee	Tur, Be	15		
Revis prospect	Ball Ground	Cherokee	Tur	8		
S.S. Densmore prospect	Ball Ground	Cherokee	Tur			
Weaver prospect	Ball Ground	Cherokee				
Cochran mine	Ball Ground (beryl-bearing)	Cherokee	Be, Tur, Grt	25	colorless, greenish-yellow	Tur, Kln, Rt, FeO, MnO, Zrn
Hendrix mine	Ball Ground (beryl-bearing)	Cherokee	Be, Tur, Grt			Kln, FeO
A.W. Amphlett mine (Franklin mine)	Ball Ground (beryl-poor)	Cherokee	Tur, Grt, Bt, Ap, Be?	25	light pinkish buff to cinnamon brown	Tur, Qtz, Kln, FeO, MnO
A.W. Amphlett mine (Franklin mine) [South Amphlett prospect]	Ball Ground (beryl-poor)	Cherokee	Tur, Grt, Bt, Ap, Be?	10	light cinnamon brown, green; some zoned	Tur, Qtz, Kln, FeO, MnO
Cook mine	Holly Springs	Cherokee		18	rum, brown	Kln, MnO
Dean mine	Holly Springs	Cherokee		10	light rum, brown	Qtz, Bt
Hause mine [1] (Toonigh Creek)	Holly Springs	Cherokee			rum, brown	Kln, Chl, MnO
Hause mine [2] (Toonigh Creek)	Holly Springs	Cherokee				
Hause mine [3] (Toonigh Creek)	Holly Springs	Cherokee		15		

CHEROKEE-PICKENS DISTRICT, GEORGIA						
Mine/Prospect	Field	County	Accessory Pegmatite Minerals	Max. Size (cm)	Color	Inclusions
Hause mine [4] (Toonigh Creek)	Holly Springs	Cherokee	Bt	20	light rum, brown	Bt
Hause prospect	Holly Springs	Cherokee				
Hillhouse prospect?	Holly Springs	Cherokee				Bt
J.D. Hillhouse mines [1]	Holly Springs	Cherokee		15	light rum, light brown	Qtz, Bt, Hem, Ms, Kln, FeO, MnO
J.D. Hillhouse mines [2]	Holly Springs	Cherokee		10	light rum	Qtz, Bt, Hem, Ms, Kln, FeO, MnO
J.D. Hillhouse mines [3]	Holly Springs	Cherokee	Bt			Qtz, Bt, Hem, Ms, Kln, FeO, MnO
J.D. Hillhouse mines [4]	Holly Springs	Cherokee		10	light rum, brown	Qtz, Bt, Hem, Ms, Kln, FeO, MnO
J.F. Hillhouse prospects [1]	Holly Springs	Cherokee		36		Bt
J.F. Hillhouse prospects [2]	Holly Springs	Cherokee		5	light rum, light brown	
J.V. Ledford mine	Holly Springs	Cherokee	Py	46	deep rum, brown	Qtz, Bt, Hem
Kuykendall prospect	Holly Springs	Cherokee				Qtz, Bt, Hem
N.M. (M.M.) Cole mine	Holly Springs	Cherokee			light rum, light brown to brownish olive	Mag, Kln, FeO, MnO
Wacaster mine [1]	Holly Springs	Cherokee		36	green to brown	Kln, FeO, MnO, Bt
Wacaster mine [2]	Holly Springs	Cherokee		10		Kln, FeO, MnO, Bt

CHEROKEE-PICKENS DISTRICT, GEORGIA						
Mine/Prospect	Field	County	Accessory Pegmatite Minerals	Max. Size (cm)	Color	Inclusions
Brady mine		Cherokee				
De Lay prospect		Cherokee		25		
F.M. Williams prospect		Cherokee		1		
G.W. Anderson prospect [1]		Cherokee		8		
G.W. Anderson prospect [2]		Cherokee				
J.B. Wheeler prospect		Cherokee		15	light colored	
J.T. Haley mine		Cherokee				
Liner mine		Cherokee				
R.M. Reece property		Cherokee				
Waltz mine (Waltz & Bates/Iza Clayton mines) [1]		Cherokee		25	green	
Waltz mine (Waltz & Bates/Iza Clayton mines) [2]		Cherokee				
Waltz mine (Waltz & Bates/Iza Clayton mines) [3]		Cherokee				
Waltz mine (Waltz & Bates/Iza Clayton mines) [4]		Cherokee	Bt	13	green	
Waltz mine (Waltz & Bates/Iza Clayton mines) [5]		Cherokee				

CHEROKEE-PICKENS DISTRICT, GEORGIA						
Mine/Prospect	Field	County	Accessory Pegmatite Minerals	Max. Size (cm)	Color	Inclusions
Allen Morton prospect	Ball Ground	Pickens		15		
C.C. West prospects [1]	Ball Ground	Pickens		13	green	
C.C. West prospects [2]	Ball Ground	Pickens		13		
C.H. Fouts property	Ball Ground	Pickens		10		
Davis mine/prospect	Ball Ground	Pickens	Tur			
E.H. Kent properties	Ball Ground	Pickens				
J.T. Worley prospect	Ball Ground	Pickens	Tur	8		
Jennie Burrell property	Ball Ground	Pickens				
Jones Bozeman mine (Jones/Bozeman mine) [1]	Ball Ground	Pickens	Tur, Be, Bt	13	light rum	Kln, FeO, MnO
Jones Bozeman mine (Jones/Bozeman mine) [2]	Ball Ground	Pickens	Tur, Be, Bt		light rum	Kln, FeO, MnO
Partain prospects [1]	Ball Ground	Pickens	Tur			
Partain prospects [2]	Ball Ground	Pickens				
Partain prospects [3]	Ball Ground	Pickens		8	Rum	
Poole mine	Ball Ground	Pickens	Tur	15		Hem, Bt

CHEROKEE-PICKENS DISTRICT, GEORGIA						
Mine/Prospect	Field	County	Accessory Pegmatite Minerals	Max. Size (cm)	Color	Inclusions
Reynolds mine	Ball Ground	Pickens	Tur, Grt, Bt	5		
Scott Byees property	Ball Ground	Pickens		15		
W.P. Stancil prospect	Ball Ground	Pickens				
Wilkie prospects	Ball Ground	Pickens	Tur			
Denson mine [1]	Ball Ground (beryl-bearing)	Pickens	Tur, Be, Grt	46	amber; zoned (yellowish-green core, brown-greenish brown rim)	Rt, FeO, MnO, Kln
Denson mine [2]	Ball Ground (beryl-bearing)	Pickens	Tur, Be, Grt	13	rum	Rt, FeO, MnO, Kln
Denson mine [3]	Ball Ground (beryl-bearing)	Pickens	Tur, Be, Grt	5		Rt, FeO, MnO, Kln
J.L. Mullinax prospect	Ball Ground (beryl-bearing)	Pickens	Tur, Be		green	Kln, MnO
F.M. Cagle mine	Ball Ground (beryl-poor)	Pickens	Tur	46		Bt, Grt, Kln, FeO, MnO
Howell mine	Ball Ground (beryl-poor)	Pickens	Tur, Py	36	light rum	Kln, FeO, MnO
J.F. Carney prospect	Ball Ground (beryl-poor)	Pickens	Tur			Kln, MnO
James Foster prospect	Ball Ground (beryl-poor)	Pickens	Tur, Bt, Grt	8		
Jones-Howell (area b/n Jones & Howell mines)	Ball Ground (beryl-poor)	Pickens				Kln, FeO, MnO

CHEROKEE-PICKENS DISTRICT, GEORGIA						
Mine/Prospect	Field	County	Accessory Pegmatite Minerals	Max. Size (cm)	Color	Inclusions
Marblehill prospect [1]	Ball Ground (beryl-poor)	Pickens	Tur, Bt, Grt			Kln, FeO, MnO
Marblehill prospect [2]	Ball Ground (beryl-poor)	Pickens	Tur, Bt, Grt			Kln, FeO, MnO
A.V. Reeves prospect		Pickens		10		
Beryl mine		Pickens				
Cochran Mine		Pickens				
Dawson mine		Pickens				
Fowler-Freeman prospect		Pickens	Tur	20		Tur
G.W. Worley property		Pickens		8		
J.M. Piyon property		Pickens				
May Davis property		Pickens				
Silver-Gray No. 8 quarry		Pickens				
W.J. Garrison property		Pickens		15		
Walker mine		Pickens				

THOMASTON-BARNESVILLE DISTRICT, GEORGIA						
Mine/Prospect	Field	County	Accessory Pegmatite Minerals	Max. Size (cm)	Color	Inclusions
Crawford Co. roadcut [1]		Crawford				
Crawford Co. roadcut [10]		Crawford				
Crawford Co. roadcut [2]		Crawford				
Crawford Co. roadcut [3]		Crawford				
Crawford Co. roadcut [4]		Crawford				
Crawford Co. roadcut [5]		Crawford				
Crawford Co. roadcut [6]		Crawford				
Crawford Co. roadcut [7]		Crawford				
Crawford Co. roadcut [8]		Crawford				
Crawford Co. roadcut [9]		Crawford				
American Feldspar Corp. Pit		Jasper				
Enon Church Mine		Jasper				
Gladesville Mine		Jasper				
J.H. Barron Property		Jasper				

THOMASTON-BARNESVILLE DISTRICT, GEORGIA						
Mine/Prospect	Field	County	Accessory Pegmatite Minerals	Max. Size (cm)	Color	Inclusions
Jasper Co. roadcut [1]		Jasper				
Jasper Co. roadcut [2]		Jasper				
Jasper Co. roadcut [3]		Jasper				
Jasper Co. roadcut [4]		Jasper				
Mrs. Athen Prospect		Jasper			greenish to clear	
Newton Prospect		Jasper			light rum	
Parker Mine		Jasper				
Coggins prospect	Lighthouse	Lamar			pinkish buff with pale greenish tinge, some green mottling	Mag
Doc Irwin mine/prospect	Lighthouse	Lamar				
J.W. Brown deposit	Lighthouse	Lamar		10		
Lamar Co. roadcut [1]	Lighthouse	Lamar				
Lamar Co. roadcut [2]	Lighthouse	Lamar				
Lamar Co. roadcut [3]	Lighthouse	Lamar				
Lamar Co. roadcut [4]	Lighthouse	Lamar				

THOMASTON-BARNESVILLE DISTRICT, GEORGIA						
Mine/Prospect	Field	County	Accessory Pegmatite Minerals	Max. Size (cm)	Color	Inclusions
Lamar Co. roadcut [5]	Lighthouse	Lamar				
Lamar Co. roadcut [6]	Lighthouse	Lamar				
Lamar Co. roadcut [7]	Lighthouse	Lamar				
Lamar Co. roadcut [8]	Lighthouse	Lamar				
Mrs. J.I. Taylor Sr. Prospect [1]	Lighthouse	Lamar		5		
Mrs. J.I. Taylor Sr. Prospect [2]	Lighthouse	Lamar	Bt	20		Grt
A.J. Thomas mine	Yatesville	Lamar			Rum	
Early Vaughn mine	Yatesville	Lamar			rum (pale pinkish buff with light greenish streaks, rare green mottling, rare brownbursts)	Mag
George R. Swift property [1]	Yatesville	Lamar			Rum	
George R. Swift property [2]	Yatesville	Lamar				
H.B. Manrey prospect	Yatesville	Lamar		5	Rum	Bt
H.S. Worsham (Manrey or Pond property)	Yatesville	Lamar			greenish rum	

THOMASTON-BARNESVILLE DISTRICT, GEORGIA						
Mine/Prospect	Field	County	Accessory Pegmatite Minerals	Max. Size (cm)	Color	Inclusions
Ingraham Prospect (old Potts Estate) [1]	Yatesville	Lamar			light rum	
Ingraham Prospect (old Potts Estate) [2]	Yatesville	Lamar			green, greenish rum	
J.T. Means mine/prospect	Yatesville	Lamar	Bt, Be	36	green, light greenish rum	Bt
Lamar Co. float [1]	Yatesville	Lamar				
Lamar Co. float [2]	Yatesville	Lamar				
Lamar Co. roadcut [10]	Yatesville	Lamar				
Lamar Co. roadcut [11]	Yatesville	Lamar				
Lamar Co. roadcut [12]	Yatesville	Lamar				
Lamar Co. roadcut [13]	Yatesville	Lamar				
Lamar Co. roadcut [14]	Yatesville	Lamar				
Lamar Co. roadcut [9]	Yatesville	Lamar				
Monroe Co. roadcut [1]	Yatesville	Lamar				
Monroe Co. roadcut [2]	Yatesville	Lamar				
Perdue prospect	Yatesville	Lamar	Bt	15	light to deep rum	Qtz

THOMASTON-BARNESVILLE DISTRICT, GEORGIA						
Mine/Prospect	Field	County	Accessory Pegmatite Minerals	Max. Size (cm)	Color	Inclusions
Williams & Holmes prospects	Yatesville	Lamar		13		
A.N. Moye property		Lamar				
Harp Mine		Lamar				
Howard mine		Lamar				
Old Childs Prospect		Lamar	Kln		Rum	
C.M. Sutton prospect [1]	Blount	Monroe	Bt			
C.M. Sutton prospect [2]	Blount	Monroe				
C.M. Sutton prospect [3]	Blount	Monroe	Bt	10		
Coleman mine/prospect	Blount	Monroe			green and rum	
E.B. Butler Property	Blount	Monroe		4		
E.J. Goggins (Goggans) prospect	Blount	Monroe		8	clear to light rum	
Goddard & Watson prospect [1]	Blount	Monroe				
Goddard & Watson prospect [2]	Blount	Monroe				
Lassiter Rd. outcrop	Blount	Monroe				

THOMASTON-BARNESVILLE DISTRICT, GEORGIA						
Mine/Prospect	Field	County	Accessory Pegmatite Minerals	Max. Size (cm)	Color	Inclusions
Marie Vaughn mine [1]	Blount	Monroe			rum	
Marie Vaughn mine [2]	Blount	Monroe	Bt			
Marie Vaughn mine [3]	Blount	Monroe	Bt	5		
Mattie Smith Mine	Blount	Monroe	Bt, Tur		rum	
Monroe Co. roadcut [1]	Blount	Monroe				
Monroe Co. roadcut [2]	Blount	Monroe				
Monroe Co. roadcut [3]	Blount	Monroe				
Monroe Co. roadcut [4]	Blount	Monroe				
Monroe Co. roadcut [5]	Blount	Monroe				
MV mine	Blount	Monroe				
unnamed mine	Blount	Monroe				
W.H. Westbrooks Prospect	Blount	Monroe	Bt		deep rum	
A.T. Redding prospect	Juliette	Monroe	Bt		rum (some green)	
Monroe Co. roadcut [10]	Juliette	Monroe				

THOMASTON-BARNESVILLE DISTRICT, GEORGIA						
Mine/Prospect	Field	County	Accessory Pegmatite Minerals	Max. Size (cm)	Color	Inclusions
Monroe Co. roadcut [8]	Juliette	Monroe				
Monroe Co. roadcut [9]	Juliette	Monroe				
New Ground mine [1]	Juliette	Monroe	Grt	15	light rum	Qtz
New Ground mine [2]	Juliette	Monroe		51		
New Ground mine [3]	Juliette	Monroe	Grt		Rum	
Owl Hollow Prospect	Juliette	Monroe	Grt			
Walker Smith mine (Old Walker Smith mine)	Juliette	Monroe		28	light rum	
Willie Bowdoin (Bowdion) Property	Juliette	Monroe		13	rum	
Brooks mine	Russellville	Monroe				
Cox Prospect	Russellville	Monroe	Bt, Vrm		light rum	Qtz, Ap, Bt, Ms
F.H. Holloway mine	Russellville	Monroe	Kln, Bt		rum	Ms, Qtz
Homer Hardin mine	Russellville	Monroe		8	rum	
Monroe Co. roadcut [12]	Russellville	Monroe				
Monroe Co. roadcut [13]	Russellville	Monroe				

THOMASTON-BARNESVILLE DISTRICT, GEORGIA						
Mine/Prospect	Field	County	Accessory Pegmatite Minerals	Max. Size (cm)	Color	Inclusions
Rosa Fletcher Prospect	Russellville	Monroe	Vrm, Grt	10	rum	Vrm
Ruffin prospect [1]	Russellville	Monroe			rum	Qtz
Ruffin prospect [2]	Russellville	Monroe	Bt	13		
Battle mine (Battles Mine)	Waymanville	Monroe	Bt, Grt		ruby; cinnamon brown; local green mottling, rare brownbursts	
Holmes mine [1]	Waymanville	Monroe	Tur		deep rum	Qtz
Holmes mine [2]	Waymanville	Monroe				
prospect pit [1]	Waymanville	Monroe				
prospect pit [2]	Waymanville	Monroe				
C.A. (C.E.) Ensign Mine	Yatesville	Monroe		10		
Dick Fletcher mine [1]	Yatesville	Monroe			clear to light rum	Qtz, Ms
Dick Fletcher mine [2]	Yatesville	Monroe	Bt	5	deep rum	Bt
F.B. Willingham Prospect	Yatesville	Monroe	Bt		rum	
Fletcher mine north	Yatesville	Monroe				

THOMASTON-BARNESVILLE DISTRICT, GEORGIA						
Mine/Prospect	Field	County	Accessory Pegmatite Minerals	Max. Size (cm)	Color	Inclusions
Florida Rock Industrial quarry	Yatesville	Monroe				
L.D. Owen prospect (Owens prospect)	Yatesville	Monroe		8	Rum	Qtz, pinholes
L.P. Goodwin mine/prospect	Yatesville	Monroe	Ap		light rum	
L.P. Phinazee mine [1]	Yatesville	Monroe	Kln	5	rum	
L.P. Phinazee mine [2]	Yatesville	Monroe		25	Rum	
Monroe Co. float	Yatesville	Monroe				
Monroe Co. roadcut [6]	Yatesville	Monroe				
O.B. Clements property	Yatesville	Monroe		10		
Persons NE prospect	Yatesville	Monroe				
Persons west prospect	Yatesville	Monroe				
Peters Mine	Yatesville	Monroe	Bt	18	Rum	Bt
T.D. Thurman Mine [1]	Yatesville	Monroe	Bt	13	rum	
T.D. Thurman Mine [2]	Yatesville	Monroe	Bt	13	rum	
Thad Persons mine (Rev. Thaddeus Persons mine) [1]	Yatesville	Monroe			rum	Qtz

THOMASTON-BARNESVILLE DISTRICT, GEORGIA						
Mine/Prospect	Field	County	Accessory Pegmatite Minerals	Max. Size (cm)	Color	Inclusions
Thad Persons mine (Rev. Thaddeus Persons mine) [2]	Yatesville	Monroe			green	
Thad Persons mine (Rev. Thaddeus Persons mine) [3]	Yatesville	Monroe			rum	
Vaughn-Butler Road	Yatesville	Monroe				Qtz, Bt
Carter Mine		Monroe				
Charlie Callaway Prospect		Monroe			rum	Qtz
Chatfield Mine		Monroe				
Goolsby prospect (Goulsby)		Monroe				
Haygood prospect		Monroe		28	rum	
Monroe Co. roadcut [11]		Monroe				
Monroe Co. roadcut [7]		Monroe				
Old Callaway Property		Monroe			light rum	pinholes
R.L. Williamson farm prospect		Monroe		30		
Smith Mine		Monroe				
Worsham & Goodwin prospect		Monroe	Bt		rum	Qtz

THOMASTON-BARNESVILLE DISTRICT, GEORGIA						
Mine/Prospect	Field	County	Accessory Pegmatite Minerals	Max. Size (cm)	Color	Inclusions
Pike Co. roadcut [2]	Concord	Pike				
Pike Co. roadcut [3]	Concord	Pike				
Pike Co. roadcut [4]	Concord	Pike				
Pike Co. roadcut [5]	Concord	Pike				
Pike Co. roadcut [6]	Concord	Pike				
Pike Co. roadcut [7]	Concord	Pike				
Pike Co. roadcut [8]	Concord	Pike				
Pike Co. roadcut [1]	Lighthouse	Pike				
E.O. Carwell Mine		Pike		30		
J.D. Pitts Property		Pike		3		
M.C. Ballard Property		Pike				
Talbot Co. roadcut [2]	Lazer Creek	Talbot				
Talbot Co. roadcut [3]	Lazer Creek	Talbot				
Talbot Co. roadcut [4]	Lazer Creek	Talbot				

THOMASTON-BARNESVILLE DISTRICT, GEORGIA						
Mine/Prospect	Field	County	Accessory Pegmatite Minerals	Max. Size (cm)	Color	Inclusions
Talbot Co. roadcut [5]	Lazer Creek	Talbot				
mica prospect (W.C. McCoy, Old Martin prospect)		Talbot				
Talbot Co. roadcut [1]		Talbot				
Talbot Co. roadcut [6]		Talbot				
Talbot Co. roadcut [7]		Talbot				
E.M. Thompson prospect	Indian Grave	Upson		15		
J.A. Partridge Mine	Indian Grave	Upson			green, rum	Bt
Upson Co. roadcut [1]	Indian Grave	Upson				
Atwater mine (Old Atwater mine) [1]	Waymanville	Upson	Kln	10	light rum-rum	Qtz
Atwater mine (Old Atwater mine) [2]	Waymanville	Upson	Kln, Bt		rum	
Atwater mine roadcut	Waymanville	Upson				
Barron Mine (see Bennie Barron/Walker Wakefield Mine)	Waymanville	Upson				
Blount #1 mine	Waymanville	Upson				

THOMASTON-BARNESVILLE DISTRICT, GEORGIA						
Mine/Prospect	Field	County	Accessory Pegmatite Minerals	Max. Size (cm)	Color	Inclusions
Boyt Mine	Waymanville	Upson			pale cinnamon brown, brownbursts rare	Ap, Bt, Hem
Brown mine (Parrish Mine)	Waymanville	Upson			pinkish buff	Mag, Hem, Bt
Charlie Nims mine [1]	Waymanville	Upson		13	Rum	Ap, pinholes
Charlie Nims mine [2]	Waymanville	Upson		8	Rum	Ap, pinholes
Corley mine	Waymanville	Upson			pinkish buff	Hem
Corley prospects [1]	Waymanville	Upson				
Corley prospects [2]	Waymanville	Upson				
Duke mine	Waymanville	Upson	Bt, Vrm		deep rum, light brown	Qtz, Bt
Emmit Trice prospects	Waymanville	Upson			Rum	
Gibson Prospect [1] (B.S. Gibson Prospects, R.S. Gibson)	Waymanville	Upson	Bt	5	rum (cinnamon brown)	
Gibson Prospect [2] (B.S. Gibson Prospects, R.S. Gibson)	Waymanville	Upson	Bt		light rum (cinnamon brown)	
Gibson Prospect [3] (B.S. Gibson Prospects, R.S. Gibson)	Waymanville	Upson	Bt	5	cinnamon brown	

THOMASTON-BARNESVILLE DISTRICT, GEORGIA						
Mine/Prospect	Field	County	Accessory Pegmatite Minerals	Max. Size (cm)	Color	Inclusions
Gordon School roadcut	Waymanville	Upson				
Grace mine/prospect	Waymanville	Upson				
Joe McKinley prospect	Waymanville	Upson	Bt	15	light rum	
Joe Persons mine	Waymanville	Upson				
King & Thurston mine (Old John Robbards Place)	Waymanville	Upson	Bt		rum	Qtz
L.M. Brooks Prospect	Waymanville	Upson				
Mauldin mine	Waymanville	Upson	Ap, Bt	20	rum (pale cinnamon brown, locally abundant brownbursts)	Ap, Bt, Hem
Mauldin Rd. prospect	Waymanville	Upson			cinnamon brown (sparse tiny brownbursts)	
Maze mine/prospect	Waymanville	Upson				
Miles B. Brown Mine	Waymanville	Upson	Bt	20	Rum	
Mitchell Creek mine	Waymanville	Upson	Bt, Ap		rum (cinnamon brown, rare brownbursts)	Qtz, Ap, Bt, Py
Mitchell Creek mine area	Waymanville	Upson				
Old Bell mine [1]	Waymanville	Upson	Tur	51		

THOMASTON-BARNESVILLE DISTRICT, GEORGIA						
Mine/Prospect	Field	County	Accessory Pegmatite Minerals	Max. Size (cm)	Color	Inclusions
Old Bell mine [2]	Waymanville	Upson	Tur		rum	
Old Cumbie Place [1] (Cumbie prospect area)	Waymanville	Upson			rum	
Old Cumbie Place [2] (Cumbie prospect area)	Waymanville	Upson			rum	
Old Cumbie Place [3] (Cumbie prospect area)	Waymanville	Upson			rum	
Old Cumbie Place [4] (Cumbie prospect area)	Waymanville	Upson				
Old Cumbie Place [5] (Cumbie prospect area)	Waymanville	Upson			rum	
Po Biddy Rd. roadcut	Waymanville	Upson				
prospect pit	Waymanville	Upson				
S.P. Cronheim prospect	Waymanville	Upson			green, light rum	
Short-Mitchell mine	Waymanville	Upson	Bt, Vrm	15	rum	
Swift Creek mine	Waymanville	Upson				
T.J. Reeves prospect	Waymanville	Upson	Bt	10	rum	
Thompson prospect	Waymanville	Upson			green	
Tomlin mine	Waymanville	Upson				

THOMASTON-BARNESVILLE DISTRICT, GEORGIA						
Mine/Prospect	Field	County	Accessory Pegmatite Minerals	Max. Size (cm)	Color	Inclusions
Triune Mills mine/prospect	Waymanville	Upson				
unnamed mine	Waymanville	Upson				
Upson Co. roadcut [10]	Waymanville	Upson				
Upson Co. roadcut [12]	Waymanville	Upson				
Upson Co. roadcut [13]	Waymanville	Upson				
Upson Co. roadcut [14]	Waymanville	Upson				
Upson Co. roadcut [15]	Waymanville	Upson				
Upson Co. roadcut [16]	Waymanville	Upson				
W.M. Dallas mine/prospects [1]	Waymanville	Upson		5	rum	
W.M. Dallas mine/prospects [2]	Waymanville	Upson			rum	
W.M. Dallas mine/prospects [3]	Waymanville	Upson	Bt	5	rum	
W.M. Dallas mine/prospects [4]	Waymanville	Upson			rum	
Walker Wakefield Mine (Benny Baron Mine)	Waymanville	Upson		15	rum; cinnamon brown	Qtz, Ap, Bt
Watson mine	Waymanville	Upson		8		

THOMASTON-BARNESVILLE DISTRICT, GEORGIA						
Mine/Prospect	Field	County	Accessory Pegmatite Minerals	Max. Size (cm)	Color	Inclusions
Wheeles mine	Waymanville	Upson				
Zorn mine/prospect area	Waymanville	Upson			light brown	
Adams Mine	Yatesville	Upson			brownish olive to cinnamon brown; widespread green mottling, sparse brownbursts	
Aggie Castlen (Castler) Property (old Mark Lions place)	Yatesville	Upson	Tur	8	rum	
Bentley prospect	Yatesville	Upson	Bt	4		
Clay Cheek mine	Yatesville	Upson				
Cliff Middlebrooks deposit	Yatesville	Upson			rose	
Colbert mine	Yatesville	Upson				
Colbert mine area	Yatesville	Upson				
D.K. Carter Mine [1]	Yatesville	Upson		5	rum	
D.K. Carter Mine [2]	Yatesville	Upson			light rum	
D.K. Carter Mine [3]	Yatesville	Upson	Bt	15	light rum	

THOMASTON-BARNESVILLE DISTRICT, GEORGIA						
Mine/Prospect	Field	County	Accessory Pegmatite Minerals	Max. Size (cm)	Color	Inclusions
Helen McDonald prospect	Yatesville	Upson				
J.H. Reynolds Mine [1]	Yatesville	Upson	Kln		rum	
J.H. Reynolds Mine [2]	Yatesville	Upson	Kln, Bt		rum	
J.M. Bevell deposit	Yatesville	Upson				
Jack Walker prospects [1]	Yatesville	Upson			rum	
Jack Walker prospects [2]	Yatesville	Upson			rum	
Jack Walker prospects [3]	Yatesville	Upson	Bt, Tur			
Jack Walker prospects [4]	Yatesville	Upson				
Johnson mine	Yatesville	Upson			cinnamon brown (rare tiny brownbursts)	Bt, Hem
Johnson mine roadcut	Yatesville	Upson				
Kelly O'Neal mine/prospects [1]	Yatesville	Upson		25		
Kelly O'Neal mine/prospects [2]	Yatesville	Upson	Bt			Qtz
Reynolds Mine [1]	Yatesville	Upson			yellowish-olive	
Reynolds Mine [2]	Yatesville	Upson			light cinnamon brown	

THOMASTON-BARNESVILLE DISTRICT, GEORGIA						
Mine/Prospect	Field	County	Accessory Pegmatite Minerals	Max. Size (cm)	Color	Inclusions
Stevens mine (Rock mine, Marshall mine, Stevens Rock mine, McKinney mine, Sullivan mine)	Yatesville	Upson	Tur, Bt, Ap	10	rum (pale cinnamon brown, much green mottling, rare brownbursts)	Bt, Py
Upson Co. roadcut [2]	Yatesville	Upson				
Upson Co. roadcut [3]	Yatesville	Upson				
Upson Co. roadcut [4]	Yatesville	Upson				
Upson Co. roadcut [5]	Yatesville	Upson				
Upson Co. roadcut [6]	Yatesville	Upson				
Upson Co. roadcut [7]	Yatesville	Upson				
Upson Co. roadcut [8]	Yatesville	Upson				
Upson Co. roadcut [9]	Yatesville	Upson				
Walker prospect [1] (Jesse Walker)	Yatesville	Upson				
Walker prospect [2] (Jesse Walker)	Yatesville	Upson				
Bell Mine		Upson		3		Qtz
Carter Mine		Upson			yellowish olive and pale cinnamon brown	

THOMASTON-BARNESVILLE DISTRICT, GEORGIA						
Mine/Prospect	Field	County	Accessory Pegmatite Minerals	Max. Size (cm)	Color	Inclusions
D.C. Ellerbee prospects		Upson		8		
E.E. Thompson property [east]		Upson		10		
E.E. Thompson property [west]		Upson		25		
F.E. Thom(p)son Prospect		Upson			Rum	
Herron mine		Upson			yellowish olive and cinnamon brown to dark brown; local green mottling	Mag, Hem
M. Richardson Property		Upson				
Nottingham prospect [1]		Upson			rum	
Nottingham prospect [2]		Upson				
Nottingham prospect [3]		Upson				
Pennyman mine		Upson				
Upson Co. roadcut [11]		Upson				
W.E. Adams Mine		Upson				
W.E. Adams Mine (Pit No. 8)		Upson	Bt		deep rum	

THOMASTON-BARNESVILLE DISTRICT, GEORGIA						
Mine/Prospect	Field	County	Accessory Pegmatite Minerals	Max. Size (cm)	Color	Inclusions
Young mine		Upson				
outcrop [1]						
outcrop [2]						
Sugar Hill No. 1 prospect						
Sugar Hill No. 2 prospect						
Taylor prospect						

NORTH GEORGIA DISTRICT, GEORGIA						
Mine/Prospect	Field	County	Accessory Pegmatite Minerals	Max. Size (cm)	Color	Inclusions
Caldwell Prospect		Lumpkin				
Camp Wahsega Prospect		Lumpkin		8	light rum	
Captain Walker Prospect		Lumpkin			light rum	
Cassity Prospect [1]		Lumpkin				
Cassity Prospect [2]		Lumpkin				
Crane Mica Mine		Lumpkin				
Gaddis Mine		Lumpkin				
Garrett Prospect		Lumpkin	FeO, MnO			
Glassy Mine Top Mine [1]		Lumpkin	Py	13	light rum	
Glassy Mine Top Mine [2]		Lumpkin		13	clear to pale green	
Green Vein Mine		Lumpkin		15	colorless to greenish	Bt
Henry Lee Mine		Lumpkin		25		
J.W. (Shotgun) Walker Prospect [1]		Lumpkin			clear to rum	
J.W. (Shotgun) Walker Prospect [2]		Lumpkin		10		

NORTH GEORGIA DISTRICT, GEORGIA						
Mine/Prospect	Field	County	Accessory Pegmatite Minerals	Max. Size (cm)	Color	Inclusions
Jones Creek Prospect		Lumpkin				
Long Mountain Mine		Lumpkin				
Old Scott Mine		Lumpkin				
prospect southeast of Ward Gap [1]		Lumpkin		10	rum	
prospect southeast of Ward Gap [2]		Lumpkin		13	rum	
Sain Mine [1]		Lumpkin		46	rum	
Sain mine [2]		Lumpkin				
Sol Walden Prospect		Lumpkin				
T.H. McDonald Prospect		Lumpkin				
Tipton Mine		Lumpkin		8		
Tucker Prospect		Lumpkin			light rum	
W.M. Gooch Mine [1]		Lumpkin		20	rum	
W.M. Gooch Mine [2]		Lumpkin		10		
Ward Gap Mine		Lumpkin		15	dark and smoky	

NORTH GEORGIA DISTRICT, GEORGIA						
Mine/Prospect	Field	County	Accessory Pegmatite Minerals	Max. Size (cm)	Color	Inclusions
Ward Mine		Lumpkin				
Wash Walker Mine ("Big" Mine)		Lumpkin		13	light-colored	
Wess Walker Mine		Lumpkin				
Williams Mica Mine		Lumpkin		30	colorless to light green	
Winn Mine (Winnie Mine)		Lumpkin				
Archie Wimpy Prospect		Union			colorless	Mag
B.F. Schuler Mine		Union		25	light rum	
Choestoe		Union				
Corley Mine		Union				
Davenport and Hedgecock Property		Union		15		
Dyer Mine		Union		10		
Eph Lee Mine		Union		13		
J.L. Weaver Prospect		Union				
J.M. Silvey Property		Union				

NORTH GEORGIA DISTRICT, GEORGIA						
Mine/Prospect	Field	County	Accessory Pegmatite Minerals	Max. Size (cm)	Color	Inclusions
James Gooch Mine		Union		15	green	
Joe Blue Mine		Union			rum	
Lot 301, District 11 Prospect		Union		15	colorless to light green in quartz; light rum in white feldspar	
Matt Gooch Mine		Union			light green	
mica mill		Union				
Mrs. Joe Stevens Prospect		Union				
Rogers and Rector Property		Union				
T.H. Saxon Mine		Union		46	light rum	
Thomas Property		Union		13		
Thomason Mine		Union			light rum	
unnamed prospect near Sarah Church		Union				
W.A. Sullivan Mine		Union			rum	Bt
Ward Gap Prospect		Union			pale rum	

HARTWELL DISTRICT, GEORGIA						
Mine/Prospect	Field	County	Accessory Pegmatite Minerals	Max. Size (cm)	Color	Inclusions
Alexander Mine [1]		Elbert		20	Clear	
Alexander Mine [2]		Elbert			white to light rum	
C.U. Gaines Prospect		Elbert		8	pale brownish olive	Mag
Chapman Mine [1]		Elbert			green	
Chapman Mine Shaft No. 2 [2]		Elbert			clear or rum	Bt
Chapman Mine [3]		Elbert		15		
Chapman Mine [4]		Elbert				
Chapman Mine [5]		Elbert		5		
Chapman Mine [6]		Elbert			white	
Chapman Mine [7]		Elbert			very light rum	
Cooley Mine		Elbert		20	pale green to light rum; yellowish green to light cinnamon brown	Mag
Craft Prospect		Elbert				
Crawford-Daniel Mine		Elbert			cinnamon brown	Mag

HARTWELL DISTRICT, GEORGIA						
Mine/Prospect	Field	County	Accessory Pegmatite Minerals	Max. Size (cm)	Color	Inclusions
Dewy Rose Prospect		Elbert		8		
J.M. Skelton Prospect		Elbert			light brownish olive to brown	Mag,Bt
M.L. Gaines Mine		Elbert			dark brownish olive, brown, yellowish olive (rare); local pale green mottling	Mag
Nancy Hart Cabin		Elbert				
New Bethel M.E. Church Prospect		Elbert		8	cinnamon brown (with concentric bands of yellowish olive)	Hem, Bt
prospect N of Chapman Mine		Elbert				
Rock Branch Church property		Elbert		5	rum	
Turner Prospect		Elbert			yellowish olive	
Ward Prospect [1]		Elbert		10	medium rum	
Ward Prospect [2]		Elbert		15	rum	
Air Line Mine		Hart				
B.W. Evans prospect [1]		Hart				

HARTWELL DISTRICT, GEORGIA						
Mine/Prospect	Field	County	Accessory Pegmatite Minerals	Max. Size (cm)	Color	Inclusions
B.W. Evans prospect [2]		Hart				
Bailey Mine		Hart			pale brownish olive to brown	Mag, Hem
Bowman		Hart				
Carter Mine		Hart			cinnamon brown with pale greenish streaks	Bt, Mag
Earl Parham farm prospect		Hart		25		
Garner Mine		Hart			pale yellowish olive to pale brown; local green mottling	Mag
Harper-Pierman Mine		Hart		8	clear (light yellowish olive with brownish streaks)	Tur, Qtz, Mag
Hartwell		Hart				
Hartwell Mine		Hart				
Horsehead Mine		Hart		25	light rum (pale yellowish to brownish olive)	Mag
J.A. Hailey farm property		Hart		13		
J.S. Heaton prospect [1]		Hart		9		

HARTWELL DISTRICT, GEORGIA						
Mine/Prospect	Field	County	Accessory Pegmatite Minerals	Max. Size (cm)	Color	Inclusions
J.S. Heaton prospect [2]		Hart		13		
J.W. Craft farm prospect		Hart		13		
Lon Allen Mine (Wood Mine; Gully Mine)		Hart			pinkish buff	
Mack Carter Prospect		Hart		8		
mine between Airline and Macedonia Church [1]		Hart		15		
mine between Airline and Macedonia Church [2]		Hart		20	light rum	Qtz
Myers Property		Hart				
R.I. Shiflett Prospect		Hart		36		
Royalston		Hart			pale brownish olive to cinnamon brown	Mag
Ruth Jones Mine		Hart			yellowish green to yellowish olive	Bt, FeO
Scrap Mine		Hart			yellowish olive (very pale green mottling)	Mag
Taylor Mine		Hart				
Tribble Prospect		Hart		15	ruby	
UNNAMED		Hart				

HARTWELL DISTRICT, GEORGIA						
Mine/Prospect	Field	County	Accessory Pegmatite Minerals	Max. Size (cm)	Color	Inclusions
W.L. Hodges farm		Hart		8		
Water Hole Mine (Waterhole Mine)		Hart			pale brown to brownish olive	

FRANKLIN-SYLVA DISTRICT, GEORGIA						
Mine/Prospect	Field	County	Accessory Pegmatite Minerals	Max. Size (cm)	Color	Inclusions
Bleckley Prospect		Rabun			green	
Hamby School Prospect [1]		Rabun			white	
Hamby School Prospect [2]		Rabun				
Hamby School Prospect [3]		Rabun			light rum	
Hamby School Prospect [4]		Rabun				
Hick's Mine		Rabun			slightly brownish	
Kell Mica Mine (Kelly Mine) [1]		Rabun		30	colorless (small books dark and opaque)	
Kell Mica Mine (Kelly Mine) [2]		Rabun		38	green (yellowish green to dark brownish olive)	
L.W. Curtis Property		Rabun				
Mark Beck Mine		Rabun		25	green	
Norton Mica Mine [JL1]		Rabun		20	light green (very pale green mottling)	
Norton Mica Mine [JL2]		Rabun			yellowish to brownish olive	
Porter McCracken Mine [1]		Rabun		10		

FRANKLIN-SYLVA DISTRICT, GEORGIA						
Mine/Prospect	Field	County	Accessory Pegmatite Minerals	Max. Size (cm)	Color	Inclusions
Porter McCracken Mine [2]		Rabun			clear to light green	
Porter McCracken Mine [3]		Rabun			green	
Porter McCracken Mine [4]		Rabun		8	green	
Rabun Bald Mine		Rabun			clear to greenish rum	
Speed - Arrendale Prospect [1]		Rabun		10	green (central portions black)	
Speed - Arrendale Prospect [2]		Rabun				
Tunnell Mine (Creighton Mine)		Rabun		25	light rum, pale green (yellowish to brownish olive)	
Westminster Road Prospect		Rabun			green	

OUTLYING DEPOSITS, GEORGIA						
Mine/Prospect	Field	County	Accessory Pegmatite Minerals	Max. Size (cm)	Color	Inclusions
Grinding Mill		Bartow				
Butts Co. roadcut [1]		Butts				
Butts Co. roadcut [2]		Butts				
B.W. Treadway and J.A. Potate Prospect		Carroll		15	green	
Bremen		Carroll				
dikes NW of Burwell		Carroll		10		
M.A. Heartley Prospect		Carroll		13	pale green	
UGA Parking Lot W03		Clarke				Qtz, Bt, Feldspar
Blackwells station occurrence		Cobb		8		
Cobb County mica-bearing pegmatites (general)		Cobb		5	slightly greenish	
Highway 41 Roadcuts		Cobb				
Luther Chalker Property		Cobb			mostly light rum (some greenish)	
Mabry Prospect [1]		Cobb		15		
Mabry Prospect [2]		Cobb				

OUTLYING DEPOSITS, GEORGIA						
Mine/Prospect	Field	County	Accessory Pegmatite Minerals	Max. Size (cm)	Color	Inclusions
Mabry Prospect [3]		Cobb				
Mabry Prospect [4]		Cobb			rum	
W.M. Davis property		Cobb		10		
McCollum Quarry		Coweta				
G.W. Elkins Property [1]		Dawson		8		
G.W. Elkins Property [2]		Dawson				
Vaughn Deposit (G.E. Vaughn Property)		DeKalb		10	green	
Pine Mountain Mine (Stockmar)		Douglas				
Villa Rica Mine (Sulfur Mining & Railroad Company Pyrite Mine)		Douglas				
Springer Mountain Mica Mine		Fannin		5		
White Mine		Fannin				
Porter Property		Fayette				
H.D. Hansard Prospect		Forsyth		5	rum	Mag
Harrison Prospect/Property		Forsyth		9	rum (brown?)	

OUTLYING DEPOSITS, GEORGIA						
Mine/Prospect	Field	County	Accessory Pegmatite Minerals	Max. Size (cm)	Color	Inclusions
McBrayer Prospect		Forsyth				
O.P. Bennett Prospect		Forsyth			colorless	
Oscar McBrayer Prospect [1]		Forsyth			Green	Mag, Grt
Oscar McBrayer Prospect [2]		Forsyth			colorless	
Cannon-Royston		Franklin				
J.L. Daniels Prospect [1]		Franklin			rum	
J.L. Daniels Prospect [2]		Franklin			rum	Grt
J.L. Daniels Prospect [3]		Franklin		5		
Lavonia Prospect [1]		Franklin			dark green	
Lavonia Prospect [2]		Franklin			green	
Roswell		Fulton				
T.M. Carter Property		Fulton				
Whitepath		Gordon				
Union Point		Greene				

OUTLYING DEPOSITS, GEORGIA						
Mine/Prospect	Field	County	Accessory Pegmatite Minerals	Max. Size (cm)	Color	Inclusions
W.M. Poss Property		Greene				
Clarkesville		Habersham				
UNNAMED		Habersham				
Merck Mine (Old Hope Mine) [1]		Hall			light rum	
Merck Mine (Old Hope Mine) [2]		Hall		36	light rum	
Merck Mine (Old Hope Mine) [JL1]		Hall			yellowish to brownish olive (very pale green mottling)	Hem
Merck Mine (Old Hope Mine) [JL2]		Hall			brownish olive to pale brown (very pale green mottling)	Mag, Hem, Bt
Merck Mine (Old Hope Mine) [JL3]		Hall			yellowish to brownish olive (very pale green mottling)	Hem
Merck Mine (Old Hope Mine) [JL4'		Hall			brownish olive to pale brown (very pale green mottling)	Mag, Hem, Bt
prospect near Gainesville		Hall		15	light rum	
prospect E of Bremen		Haralson		8		
railroad cut E of Bremen		Haralson		5		

OUTLYING DEPOSITS, GEORGIA						
Mine/Prospect	Field	County	Accessory Pegmatite Minerals	Max. Size (cm)	Color	Inclusions
Reeds Mountain Pyrite Mine		Haralson				
mica prospect (Long 73)		Heard				
Upson Clark prospect		Heard		15	greenish	
Maddox Mine		Henry		69	light rum	
Pendergrass		Jackson				
Ruby Quarry		Jones				
Graves Mountain Mines		Lincoln				
A.B. Snelson Prospect/Mine		Meriwether		15	rum	
mica mine (Keith Property, Long 73)		Meriwether		10	green	
Rufus Martin Prospect		Meriwether				
UNNAMED		Meriwether				
Adair Plantation		Morgan				
Alliston Prospect		Morgan		36		
D.S. Thomas farm property		Oconee				

OUTLYING DEPOSITS, GEORGIA						
Mine/Prospect	Field	County	Accessory Pegmatite Minerals	Max. Size (cm)	Color	Inclusions
Dickens Mine		Oconee				
Dixon Property		Oconee				
J.J. Branch property		Oconee		13		
B.F. Choran Property		Paulding		5	extremely green	
C.H. Miller Property		Paulding		15		
Cole Mine		Paulding				
Dr. C.W. Dean Mine (E.W. Dean Property)		Paulding		20	light rum (green in quartz)	Mag
J.F. Poole Property		Paulding			green	
Kirk Property		Paulding				
M.J. Petty		Paulding				
pegmatite east of New Georgia Church		Paulding				
R.S. Cole Mine		Paulding		30	light rum	
Turner Mine		Paulding				
W.J. Miller Property		Paulding			green	

OUTLYING DEPOSITS, GEORGIA						
Mine/Prospect	Field	County	Accessory Pegmatite Minerals	Max. Size (cm)	Color	Inclusions
Jack Bell Prospect		Rockdale		8	colorless	
H.B. Melton property [1]		Spaulding			rum	
H.B. Melton property [2]		Spaulding		3	rum	
Hunter Knob		Towns				
O.L. Burch Mine [1]		Towns			light green	
O.L. Burch Mine [2]		Towns		10		
Spanish Mountain Mine		Towns		25	colorless	
W.A. Henson Mine		Towns		20	smoky to rum	
Winchester Creek		Towns				
Ben Burts Mine		Troup		13	colorless	
Lee and Cline Prospect		Troup		20	green	Grt
Minerals Processing Company Mine (Foley Mine)		Troup				
Minerals Processing Company Mine No. 8 (Hogg Estate Mine) [core-margin]		Troup			green, rum (yellowish green to yellowish olive)	Grt

OUTLYING DEPOSITS, GEORGIA						
Mine/Prospect	Field	County	Accessory Pegmatite Minerals	Max. Size (cm)	Color	Inclusions
Minerals Processing Company Mine No. 8 (Hogg Estate Mine) [wall zone]		Troup			yellowish to brownish olive	Bt, Hem
prospect south of Smith's Store		Troup			yellowish olive	Hem
prospect west of Smith's store		Troup				
Smith's Store Prospect (Smith Store Prospect)		Troup		8	medium green (yellowish olive)	Hem
Virgil E. Davis property		Troup		14		
W.B. Word Property		Troup			greenish-rum	
Word Prospect (W. Hugh Allen Property)		Troup				
Lake Walton		Walton				Qtz, Bt, Hem?
unnamed prospect		Walton		13	green	
UNNAMED Prospect (10167921)		Walton				
Youngs Chapel Prospect		Wilkes				
Unknown mine 1					yellowish olive	Hem
Unknown mine 2					cinnamon brown	

APPENDIX C

PXRF ANALYTICAL RESULTS

Sample		As		Ba		Ca		Cd	
Sample #	District	As	± 2σ	Ba	± 2σ	Ca	± 2σ	Cd	± 2σ
1027 (1017)	ARTIFACT	< LOD	8	< LOD	63	< LOD	349	< LOD	8
1311 (1017)	ARTIFACT	< LOD	8	901	50	< LOD	358	< LOD	10
2430 (1019)	ARTIFACT	< LOD	11	< LOD	48	< LOD	448	< LOD	7
2518 (1019)	ARTIFACT	< LOD	10	326	45	< LOD	304	< LOD	9
3236 (1019)	ARTIFACT	< LOD	9	512	47	< LOD	280	< LOD	10
1332-1 (1017)	ARTIFACT	< LOD	7	< LOD	54	< LOD	283	< LOD	8
1350-1 (1017)	ARTIFACT	< LOD	9	915	48	1861	287	< LOD	9
1350-2 (1017)	ARTIFACT	< LOD	8	61	40	2256	274	< LOD	9
308-2 (1017)	ARTIFACT	< LOD	8	293	45	< LOD	440	< LOD	9
308-4 (1017)	ARTIFACT	< LOD	8	289	44	4318	325	< LOD	9
308-5 (1017)	ARTIFACT	< LOD	9	< LOD	58	8048	412	< LOD	8
PM1	CP (BG)	< LOD	8	1141	50	< LOD	374	< LOD	10
PM2	CP (BG)	< LOD	8	127	50	< LOD	335	< LOD	11
PM4	CP (BG)	< LOD	8	< LOD	62	< LOD	400	< LOD	9
PM5	CP (BG)	< LOD	8	420	46	< LOD	334	< LOD	9
PM7	CP (BG)	< LOD	9	344	45	< LOD	364	< LOD	9
PM8	CP (BG)	< LOD	8	< LOD	59	< LOD	359	< LOD	8
PM9	CP (BG)	< LOD	10	< LOD	60	< LOD	378	< LOD	8
PM11	CP (BG)	< LOD	8	112	42	< LOD	369	< LOD	8
RM8	CP (BG)	< LOD	10	522	48	< LOD	295	< LOD	10
RM9	CP (BG)	< LOD	10	149	45	< LOD	303	< LOD	10
RM10	CP (BG)	< LOD	10	< LOD	61	< LOD	356	< LOD	9
RM11	CP (BG)	< LOD	9	436	46	< LOD	351	< LOD	10
RM18	CP (BG)	< LOD	8	< LOD	55	< LOD	303	< LOD	8
RM21	CP (BG)	< LOD	11	86	43	< LOD	305	< LOD	9
RM23	CP (BG)	< LOD	9	< LOD	55	< LOD	252	< LOD	8
RM24	CP (BG)	< LOD	9	< LOD	49	< LOD	334	< LOD	7
RM25	CP (BG)	< LOD	9	< LOD	52	< LOD	347	< LOD	7
RM27	CP (BG)	< LOD	9	< LOD	49	< LOD	310	< LOD	7
RM28	CP (BG)	10	6	< LOD	52	< LOD	294	< LOD	8

Sample		As		Ba		Ca		Cd	
Sample #	District	As	± 2σ	Ba	± 2σ	Ca	± 2σ	Cd	± 2σ
RM29	CP (BG)	< LOD	11	< LOD	52	< LOD	308	< LOD	8
RM31	CP (BG)	< LOD	8	< LOD	51	< LOD	333	< LOD	7
RM33	CP (BG)	< LOD	9	< LOD	55	< LOD	313	< LOD	8
RM35	CP (BG)	< LOD	9	< LOD	47	< LOD	333	< LOD	7
RM40	CP (BG)	< LOD	10	< LOD	63	< LOD	339	< LOD	9
RM42	CP (BG)	< LOD	9	121	43	< LOD	353	< LOD	9
RM48	CP (BG)	< LOD	9	< LOD	45	< LOD	366	< LOD	6
RM51	CP (BG)	< LOD	8	< LOD	51	< LOD	339	< LOD	7
RM52	CP (BG)	< LOD	10	< LOD	51	< LOD	285	< LOD	7
RM53	CP (BG)	11	6	< LOD	50	< LOD	337	< LOD	7
RM62	CP (BG)	< LOD	9	< LOD	44	< LOD	347	< LOD	6
RM65	CP (BG)	< LOD	9	< LOD	46	< LOD	334	< LOD	6
RM66	CP (BG)	< LOD	8	< LOD	45	< LOD	376	< LOD	6
RM76	CP (BG)	< LOD	9	< LOD	45	< LOD	318	< LOD	6
RM81	CP (BG)	< LOD	9	< LOD	46	< LOD	352	< LOD	6
RM87	CP (BG)	< LOD	8	< LOD	50	< LOD	304	< LOD	7
DM1	CP (HS)	< LOD	7	2053	58	< LOD	376	< LOD	10
DM3	CP (HS)	< LOD	8	698	47	< LOD	412	< LOD	9
DM4	CP (HS)	< LOD	8	4148	72	< LOD	395	< LOD	11
DM5	CP (HS)	< LOD	7	2896	63	< LOD	357	< LOD	10
DM9	CP (HS)	< LOD	8	1262	53	< LOD	358	< LOD	10
DM10	CP (HS)	< LOD	7	2354	59	< LOD	386	< LOD	10
DM11	CP (HS)	< LOD	8	3204	67	< LOD	386	< LOD	11
DM14	CP (HS)	< LOD	8	435	48	< LOD	341	< LOD	9
DM17	CP (HS)	< LOD	8	3226	65	< LOD	380	< LOD	10
DM18	CP (HS)	< LOD	8	2150	57	< LOD	393	< LOD	10
DM19	CP (HS)	< LOD	8	939	49	< LOD	402	< LOD	9
DM20	CP (HS)	< LOD	8	4479	73	< LOD	405	< LOD	11
DM21	CP (HS)	< LOD	7	2896	63	< LOD	385	< LOD	10
DM22	CP (HS)	< LOD	7	1733	54	< LOD	406	< LOD	10

Sample		As		Ba		Ca		Cd	
Sample #	District	As	± 2σ	Ba	± 2σ	Ca	± 2σ	Cd	± 2σ
DM25	CP (HS)	< LOD	7	1345	53	< LOD	392	< LOD	10
DM29	CP (HS)	< LOD	8	2098	58	< LOD	356	< LOD	10
DM30	CP (HS)	< LOD	8	3271	68	< LOD	371	< LOD	11
DM31	CP (HS)	< LOD	8	3224	68	< LOD	354	< LOD	11
DM32	CP (HS)	< LOD	7	1812	56	< LOD	384	< LOD	10
DM33	CP (HS)	< LOD	8	1631	55	< LOD	364	< LOD	10
DM34	CP (HS)	< LOD	8	1637	55	< LOD	397	< LOD	10
JDHM1	CP (HS)	< LOD	9	< LOD	56	< LOD	349	< LOD	8
JDHM4	CP (HS)	< LOD	8	469	45	< LOD	422	< LOD	9
JDHM8	CP (HS)	< LOD	8	149	47	< LOD	278	< LOD	10
JDHM9	CP (HS)	< LOD	8	362	44	< LOD	395	< LOD	9
JDHM10	CP (HS)	< LOD	8	757	49	< LOD	346	< LOD	10
JDHM11	CP (HS)	< LOD	8	806	47	< LOD	389	< LOD	9
JDHM12	CP (HS)	< LOD	8	1203	52	< LOD	404	< LOD	10
JDHM14	CP (HS)	< LOD	9	558	49	< LOD	308	< LOD	10
JDHM17	CP (HS)	< LOD	8	611	48	< LOD	395	< LOD	10
JDHM22	CP (HS)	< LOD	9	399	47	< LOD	336	< LOD	10
JDHM26	CP (HS)	< LOD	9	< LOD	60	< LOD	340	< LOD	9
JDHM27	CP (HS)	< LOD	8	186	43	< LOD	378	< LOD	9
JDHM29	CP (HS)	< LOD	8	1295	52	< LOD	395	< LOD	10
JDHM32	CP (HS)	< LOD	8	1047	50	< LOD	398	< LOD	10
JDHM33	CP (HS)	< LOD	8	1141	53	< LOD	330	< LOD	11
JDHM34	CP (HS)	< LOD	9	< LOD	58	< LOD	364	< LOD	9
JDHM35	CP (HS)	< LOD	8	1742	56	< LOD	423	< LOD	10
JDHM43	CP (HS)	< LOD	8	< LOD	61	< LOD	346	< LOD	9
JDHM44	CP (HS)	< LOD	8	1188	54	< LOD	320	< LOD	11
JDHM45	CP (HS)	< LOD	8	< LOD	64	< LOD	323	< LOD	9
JDHM46	CP (HS)	< LOD	9	114	43	< LOD	339	< LOD	9
JDHM48-1	CP (HS)	< LOD	8	1586	55	< LOD	417	< LOD	10
JDHM48-2	CP (HS)	< LOD	9	1499	55	< LOD	359	< LOD	10

Sample		As		Ba		Ca		Cd	
Sample #	District	As	± 2σ	Ba	± 2σ	Ca	± 2σ	Cd	± 2σ
JDHM48-3	CP (HS)	< LOD	8	1488	55	< LOD	369	< LOD	10
JDHM48-4	CP (HS)	< LOD	8	1526	55	< LOD	405	< LOD	10
JDHM48-5	CP (HS)	< LOD	8	1399	52	< LOD	419	< LOD	10
JDHM48-6	CP (HS)	< LOD	9	1433	53	< LOD	413	< LOD	10
JDHM48-7	CP (HS)	< LOD	8	1617	56	< LOD	393	< LOD	11
JDHM48-8	CP (HS)	< LOD	8	1514	55	< LOD	407	< LOD	10
JDHM49	CP (HS)	< LOD	9	< LOD	55	< LOD	388	< LOD	8
JDHM50	CP (HS)	< LOD	9	1357	53	< LOD	396	< LOD	10
JDHM52	CP (HS)	< LOD	8	734	48	< LOD	385	< LOD	10
JDHM54	CP (HS)	< LOD	8	269	44	< LOD	387	< LOD	10
JDHM56	CP (HS)	< LOD	8	< LOD	62	< LOD	347	< LOD	9
JDHM57	CP (HS)	< LOD	8	301	44	< LOD	386	< LOD	9
JDHM58	CP (HS)	< LOD	8	< LOD	62	< LOD	407	< LOD	9
JDHM59	CP (HS)	< LOD	8	999	51	< LOD	387	< LOD	10
JDHP1	CP (HS)	9	6	655	48	< LOD	430	< LOD	9
JDHP2	CP (HS)	< LOD	8	2014	56	< LOD	412	< LOD	10
JDHP6	CP (HS)	< LOD	8	741	47	< LOD	415	< LOD	9
JDHP9	CP (HS)	< LOD	9	< LOD	60	< LOD	403	< LOD	9
JDHP10	CP (HS)	< LOD	8	1306	52	< LOD	404	< LOD	10
JDHP11	CP (HS)	< LOD	8	1233	52	< LOD	372	< LOD	10
KP2	CP (HS)	< LOD	8	1078	50	< LOD	418	< LOD	10
KP3	CP (HS)	< LOD	8	3126	64	< LOD	407	< LOD	11
KP4	CP (HS)	< LOD	9	1576	56	< LOD	398	< LOD	10
KP5	CP (HS)	< LOD	8	2159	59	< LOD	391	< LOD	10
KP7	CP (HS)	< LOD	8	1841	57	< LOD	383	< LOD	10
KP8	CP (HS)	< LOD	9	< LOD	57	< LOD	340	< LOD	8
KP9	CP (HS)	< LOD	8	1067	50	< LOD	428	< LOD	9
KP13	CP (HS)	< LOD	8	2805	64	< LOD	371	< LOD	11
KP14	CP (HS)	< LOD	8	3942	71	< LOD	395	< LOD	11
KP17	CP (HS)	< LOD	8	2920	65	< LOD	363	< LOD	11

Sample		As		Ba		Ca		Cd	
Sample #	District	As	± 2σ	Ba	± 2σ	Ca	± 2σ	Cd	± 2σ
KP19	CP (HS)	< LOD	9	1490	54	< LOD	417	< LOD	10
KP21	CP (HS)	< LOD	8	2653	62	< LOD	392	< LOD	10
KP23	CP (HS)	< LOD	9	451	45	< LOD	407	< LOD	9
KP25	CP (HS)	< LOD	8	3674	69	< LOD	391	< LOD	11
LM1	CP (HS)	< LOD	8	3744	68	< LOD	426	< LOD	11
LM4	CP (HS)	< LOD	8	3676	67	< LOD	411	< LOD	11
LM8	CP (HS)	< LOD	8	3686	67	< LOD	385	< LOD	11
LM10	CP (HS)	< LOD	8	802	48	< LOD	378	< LOD	9
LM11	CP (HS)	< LOD	8	874	48	< LOD	402	< LOD	9
LM18	CP (HS)	< LOD	9	1545	53	< LOD	395	< LOD	10
LM20	CP (HS)	< LOD	9	478	46	< LOD	360	< LOD	9
LM21	CP (HS)	< LOD	8	981	50	< LOD	382	< LOD	9
LM27	CP (HS)	< LOD	8	2278	58	< LOD	423	< LOD	10
LM28	CP (HS)	< LOD	8	2187	58	< LOD	375	< LOD	10
LM29	CP (HS)	< LOD	8	1250	51	< LOD	390	< LOD	9
WM1	CP (HS)	< LOD	8	212	46	< LOD	287	< LOD	10
WM4	CP (HS)	< LOD	9	411	54	< LOD	231	12	8
WM5	CP (HS)	< LOD	8	< LOD	59	< LOD	324	< LOD	9
WM11	CP (HS)	< LOD	8	< LOD	59	< LOD	368	< LOD	8
WM17	CP (HS)	< LOD	8	< LOD	60	< LOD	341	< LOD	9
WM21	CP (HS)	< LOD	7	316	44	< LOD	376	< LOD	9
WM24	CP (HS)	< LOD	8	< LOD	59	< LOD	318	< LOD	9
WM27	CP (HS)	< LOD	8	229	43	< LOD	375	< LOD	9
WM32	CP (HS)	< LOD	8	< LOD	60	< LOD	358	< LOD	9
WM35	CP (HS)	10	5	237	44	< LOD	370	< LOD	9
WM45	CP (HS)	< LOD	8	< LOD	59	< LOD	349	< LOD	9
WM59	CP (HS)	< LOD	8	< LOD	63	< LOD	369	< LOD	9
WM66	CP (HS)	< LOD	8	< LOD	60	< LOD	376	< LOD	9
WM68	CP (HS)	< LOD	7	< LOD	62	< LOD	359	< LOD	9
WM89	CP (HS)	< LOD	8	< LOD	58	< LOD	346	< LOD	9

Sample		As		Ba		Ca		Cd	
Sample #	District	As	± 2σ	Ba	± 2σ	Ca	± 2σ	Cd	± 2σ
WM90	CP (HS)	< LOD	8	< LOD	58	< LOD	381	< LOD	9
WM91	CP (HS)	< LOD	8	< LOD	64	< LOD	344	< LOD	9
WM100	CP (HS)	< LOD	9	< LOD	58	< LOD	368	< LOD	8
WM112	CP (HS)	< LOD	9	< LOD	54	< LOD	331	< LOD	8
WM120	CP (HS)	< LOD	8	68	41	< LOD	380	< LOD	9
WM124-1	CP (HS)	< LOD	8	112	43	< LOD	388	< LOD	9
WM124-2	CP (HS)	< LOD	7	76	42	< LOD	396	< LOD	9
WM124-3	CP (HS)	< LOD	7	68	42	< LOD	398	< LOD	9
WM124-4	CP (HS)	< LOD	8	112	42	< LOD	398	< LOD	9
WM124-5	CP (HS)	< LOD	8	76	42	< LOD	389	< LOD	9
WM124-6	CP (HS)	< LOD	7	62	42	< LOD	396	< LOD	9
WM124-7	CP (HS)	< LOD	8	65	42	< LOD	376	< LOD	9
WM124-8	CP (HS)	< LOD	7	117	43	< LOD	381	< LOD	9
WM125	CP (HS)	< LOD	8	187	44	< LOD	313	< LOD	10
WM138	CP (HS)	< LOD	8	101	42	< LOD	372	< LOD	9
WM140	CP (HS)	< LOD	8	< LOD	63	< LOD	385	< LOD	9
WM149	CP (HS)	< LOD	7	185	42	< LOD	368	< LOD	9
WM156	CP (HS)	< LOD	8	120	44	< LOD	313	< LOD	10
WM161	CP (HS)	< LOD	7	< LOD	57	< LOD	365	< LOD	8
WM162	CP (HS)	< LOD	8	< LOD	61	< LOD	356	< LOD	9
WM166	CP (HS)	< LOD	8	< LOD	62	< LOD	365	< LOD	9
WM170	CP (HS)	< LOD	8	114	43	< LOD	353	< LOD	9
WM177	CP (HS)	< LOD	8	< LOD	62	< LOD	321	< LOD	9
DPM1	SP	< LOD	10	< LOD	51	< LOD	400	< LOD	7
DPM2	SP	< LOD	11	< LOD	64	< LOD	308	< LOD	9
DPM3	SP	< LOD	8	< LOD	62	< LOD	443	< LOD	9
DPM4	SP	12	7	< LOD	56	< LOD	345	< LOD	8
DPM5	SP	< LOD	9	< LOD	53	< LOD	448	< LOD	8
DPM6	SP	11	7	< LOD	47	< LOD	412	< LOD	7
DPM7	SP	12	7	< LOD	47	< LOD	448	< LOD	6

Sample		As		Ba		Ca		Cd	
Sample #	District	As	± 2σ	Ba	± 2σ	Ca	± 2σ	Cd	± 2σ
DPM8	SP	< LOD	8	< LOD	56	< LOD	432	< LOD	8
DPM10	SP	< LOD	10	< LOD	54	< LOD	383	< LOD	7
DPM10-2	SP	10	6	< LOD	49	< LOD	369	< LOD	7
DPM11	SP	< LOD	9	< LOD	57	< LOD	434	< LOD	8
DPM12	SP	< LOD	10	< LOD	50	< LOD	385	< LOD	7
DPM13	SP	< LOD	11	< LOD	56	< LOD	417	< LOD	8
DPM16	SP	< LOD	10	< LOD	49	< LOD	398	< LOD	7
DPM18	SP	< LOD	10	< LOD	47	< LOD	438	< LOD	7
DPM20	SP	< LOD	10	< LOD	54	< LOD	399	< LOD	8
DPM24	SP	< LOD	11	< LOD	64	< LOD	424	< LOD	9
DPM27	SP	< LOD	10	< LOD	52	< LOD	357	< LOD	7
DPM28	SP	< LOD	11	< LOD	63	< LOD	346	< LOD	9
DPM29	SP	< LOD	10	< LOD	58	< LOD	434	< LOD	8
DPM31	SP	< LOD	10	< LOD	58	< LOD	344	< LOD	8
DPM32	SP	< LOD	11	< LOD	51	< LOD	432	< LOD	7
DPM33	SP	< LOD	10	< LOD	66	< LOD	332	< LOD	9
DPM34	SP	< LOD	9	123	44	< LOD	367	< LOD	9
DPM35	SP	< LOD	10	< LOD	58	< LOD	354	< LOD	8
DPM36	SP	< LOD	10	< LOD	60	< LOD	299	< LOD	8
DPM37	SP	< LOD	9	263	46	< LOD	368	< LOD	10
DPM38	SP	< LOD	9	234	49	< LOD	303	< LOD	10
DPM39	SP	< LOD	9	< LOD	62	< LOD	356	< LOD	9
DPM39-2	SP	< LOD	9	80	45	< LOD	360	< LOD	9
McK1	SP	16	8	< LOD	49	< LOD	460	< LOD	7
McK2	SP	< LOD	12	< LOD	51	< LOD	380	< LOD	7
McK3	SP	15	9	< LOD	51	< LOD	399	< LOD	7
McK4	SP	< LOD	12	< LOD	54	< LOD	398	< LOD	7
McK5	SP	< LOD	12	< LOD	48	< LOD	439	< LOD	7
McK6	SP	< LOD	12	< LOD	50	< LOD	401	< LOD	7
McK7	SP	< LOD	13	< LOD	52	< LOD	404	< LOD	7

Sample		As		Ba		Ca		Cd	
Sample #	District	As	± 2σ	Ba	± 2σ	Ca	± 2σ	Cd	± 2σ
McK8	SP	< LOD	14	< LOD	56	< LOD	395	< LOD	8
McK9	SP	< LOD	14	< LOD	52	< LOD	353	< LOD	7
McK10	SP	< LOD	12	< LOD	46	< LOD	437	< LOD	6
McK11	SP	< LOD	12	< LOD	44	< LOD	400	< LOD	6
McK12	SP	< LOD	13	< LOD	49	< LOD	459	< LOD	7
McK13	SP	< LOD	13	< LOD	49	< LOD	427	< LOD	7
McK15	SP	14	9	< LOD	51	< LOD	428	< LOD	7
Pink1	SP	< LOD	11	< LOD	58	< LOD	411	< LOD	8
Pink2	SP	< LOD	11	< LOD	58	< LOD	449	< LOD	8
Pink3	SP	14	7	< LOD	52	< LOD	480	< LOD	7
Pink4	SP	< LOD	10	< LOD	62	< LOD	401	< LOD	9
Pink7	SP	< LOD	11	< LOD	67	< LOD	319	< LOD	9
Pink8	SP	< LOD	9	< LOD	53	< LOD	470	< LOD	7
Pink9	SP	< LOD	10	< LOD	62	< LOD	336	< LOD	9
Pink10	SP	< LOD	10	< LOD	54	< LOD	485	< LOD	8
Pink11	SP	< LOD	12	< LOD	66	< LOD	360	< LOD	9
Pink12	SP	< LOD	10	< LOD	54	< LOD	380	< LOD	7
JAPM2	TB (IG)	< LOD	11	< LOD	47	< LOD	388	< LOD	7
JAPM8	TB (IG)	< LOD	11	< LOD	53	< LOD	365	< LOD	8
JAPM9	TB (IG)	< LOD	10	< LOD	52	< LOD	420	< LOD	8
JAPM10	TB (IG)	< LOD	12	< LOD	50	< LOD	420	< LOD	7
JAPM15	TB (IG)	< LOD	10	< LOD	55	< LOD	418	< LOD	8
JAPM17	TB (IG)	< LOD	13	< LOD	70	< LOD	431	< LOD	10
MM1	TB (WV)	< LOD	8	961	50	< LOD	345	< LOD	10
MM2	TB (WV)	< LOD	8	658	49	< LOD	301	< LOD	10
MM3	TB (WV)	< LOD	7	787	49	< LOD	340	< LOD	10
MM4	TB (WV)	< LOD	8	921	51	< LOD	304	< LOD	10
MM5	TB (WV)	< LOD	8	755	50	< LOD	323	< LOD	10
MM6	TB (WV)	< LOD	8	755	48	< LOD	362	< LOD	10
MM7	TB (WV)	< LOD	7	748	49	< LOD	349	< LOD	10

Sample		As		Ba		Ca		Cd	
Sample #	District	As	± 2σ	Ba	± 2σ	Ca	± 2σ	Cd	± 2σ
MM8	TB (WV)	< LOD	7	574	45	< LOD	348	< LOD	9
MM9	TB (WV)	< LOD	7	543	46	< LOD	350	< LOD	9
MM10	TB (WV)	< LOD	7	678	47	< LOD	369	< LOD	10
MM11	TB (WV)	< LOD	8	< LOD	58	< LOD	365	< LOD	9
MM13	TB (WV)	< LOD	8	148	44	< LOD	320	< LOD	10
MM14	TB (WV)	< LOD	8	820	48	< LOD	337	< LOD	10
MM15	TB (WV)	< LOD	8	110	42	< LOD	341	< LOD	9
MM16	TB (WV)	< LOD	8	75	41	< LOD	358	< LOD	9
MM24	TB (WV)	< LOD	8	782	48	< LOD	352	< LOD	10
MM28	TB (WV)	< LOD	8	127	46	< LOD	260	< LOD	10
MM31	TB (WV)	< LOD	8	957	51	< LOD	339	< LOD	10
MM32	TB (WV)	< LOD	8	< LOD	65	< LOD	264	< LOD	10
MM33	TB (WV)	< LOD	7	614	46	< LOD	356	< LOD	9
MM34	TB (WV)	< LOD	8	1001	49	< LOD	348	< LOD	10
MM35	TB (WV)	< LOD	7	694	48	< LOD	362	< LOD	10
MM36	TB (WV)	< LOD	8	744	53	< LOD	257	< LOD	11
MM37	TB (WV)	< LOD	8	951	52	< LOD	292	< LOD	10
MM40	TB (WV)	< LOD	7	< LOD	61	< LOD	356	< LOD	9
MM42	TB (WV)	< LOD	8	313	45	< LOD	339	< LOD	9
MM45	TB (WV)	< LOD	7	473	46	< LOD	338	< LOD	10
MM47	TB (WV)	< LOD	7	415	45	< LOD	356	< LOD	10
MM48	TB (WV)	< LOD	8	741	48	< LOD	335	< LOD	9
MM50	TB (WV)	< LOD	8	470	45	< LOD	347	< LOD	9
MM51	TB (WV)	< LOD	8	131	41	< LOD	354	< LOD	9
MM58	TB (WV)	< LOD	8	242	44	< LOD	332	< LOD	9
MM59	TB (WV)	< LOD	8	618	47	< LOD	339	< LOD	10
MM66	TB (WV)	< LOD	8	881	48	< LOD	355	< LOD	10
MM69	TB (WV)	< LOD	7	755	47	< LOD	363	< LOD	10
MM73	TB (WV)	< LOD	8	456	46	< LOD	339	< LOD	10
MM74	TB (WV)	< LOD	7	455	47	< LOD	323	< LOD	10

Sample		As		Ba		Ca		Cd	
Sample #	District	As	± 2σ	Ba	± 2σ	Ca	± 2σ	Cd	± 2σ
MM76	TB (WV)	< LOD	8	< LOD	61	< LOD	298	< LOD	9
MM86	TB (WV)	< LOD	7	< LOD	65	< LOD	337	< LOD	10
MM93-1	TB (WV)	9	5	204	44	< LOD	345	< LOD	9
MM93-2	TB (WV)	< LOD	8	696	48	< LOD	356	< LOD	10
MM93-3	TB (WV)	< LOD	8	343	44	< LOD	363	< LOD	9
MM93-4	TB (WV)	< LOD	7	592	46	< LOD	363	< LOD	9
MM93-5	TB (WV)	< LOD	8	357	45	< LOD	365	< LOD	10
MM93-6	TB (WV)	< LOD	7	566	46	< LOD	356	< LOD	9
MM93-7	TB (WV)	< LOD	8	619	46	< LOD	357	< LOD	10
MM93-8	TB (WV)	< LOD	8	569	45	< LOD	362	< LOD	9
MM93-9	TB (WV)	< LOD	7	622	46	< LOD	358	< LOD	10
VB2	TB (YV)	< LOD	7	255	43	< LOD	354	< LOD	9
VB3	TB (YV)	< LOD	7	< LOD	61	< LOD	357	< LOD	9
VB6	TB (YV)	< LOD	7	< LOD	59	< LOD	362	< LOD	9
VB7	TB (YV)	< LOD	8	427	46	< LOD	346	< LOD	10
VB9	TB (YV)	< LOD	8	< LOD	55	< LOD	367	< LOD	8
VB10	TB (YV)	< LOD	8	< LOD	59	< LOD	346	< LOD	9
VB11	TB (YV)	< LOD	7	349	43	< LOD	353	< LOD	9
VB14	TB (YV)	< LOD	7	< LOD	59	< LOD	335	< LOD	8

Sample		Co		Cr		Cs		Cu	
Sample #	District	Co	± 2σ	Cr	± 2σ	Cs	± 2σ	Cu	± 2σ
1027 (1017)	ARTIFACT	< LOD	104	122	24	< LOD	22	< LOD	27
1311 (1017)	ARTIFACT	< LOD	147	96	26	< LOD	25	< LOD	29
2430 (1019)	ARTIFACT	< LOD	184	< LOD	39	< LOD	18	37	23
2518 (1019)	ARTIFACT	< LOD	84	68	19	< LOD	24	< LOD	24
3236 (1019)	ARTIFACT	< LOD	80	< LOD	20	< LOD	25	< LOD	29
1332-1 (1017)	ARTIFACT	< LOD	81	< LOD	20	< LOD	21	< LOD	25
1350-1 (1017)	ARTIFACT	< LOD	121	164	28	< LOD	23	< LOD	27
1350-2 (1017)	ARTIFACT	< LOD	94	160	23	< LOD	22	< LOD	25
308-2 (1017)	ARTIFACT	< LOD	158	66	26	< LOD	24	< LOD	29
308-4 (1017)	ARTIFACT	< LOD	147	79	27	< LOD	22	< LOD	29
308-5 (1017)	ARTIFACT	< LOD	170	88	28	< LOD	22	< LOD	29
PM1	CP (BG)	< LOD	113	99	23	< LOD	24	< LOD	27
PM2	CP (BG)	< LOD	121	< LOD	28	< LOD	27	< LOD	30
PM4	CP (BG)	< LOD	144	92	25	< LOD	22	< LOD	27
PM5	CP (BG)	< LOD	115	33	20	< LOD	23	< LOD	28
PM7	CP (BG)	< LOD	143	< LOD	32	< LOD	24	< LOD	30
PM8	CP (BG)	< LOD	132	74	22	< LOD	21	< LOD	30
PM9	CP (BG)	< LOD	160	< LOD	34	< LOD	22	< LOD	31
PM11	CP (BG)	140	80	90	23	< LOD	22	< LOD	27
RM8	CP (BG)	< LOD	128	< LOD	24	73	17	< LOD	30
RM9	CP (BG)	< LOD	116	< LOD	25	< LOD	25	< LOD	28
RM10	CP (BG)	122	78	64	22	< LOD	23	< LOD	26
RM11	CP (BG)	< LOD	121	88	23	< LOD	25	< LOD	27
RM18	CP (BG)	< LOD	100	< LOD	23	< LOD	21	< LOD	31
RM21	CP (BG)	< LOD	83	63	18	< LOD	24	< LOD	27
RM23	CP (BG)	< LOD	107	< LOD	20	< LOD	21	< LOD	31
RM24	CP (BG)	< LOD	102	< LOD	25	< LOD	19	< LOD	30
RM25	CP (BG)	< LOD	102	< LOD	28	< LOD	20	< LOD	28
RM27	CP (BG)	< LOD	106	< LOD	26	< LOD	19	< LOD	30
RM28	CP (BG)	< LOD	99	< LOD	21	< LOD	20	< LOD	29

Sample		Co		Cr		Cs		Cu	
Sample #	District	Co	± 2σ	Cr	± 2σ	Cs	± 2σ	Cu	± 2σ
RM29	CP (BG)	< LOD	102	< LOD	22	< LOD	20	35	23
RM31	CP (BG)	< LOD	99	< LOD	27	< LOD	19	< LOD	29
RM33	CP (BG)	< LOD	96	85	20	< LOD	21	< LOD	29
RM35	CP (BG)	< LOD	99	< LOD	29	< LOD	18	< LOD	31
RM40	CP (BG)	< LOD	119	55	21	< LOD	23	< LOD	28
RM42	CP (BG)	< LOD	120	< LOD	30	< LOD	24	< LOD	27
RM48	CP (BG)	< LOD	111	< LOD	30	< LOD	18	37	21
RM51	CP (BG)	< LOD	98	< LOD	28	< LOD	20	< LOD	27
RM52	CP (BG)	< LOD	98	< LOD	21	< LOD	20	< LOD	31
RM53	CP (BG)	< LOD	106	< LOD	27	< LOD	19	< LOD	29
RM62	CP (BG)	< LOD	110	< LOD	30	< LOD	17	< LOD	30
RM65	CP (BG)	127	67	< LOD	27	< LOD	18	< LOD	30
RM66	CP (BG)	< LOD	105	207	27	< LOD	17	< LOD	27
RM76	CP (BG)	< LOD	110	< LOD	23	< LOD	18	< LOD	32
RM81	CP (BG)	< LOD	119	88	22	< LOD	18	< LOD	33
RM87	CP (BG)	< LOD	103	< LOD	23	< LOD	19	< LOD	29
DM1	CP (HS)	< LOD	148	56	26	< LOD	25	< LOD	29
DM3	CP (HS)	< LOD	146	131	28	< LOD	23	< LOD	27
DM4	CP (HS)	< LOD	146	67	27	116	19	< LOD	28
DM5	CP (HS)	162	88	< LOD	33	39	18	< LOD	30
DM9	CP (HS)	< LOD	154	< LOD	35	< LOD	25	< LOD	30
DM10	CP (HS)	< LOD	133	< LOD	33	35	17	< LOD	30
DM11	CP (HS)	< LOD	150	80	26	122	19	< LOD	29
DM14	CP (HS)	< LOD	150	< LOD	30	< LOD	24	< LOD	30
DM17	CP (HS)	< LOD	131	< LOD	35	105	18	< LOD	30
DM18	CP (HS)	< LOD	130	168	28	< LOD	25	< LOD	28
DM19	CP (HS)	< LOD	150	135	29	< LOD	23	< LOD	29
DM20	CP (HS)	< LOD	145	184	30	135	19	< LOD	27
DM21	CP (HS)	< LOD	141	< LOD	35	27	18	< LOD	28
DM22	CP (HS)	< LOD	148	78	27	< LOD	24	< LOD	28

Sample		Co		Cr		Cs		Cu	
Sample #	District	Co	± 2σ	Cr	± 2σ	Cs	± 2σ	Cu	± 2σ
DM25	CP (HS)	< LOD	134	200	29	< LOD	25	< LOD	26
DM29	CP (HS)	< LOD	139	< LOD	30	< LOD	26	< LOD	32
DM30	CP (HS)	< LOD	150	< LOD	31	145	19	< LOD	31
DM31	CP (HS)	< LOD	150	< LOD	31	128	19	< LOD	31
DM32	CP (HS)	< LOD	145	< LOD	36	< LOD	25	< LOD	30
DM33	CP (HS)	< LOD	133	53	24	< LOD	25	< LOD	27
DM34	CP (HS)	< LOD	145	159	28	< LOD	26	< LOD	27
JDHM1	CP (HS)	< LOD	120	< LOD	28	< LOD	22	< LOD	29
JDHM4	CP (HS)	< LOD	151	109	27	< LOD	23	< LOD	28
JDHM8	CP (HS)	< LOD	123	< LOD	21	< LOD	26	< LOD	31
JDHM9	CP (HS)	< LOD	139	97	25	< LOD	23	< LOD	27
JDHM10	CP (HS)	149	87	< LOD	30	< LOD	25	< LOD	28
JDHM11	CP (HS)	< LOD	116	81	23	< LOD	24	< LOD	26
JDHM12	CP (HS)	< LOD	144	82	25	42	17	< LOD	27
JDHM14	CP (HS)	< LOD	129	< LOD	26	< LOD	25	< LOD	29
JDHM17	CP (HS)	< LOD	153	161	28	< LOD	24	< LOD	29
JDHM22	CP (HS)	< LOD	122	< LOD	27	< LOD	25	< LOD	27
JDHM26	CP (HS)	< LOD	112	< LOD	28	< LOD	22	< LOD	27
JDHM27	CP (HS)	< LOD	117	151	24	< LOD	24	< LOD	27
JDHM29	CP (HS)	< LOD	137	46	24	38	17	< LOD	28
JDHM32	CP (HS)	< LOD	126	97	25	35	17	< LOD	26
JDHM33	CP (HS)	< LOD	117	88	21	71	18	< LOD	28
JDHM34	CP (HS)	< LOD	119	< LOD	31	< LOD	22	< LOD	28
JDHM35	CP (HS)	< LOD	150	71	26	67	17	< LOD	30
JDHM43	CP (HS)	< LOD	119	< LOD	27	< LOD	23	< LOD	29
JDHM44	CP (HS)	< LOD	139	< LOD	26	36	18	< LOD	28
JDHM45	CP (HS)	< LOD	134	< LOD	24	< LOD	23	< LOD	29
JDHM46	CP (HS)	< LOD	124	75	21	< LOD	23	< LOD	29
JDHM48-1	CP (HS)	< LOD	152	60	26	48	17	< LOD	27
JDHM48-2	CP (HS)	< LOD	151	< LOD	31	42	18	< LOD	30

Sample		Co		Cr		Cs		Cu	
Sample #	District	Co	± 2σ	Cr	± 2σ	Cs	± 2σ	Cu	± 2σ
JDHM48-3	CP (HS)	< LOD	156	37	23	27	18	< LOD	30
JDHM48-4	CP (HS)	< LOD	152	69	26	33	17	< LOD	28
JDHM48-5	CP (HS)	< LOD	152	79	26	< LOD	25	< LOD	28
JDHM48-6	CP (HS)	< LOD	151	77	26	27	17	< LOD	27
JDHM48-7	CP (HS)	< LOD	152	67	25	41	18	< LOD	28
JDHM48-8	CP (HS)	< LOD	153	121	27	33	17	< LOD	29
JDHM49	CP (HS)	< LOD	130	67	23	< LOD	21	< LOD	25
JDHM50	CP (HS)	< LOD	147	< LOD	34	34	17	< LOD	26
JDHM52	CP (HS)	< LOD	141	115	25	< LOD	24	< LOD	28
JDHM54	CP (HS)	< LOD	116	101	23	< LOD	24	< LOD	24
JDHM56	CP (HS)	< LOD	141	< LOD	27	< LOD	22	< LOD	30
JDHM57	CP (HS)	< LOD	133	49	23	< LOD	23	< LOD	27
JDHM58	CP (HS)	< LOD	149	86	26	< LOD	22	< LOD	28
JDHM59	CP (HS)	< LOD	137	99	24	< LOD	25	< LOD	26
JDHP1	CP (HS)	< LOD	170	118	30	< LOD	24	< LOD	29
JDHP2	CP (HS)	< LOD	139	70	27	< LOD	24	< LOD	28
JDHP6	CP (HS)	190	99	129	29	< LOD	23	< LOD	28
JDHP9	CP (HS)	< LOD	161	< LOD	34	< LOD	23	< LOD	29
JDHP10	CP (HS)	< LOD	140	90	27	< LOD	24	< LOD	28
JDHP11	CP (HS)	< LOD	144	< LOD	33	< LOD	24	< LOD	28
KP2	CP (HS)	< LOD	159	122	29	< LOD	24	< LOD	28
KP3	CP (HS)	< LOD	152	< LOD	40	41	18	< LOD	30
KP4	CP (HS)	< LOD	166	113	29	< LOD	25	< LOD	29
KP5	CP (HS)	< LOD	151	< LOD	38	< LOD	26	< LOD	30
KP7	CP (HS)	< LOD	164	79	27	< LOD	25	< LOD	29
KP8	CP (HS)	< LOD	112	< LOD	27	< LOD	22	< LOD	30
KP9	CP (HS)	< LOD	171	84	29	< LOD	23	< LOD	30
KP13	CP (HS)	< LOD	161	< LOD	37	< LOD	27	< LOD	29
KP14	CP (HS)	< LOD	151	114	28	121	19	< LOD	28
KP17	CP (HS)	< LOD	156	< LOD	34	< LOD	27	< LOD	29

Sample		Co		Cr		Cs		Cu	
Sample #	District	Co	± 2σ	Cr	± 2σ	Cs	± 2σ	Cu	± 2σ
KP19	CP (HS)	< LOD	158	118	29	< LOD	25	< LOD	27
KP21	CP (HS)	< LOD	160	102	28	< LOD	26	< LOD	31
KP23	CP (HS)	< LOD	163	97	27	< LOD	22	< LOD	29
KP25	CP (HS)	< LOD	163	53	27	58	18	< LOD	29
LM1	CP (HS)	< LOD	150	50	29	42	18	< LOD	29
LM4	CP (HS)	229	99	96	29	42	18	< LOD	30
LM8	CP (HS)	< LOD	137	118	29	65	18	< LOD	27
LM10	CP (HS)	< LOD	149	110	28	< LOD	23	< LOD	30
LM11	CP (HS)	< LOD	150	91	28	< LOD	23	< LOD	30
LM18	CP (HS)	< LOD	152	59	28	< LOD	24	< LOD	28
LM20	CP (HS)	< LOD	156	< LOD	37	< LOD	22	< LOD	31
LM21	CP (HS)	156	102	64	26	< LOD	23	< LOD	30
LM27	CP (HS)	< LOD	150	105	30	< LOD	25	< LOD	28
LM28	CP (HS)	< LOD	141	64	26	< LOD	25	< LOD	29
LM29	CP (HS)	< LOD	148	< LOD	40	< LOD	23	< LOD	30
WM1	CP (HS)	< LOD	110	< LOD	20	47	17	< LOD	29
WM4	CP (HS)	< LOD	150	< LOD	23	87	20	< LOD	36
WM5	CP (HS)	< LOD	137	< LOD	25	< LOD	23	< LOD	30
WM11	CP (HS)	132	80	113	23	< LOD	22	< LOD	27
WM17	CP (HS)	< LOD	109	58	20	< LOD	23	< LOD	27
WM21	CP (HS)	< LOD	119	34	21	29	16	32	20
WM24	CP (HS)	< LOD	108	< LOD	23	< LOD	23	< LOD	27
WM27	CP (HS)	< LOD	105	123	22	30	16	< LOD	27
WM32	CP (HS)	< LOD	114	32	20	< LOD	22	< LOD	26
WM35	CP (HS)	120	78	139	24	< LOD	24	< LOD	27
WM45	CP (HS)	< LOD	108	43	20	< LOD	22	< LOD	25
WM59	CP (HS)	< LOD	125	77	22	< LOD	23	< LOD	28
WM66	CP (HS)	< LOD	109	71	21	< LOD	22	< LOD	25
WM68	CP (HS)	< LOD	107	124	22	< LOD	23	< LOD	27
WM89	CP (HS)	< LOD	110	60	20	< LOD	22	< LOD	26

Sample		Co		Cr		Cs		Cu	
Sample #	District	Co	± 2σ	Cr	± 2σ	Cs	± 2σ	Cu	± 2σ
WM90	CP (HS)	< LOD	115	190	25	< LOD	22	< LOD	25
WM91	CP (HS)	< LOD	109	51	19	< LOD	24	< LOD	28
WM100	CP (HS)	< LOD	159	< LOD	31	< LOD	22	< LOD	31
WM112	CP (HS)	< LOD	112	28	19	< LOD	21	< LOD	29
WM120	CP (HS)	< LOD	113	63	22	< LOD	23	< LOD	26
WM124-1	CP (HS)	< LOD	120	139	24	< LOD	23	< LOD	26
WM124-2	CP (HS)	< LOD	123	87	23	< LOD	23	< LOD	26
WM124-3	CP (HS)	< LOD	125	108	24	< LOD	23	< LOD	27
WM124-4	CP (HS)	< LOD	124	89	24	< LOD	23	< LOD	27
WM124-5	CP (HS)	< LOD	126	100	24	< LOD	23	< LOD	27
WM124-6	CP (HS)	< LOD	125	93	24	< LOD	23	< LOD	27
WM124-7	CP (HS)	< LOD	121	67	22	< LOD	23	< LOD	29
WM124-8	CP (HS)	< LOD	121	78	23	< LOD	24	< LOD	25
WM125	CP (HS)	< LOD	111	< LOD	24	36	16	< LOD	27
WM138	CP (HS)	< LOD	112	96	22	< LOD	23	< LOD	27
WM140	CP (HS)	< LOD	115	96	23	< LOD	24	< LOD	28
WM149	CP (HS)	< LOD	107	91	22	< LOD	23	< LOD	27
WM156	CP (HS)	< LOD	105	< LOD	23	< LOD	24	< LOD	29
WM161	CP (HS)	< LOD	109	103	22	< LOD	21	< LOD	27
WM162	CP (HS)	< LOD	108	237	25	< LOD	23	< LOD	27
WM166	CP (HS)	< LOD	108	< LOD	26	< LOD	23	< LOD	25
WM170	CP (HS)	< LOD	111	< LOD	25	< LOD	24	< LOD	27
WM177	CP (HS)	< LOD	130	< LOD	24	< LOD	24	< LOD	30
DPM1	SP	< LOD	192	< LOD	36	< LOD	20	< LOD	32
DPM2	SP	< LOD	200	< LOD	25	< LOD	24	< LOD	40
DPM3	SP	< LOD	170	66	27	< LOD	23	< LOD	28
DPM4	SP	< LOD	174	< LOD	28	< LOD	21	37	24
DPM5	SP	< LOD	187	< LOD	39	< LOD	21	< LOD	29
DPM6	SP	< LOD	180	< LOD	38	< LOD	18	< LOD	32
DPM7	SP	< LOD	196	42	27	< LOD	18	43	24

Sample		Co		Cr		Cs		Cu	
Sample #	District	Co	± 2σ	Cr	± 2σ	Cs	± 2σ	Cu	± 2σ
DPM8	SP	< LOD	177	63	26	< LOD	21	< LOD	30
DPM10	SP	< LOD	171	< LOD	31	< LOD	20	< LOD	32
DPM10-2	SP	< LOD	166	< LOD	26	< LOD	19	< LOD	32
DPM11	SP	< LOD	182	46	26	< LOD	22	< LOD	30
DPM12	SP	189	122	< LOD	34	< LOD	19	< LOD	34
DPM13	SP	< LOD	181	174	29	< LOD	21	< LOD	30
DPM16	SP	< LOD	170	< LOD	36	< LOD	19	< LOD	33
DPM18	SP	< LOD	187	66	27	< LOD	18	< LOD	32
DPM20	SP	< LOD	186	< LOD	32	< LOD	21	< LOD	32
DPM24	SP	< LOD	189	127	28	< LOD	24	< LOD	33
DPM27	SP	< LOD	195	< LOD	28	< LOD	20	< LOD	36
DPM28	SP	< LOD	186	< LOD	26	< LOD	23	< LOD	34
DPM29	SP	< LOD	201	< LOD	38	< LOD	22	< LOD	33
DPM31	SP	< LOD	182	< LOD	27	< LOD	22	< LOD	35
DPM32	SP	< LOD	207	71	28	< LOD	20	< LOD	36
DPM33	SP	< LOD	214	< LOD	27	< LOD	25	< LOD	37
DPM34	SP	< LOD	177	< LOD	30	< LOD	24	< LOD	32
DPM35	SP	< LOD	178	< LOD	26	< LOD	22	40	25
DPM36	SP	< LOD	176	< LOD	23	< LOD	23	40	26
DPM37	SP	< LOD	177	< LOD	28	< LOD	25	< LOD	33
DPM38	SP	< LOD	185	< LOD	22	< LOD	27	< LOD	36
DPM39	SP	< LOD	178	< LOD	28	< LOD	23	< LOD	34
DPM39-2	SP	< LOD	179	< LOD	28	< LOD	25	< LOD	32
McK1	SP	< LOD	191	54	29	< LOD	19	< LOD	33
McK2	SP	< LOD	198	< LOD	34	< LOD	20	< LOD	35
McK3	SP	< LOD	187	< LOD	29	< LOD	20	61	25
McK4	SP	< LOD	159	< LOD	37	< LOD	21	55	24
McK5	SP	< LOD	200	< LOD	41	< LOD	19	< LOD	31
McK6	SP	< LOD	190	< LOD	34	< LOD	19	< LOD	33
McK7	SP	< LOD	172	< LOD	34	< LOD	20	37	24

Sample		Co		Cr		Cs		Cu	
Sample #	District	Co	± 2σ	Cr	± 2σ	Cs	± 2σ	Cu	± 2σ
McK8	SP	< LOD	174	< LOD	33	< LOD	21	< LOD	34
McK9	SP	< LOD	193	< LOD	28	< LOD	20	< LOD	35
McK10	SP	< LOD	192	144	31	< LOD	18	< LOD	33
McK11	SP	< LOD	191	< LOD	31	< LOD	17	< LOD	36
McK12	SP	< LOD	181	< LOD	44	< LOD	19	83	26
McK13	SP	< LOD	184	< LOD	34	< LOD	19	51	24
McK15	SP	< LOD	176	< LOD	39	< LOD	20	38	23
Pink1	SP	< LOD	204	< LOD	35	< LOD	22	< LOD	34
Pink2	SP	< LOD	195	< LOD	34	< LOD	22	< LOD	35
Pink3	SP	240	139	< LOD	40	< LOD	20	< LOD	34
Pink4	SP	< LOD	193	< LOD	34	< LOD	23	< LOD	33
Pink7	SP	< LOD	204	< LOD	24	< LOD	25	< LOD	40
Pink8	SP	< LOD	195	62	29	< LOD	20	< LOD	33
Pink9	SP	< LOD	199	< LOD	27	< LOD	23	< LOD	32
Pink10	SP	< LOD	190	< LOD	36	< LOD	20	< LOD	30
Pink11	SP	< LOD	299	< LOD	32	< LOD	25	< LOD	40
Pink12	SP	< LOD	196	< LOD	30	< LOD	21	< LOD	35
JAPM2	TB (IG)	< LOD	160	< LOD	33	< LOD	19	< LOD	33
JAPM8	TB (IG)	< LOD	163	< LOD	30	< LOD	20	< LOD	30
JAPM9	TB (IG)	< LOD	150	< LOD	35	< LOD	20	< LOD	29
JAPM10	TB (IG)	< LOD	186	< LOD	35	< LOD	20	< LOD	31
JAPM15	TB (IG)	< LOD	157	< LOD	38	< LOD	21	< LOD	31
JAPM17	TB (IG)	< LOD	438	< LOD	62	< LOD	26	< LOD	40
MM1	TB (WV)	< LOD	86	87	21	93	17	< LOD	25
MM2	TB (WV)	< LOD	97	< LOD	23	64	17	< LOD	29
MM3	TB (WV)	< LOD	95	77	20	90	17	< LOD	27
MM4	TB (WV)	< LOD	91	30	18	92	17	< LOD	26
MM5	TB (WV)	< LOD	97	< LOD	27	100	17	< LOD	27
MM6	TB (WV)	< LOD	94	41	20	98	17	< LOD	25
MM7	TB (WV)	< LOD	93	< LOD	29	79	17	< LOD	26

Sample		Co		Cr		Cs		Cu	
Sample #	District	Co	± 2σ	Cr	± 2σ	Cs	± 2σ	Cu	± 2σ
MM8	TB (WV)	< LOD	86	83	21	< LOD	24	< LOD	24
MM9	TB (WV)	< LOD	95	104	21	27	16	< LOD	27
MM10	TB (WV)	< LOD	99	117	22	94	17	< LOD	26
MM11	TB (WV)	< LOD	101	92	22	< LOD	22	< LOD	26
MM13	TB (WV)	< LOD	99	< LOD	24	< LOD	24	< LOD	28
MM14	TB (WV)	< LOD	89	41	19	67	17	< LOD	25
MM15	TB (WV)	< LOD	93	< LOD	27	< LOD	23	< LOD	27
MM16	TB (WV)	< LOD	93	133	22	< LOD	22	< LOD	24
MM24	TB (WV)	< LOD	88	46	20	57	16	< LOD	25
MM28	TB (WV)	< LOD	94	< LOD	20	< LOD	25	< LOD	30
MM31	TB (WV)	< LOD	93	70	20	108	17	< LOD	26
MM32	TB (WV)	< LOD	98	< LOD	19	< LOD	24	< LOD	28
MM33	TB (WV)	< LOD	91	84	21	40	16	< LOD	26
MM34	TB (WV)	< LOD	87	53	20	96	17	< LOD	26
MM35	TB (WV)	< LOD	97	< LOD	29	83	17	< LOD	27
MM36	TB (WV)	< LOD	100	< LOD	19	119	19	< LOD	30
MM37	TB (WV)	< LOD	94	< LOD	21	80	18	< LOD	27
MM40	TB (WV)	< LOD	89	71	21	< LOD	23	< LOD	24
MM42	TB (WV)	< LOD	96	34	19	< LOD	24	< LOD	26
MM45	TB (WV)	< LOD	94	< LOD	28	< LOD	24	< LOD	25
MM47	TB (WV)	< LOD	95	< LOD	29	31	16	< LOD	25
MM48	TB (WV)	< LOD	88	33	19	62	17	< LOD	27
MM50	TB (WV)	< LOD	92	73	20	< LOD	24	< LOD	24
MM51	TB (WV)	< LOD	91	123	22	< LOD	22	< LOD	26
MM58	TB (WV)	< LOD	99	34	19	< LOD	24	< LOD	26
MM59	TB (WV)	< LOD	89	32	19	39	16	< LOD	26
MM66	TB (WV)	< LOD	88	< LOD	27	70	16	< LOD	25
MM69	TB (WV)	< LOD	88	89	21	63	16	< LOD	25
MM73	TB (WV)	< LOD	92	93	21	< LOD	24	< LOD	25
MM74	TB (WV)	< LOD	94	< LOD	24	32	17	< LOD	25

Sample		Co		Cr		Cs		Cu	
Sample #	District	Co	± 2σ	Cr	± 2σ	Cs	± 2σ	Cu	± 2σ
MM76	TB (WV)	< LOD	103	< LOD	24	< LOD	23	< LOD	28
MM86	TB (WV)	< LOD	101	64	20	< LOD	24	< LOD	26
MM93-1	TB (WV)	< LOD	92	104	21	< LOD	24	< LOD	25
MM93-2	TB (WV)	< LOD	93	< LOD	29	65	17	< LOD	27
MM93-3	TB (WV)	< LOD	92	86	21	< LOD	24	< LOD	25
MM93-4	TB (WV)	< LOD	92	94	21	44	16	< LOD	25
MM93-5	TB (WV)	< LOD	91	71	21	< LOD	24	< LOD	25
MM93-6	TB (WV)	< LOD	90	66	20	39	16	< LOD	25
MM93-7	TB (WV)	< LOD	91	57	20	52	16	< LOD	27
MM93-8	TB (WV)	< LOD	93	67	21	33	16	< LOD	27
MM93-9	TB (WV)	< LOD	92	79	21	41	16	< LOD	26
VB2	TB (YV)	< LOD	90	129	22	< LOD	23	< LOD	26
VB3	TB (YV)	< LOD	89	114	22	< LOD	22	< LOD	26
VB6	TB (YV)	< LOD	89	81	22	< LOD	21	< LOD	25
VB7	TB (YV)	< LOD	104	89	22	< LOD	25	< LOD	25
VB9	TB (YV)	< LOD	105	161	24	< LOD	21	< LOD	26
VB10	TB (YV)	< LOD	90	97	21	< LOD	22	< LOD	24
VB11	TB (YV)	< LOD	86	86	21	< LOD	23	< LOD	27
VB14	TB (YV)	< LOD	88	47	19	< LOD	22	< LOD	25

Sample		Fe		Hg		K		Mn	
Sample #	District	Fe	± 2σ	Hg	± 2σ	K	± 2σ	Mn	± 2σ
1027 (1017)	ARTIFACT	12351	293	< LOD	9	88435	1107	124	60
1311 (1017)	ARTIFACT	23442	415	< LOD	10	67238	1072	286	80
2430 (1019)	ARTIFACT	35365	520	< LOD	12	87811	1347	325	90
2518 (1019)	ARTIFACT	8188	231	< LOD	9	76587	950	81	52
3236 (1019)	ARTIFACT	7476	226	< LOD	10	71002	877	< LOD	76
1332-1 (1017)	ARTIFACT	8838	229	< LOD	8	71199	898	100	51
1350-1 (1017)	ARTIFACT	17396	344	< LOD	9	84246	1171	157	65
1350-2 (1017)	ARTIFACT	10167	257	< LOD	9	90099	1120	113	56
308-2 (1017)	ARTIFACT	27790	451	< LOD	10	91322	1311	322	84
308-4 (1017)	ARTIFACT	22476	411	< LOD	10	78442	1170	568	99
308-5 (1017)	ARTIFACT	31099	485	< LOD	10	87763	1333	888	120
PM1	CP (BG)	14903	318	< LOD	9	92300	1181	124	61
PM2	CP (BG)	15564	339	< LOD	10	80354	1057	268	75
PM4	CP (BG)	23141	410	< LOD	10	90471	1251	119	66
PM5	CP (BG)	14626	323	< LOD	10	81887	1063	109	60
PM7	CP (BG)	22008	406	< LOD	10	80458	1154	123	67
PM8	CP (BG)	18182	368	< LOD	10	84123	1122	131	65
PM9	CP (BG)	24820	444	< LOD	11	83616	1192	120	71
PM11	CP (BG)	15268	325	< LOD	9	93137	1189	134	62
RM8	CP (BG)	16301	365	< LOD	10	66215	925	209	74
RM9	CP (BG)	14846	327	< LOD	10	70357	956	223	71
RM10	CP (BG)	15474	319	< LOD	9	82831	1126	< LOD	77
RM11	CP (BG)	17196	344	< LOD	10	79920	1109	137	63
RM18	CP (BG)	9910	274	< LOD	10	76581	952	< LOD	83
RM21	CP (BG)	8360	237	< LOD	9	80367	973	< LOD	74
RM23	CP (BG)	10567	295	< LOD	12	59708	795	< LOD	83
RM24	CP (BG)	10761	280	< LOD	11	86276	1057	< LOD	79
RM25	CP (BG)	11576	284	< LOD	11	86883	1089	< LOD	84
RM27	CP (BG)	12417	304	< LOD	11	74781	974	< LOD	84
RM28	CP (BG)	10048	276	< LOD	11	70797	912	< LOD	82

Sample		Fe		Hg		K		Mn	
Sample #	District	Fe	± 2σ	Hg	± 2σ	K	± 2σ	Mn	± 2σ
RM29	CP (BG)	9989	283	< LOD	13	77386	981	< LOD	88
RM31	CP (BG)	10573	274	< LOD	10	84359	1058	< LOD	84
RM33	CP (BG)	10128	274	< LOD	11	77761	993	< LOD	79
RM35	CP (BG)	10830	283	< LOD	11	86553	1068	< LOD	77
RM40	CP (BG)	15947	331	< LOD	10	76650	1054	< LOD	83
RM42	CP (BG)	16312	333	< LOD	9	80333	1105	175	65
RM48	CP (BG)	13240	308	< LOD	11	88571	1128	< LOD	81
RM51	CP (BG)	10744	271	< LOD	10	85971	1079	< LOD	80
RM52	CP (BG)	9636	274	< LOD	11	68321	891	< LOD	83
RM53	CP (BG)	11982	291	< LOD	10	81954	1068	179	65
RM62	CP (BG)	12957	309	< LOD	11	75791	1041	90	59
RM65	CP (BG)	10360	271	< LOD	11	81503	1031	< LOD	74
RM66	CP (BG)	13814	304	11	7	89538	1182	93	58
RM76	CP (BG)	12574	312	< LOD	11	76066	1003	< LOD	81
RM81	CP (BG)	13729	324	< LOD	12	90380	1126	< LOD	88
RM87	CP (BG)	11277	290	< LOD	11	73058	959	118	61
DM1	CP (HS)	22830	414	< LOD	10	85283	1199	227	77
DM3	CP (HS)	23411	413	< LOD	10	94070	1292	124	67
DM4	CP (HS)	22559	408	< LOD	9	85386	1234	142	69
DM5	CP (HS)	17631	361	< LOD	10	82948	1140	124	65
DM9	CP (HS)	23159	427	< LOD	10	81294	1135	< LOD	98
DM10	CP (HS)	19290	373	< LOD	10	91047	1217	128	65
DM11	CP (HS)	23938	427	< LOD	10	85849	1212	155	72
DM14	CP (HS)	21847	420	< LOD	11	75150	1059	110	69
DM17	CP (HS)	18751	369	< LOD	10	88376	1207	< LOD	93
DM18	CP (HS)	18785	368	< LOD	9	90260	1221	< LOD	84
DM19	CP (HS)	23942	421	< LOD	10	93065	1277	< LOD	94
DM20	CP (HS)	23101	413	< LOD	10	90413	1275	142	71
DM21	CP (HS)	21156	394	< LOD	10	87280	1209	157	70
DM22	CP (HS)	23704	412	< LOD	10	92354	1285	180	72

Sample		Fe		Hg		K		Mn	
Sample #	District	Fe	± 2σ	Hg	± 2σ	K	± 2σ	Mn	± 2σ
DM25	CP (HS)	21182	371	< LOD	10	87498	1237	130	63
DM29	CP (HS)	19323	392	< LOD	11	79059	1117	123	69
DM30	CP (HS)	22617	417	< LOD	10	84049	1178	150	71
DM31	CP (HS)	22039	421	< LOD	11	78260	1108	152	72
DM32	CP (HS)	22198	406	< LOD	10	88637	1226	159	72
DM33	CP (HS)	19076	372	< LOD	10	82891	1138	< LOD	87
DM34	CP (HS)	23223	412	< LOD	11	87486	1250	126	68
JDHM1	CP (HS)	16736	347	< LOD	10	84060	1111	99	60
JDHM4	CP (HS)	25630	425	< LOD	10	95001	1338	270	78
JDHM8	CP (HS)	15156	348	< LOD	10	64508	874	118	65
JDHM9	CP (HS)	21923	395	< LOD	10	93704	1272	272	76
JDHM10	CP (HS)	17636	358	< LOD	10	81455	1102	189	70
JDHM11	CP (HS)	16759	335	< LOD	9	95580	1236	245	71
JDHM12	CP (HS)	23057	406	< LOD	10	91921	1273	166	70
JDHM14	CP (HS)	16529	360	< LOD	10	71483	977	120	65
JDHM17	CP (HS)	25717	434	< LOD	9	87915	1262	223	76
JDHM22	CP (HS)	15619	338	< LOD	10	80985	1068	< LOD	78
JDHM26	CP (HS)	13444	309	< LOD	10	86631	1084	337	77
JDHM27	CP (HS)	15918	327	< LOD	9	91627	1192	159	63
JDHM29	CP (HS)	20706	380	< LOD	9	92340	1259	215	72
JDHM32	CP (HS)	18406	355	< LOD	9	95671	1266	310	77
JDHM33	CP (HS)	14339	320	< LOD	9	79714	1038	149	64
JDHM34	CP (HS)	15242	328	< LOD	10	91204	1156	344	79
JDHM35	CP (HS)	25495	428	< LOD	10	93588	1319	236	76
JDHM43	CP (HS)	15340	329	< LOD	9	82330	1089	< LOD	88
JDHM44	CP (HS)	19869	392	< LOD	11	73850	1029	237	77
JDHM45	CP (HS)	18435	379	< LOD	10	74016	1020	280	79
JDHM46	CP (HS)	16637	350	< LOD	10	81915	1080	162	67
JDHM48-1	CP (HS)	25457	427	< LOD	10	94911	1324	366	86
JDHM48-2	CP (HS)	23088	428	< LOD	10	78595	1130	254	80

Sample		Fe		Hg		K		Mn	
Sample #	District	Fe	± 2σ	Hg	± 2σ	K	± 2σ	Mn	± 2σ
JDHM48-3	CP (HS)	24842	433	< LOD	10	82115	1174	283	82
JDHM48-4	CP (HS)	25186	425	< LOD	10	91232	1294	261	78
JDHM48-5	CP (HS)	25630	430	< LOD	10	93579	1317	343	83
JDHM48-6	CP (HS)	25145	427	< LOD	9	91781	1303	277	80
JDHM48-7	CP (HS)	24164	421	< LOD	10	86868	1239	259	79
JDHM48-8	CP (HS)	25244	428	< LOD	10	91998	1296	341	85
JDHM49	CP (HS)	19022	367	< LOD	10	93984	1230	103	61
JDHM50	CP (HS)	23045	408	< LOD	10	90909	1257	156	69
JDHM52	CP (HS)	21896	397	< LOD	10	88303	1219	299	80
JDHM54	CP (HS)	15785	324	< LOD	9	95933	1224	97	58
JDHM56	CP (HS)	20752	395	< LOD	10	81511	1104	295	80
JDHM57	CP (HS)	19932	370	< LOD	9	91651	1225	303	77
JDHM58	CP (HS)	23901	417	< LOD	9	93231	1285	301	81
JDHM59	CP (HS)	20326	379	< LOD	9	90479	1223	156	67
JDHP1	CP (HS)	30284	480	< LOD	11	94804	1371	361	89
JDHP2	CP (HS)	21244	388	< LOD	10	94422	1288	283	78
JDHP6	CP (HS)	22282	405	< LOD	10	94908	1293	216	74
JDHP9	CP (HS)	26371	446	< LOD	11	89190	1271	319	84
JDHP10	CP (HS)	21898	402	< LOD	10	94890	1291	335	84
JDHP11	CP (HS)	22035	402	< LOD	10	85195	1176	180	71
KP2	CP (HS)	27969	452	< LOD	11	93376	1335	269	81
KP3	CP (HS)	25201	431	< LOD	10	90713	1297	166	73
KP4	CP (HS)	29055	470	< LOD	10	87608	1275	183	77
KP5	CP (HS)	24850	431	< LOD	10	84773	1224	183	73
KP7	CP (HS)	27239	462	< LOD	10	77979	1183	282	84
KP8	CP (HS)	13138	306	< LOD	10	83201	1073	260	73
KP9	CP (HS)	29993	476	< LOD	10	93327	1348	239	82
KP13	CP (HS)	26355	458	< LOD	11	79805	1169	327	88
KP14	CP (HS)	26050	430	< LOD	10	87877	1262	318	82
KP17	CP (HS)	24303	437	< LOD	10	77218	1135	181	75

Sample		Fe		Hg		K		Mn	
Sample #	District	Fe	± 2σ	Hg	± 2σ	K	± 2σ	Mn	± 2σ
KP19	CP (HS)	27027	446	< LOD	10	92584	1324	308	82
KP21	CP (HS)	26574	451	< LOD	10	84266	1238	285	83
KP23	CP (HS)	27623	458	< LOD	11	92568	1295	347	88
KP25	CP (HS)	26676	455	< LOD	10	83363	1233	259	82
LM1	CP (HS)	24464	422	< LOD	10	95096	1324	192	74
LM4	CP (HS)	22720	402	< LOD	10	92431	1297	185	72
LM8	CP (HS)	20687	384	< LOD	9	87860	1229	< LOD	93
LM10	CP (HS)	23625	426	< LOD	10	85265	1201	< LOD	100
LM11	CP (HS)	23989	422	< LOD	10	90382	1269	173	73
LM18	CP (HS)	24383	427	< LOD	11	89008	1261	113	69
LM20	CP (HS)	24063	439	< LOD	10	78834	1138	120	72
LM21	CP (HS)	22997	422	< LOD	10	83512	1182	< LOD	97
LM27	CP (HS)	25152	421	< LOD	9	92606	1323	208	74
LM28	CP (HS)	21271	391	< LOD	9	83906	1200	133	67
LM29	CP (HS)	22911	414	< LOD	10	86214	1221	131	69
WM1	CP (HS)	12041	303	< LOD	10	70062	917	154	66
WM4	CP (HS)	18707	414	< LOD	11	42514	709	241	84
WM5	CP (HS)	18729	385	< LOD	10	74170	1025	263	79
WM11	CP (HS)	15240	326	< LOD	10	88781	1154	89	58
WM17	CP (HS)	14013	315	< LOD	9	83103	1091	132	62
WM21	CP (HS)	16240	333	< LOD	10	89666	1177	< LOD	87
WM24	CP (HS)	13110	303	< LOD	10	80413	1026	103	58
WM27	CP (HS)	13313	297	< LOD	9	94084	1174	151	61
WM32	CP (HS)	14645	317	< LOD	9	88347	1139	156	63
WM35	CP (HS)	14993	322	< LOD	10	91549	1181	101	59
WM45	CP (HS)	13403	304	< LOD	9	88156	1115	163	63
WM59	CP (HS)	17694	357	< LOD	10	89112	1170	146	65
WM66	CP (HS)	13938	305	< LOD	9	96114	1192	95	57
WM68	CP (HS)	13054	296	< LOD	9	88904	1133	149	61
WM89	CP (HS)	13482	304	< LOD	10	84192	1083	95	58

Sample		Fe		Hg		K		Mn	
Sample #	District	Fe	± 2σ	Hg	± 2σ	K	± 2σ	Mn	± 2σ
WM90	CP (HS)	15576	323	< LOD	9	94069	1213	157	64
WM91	CP (HS)	12831	303	< LOD	10	82010	1063	107	59
WM100	CP (HS)	24499	443	< LOD	11	82608	1174	209	79
WM112	CP (HS)	13663	314	< LOD	9	83708	1054	118	61
WM120	CP (HS)	15312	324	< LOD	9	94439	1204	144	63
WM124-1	CP (HS)	16895	338	< LOD	10	95100	1234	91	58
WM124-2	CP (HS)	17323	343	< LOD	10	96393	1255	168	66
WM124-3	CP (HS)	17507	345	< LOD	9	96286	1261	174	66
WM124-4	CP (HS)	17662	348	< LOD	9	96885	1266	170	67
WM124-5	CP (HS)	17768	353	< LOD	10	94696	1238	180	68
WM124-6	CP (HS)	17572	347	< LOD	10	96194	1260	195	68
WM124-7	CP (HS)	16857	342	< LOD	9	91061	1187	222	70
WM124-8	CP (HS)	16982	340	< LOD	9	92803	1217	161	64
WM125	CP (HS)	13117	310	< LOD	10	77021	989	149	64
WM138	CP (HS)	14206	312	< LOD	9	94131	1184	92	57
WM140	CP (HS)	15544	324	< LOD	10	95417	1226	153	63
WM149	CP (HS)	13115	297	< LOD	9	93204	1173	169	63
WM156	CP (HS)	12584	306	< LOD	9	77267	991	194	68
WM161	CP (HS)	13802	304	< LOD	9	91744	1164	169	64
WM162	CP (HS)	13717	306	< LOD	9	86867	1121	102	58
WM166	CP (HS)	14446	311	< LOD	9	88197	1145	148	63
WM170	CP (HS)	14017	313	< LOD	9	86862	1121	156	64
WM177	CP (HS)	17461	370	< LOD	10	73074	998	170	70
DPM1	SP	34626	542	< LOD	12	81589	1260	406	100
DPM2	SP	32906	567	< LOD	13	61400	984	476	111
DPM3	SP	30664	479	< LOD	10	95400	1382	427	93
DPM4	SP	27007	485	< LOD	11	73378	1093	327	91
DPM5	SP	35075	522	< LOD	10	96253	1404	455	98
DPM6	SP	32020	508	< LOD	10	87207	1303	332	91
DPM7	SP	37570	553	< LOD	12	93717	1404	533	106

Sample		Fe		Hg		K		Mn	
Sample #	District	Fe	± 2σ	Hg	± 2σ	K	± 2σ	Mn	± 2σ
DPM8	SP	32209	498	< LOD	11	94245	1372	325	88
DPM10	SP	28186	483	< LOD	11	82584	1198	400	96
DPM10-2	SP	27495	472	< LOD	11	80461	1164	266	85
DPM11	SP	33623	513	< LOD	11	92875	1366	352	91
DPM12	SP	30988	508	< LOD	12	82689	1226	430	99
DPM13	SP	32387	509	< LOD	11	86661	1309	353	92
DPM16	SP	28170	475	< LOD	12	86240	1247	333	90
DPM18	SP	34349	525	< LOD	12	95651	1394	428	97
DPM20	SP	32638	520	< LOD	11	83478	1243	526	105
DPM24	SP	34622	533	< LOD	11	86381	1310	406	98
DPM27	SP	34344	558	< LOD	12	73041	1134	621	116
DPM28	SP	30176	523	< LOD	12	71509	1097	282	91
DPM29	SP	37945	562	< LOD	11	88859	1376	552	109
DPM31	SP	29281	512	< LOD	12	72171	1080	378	99
DPM32	SP	40419	591	< LOD	12	88030	1361	649	117
DPM33	SP	37007	599	< LOD	13	63453	1036	549	117
DPM34	SP	29255	495	< LOD	11	80088	1180	387	95
DPM35	SP	28168	500	< LOD	12	75757	1109	283	90
DPM36	SP	26182	489	< LOD	12	62841	942	366	96
DPM37	SP	29456	497	< LOD	11	77467	1159	440	99
DPM38	SP	28976	522	< LOD	12	61021	945	430	104
DPM39	SP	29584	502	< LOD	11	74562	1117	571	108
DPM39-2	SP	29823	502	< LOD	11	75226	1132	505	104
McK1	SP	36206	537	< LOD	11	97471	1447	461	100
McK2	SP	35334	553	< LOD	12	80365	1231	338	98
McK3	SP	31856	519	< LOD	12	83742	1249	359	95
McK4	SP	25273	448	15	8	89366	1265	183	77
McK5	SP	38007	566	< LOD	13	90192	1370	291	93
McK6	SP	33615	537	< LOD	12	84887	1286	396	99
McK7	SP	27612	478	< LOD	12	86318	1264	238	84

Sample		Fe		Hg		K		Mn	
Sample #	District	Fe	± 2σ	Hg	± 2σ	K	± 2σ	Mn	± 2σ
McK8	SP	28527	487	< LOD	12	81270	1228	263	86
McK9	SP	34384	548	< LOD	12	70401	1107	344	97
McK10	SP	35228	541	< LOD	12	94003	1411	383	98
McK11	SP	33620	538	< LOD	12	81277	1239	204	84
McK12	SP	33094	508	< LOD	12	100530	1461	457	99
McK13	SP	32486	517	< LOD	12	92504	1353	185	81
McK15	SP	30514	493	< LOD	12	93668	1361	273	85
Pink1	SP	39051	577	< LOD	12	83207	1311	312	95
Pink2	SP	36724	550	< LOD	12	94089	1412	439	101
Pink3	SP	40679	581	< LOD	12	100312	1510	488	107
Pink4	SP	36470	549	< LOD	12	83377	1278	210	85
Pink7	SP	33763	575	< LOD	12	64018	1003	369	104
Pink8	SP	38298	548	< LOD	11	94304	1452	390	95
Pink9	SP	35851	559	< LOD	11	66955	1055	414	101
Pink10	SP	37727	536	< LOD	11	100439	1508	498	100
Pink11	SP	70174	848	< LOD	12	62715	1106	676	140
Pink12	SP	35432	554	< LOD	12	76958	1203	394	100
JAPM2	TB (IG)	26076	454	< LOD	12	85039	1223	564	103
JAPM8	TB (IG)	26642	461	< LOD	12	76948	1139	578	104
JAPM9	TB (IG)	23591	419	< LOD	11	96744	1324	441	91
JAPM10	TB (IG)	32999	520	< LOD	12	80893	1270	1070	134
JAPM15	TB (IG)	25674	443	< LOD	11	89865	1290	512	97
JAPM17	TB (IG)	150084	1243	< LOD	14	40731	1269	649	162
MM1	TB (WV)	9083	241	< LOD	9	90924	1097	< LOD	73
MM2	TB (WV)	10322	269	< LOD	10	76835	958	< LOD	77
MM3	TB (WV)	10111	259	< LOD	9	89832	1101	< LOD	75
MM4	TB (WV)	9160	253	< LOD	9	79614	977	< LOD	79
MM5	TB (WV)	10602	272	< LOD	9	83348	1029	87	55
MM6	TB (WV)	10633	263	< LOD	9	94058	1148	87	53
MM7	TB (WV)	10166	256	< LOD	10	91828	1113	< LOD	77

Sample		Fe		Hg		K		Mn	
Sample #	District	Fe	± 2σ	Hg	± 2σ	K	± 2σ	Mn	± 2σ
MM8	TB (WV)	8922	240	< LOD	8	92935	1107	< LOD	74
MM9	TB (WV)	10243	259	< LOD	9	92154	1114	< LOD	74
MM10	TB (WV)	11728	279	< LOD	9	95540	1169	93	55
MM11	TB (WV)	12256	284	< LOD	9	95226	1168	< LOD	80
MM13	TB (WV)	10968	276	< LOD	9	81568	1018	< LOD	79
MM14	TB (WV)	9414	250	< LOD	9	87119	1052	< LOD	75
MM15	TB (WV)	10025	261	< LOD	10	89012	1071	< LOD	69
MM16	TB (WV)	11058	265	< LOD	9	92731	1139	< LOD	73
MM24	TB (WV)	9012	243	< LOD	9	93226	1116	< LOD	76
MM28	TB (WV)	8604	257	< LOD	10	66374	831	< LOD	84
MM31	TB (WV)	9918	258	< LOD	9	88561	1076	< LOD	77
MM32	TB (WV)	10227	278	< LOD	10	66418	841	< LOD	76
MM33	TB (WV)	10014	255	< LOD	9	96633	1147	< LOD	73
MM34	TB (WV)	9120	246	< LOD	9	94528	1117	83	53
MM35	TB (WV)	11149	272	< LOD	9	92162	1139	< LOD	77
MM36	TB (WV)	9955	280	< LOD	10	64265	824	95	59
MM37	TB (WV)	9630	264	< LOD	10	73785	922	137	62
MM40	TB (WV)	11504	255	< LOD	9	93229	1137	< LOD	67
MM42	TB (WV)	10400	264	< LOD	9	88154	1076	100	54
MM45	TB (WV)	10563	264	< LOD	9	88443	1074	< LOD	78
MM47	TB (WV)	10918	267	< LOD	8	94386	1144	< LOD	77
MM48	TB (WV)	9101	247	< LOD	9	86851	1062	< LOD	77
MM50	TB (WV)	9847	255	< LOD	9	89263	1097	< LOD	76
MM51	TB (WV)	9421	250	< LOD	9	93822	1119	< LOD	72
MM58	TB (WV)	10729	271	< LOD	10	85916	1051	149	60
MM59	TB (WV)	9212	249	< LOD	9	87387	1070	86	55
MM66	TB (WV)	9071	243	< LOD	9	90203	1107	< LOD	74
MM69	TB (WV)	9184	243	< LOD	9	94939	1140	< LOD	75
MM73	TB (WV)	10163	258	< LOD	9	89309	1084	84	53
MM74	TB (WV)	10147	264	< LOD	9	82317	1026	< LOD	78

Sample		Fe		Hg		K		Mn	
Sample #	District	Fe	± 2σ	Hg	± 2σ	K	± 2σ	Mn	± 2σ
MM76	TB (WV)	11212	286	< LOD	10	76850	962	< LOD	80
MM86	TB (WV)	11618	278	< LOD	9	85163	1065	< LOD	77
MM93-1	TB (WV)	10215	259	< LOD	9	87849	1090	159	60
MM93-2	TB (WV)	10148	256	< LOD	10	91956	1129	< LOD	74
MM93-3	TB (WV)	10071	254	< LOD	9	93546	1137	< LOD	71
MM93-4	TB (WV)	10099	256	< LOD	9	94047	1137	< LOD	74
MM93-5	TB (WV)	10121	253	< LOD	9	95383	1154	113	55
MM93-6	TB (WV)	9851	253	< LOD	9	93808	1130	98	54
MM93-7	TB (WV)	9861	254	< LOD	9	93890	1132	104	54
MM93-8	TB (WV)	10118	255	< LOD	9	94586	1143	< LOD	76
MM93-9	TB (WV)	9878	252	< LOD	9	94282	1134	105	55
VB2	TB (YV)	9599	250	< LOD	9	93319	1134	90	53
VB3	TB (YV)	9535	247	< LOD	9	95734	1132	< LOD	76
VB6	TB (YV)	9428	244	< LOD	9	92112	1128	93	52
VB7	TB (YV)	13862	305	< LOD	9	79549	1080	< LOD	84
VB9	TB (YV)	13137	299	< LOD	10	89789	1144	156	62
VB10	TB (YV)	9737	251	< LOD	9	92665	1108	< LOD	73
VB11	TB (YV)	8920	242	< LOD	9	94777	1116	< LOD	74
VB14	TB (YV)	9105	245	< LOD	9	89117	1068	< LOD	76

Sample		Pb		Rb		Sb		Sc	
Sample #	District	Pb	± 2σ	Rb	± 2σ	Sb	± 2σ	Sc	± 2σ
1027 (1017)	ARTIFACT	< LOD	10	135	8	< LOD	23	< LOD	25
1311 (1017)	ARTIFACT	< LOD	10	166	9	< LOD	27	< LOD	29
2430 (1019)	ARTIFACT	< LOD	15	2556	35	< LOD	19	< LOD	31
2518 (1019)	ARTIFACT	21	8	350	12	< LOD	26	< LOD	19
3236 (1019)	ARTIFACT	< LOD	12	330	12	< LOD	27	< LOD	17
1332-1 (1017)	ARTIFACT	< LOD	10	805	17	< LOD	22	< LOD	17
1350-1 (1017)	ARTIFACT	< LOD	12	249	10	< LOD	25	< LOD	37
1350-2 (1017)	ARTIFACT	< LOD	11	495	14	< LOD	24	< LOD	31
308-2 (1017)	ARTIFACT	< LOD	11	289	12	< LOD	26	< LOD	33
308-4 (1017)	ARTIFACT	< LOD	11	188	10	< LOD	23	< LOD	45
308-5 (1017)	ARTIFACT	< LOD	13	334	13	< LOD	23	< LOD	57
PM1	CP (BG)	< LOD	10	191	9	< LOD	27	< LOD	24
PM2	CP (BG)	< LOD	10	197	10	< LOD	29	< LOD	21
PM4	CP (BG)	< LOD	11	215	10	< LOD	24	< LOD	27
PM5	CP (BG)	< LOD	10	200	9	< LOD	26	< LOD	21
PM7	CP (BG)	< LOD	11	220	10	< LOD	26	< LOD	25
PM8	CP (BG)	< LOD	11	184	9	< LOD	22	< LOD	24
PM9	CP (BG)	< LOD	12	210	10	< LOD	23	< LOD	26
PM11	CP (BG)	< LOD	10	184	9	< LOD	23	< LOD	25
RM8	CP (BG)	14	9	244	11	< LOD	28	< LOD	19
RM9	CP (BG)	21	9	275	11	< LOD	28	< LOD	18
RM10	CP (BG)	21	8	268	11	< LOD	25	< LOD	21
RM11	CP (BG)	14	8	272	11	< LOD	27	< LOD	22
RM18	CP (BG)	< LOD	12	995	21	< LOD	22	< LOD	17
RM21	CP (BG)	37	10	355	12	< LOD	26	< LOD	17
RM23	CP (BG)	< LOD	12	1072	23	< LOD	23	< LOD	15
RM24	CP (BG)	< LOD	13	1392	25	< LOD	20	< LOD	21
RM25	CP (BG)	< LOD	12	1118	22	< LOD	21	< LOD	21
RM27	CP (BG)	< LOD	12	1351	25	< LOD	19	< LOD	18
RM28	CP (BG)	< LOD	12	1117	23	< LOD	21	< LOD	17

Sample		Pb		Rb		Sb		Sc	
Sample #	District	Pb	± 2σ	Rb	± 2σ	Sb	± 2σ	Sc	± 2σ
RM29	CP (BG)	< LOD	16	3271	40	< LOD	21	< LOD	18
RM31	CP (BG)	< LOD	12	1038	21	< LOD	21	< LOD	20
RM33	CP (BG)	< LOD	12	1084	22	< LOD	22	< LOD	18
RM35	CP (BG)	< LOD	13	1225	24	< LOD	19	< LOD	19
RM40	CP (BG)	18	8	256	11	< LOD	26	< LOD	21
RM42	CP (BG)	17	8	257	11	< LOD	26	< LOD	21
RM48	CP (BG)	< LOD	13	1414	25	< LOD	18	< LOD	23
RM51	CP (BG)	< LOD	12	1029	21	< LOD	21	< LOD	19
RM52	CP (BG)	< LOD	13	1286	25	< LOD	20	< LOD	16
RM53	CP (BG)	< LOD	11	1122	22	< LOD	20	< LOD	19
RM62	CP (BG)	< LOD	13	1957	30	< LOD	18	< LOD	24
RM65	CP (BG)	< LOD	12	1347	24	< LOD	18	< LOD	20
RM66	CP (BG)	< LOD	11	1445	24	< LOD	18	< LOD	21
RM76	CP (BG)	< LOD	13	1613	28	< LOD	18	< LOD	19
RM81	CP (BG)	< LOD	13	1061	22	< LOD	18	< LOD	21
RM87	CP (BG)	< LOD	12	1143	23	< LOD	20	< LOD	18
DM1	CP (HS)	< LOD	9	206	10	< LOD	27	30	20
DM3	CP (HS)	< LOD	10	203	10	< LOD	25	33	21
DM4	CP (HS)	< LOD	11	199	10	< LOD	31	< LOD	30
DM5	CP (HS)	< LOD	9	181	9	< LOD	29	< LOD	26
DM9	CP (HS)	< LOD	10	188	10	< LOD	26	31	19
DM10	CP (HS)	< LOD	9	195	10	< LOD	28	< LOD	29
DM11	CP (HS)	< LOD	10	189	10	32	21	< LOD	28
DM14	CP (HS)	< LOD	11	196	10	< LOD	26	< LOD	25
DM17	CP (HS)	< LOD	10	202	10	< LOD	29	< LOD	29
DM18	CP (HS)	< LOD	10	197	10	< LOD	28	< LOD	29
DM19	CP (HS)	< LOD	10	188	9	< LOD	25	33	21
DM20	CP (HS)	< LOD	11	202	10	36	21	< LOD	32
DM21	CP (HS)	< LOD	10	211	10	< LOD	29	< LOD	29
DM22	CP (HS)	< LOD	9	205	10	< LOD	26	< LOD	31

Sample		Pb		Rb		Sb		Sc	
Sample #	District	Pb	± 2σ	Rb	± 2σ	Sb	± 2σ	Sc	± 2σ
DM25	CP (HS)	< LOD	9	203	9	< LOD	27	41	21
DM29	CP (HS)	< LOD	10	180	10	< LOD	28	< LOD	27
DM30	CP (HS)	< LOD	10	196	10	50	21	< LOD	28
DM31	CP (HS)	< LOD	10	185	10	31	21	< LOD	26
DM32	CP (HS)	< LOD	10	194	10	< LOD	28	< LOD	28
DM33	CP (HS)	< LOD	10	210	10	< LOD	27	< LOD	26
DM34	CP (HS)	< LOD	10	200	10	< LOD	28	< LOD	30
JDHM1	CP (HS)	13	8	230	10	< LOD	23	< LOD	21
JDHM4	CP (HS)	< LOD	10	221	10	< LOD	25	< LOD	27
JDHM8	CP (HS)	< LOD	12	208	10	< LOD	28	< LOD	16
JDHM9	CP (HS)	< LOD	10	210	10	< LOD	25	< LOD	26
JDHM10	CP (HS)	< LOD	10	204	10	< LOD	27	< LOD	21
JDHM11	CP (HS)	< LOD	9	220	10	< LOD	26	< LOD	23
JDHM12	CP (HS)	< LOD	11	210	10	< LOD	28	< LOD	26
JDHM14	CP (HS)	< LOD	12	203	10	< LOD	28	< LOD	18
JDHM17	CP (HS)	< LOD	11	206	10	< LOD	26	< LOD	27
JDHM22	CP (HS)	< LOD	11	219	10	< LOD	27	< LOD	21
JDHM26	CP (HS)	< LOD	11	244	10	< LOD	24	< LOD	20
JDHM27	CP (HS)	< LOD	11	244	10	< LOD	26	< LOD	21
JDHM29	CP (HS)	< LOD	11	204	10	< LOD	28	< LOD	26
JDHM32	CP (HS)	< LOD	11	214	10	< LOD	27	< LOD	25
JDHM33	CP (HS)	< LOD	10	192	9	< LOD	29	< LOD	19
JDHM34	CP (HS)	< LOD	12	236	10	< LOD	23	< LOD	21
JDHM35	CP (HS)	< LOD	11	220	10	< LOD	29	< LOD	28
JDHM43	CP (HS)	< LOD	11	256	11	< LOD	25	< LOD	20
JDHM44	CP (HS)	< LOD	10	198	10	< LOD	29	< LOD	20
JDHM45	CP (HS)	< LOD	10	191	10	< LOD	25	< LOD	19
JDHM46	CP (HS)	< LOD	11	219	10	< LOD	25	< LOD	21
JDHM48-1	CP (HS)	< LOD	11	213	10	< LOD	28	< LOD	29
JDHM48-2	CP (HS)	< LOD	11	206	10	< LOD	29	< LOD	23

Sample		Pb		Rb		Sb		Sc	
Sample #	District	Pb	± 2σ	Rb	± 2σ	Sb	± 2σ	Sc	± 2σ
JDHM48-3	CP (HS)	< LOD	11	214	10	< LOD	29	< LOD	25
JDHM48-4	CP (HS)	< LOD	9	209	10	< LOD	28	< LOD	26
JDHM48-5	CP (HS)	< LOD	10	225	10	< LOD	27	< LOD	26
JDHM48-6	CP (HS)	< LOD	12	220	10	< LOD	28	< LOD	29
JDHM48-7	CP (HS)	< LOD	10	209	10	< LOD	29	< LOD	26
JDHM48-8	CP (HS)	< LOD	11	218	10	< LOD	28	< LOD	28
JDHM49	CP (HS)	20	9	246	10	< LOD	22	< LOD	23
JDHM50	CP (HS)	< LOD	11	219	10	< LOD	28	< LOD	25
JDHM52	CP (HS)	< LOD	11	205	10	< LOD	26	< LOD	24
JDHM54	CP (HS)	< LOD	10	266	11	< LOD	27	< LOD	22
JDHM56	CP (HS)	< LOD	11	201	10	< LOD	24	< LOD	22
JDHM57	CP (HS)	< LOD	10	205	9	< LOD	25	< LOD	23
JDHM58	CP (HS)	< LOD	10	219	10	< LOD	24	< LOD	26
JDHM59	CP (HS)	< LOD	10	214	10	< LOD	27	< LOD	24
JDHP1	CP (HS)	< LOD	9	201	10	< LOD	26	< LOD	32
JDHP2	CP (HS)	< LOD	10	185	9	< LOD	27	< LOD	31
JDHP6	CP (HS)	< LOD	10	185	9	< LOD	24	35	22
JDHP9	CP (HS)	< LOD	12	233	11	< LOD	24	< LOD	27
JDHP10	CP (HS)	< LOD	10	178	9	< LOD	26	42	21
JDHP11	CP (HS)	< LOD	10	181	9	< LOD	26	< LOD	28
KP2	CP (HS)	< LOD	11	236	10	< LOD	25	< LOD	31
KP3	CP (HS)	< LOD	10	229	10	< LOD	29	< LOD	30
KP4	CP (HS)	< LOD	11	253	11	< LOD	27	40	21
KP5	CP (HS)	< LOD	10	234	11	< LOD	28	< LOD	27
KP7	CP (HS)	< LOD	11	233	11	< LOD	27	< LOD	30
KP8	CP (HS)	< LOD	12	589	16	< LOD	23	< LOD	20
KP9	CP (HS)	< LOD	11	245	11	< LOD	24	< LOD	33
KP13	CP (HS)	< LOD	11	231	11	< LOD	29	< LOD	28
KP14	CP (HS)	< LOD	10	221	10	36	21	< LOD	31
KP17	CP (HS)	< LOD	10	235	11	< LOD	29	< LOD	28

Sample		Pb		Rb		Sb		Sc	
Sample #	District	Pb	± 2σ	Rb	± 2σ	Sb	± 2σ	Sc	± 2σ
KP19	CP (HS)	< LOD	11	239	11	< LOD	27	< LOD	31
KP21	CP (HS)	< LOD	11	232	11	< LOD	28	< LOD	31
KP23	CP (HS)	< LOD	12	237	11	< LOD	24	< LOD	28
KP25	CP (HS)	< LOD	10	236	11	< LOD	30	< LOD	31
LM1	CP (HS)	< LOD	10	219	10	< LOD	29	< LOD	33
LM4	CP (HS)	< LOD	11	215	10	< LOD	29	< LOD	31
LM8	CP (HS)	< LOD	10	213	10	< LOD	30	< LOD	30
LM10	CP (HS)	< LOD	10	211	10	< LOD	24	< LOD	28
LM11	CP (HS)	< LOD	11	221	10	< LOD	24	< LOD	30
LM18	CP (HS)	< LOD	11	213	10	< LOD	25	< LOD	32
LM20	CP (HS)	< LOD	12	204	10	< LOD	24	< LOD	28
LM21	CP (HS)	< LOD	11	203	10	< LOD	25	< LOD	28
LM27	CP (HS)	< LOD	9	226	10	< LOD	27	< LOD	33
LM28	CP (HS)	< LOD	11	201	10	< LOD	28	< LOD	28
LM29	CP (HS)	< LOD	11	206	10	< LOD	25	< LOD	31
WM1	CP (HS)	< LOD	10	299	12	< LOD	28	< LOD	17
WM4	CP (HS)	< LOD	12	332	14	48	22	< LOD	16
WM5	CP (HS)	< LOD	11	496	16	< LOD	24	< LOD	19
WM11	CP (HS)	< LOD	10	293	11	< LOD	24	< LOD	24
WM17	CP (HS)	< LOD	10	306	12	< LOD	25	< LOD	21
WM21	CP (HS)	< LOD	9	325	12	< LOD	26	< LOD	23
WM24	CP (HS)	< LOD	9	312	12	< LOD	24	< LOD	19
WM27	CP (HS)	< LOD	10	315	11	< LOD	26	< LOD	22
WM32	CP (HS)	< LOD	11	311	12	< LOD	24	< LOD	21
WM35	CP (HS)	< LOD	9	310	12	< LOD	26	< LOD	23
WM45	CP (HS)	< LOD	10	355	12	< LOD	24	< LOD	21
WM59	CP (HS)	< LOD	10	308	12	< LOD	25	< LOD	24
WM66	CP (HS)	< LOD	10	360	12	< LOD	24	< LOD	22
WM68	CP (HS)	< LOD	10	295	11	< LOD	25	< LOD	22
WM89	CP (HS)	< LOD	10	338	12	< LOD	24	< LOD	21

Sample		Pb		Rb		Sb		Sc	
Sample #	District	Pb	± 2σ	Rb	± 2σ	Sb	± 2σ	Sc	± 2σ
WM90	CP (HS)	< LOD	10	333	12	< LOD	24	< LOD	23
WM91	CP (HS)	< LOD	10	347	12	< LOD	26	< LOD	21
WM100	CP (HS)	< LOD	12	813	20	< LOD	23	< LOD	23
WM112	CP (HS)	< LOD	11	428	14	< LOD	22	< LOD	19
WM120	CP (HS)	< LOD	11	483	14	< LOD	25	< LOD	22
WM124-1	CP (HS)	< LOD	9	305	11	< LOD	26	< LOD	25
WM124-2	CP (HS)	< LOD	9	311	12	< LOD	25	< LOD	25
WM124-3	CP (HS)	< LOD	9	324	12	< LOD	25	< LOD	25
WM124-4	CP (HS)	< LOD	11	310	12	< LOD	26	< LOD	26
WM124-5	CP (HS)	< LOD	11	327	12	< LOD	25	< LOD	25
WM124-6	CP (HS)	< LOD	10	325	12	< LOD	25	< LOD	25
WM124-7	CP (HS)	< LOD	10	300	11	< LOD	25	< LOD	23
WM124-8	CP (HS)	< LOD	9	306	11	< LOD	26	< LOD	25
WM125	CP (HS)	< LOD	9	305	12	< LOD	27	< LOD	18
WM138	CP (HS)	< LOD	11	301	11	< LOD	25	< LOD	21
WM140	CP (HS)	< LOD	9	359	12	< LOD	26	< LOD	23
WM149	CP (HS)	< LOD	9	287	11	< LOD	25	< LOD	23
WM156	CP (HS)	< LOD	10	284	12	< LOD	26	< LOD	19
WM161	CP (HS)	< LOD	10	318	12	< LOD	23	< LOD	22
WM162	CP (HS)	< LOD	10	342	12	< LOD	25	< LOD	22
WM166	CP (HS)	< LOD	11	346	12	< LOD	25	< LOD	23
WM170	CP (HS)	< LOD	10	382	13	< LOD	26	< LOD	21
WM177	CP (HS)	< LOD	11	302	12	< LOD	25	< LOD	21
DPM1	SP	< LOD	13	1094	24	< LOD	20	< LOD	24
DPM2	SP	< LOD	14	912	23	< LOD	25	22	14
DPM3	SP	< LOD	10	541	16	< LOD	24	< LOD	28
DPM4	SP	< LOD	13	885	22	< LOD	22	< LOD	20
DPM5	SP	< LOD	12	587	17	< LOD	21	< LOD	28
DPM6	SP	< LOD	13	963	22	< LOD	19	< LOD	25
DPM7	SP	< LOD	13	1023	23	< LOD	19	< LOD	29

Sample		Pb		Rb		Sb		Sc	
Sample #	District	Pb	± 2σ	Rb	± 2σ	Sb	± 2σ	Sc	± 2σ
DPM8	SP	< LOD	11	544	16	< LOD	23	< LOD	27
DPM10	SP	< LOD	14	1011	23	< LOD	21	< LOD	24
DPM10-2	SP	< LOD	12	980	22	< LOD	19	< LOD	24
DPM11	SP	< LOD	12	561	17	< LOD	23	< LOD	27
DPM12	SP	< LOD	13	982	22	< LOD	20	< LOD	25
DPM13	SP	< LOD	13	890	21	< LOD	22	< LOD	28
DPM16	SP	< LOD	13	973	22	< LOD	19	< LOD	25
DPM18	SP	< LOD	13	1038	23	< LOD	19	< LOD	28
DPM20	SP	< LOD	13	543	17	< LOD	22	< LOD	25
DPM24	SP	< LOD	14	748	20	< LOD	25	< LOD	27
DPM27	SP	< LOD	14	953	23	< LOD	21	< LOD	24
DPM28	SP	< LOD	14	834	22	< LOD	25	< LOD	23
DPM29	SP	< LOD	13	968	22	< LOD	23	< LOD	29
DPM31	SP	< LOD	14	940	23	< LOD	23	< LOD	22
DPM32	SP	< LOD	14	1022	23	< LOD	20	< LOD	28
DPM33	SP	< LOD	13	911	23	< LOD	26	< LOD	22
DPM34	SP	< LOD	11	498	16	< LOD	26	< LOD	24
DPM35	SP	< LOD	13	848	22	< LOD	23	< LOD	23
DPM36	SP	< LOD	13	899	23	< LOD	24	< LOD	19
DPM37	SP	< LOD	12	534	17	< LOD	27	< LOD	24
DPM38	SP	< LOD	13	500	17	< LOD	29	< LOD	19
DPM39	SP	< LOD	13	498	16	< LOD	25	< LOD	23
DPM39-2	SP	< LOD	13	503	16	< LOD	26	< LOD	24
McK1	SP	< LOD	14	1513	27	< LOD	19	< LOD	30
McK2	SP	19	12	1933	32	< LOD	20	< LOD	25
McK3	SP	< LOD	16	1846	31	< LOD	20	< LOD	26
McK4	SP	17	11	2050	32	< LOD	22	< LOD	24
McK5	SP	17	11	1424	27	< LOD	19	< LOD	28
McK6	SP	< LOD	16	1999	33	< LOD	19	< LOD	25
McK7	SP	25	12	2403	35	< LOD	21	< LOD	25

Sample		Pb		Rb		Sb		Sc	
Sample #	District	Pb	± 2σ	Rb	± 2σ	Sb	± 2σ	Sc	± 2σ
McK8	SP	24	12	2011	32	< LOD	22	< LOD	25
McK9	SP	38	13	1743	31	< LOD	20	< LOD	23
McK10	SP	< LOD	16	1942	32	< LOD	18	< LOD	27
McK11	SP	< LOD	16	1778	31	< LOD	17	< LOD	24
McK12	SP	19	11	1967	31	< LOD	20	< LOD	30
McK13	SP	< LOD	17	1840	31	< LOD	19	< LOD	27
McK15	SP	30	12	2096	32	< LOD	20	< LOD	25
Pink1	SP	< LOD	14	1025	23	< LOD	22	< LOD	28
Pink2	SP	< LOD	14	840	21	< LOD	23	< LOD	28
Pink3	SP	< LOD	13	1185	25	< LOD	20	< LOD	31
Pink4	SP	< LOD	13	816	20	< LOD	25	< LOD	26
Pink7	SP	< LOD	14	776	22	< LOD	26	< LOD	21
Pink8	SP	< LOD	13	1058	23	< LOD	21	< LOD	30
Pink9	SP	< LOD	14	994	23	< LOD	24	< LOD	23
Pink10	SP	< LOD	13	837	20	< LOD	22	< LOD	33
Pink11	SP	< LOD	15	683	21	< LOD	26	< LOD	26
Pink12	SP	< LOD	15	1016	23	< LOD	22	< LOD	24
JAPM2	TB (IG)	< LOD	14	1201	24	< LOD	19	< LOD	26
JAPM8	TB (IG)	< LOD	14	1278	25	< LOD	21	< LOD	23
JAPM9	TB (IG)	< LOD	14	1296	24	< LOD	21	< LOD	25
JAPM10	TB (IG)	< LOD	15	1610	28	< LOD	20	< LOD	28
JAPM15	TB (IG)	< LOD	13	1277	25	< LOD	22	< LOD	27
JAPM17	TB (IG)	< LOD	16	690	21	< LOD	28	62	33
MM1	TB (WV)	< LOD	10	260	10	35	19	< LOD	22
MM2	TB (WV)	< LOD	10	292	11	< LOD	28	< LOD	18
MM3	TB (WV)	< LOD	9	280	11	< LOD	28	25	15
MM4	TB (WV)	< LOD	10	278	11	< LOD	29	27	14
MM5	TB (WV)	< LOD	10	289	11	36	19	< LOD	20
MM6	TB (WV)	< LOD	10	307	11	39	19	< LOD	22
MM7	TB (WV)	< LOD	9	286	11	34	19	< LOD	22

Sample		Pb		Rb		Sb		Sc	
Sample #	District	Pb	± 2σ	Rb	± 2σ	Sb	± 2σ	Sc	± 2σ
MM8	TB (WV)	< LOD	10	270	10	< LOD	26	32	16
MM9	TB (WV)	< LOD	9	269	10	< LOD	27	< LOD	22
MM10	TB (WV)	< LOD	10	322	12	30	18	< LOD	23
MM11	TB (WV)	< LOD	10	314	11	< LOD	24	< LOD	23
MM13	TB (WV)	< LOD	11	310	12	< LOD	26	< LOD	18
MM14	TB (WV)	< LOD	9	266	10	< LOD	28	< LOD	21
MM15	TB (WV)	< LOD	10	289	11	< LOD	25	< LOD	21
MM16	TB (WV)	< LOD	10	309	11	< LOD	24	< LOD	22
MM24	TB (WV)	< LOD	10	260	10	< LOD	27	< LOD	23
MM28	TB (WV)	< LOD	11	246	11	< LOD	27	22	12
MM31	TB (WV)	< LOD	10	287	11	47	19	< LOD	21
MM32	TB (WV)	< LOD	11	296	12	< LOD	26	< LOD	17
MM33	TB (WV)	< LOD	9	278	11	< LOD	26	< LOD	22
MM34	TB (WV)	< LOD	10	270	11	< LOD	27	< LOD	22
MM35	TB (WV)	< LOD	10	315	11	< LOD	28	< LOD	21
MM36	TB (WV)	< LOD	11	306	12	< LOD	31	< LOD	16
MM37	TB (WV)	< LOD	10	269	11	36	20	< LOD	19
MM40	TB (WV)	< LOD	9	317	11	< LOD	25	< LOD	21
MM42	TB (WV)	< LOD	10	297	11	< LOD	26	< LOD	21
MM45	TB (WV)	< LOD	10	292	11	< LOD	27	< LOD	21
MM47	TB (WV)	< LOD	9	312	11	< LOD	27	< LOD	22
MM48	TB (WV)	< LOD	11	263	11	< LOD	27	< LOD	22
MM50	TB (WV)	< LOD	10	285	11	< LOD	26	< LOD	22
MM51	TB (WV)	< LOD	11	259	10	< LOD	24	< LOD	24
MM58	TB (WV)	< LOD	10	310	11	< LOD	26	< LOD	22
MM59	TB (WV)	< LOD	9	257	10	< LOD	27	34	16
MM66	TB (WV)	< LOD	11	263	10	< LOD	27	< LOD	22
MM69	TB (WV)	< LOD	9	272	10	< LOD	27	< LOD	24
MM73	TB (WV)	< LOD	9	283	11	< LOD	27	< LOD	21
MM74	TB (WV)	< LOD	9	292	11	< LOD	28	< LOD	20

Sample		Pb		Rb		Sb		Sc	
Sample #	District	Pb	± 2σ	Rb	± 2σ	Sb	± 2σ	Sc	± 2σ
MM76	TB (WV)	< LOD	10	305	12	< LOD	25	< LOD	19
MM86	TB (WV)	< LOD	10	305	11	< LOD	26	< LOD	20
MM93-1	TB (WV)	< LOD	9	297	11	< LOD	26	< LOD	21
MM93-2	TB (WV)	< LOD	10	290	11	< LOD	28	< LOD	22
MM93-3	TB (WV)	< LOD	9	289	11	< LOD	26	< LOD	22
MM93-4	TB (WV)	< LOD	9	293	11	< LOD	26	< LOD	22
MM93-5	TB (WV)	< LOD	10	288	11	< LOD	26	< LOD	22
MM93-6	TB (WV)	< LOD	9	286	11	< LOD	27	< LOD	22
MM93-7	TB (WV)	< LOD	10	292	11	< LOD	27	< LOD	23
MM93-8	TB (WV)	< LOD	10	289	11	< LOD	26	< LOD	22
MM93-9	TB (WV)	< LOD	10	297	11	< LOD	27	< LOD	22
VB2	TB (YV)	< LOD	9	196	9	< LOD	25	< LOD	23
VB3	TB (YV)	< LOD	10	204	9	< LOD	24	< LOD	23
VB6	TB (YV)	< LOD	10	210	9	< LOD	23	< LOD	23
VB7	TB (YV)	< LOD	10	216	10	< LOD	27	< LOD	22
VB9	TB (YV)	< LOD	10	214	10	< LOD	22	< LOD	26
VB10	TB (YV)	< LOD	9	210	9	< LOD	23	< LOD	21
VB11	TB (YV)	< LOD	9	203	9	< LOD	25	< LOD	22
VB14	TB (YV)	< LOD	10	209	9	< LOD	23	< LOD	21

Sample		Sn		Sr		Te		Ti	
Sample #	District	Sn	± 2σ	Sr	± 2σ	Te	± 2σ	Ti	± 2σ
1027 (1017)	ARTIFACT	< LOD	22	54	4	< LOD	48	5062	198
1311 (1017)	ARTIFACT	< LOD	26	40	4	< LOD	55	4149	184
2430 (1019)	ARTIFACT	< LOD	18	< LOD	4	< LOD	40	826	101
2518 (1019)	ARTIFACT	< LOD	25	24	3	< LOD	53	936	99
3236 (1019)	ARTIFACT	< LOD	27	24	3	< LOD	55	865	90
1332-1 (1017)	ARTIFACT	< LOD	22	3	2	< LOD	46	1162	71
1350-1 (1017)	ARTIFACT	< LOD	24	49	4	< LOD	51	4712	214
1350-2 (1017)	ARTIFACT	< LOD	24	17	3	< LOD	50	1771	107
308-2 (1017)	ARTIFACT	< LOD	25	25	3	< LOD	53	3117	175
308-4 (1017)	ARTIFACT	< LOD	23	59	5	< LOD	48	5147	225
308-5 (1017)	ARTIFACT	< LOD	22	109	6	< LOD	48	2538	156
PM1	CP (BG)	< LOD	26	24	3	< LOD	55	3447	164
PM2	CP (BG)	< LOD	28	23	3	< LOD	60	1707	120
PM4	CP (BG)	< LOD	23	25	3	< LOD	49	3370	166
PM5	CP (BG)	< LOD	25	23	3	< LOD	53	2645	143
PM7	CP (BG)	< LOD	25	23	3	< LOD	53	3188	152
PM8	CP (BG)	< LOD	21	26	4	< LOD	47	2895	155
PM9	CP (BG)	< LOD	22	24	4	< LOD	48	3089	160
PM11	CP (BG)	< LOD	23	27	3	< LOD	48	3866	171
RM8	CP (BG)	41	19	8	3	80	39	1247	87
RM9	CP (BG)	< LOD	27	4	2	< LOD	57	595	71
RM10	CP (BG)	< LOD	24	9	2	< LOD	51	1063	94
RM11	CP (BG)	< LOD	26	9	3	< LOD	56	823	94
RM18	CP (BG)	< LOD	23	< LOD	3	< LOD	46	1214	74
RM21	CP (BG)	< LOD	26	14	3	< LOD	54	134	45
RM23	CP (BG)	< LOD	23	< LOD	4	< LOD	47	1073	65
RM24	CP (BG)	< LOD	21	< LOD	4	< LOD	41	1292	79
RM25	CP (BG)	< LOD	22	6	3	< LOD	44	1494	87
RM27	CP (BG)	< LOD	20	< LOD	4	< LOD	41	1272	76
RM28	CP (BG)	< LOD	22	< LOD	4	< LOD	44	1171	71

Sample		Sn		Sr		Te		Ti	
Sample #	District	Sn	± 2σ	Sr	± 2σ	Te	± 2σ	Ti	± 2σ
RM29	CP (BG)	115	16	< LOD	5	< LOD	44	545	62
RM31	CP (BG)	< LOD	21	< LOD	3	< LOD	43	1254	82
RM33	CP (BG)	37	16	< LOD	4	< LOD	46	1189	79
RM35	CP (BG)	< LOD	19	< LOD	4	< LOD	40	1411	84
RM40	CP (BG)	< LOD	25	14	3	< LOD	53	1306	99
RM42	CP (BG)	< LOD	26	6	2	< LOD	54	1363	102
RM48	CP (BG)	< LOD	19	< LOD	4	< LOD	38	1278	87
RM51	CP (BG)	< LOD	21	< LOD	3	< LOD	43	1346	87
RM52	CP (BG)	< LOD	21	< LOD	4	< LOD	43	1073	70
RM53	CP (BG)	< LOD	21	< LOD	3	< LOD	42	1369	85
RM62	CP (BG)	< LOD	18	< LOD	4	< LOD	37	1014	80
RM65	CP (BG)	< LOD	19	5	3	< LOD	38	1363	81
RM66	CP (BG)	< LOD	18	< LOD	4	< LOD	37	1305	93
RM76	CP (BG)	< LOD	18	5	3	< LOD	38	1044	78
RM81	CP (BG)	< LOD	18	7	3	< LOD	38	1594	92
RM87	CP (BG)	< LOD	21	< LOD	4	< LOD	43	1104	78
DM1	CP (HS)	< LOD	28	37	4	< LOD	57	4621	224
DM3	CP (HS)	< LOD	25	34	4	< LOD	51	5431	224
DM4	CP (HS)	82	21	47	4	128	43	4342	235
DM5	CP (HS)	41	20	46	4	< LOD	60	3882	197
DM9	CP (HS)	< LOD	26	46	4	< LOD	55	4389	216
DM10	CP (HS)	54	19	37	4	< LOD	58	5579	216
DM11	CP (HS)	99	21	40	4	133	43	5198	213
DM14	CP (HS)	< LOD	25	32	4	< LOD	54	4466	187
DM17	CP (HS)	88	20	44	4	63	40	6014	224
DM18	CP (HS)	44	19	50	4	< LOD	57	5875	224
DM19	CP (HS)	< LOD	25	46	4	< LOD	51	5834	248
DM20	CP (HS)	83	21	46	4	127	43	4195	235
DM21	CP (HS)	33	20	35	4	< LOD	60	4914	221
DM22	CP (HS)	< LOD	27	32	4	< LOD	55	4393	224

Sample		Sn		Sr		Te		Ti	
Sample #	District	Sn	± 2σ	Sr	± 2σ	Te	± 2σ	Ti	± 2σ
DM25	CP (HS)	< LOD	27	39	4	< LOD	55	6126	236
DM29	CP (HS)	37	19	39	4	< LOD	59	5559	212
DM30	CP (HS)	124	22	38	4	109	43	5155	207
DM31	CP (HS)	119	22	37	4	125	43	4941	199
DM32	CP (HS)	31	19	36	4	< LOD	57	5423	216
DM33	CP (HS)	< LOD	27	46	4	< LOD	56	3682	191
DM34	CP (HS)	50	19	35	4	< LOD	57	5418	215
JDHM1	CP (HS)	< LOD	22	13	3	< LOD	47	346	78
JDHM4	CP (HS)	< LOD	24	32	4	< LOD	51	1899	167
JDHM8	CP (HS)	< LOD	27	8	3	< LOD	58	306	61
JDHM9	CP (HS)	< LOD	24	23	3	< LOD	51	781	131
JDHM10	CP (HS)	< LOD	26	20	3	< LOD	56	420	102
JDHM11	CP (HS)	< LOD	26	16	3	< LOD	55	406	107
JDHM12	CP (HS)	< LOD	28	25	3	< LOD	59	1264	142
JDHM14	CP (HS)	< LOD	27	19	3	< LOD	57	420	89
JDHM17	CP (HS)	< LOD	25	27	4	< LOD	54	2022	164
JDHM22	CP (HS)	< LOD	27	13	3	< LOD	57	380	79
JDHM26	CP (HS)	< LOD	24	8	2	< LOD	50	492	71
JDHM27	CP (HS)	< LOD	25	10	3	< LOD	53	408	84
JDHM29	CP (HS)	< LOD	27	27	3	< LOD	57	842	131
JDHM32	CP (HS)	< LOD	27	18	3	< LOD	56	402	119
JDHM33	CP (HS)	43	19	13	3	115	41	232	88
JDHM34	CP (HS)	< LOD	22	14	3	< LOD	48	288	90
JDHM35	CP (HS)	41	19	35	4	60	39	1861	164
JDHM43	CP (HS)	< LOD	24	10	3	< LOD	51	246	66
JDHM44	CP (HS)	< LOD	29	21	3	64	41	745	104
JDHM45	CP (HS)	< LOD	24	20	3	< LOD	51	509	97
JDHM46	CP (HS)	< LOD	24	16	3	< LOD	51	336	93
JDHM48-1	CP (HS)	< LOD	28	33	4	< LOD	58	1985	168
JDHM48-2	CP (HS)	29	19	26	4	< LOD	60	1605	141

Sample		Sn		Sr		Te		Ti	
Sample #	District	Sn	± 2σ	Sr	± 2σ	Te	± 2σ	Ti	± 2σ
JDHM48-3	CP (HS)	< LOD	29	31	4	< LOD	60	1730	149
JDHM48-4	CP (HS)	< LOD	28	31	4	< LOD	59	2009	162
JDHM48-5	CP (HS)	< LOD	27	31	4	< LOD	56	1848	167
JDHM48-6	CP (HS)	< LOD	27	34	4	< LOD	57	1936	164
JDHM48-7	CP (HS)	32	19	29	4	< LOD	60	1901	156
JDHM48-8	CP (HS)	< LOD	28	33	4	< LOD	58	1905	159
JDHM49	CP (HS)	< LOD	21	14	3	< LOD	46	511	85
JDHM50	CP (HS)	< LOD	28	28	4	< LOD	58	1461	145
JDHM52	CP (HS)	< LOD	26	26	3	< LOD	54	953	128
JDHM54	CP (HS)	31	18	8	2	< LOD	55	186	73
JDHM56	CP (HS)	< LOD	23	22	3	< LOD	49	579	113
JDHM57	CP (HS)	< LOD	24	22	3	< LOD	51	575	119
JDHM58	CP (HS)	< LOD	23	28	4	< LOD	49	951	138
JDHM59	CP (HS)	< LOD	27	25	3	< LOD	57	730	125
JDHP1	CP (HS)	< LOD	25	41	4	< LOD	53	4748	229
JDHP2	CP (HS)	< LOD	26	39	4	< LOD	55	5454	237
JDHP6	CP (HS)	< LOD	24	40	4	< LOD	50	6532	247
JDHP9	CP (HS)	< LOD	23	26	4	< LOD	50	3567	158
JDHP10	CP (HS)	< LOD	25	42	4	< LOD	53	6486	245
JDHP11	CP (HS)	< LOD	26	46	4	< LOD	55	4679	211
KP2	CP (HS)	< LOD	25	40	4	< LOD	53	2607	210
KP3	CP (HS)	< LOD	29	53	5	< LOD	60	2918	220
KP4	CP (HS)	< LOD	27	48	5	< LOD	57	2755	223
KP5	CP (HS)	< LOD	28	45	4	< LOD	58	1936	189
KP7	CP (HS)	< LOD	27	45	4	< LOD	56	2729	213
KP8	CP (HS)	< LOD	23	< LOD	3	< LOD	48	412	58
KP9	CP (HS)	< LOD	24	48	5	< LOD	51	3010	236
KP13	CP (HS)	< LOD	29	49	5	< LOD	61	2703	206
KP14	CP (HS)	64	21	50	4	127	43	3007	216
KP17	CP (HS)	< LOD	29	54	5	< LOD	61	2588	208

Sample		Sn		Sr		Te		Ti	
Sample #	District	Sn	± 2σ	Sr	± 2σ	Te	± 2σ	Ti	± 2σ
KP19	CP (HS)	< LOD	27	39	4	< LOD	55	2566	205
KP21	CP (HS)	< LOD	28	44	4	< LOD	58	2870	217
KP23	CP (HS)	< LOD	23	40	4	< LOD	49	1865	184
KP25	CP (HS)	33	20	46	4	< LOD	62	2824	215
LM1	CP (HS)	34	20	68	5	< LOD	60	5281	265
LM4	CP (HS)	< LOD	29	74	5	< LOD	60	4651	254
LM8	CP (HS)	< LOD	30	67	5	72	41	4460	241
LM10	CP (HS)	< LOD	24	72	5	< LOD	50	4062	228
LM11	CP (HS)	< LOD	24	74	5	< LOD	50	3635	231
LM18	CP (HS)	< LOD	25	77	5	< LOD	53	5027	250
LM20	CP (HS)	< LOD	23	71	5	< LOD	49	4548	228
LM21	CP (HS)	< LOD	24	74	5	< LOD	52	3442	216
LM27	CP (HS)	< LOD	26	69	5	< LOD	55	5104	259
LM28	CP (HS)	< LOD	28	67	5	< LOD	57	3923	220
LM29	CP (HS)	< LOD	24	76	5	< LOD	51	5741	251
WM1	CP (HS)	62	19	5	2	< LOD	57	1346	78
WM4	CP (HS)	62	21	8	3	115	45	2179	99
WM5	CP (HS)	< LOD	24	< LOD	3	< LOD	50	796	75
WM11	CP (HS)	< LOD	24	13	3	< LOD	49	2867	129
WM17	CP (HS)	< LOD	24	4	2	< LOD	51	1919	100
WM21	CP (HS)	44	18	8	2	< LOD	55	1491	103
WM24	CP (HS)	< LOD	24	7	2	< LOD	50	1489	87
WM27	CP (HS)	38	17	9	2	< LOD	54	2184	110
WM32	CP (HS)	< LOD	25	8	2	< LOD	51	1616	99
WM35	CP (HS)	40	17	10	3	< LOD	54	2629	125
WM45	CP (HS)	< LOD	24	4	2	< LOD	50	1636	92
WM59	CP (HS)	< LOD	26	10	3	< LOD	53	2672	124
WM66	CP (HS)	< LOD	24	5	2	< LOD	50	2075	107
WM68	CP (HS)	< LOD	25	9	2	< LOD	52	2638	119
WM89	CP (HS)	< LOD	24	5	2	< LOD	49	1824	99

Sample		Sn		Sr		Te		Ti	
Sample #	District	Sn	± 2σ	Sr	± 2σ	Te	± 2σ	Ti	± 2σ
WM90	CP (HS)	< LOD	23	6	2	< LOD	49	2378	117
WM91	CP (HS)	< LOD	26	6	2	< LOD	55	1534	91
WM100	CP (HS)	< LOD	24	< LOD	4	< LOD	49	706	80
WM112	CP (HS)	< LOD	21	< LOD	3	< LOD	46	1494	86
WM120	CP (HS)	27	17	< LOD	3	< LOD	51	1369	93
WM124-1	CP (HS)	< LOD	26	8	2	< LOD	53	2789	127
WM124-2	CP (HS)	26	17	11	3	< LOD	52	2765	128
WM124-3	CP (HS)	26	17	7	2	< LOD	52	2752	132
WM124-4	CP (HS)	43	17	7	2	< LOD	53	2790	131
WM124-5	CP (HS)	29	17	10	3	< LOD	53	2601	130
WM124-6	CP (HS)	< LOD	25	9	3	< LOD	52	2688	130
WM124-7	CP (HS)	< LOD	25	9	3	< LOD	53	2592	123
WM124-8	CP (HS)	48	18	10	3	< LOD	54	2603	127
WM125	CP (HS)	77	18	6	2	< LOD	55	1378	86
WM138	CP (HS)	44	17	11	3	< LOD	52	2522	121
WM140	CP (HS)	< LOD	26	4	2	< LOD	54	1819	105
WM149	CP (HS)	35	17	11	3	< LOD	52	2815	126
WM156	CP (HS)	< LOD	26	9	3	< LOD	54	2186	101
WM161	CP (HS)	< LOD	23	8	2	< LOD	47	1875	104
WM162	CP (HS)	< LOD	25	5	2	< LOD	52	1860	103
WM166	CP (HS)	< LOD	25	6	2	< LOD	53	1817	101
WM170	CP (HS)	< LOD	26	6	2	< LOD	55	1556	93
WM177	CP (HS)	< LOD	25	8	3	< LOD	53	2180	103
DPM1	SP	< LOD	20	< LOD	4	< LOD	43	1019	98
DPM2	SP	< LOD	24	< LOD	4	< LOD	53	784	78
DPM3	SP	< LOD	24	13	3	< LOD	51	1202	123
DPM4	SP	< LOD	22	5	3	< LOD	47	791	85
DPM5	SP	< LOD	21	8	3	< LOD	45	1113	109
DPM6	SP	< LOD	18	< LOD	4	< LOD	40	938	99
DPM7	SP	< LOD	18	< LOD	4	< LOD	39	1084	110

Sample		Sn		Sr		Te		Ti	
Sample #	District	Sn	± 2σ	Sr	± 2σ	Te	± 2σ	Ti	± 2σ
DPM8	SP	< LOD	22	6	3	< LOD	47	1186	113
DPM10	SP	< LOD	21	< LOD	4	< LOD	45	1022	92
DPM10-2	SP	< LOD	19	< LOD	4	< LOD	41	901	89
DPM11	SP	< LOD	23	18	3	< LOD	48	1010	110
DPM12	SP	< LOD	19	< LOD	4	< LOD	42	944	92
DPM13	SP	< LOD	22	4	3	< LOD	47	1045	108
DPM16	SP	< LOD	19	< LOD	4	< LOD	41	931	93
DPM18	SP	< LOD	18	4	3	< LOD	39	1025	108
DPM20	SP	< LOD	21	9	3	< LOD	45	878	96
DPM24	SP	< LOD	25	7	3	< LOD	53	1116	106
DPM27	SP	< LOD	20	5	3	< LOD	44	784	89
DPM28	SP	< LOD	24	< LOD	4	< LOD	52	923	84
DPM29	SP	< LOD	23	< LOD	4	< LOD	48	1028	109
DPM31	SP	< LOD	23	< LOD	4	< LOD	48	832	81
DPM32	SP	< LOD	19	< LOD	4	< LOD	42	948	104
DPM33	SP	< LOD	26	< LOD	4	< LOD	55	789	86
DPM34	SP	< LOD	26	5	3	< LOD	55	981	96
DPM35	SP	< LOD	22	6	3	< LOD	49	795	85
DPM36	SP	< LOD	23	4	3	< LOD	50	577	75
DPM37	SP	< LOD	27	9	3	< LOD	57	917	93
DPM38	SP	< LOD	28	6	3	< LOD	61	726	75
DPM39	SP	< LOD	25	6	3	< LOD	52	772	92
DPM39-2	SP	< LOD	26	6	3	< LOD	55	886	90
McK1	SP	< LOD	19	< LOD	4	< LOD	41	580	97
McK2	SP	< LOD	20	< LOD	4	< LOD	42	493	85
McK3	SP	< LOD	20	< LOD	4	< LOD	42	1089	100
McK4	SP	< LOD	21	< LOD	4	< LOD	45	554	89
McK5	SP	< LOD	18	< LOD	4	< LOD	40	449	97
McK6	SP	< LOD	19	< LOD	4	< LOD	41	505	86
McK7	SP	< LOD	20	< LOD	5	< LOD	43	543	84

Sample		Sn		Sr		Te		Ti	
Sample #	District	Sn	± 2σ	Sr	± 2σ	Te	± 2σ	Ti	± 2σ
McK8	SP	< LOD	21	5	3	< LOD	46	532	85
McK9	SP	< LOD	19	< LOD	4	< LOD	43	554	82
McK10	SP	< LOD	17	< LOD	4	< LOD	38	590	96
McK11	SP	< LOD	16	< LOD	4	< LOD	36	537	85
McK12	SP	< LOD	19	< LOD	4	< LOD	41	2131	138
McK13	SP	< LOD	18	6	3	< LOD	41	840	98
McK15	SP	< LOD	20	< LOD	4	< LOD	43	784	98
Pink1	SP	< LOD	22	5	3	< LOD	47	545	86
Pink2	SP	< LOD	23	5	3	< LOD	49	608	101
Pink3	SP	< LOD	20	4	3	< LOD	43	571	103
Pink4	SP	< LOD	24	< LOD	3	< LOD	51	665	90
Pink7	SP	< LOD	26	6	3	< LOD	55	414	76
Pink8	SP	< LOD	20	< LOD	4	< LOD	44	520	99
Pink9	SP	< LOD	24	5	3	< LOD	51	486	76
Pink10	SP	< LOD	21	8	3	< LOD	45	807	106
Pink11	SP	< LOD	26	9	3	< LOD	55	575	94
Pink12	SP	< LOD	21	7	3	< LOD	45	594	86
JAPM2	TB (IG)	22	14	< LOD	4	< LOD	40	1680	115
JAPM8	TB (IG)	163	17	< LOD	4	< LOD	45	1532	104
JAPM9	TB (IG)	269	17	5	3	< LOD	43	1726	112
JAPM10	TB (IG)	174	17	11	3	< LOD	42	1235	110
JAPM15	TB (IG)	301	18	< LOD	4	< LOD	46	1693	116
JAPM17	TB (IG)	409	24	< LOD	4	< LOD	59	583	180
MM1	TB (WV)	74	19	15	3	104	39	4818	152
MM2	TB (WV)	45	19	12	3	115	39	2386	106
MM3	TB (WV)	78	19	15	3	96	38	3328	129
MM4	TB (WV)	58	19	14	3	87	39	3585	126
MM5	TB (WV)	64	19	10	3	102	39	2641	116
MM6	TB (WV)	68	19	13	3	93	38	2939	129
MM7	TB (WV)	52	19	13	3	98	39	3307	134

Sample		Sn		Sr		Te		Ti	
Sample #	District	Sn	± 2σ	Sr	± 2σ	Te	± 2σ	Ti	± 2σ
MM8	TB (WV)	< LOD	26	14	3	< LOD	54	5890	165
MM9	TB (WV)	36	18	14	3	< LOD	55	3623	139
MM10	TB (WV)	61	18	13	3	83	38	2484	124
MM11	TB (WV)	< LOD	23	13	3	< LOD	48	2791	126
MM13	TB (WV)	< LOD	26	12	3	< LOD	54	2277	110
MM14	TB (WV)	49	18	14	3	72	38	3819	135
MM15	TB (WV)	< LOD	24	12	3	< LOD	51	3922	136
MM16	TB (WV)	< LOD	24	15	3	< LOD	51	3003	128
MM24	TB (WV)	41	18	18	3	< LOD	56	4928	156
MM28	TB (WV)	< LOD	27	14	3	< LOD	57	3572	117
MM31	TB (WV)	76	19	16	3	138	40	3791	136
MM32	TB (WV)	< LOD	25	12	3	< LOD	54	2083	93
MM33	TB (WV)	< LOD	26	12	3	< LOD	54	4131	146
MM34	TB (WV)	56	18	17	3	78	38	4956	157
MM35	TB (WV)	54	18	11	3	94	38	2466	119
MM36	TB (WV)	94	21	9	3	165	43	1822	87
MM37	TB (WV)	47	19	16	3	76	40	3714	127
MM40	TB (WV)	< LOD	24	13	2	< LOD	51	2603	121
MM42	TB (WV)	< LOD	26	13	3	< LOD	54	2448	117
MM45	TB (WV)	32	18	10	3	< LOD	55	2727	117
MM47	TB (WV)	42	18	10	2	< LOD	54	2658	122
MM48	TB (WV)	40	18	14	3	< LOD	56	4736	149
MM50	TB (WV)	< LOD	26	16	3	< LOD	54	3409	133
MM51	TB (WV)	< LOD	24	17	3	< LOD	50	4877	157
MM58	TB (WV)	< LOD	26	12	3	< LOD	54	2848	117
MM59	TB (WV)	30	18	14	3	< LOD	56	5540	160
MM66	TB (WV)	< LOD	27	13	3	< LOD	56	3717	140
MM69	TB (WV)	55	18	17	3	73	37	4948	156
MM73	TB (WV)	< LOD	27	11	3	< LOD	56	3237	129
MM74	TB (WV)	42	18	13	3	< LOD	57	2617	117

Sample		Sn		Sr		Te		Ti	
Sample #	District	Sn	± 2σ	Sr	± 2σ	Te	± 2σ	Ti	± 2σ
MM76	TB (WV)	< LOD	23	14	3	< LOD	50	2350	105
MM86	TB (WV)	< LOD	25	11	3	< LOD	53	2606	116
MM93-1	TB (WV)	< LOD	26	12	3	< LOD	54	3256	129
MM93-2	TB (WV)	52	18	14	3	72	38	3593	136
MM93-3	TB (WV)	< LOD	25	13	3	< LOD	53	3161	131
MM93-4	TB (WV)	30	17	14	3	< LOD	54	3563	137
MM93-5	TB (WV)	< LOD	26	13	3	< LOD	54	3473	140
MM93-6	TB (WV)	27	17	13	3	< LOD	55	3643	136
MM93-7	TB (WV)	48	18	14	3	< LOD	55	3571	140
MM93-8	TB (WV)	< LOD	26	14	3	< LOD	54	3623	137
MM93-9	TB (WV)	54	18	14	3	< LOD	55	3699	141
VB2	TB (YV)	< LOD	24	20	3	< LOD	51	3354	141
VB3	TB (YV)	< LOD	23	20	3	< LOD	49	3741	145
VB6	TB (YV)	< LOD	22	18	3	< LOD	48	3376	147
VB7	TB (YV)	< LOD	27	14	3	< LOD	56	1550	107
VB9	TB (YV)	< LOD	21	21	3	< LOD	45	3489	149
VB10	TB (YV)	< LOD	23	21	3	< LOD	48	3367	140
VB11	TB (YV)	< LOD	24	23	3	< LOD	51	3719	142
VB14	TB (YV)	< LOD	22	19	3	< LOD	48	3394	137

Sample		V		W		Zn		Zr	
Sample #	District	V	± 2σ	W	± 2σ	Zn	± 2σ	Zr	± 2σ
1027 (1017)	ARTIFACT	< LOD	81	< LOD	64	34	12	7	4
1311 (1017)	ARTIFACT	< LOD	76	78	48	25	12	20	5
2430 (1019)	ARTIFACT	< LOD	44	< LOD	80	310	28	< LOD	6
2518 (1019)	ARTIFACT	< LOD	43	< LOD	60	47	13	< LOD	5
3236 (1019)	ARTIFACT	< LOD	40	< LOD	65	49	13	< LOD	5
1332-1 (1017)	ARTIFACT	< LOD	29	< LOD	61	33	11	6	3
1350-1 (1017)	ARTIFACT	< LOD	89	< LOD	64	67	14	< LOD	6
1350-2 (1017)	ARTIFACT	< LOD	44	< LOD	60	53	13	< LOD	5
308-2 (1017)	ARTIFACT	< LOD	73	< LOD	69	30	12	< LOD	6
308-4 (1017)	ARTIFACT	< LOD	93	< LOD	71	25	12	18	5
308-5 (1017)	ARTIFACT	< LOD	64	< LOD	73	70	16	60	6
PM1	CP (BG)	< LOD	67	< LOD	64	18	11	7	4
PM2	CP (BG)	< LOD	51	< LOD	69	21	12	7	4
PM4	CP (BG)	< LOD	67	< LOD	71	23	12	8	4
PM5	CP (BG)	< LOD	59	< LOD	66	18	11	9	4
PM7	CP (BG)	< LOD	62	< LOD	67	20	11	< LOD	6
PM8	CP (BG)	< LOD	64	< LOD	68	18	11	65	6
PM9	CP (BG)	< LOD	67	< LOD	72	30	13	15	4
PM11	CP (BG)	< LOD	70	< LOD	61	17	10	7	4
RM8	CP (BG)	< LOD	37	< LOD	68	30	13	< LOD	6
RM9	CP (BG)	< LOD	30	< LOD	66	51	14	< LOD	5
RM10	CP (BG)	< LOD	41	< LOD	60	19	10	< LOD	5
RM11	CP (BG)	< LOD	41	< LOD	60	< LOD	15	< LOD	5
RM18	CP (BG)	< LOD	30	< LOD	71	56	15	7	4
RM21	CP (BG)	< LOD	22	< LOD	61	51	13	7	4
RM23	CP (BG)	< LOD	25	< LOD	76	55	15	< LOD	6
RM24	CP (BG)	< LOD	32	< LOD	73	83	16	< LOD	6
RM25	CP (BG)	< LOD	35	99	49	66	15	11	4
RM27	CP (BG)	< LOD	30	< LOD	68	83	16	< LOD	6
RM28	CP (BG)	< LOD	28	< LOD	71	57	15	11	4

Sample		V		W		Zn		Zr	
Sample #	District	V	± 2σ	W	± 2σ	Zn	± 2σ	Zr	± 2σ
RM29	CP (BG)	< LOD	27	86	55	111	19	< LOD	6
RM31	CP (BG)	< LOD	33	< LOD	68	40	13	< LOD	5
RM33	CP (BG)	< LOD	32	< LOD	67	55	14	< LOD	6
RM35	CP (BG)	< LOD	33	< LOD	68	75	16	9	4
RM40	CP (BG)	< LOD	42	< LOD	61	22	11	< LOD	5
RM42	CP (BG)	< LOD	43	< LOD	61	42	13	< LOD	5
RM48	CP (BG)	< LOD	35	97	51	100	18	9	4
RM51	CP (BG)	< LOD	34	< LOD	68	49	14	< LOD	5
RM52	CP (BG)	< LOD	29	< LOD	74	54	15	< LOD	6
RM53	CP (BG)	< LOD	34	< LOD	68	104	17	< LOD	5
RM62	CP (BG)	< LOD	33	< LOD	74	95	17	< LOD	6
RM65	CP (BG)	< LOD	33	< LOD	70	65	15	< LOD	6
RM66	CP (BG)	< LOD	37	< LOD	67	164	20	< LOD	5
RM76	CP (BG)	< LOD	32	98	54	82	17	< LOD	6
RM81	CP (BG)	< LOD	36	< LOD	75	103	18	27	5
RM87	CP (BG)	< LOD	32	< LOD	71	105	18	< LOD	6
DM1	CP (HS)	< LOD	94	< LOD	66	21	12	< LOD	6
DM3	CP (HS)	< LOD	92	< LOD	67	32	12	23	5
DM4	CP (HS)	< LOD	99	< LOD	67	24	12	< LOD	6
DM5	CP (HS)	< LOD	83	< LOD	65	19	11	< LOD	6
DM9	CP (HS)	< LOD	92	< LOD	72	< LOD	18	29	5
DM10	CP (HS)	< LOD	88	< LOD	65	27	12	8	4
DM11	CP (HS)	< LOD	87	< LOD	68	37	13	< LOD	6
DM14	CP (HS)	< LOD	77	< LOD	73	26	13	7	4
DM17	CP (HS)	< LOD	92	< LOD	68	< LOD	16	< LOD	6
DM18	CP (HS)	< LOD	93	< LOD	64	27	12	< LOD	6
DM19	CP (HS)	< LOD	103	75	49	25	12	12	4
DM20	CP (HS)	< LOD	101	< LOD	72	31	13	< LOD	6
DM21	CP (HS)	< LOD	91	< LOD	68	< LOD	17	< LOD	6
DM22	CP (HS)	< LOD	93	< LOD	65	25	12	7	4

Sample		V		W		Zn		Zr	
Sample #	District	V	± 2σ	W	± 2σ	Zn	± 2σ	Zr	± 2σ
DM25	CP (HS)	< LOD	98	< LOD	64	30	12	< LOD	6
DM29	CP (HS)	< LOD	88	83	52	23	13	< LOD	6
DM30	CP (HS)	< LOD	85	< LOD	66	32	13	6	4
DM31	CP (HS)	< LOD	82	< LOD	74	44	14	< LOD	6
DM32	CP (HS)	< LOD	88	< LOD	62	24	12	12	4
DM33	CP (HS)	< LOD	80	< LOD	66	37	13	< LOD	6
DM34	CP (HS)	< LOD	87	< LOD	68	< LOD	17	< LOD	6
JDHM1	CP (HS)	< LOD	36	< LOD	66	38	13	9	4
JDHM4	CP (HS)	< LOD	71	< LOD	69	33	12	< LOD	6
JDHM8	CP (HS)	< LOD	30	< LOD	68	30	13	< LOD	6
JDHM9	CP (HS)	< LOD	57	< LOD	67	27	12	< LOD	5
JDHM10	CP (HS)	< LOD	47	< LOD	67	43	13	< LOD	5
JDHM11	CP (HS)	< LOD	49	< LOD	63	42	13	< LOD	5
JDHM12	CP (HS)	< LOD	62	< LOD	65	33	12	< LOD	6
JDHM14	CP (HS)	< LOD	40	< LOD	68	53	15	< LOD	6
JDHM17	CP (HS)	< LOD	70	< LOD	65	39	13	< LOD	6
JDHM22	CP (HS)	< LOD	37	< LOD	66	25	12	7	4
JDHM26	CP (HS)	< LOD	34	< LOD	65	47	13	< LOD	5
JDHM27	CP (HS)	< LOD	38	< LOD	60	33	12	< LOD	5
JDHM29	CP (HS)	< LOD	58	< LOD	64	35	12	< LOD	5
JDHM32	CP (HS)	< LOD	54	< LOD	61	43	13	< LOD	5
JDHM33	CP (HS)	< LOD	40	< LOD	64	32	12	< LOD	5
JDHM34	CP (HS)	< LOD	42	< LOD	68	61	15	< LOD	5
JDHM35	CP (HS)	< LOD	70	< LOD	64	32	12	< LOD	6
JDHM43	CP (HS)	< LOD	31	< LOD	61	41	13	< LOD	5
JDHM44	CP (HS)	< LOD	46	< LOD	72	36	13	< LOD	6
JDHM45	CP (HS)	< LOD	44	< LOD	72	37	13	< LOD	6
JDHM46	CP (HS)	< LOD	42	< LOD	68	31	12	< LOD	6
JDHM48-1	CP (HS)	< LOD	71	< LOD	62	40	13	< LOD	6
JDHM48-2	CP (HS)	< LOD	61	< LOD	71	23	12	7	4

Sample		V		W		Zn		Zr	
Sample #	District	V	± 2σ	W	± 2σ	Zn	± 2σ	Zr	± 2σ
JDHM48-3	CP (HS)	< LOD	64	< LOD	73	41	14	< LOD	6
JDHM48-4	CP (HS)	< LOD	69	< LOD	66	45	13	< LOD	6
JDHM48-5	CP (HS)	< LOD	71	< LOD	64	38	13	< LOD	6
JDHM48-6	CP (HS)	< LOD	71	< LOD	63	44	13	< LOD	6
JDHM48-7	CP (HS)	< LOD	66	< LOD	66	44	13	< LOD	6
JDHM48-8	CP (HS)	< LOD	68	< LOD	71	33	13	< LOD	6
JDHM49	CP (HS)	< LOD	40	< LOD	66	32	12	6	4
JDHM50	CP (HS)	< LOD	63	< LOD	64	38	13	< LOD	5
JDHM52	CP (HS)	< LOD	56	< LOD	66	48	14	< LOD	6
JDHM54	CP (HS)	< LOD	33	< LOD	63	44	13	< LOD	5
JDHM56	CP (HS)	< LOD	50	< LOD	66	37	13	6	4
JDHM57	CP (HS)	< LOD	53	< LOD	66	35	12	< LOD	6
JDHM58	CP (HS)	< LOD	61	< LOD	65	31	12	10	4
JDHM59	CP (HS)	< LOD	55	< LOD	64	49	13	< LOD	5
JDHP1	CP (HS)	< LOD	96	< LOD	71	33	13	< LOD	6
JDHP2	CP (HS)	< LOD	99	< LOD	64	28	12	< LOD	6
JDHP6	CP (HS)	111	69	< LOD	64	24	12	9	4
JDHP9	CP (HS)	< LOD	65	< LOD	68	52	14	185	9
JDHP10	CP (HS)	< LOD	102	< LOD	67	< LOD	17	7	4
JDHP11	CP (HS)	100	60	81	49	29	13	< LOD	6
KP2	CP (HS)	< LOD	90	< LOD	68	50	14	< LOD	6
KP3	CP (HS)	< LOD	94	< LOD	62	34	12	< LOD	6
KP4	CP (HS)	< LOD	95	< LOD	71	28	12	8	4
KP5	CP (HS)	< LOD	83	< LOD	70	23	12	< LOD	6
KP7	CP (HS)	< LOD	92	< LOD	67	40	13	< LOD	6
KP8	CP (HS)	< LOD	27	< LOD	67	213	23	22	4
KP9	CP (HS)	< LOD	101	< LOD	67	39	13	< LOD	6
KP13	CP (HS)	< LOD	88	< LOD	69	33	13	< LOD	6
KP14	CP (HS)	< LOD	93	< LOD	63	49	13	< LOD	6
KP17	CP (HS)	< LOD	90	< LOD	67	26	12	< LOD	6

Sample		V		W		Zn		Zr	
Sample #	District	V	± 2σ	W	± 2σ	Zn	± 2σ	Zr	± 2σ
KP19	CP (HS)	< LOD	87	< LOD	65	43	13	13	4
KP21	CP (HS)	< LOD	93	< LOD	70	44	14	< LOD	6
KP23	CP (HS)	< LOD	80	< LOD	70	51	14	16	5
KP25	CP (HS)	< LOD	92	< LOD	68	40	13	< LOD	6
LM1	CP (HS)	< LOD	114	< LOD	67	17	11	< LOD	6
LM4	CP (HS)	< LOD	110	< LOD	67	< LOD	15	< LOD	6
LM8	CP (HS)	108	70	< LOD	66	< LOD	16	7	4
LM10	CP (HS)	< LOD	98	< LOD	64	< LOD	16	< LOD	7
LM11	CP (HS)	< LOD	101	< LOD	67	< LOD	16	19	5
LM18	CP (HS)	< LOD	108	77	49	< LOD	16	< LOD	6
LM20	CP (HS)	107	66	< LOD	71	< LOD	17	23	5
LM21	CP (HS)	< LOD	94	< LOD	70	21	12	12	5
LM27	CP (HS)	< LOD	112	< LOD	63	16	11	8	4
LM28	CP (HS)	< LOD	95	< LOD	66	17	11	< LOD	6
LM29	CP (HS)	122	72	< LOD	70	< LOD	17	8	4
WM1	CP (HS)	< LOD	31	< LOD	71	27	12	< LOD	6
WM4	CP (HS)	< LOD	40	< LOD	80	32	14	< LOD	6
WM5	CP (HS)	< LOD	32	< LOD	65	95	17	10	4
WM11	CP (HS)	< LOD	50	< LOD	68	38	13	8	4
WM17	CP (HS)	< LOD	39	< LOD	62	27	11	< LOD	6
WM21	CP (HS)	< LOD	43	< LOD	63	24	11	< LOD	5
WM24	CP (HS)	< LOD	35	< LOD	66	35	12	< LOD	5
WM27	CP (HS)	< LOD	42	< LOD	60	32	12	< LOD	5
WM32	CP (HS)	< LOD	39	< LOD	63	35	12	< LOD	5
WM35	CP (HS)	< LOD	49	< LOD	62	28	12	< LOD	5
WM45	CP (HS)	< LOD	36	< LOD	65	40	13	< LOD	5
WM59	CP (HS)	< LOD	48	< LOD	69	41	13	< LOD	6
WM66	CP (HS)	< LOD	42	< LOD	59	38	12	< LOD	5
WM68	CP (HS)	< LOD	46	< LOD	59	36	12	< LOD	5
WM89	CP (HS)	< LOD	40	< LOD	66	24	11	< LOD	5

Sample		V		W		Zn		Zr	
Sample #	District	V	± 2σ	W	± 2σ	Zn	± 2σ	Zr	± 2σ
WM90	CP (HS)	< LOD	45	< LOD	65	44	13	7	4
WM91	CP (HS)	< LOD	36	< LOD	65	40	13	< LOD	6
WM100	CP (HS)	< LOD	35	< LOD	76	94	18	< LOD	6
WM112	CP (HS)	< LOD	34	< LOD	64	54	14	7	4
WM120	CP (HS)	< LOD	36	< LOD	63	45	13	< LOD	5
WM124-1	CP (HS)	< LOD	49	< LOD	62	47	13	< LOD	5
WM124-2	CP (HS)	< LOD	49	68	45	34	12	< LOD	5
WM124-3	CP (HS)	< LOD	51	< LOD	62	42	13	< LOD	5
WM124-4	CP (HS)	< LOD	51	< LOD	60	44	13	6	4
WM124-5	CP (HS)	< LOD	50	< LOD	63	56	14	< LOD	6
WM124-6	CP (HS)	< LOD	51	< LOD	63	36	12	< LOD	5
WM124-7	CP (HS)	< LOD	48	< LOD	65	36	12	< LOD	5
WM124-8	CP (HS)	< LOD	49	< LOD	60	44	13	< LOD	5
WM125	CP (HS)	< LOD	35	< LOD	70	22	12	< LOD	6
WM138	CP (HS)	< LOD	47	< LOD	59	38	12	7	4
WM140	CP (HS)	< LOD	41	< LOD	61	29	11	< LOD	5
WM149	CP (HS)	< LOD	49	< LOD	66	29	12	< LOD	5
WM156	CP (HS)	< LOD	40	< LOD	67	39	13	< LOD	6
WM161	CP (HS)	< LOD	41	< LOD	63	27	11	< LOD	5
WM162	CP (HS)	< LOD	40	< LOD	60	34	12	< LOD	5
WM166	CP (HS)	< LOD	40	< LOD	62	39	12	27	4
WM170	CP (HS)	< LOD	37	< LOD	64	43	13	< LOD	5
WM177	CP (HS)	< LOD	40	< LOD	72	41	14	9	4
DPM1	SP	< LOD	42	< LOD	78	356	31	< LOD	6
DPM2	SP	< LOD	34	< LOD	92	238	29	< LOD	7
DPM3	SP	< LOD	52	< LOD	70	221	24	< LOD	6
DPM4	SP	< LOD	37	< LOD	75	146	22	< LOD	6
DPM5	SP	< LOD	46	< LOD	75	282	27	< LOD	6
DPM6	SP	< LOD	41	< LOD	76	170	22	9	4
DPM7	SP	< LOD	46	< LOD	82	486	36	13	4

Sample		V		W		Zn		Zr	
Sample #	District	V	± 2σ	W	± 2σ	Zn	± 2σ	Zr	± 2σ
DPM8	SP	< LOD	47	< LOD	73	237	25	< LOD	6
DPM10	SP	< LOD	39	< LOD	78	166	23	7	4
DPM10-2	SP	< LOD	39	< LOD	77	135	21	< LOD	6
DPM11	SP	< LOD	47	< LOD	70	267	27	21	5
DPM12	SP	< LOD	39	< LOD	77	208	25	< LOD	6
DPM13	SP	< LOD	45	< LOD	71	260	26	< LOD	6
DPM16	SP	< LOD	39	< LOD	78	147	21	< LOD	6
DPM18	SP	< LOD	46	< LOD	75	212	25	< LOD	6
DPM20	SP	< LOD	41	< LOD	75	259	27	< LOD	6
DPM24	SP	< LOD	44	< LOD	71	248	26	< LOD	6
DPM27	SP	< LOD	37	< LOD	84	567	40	< LOD	7
DPM28	SP	< LOD	37	< LOD	83	168	24	< LOD	6
DPM29	SP	< LOD	45	< LOD	74	547	38	< LOD	6
DPM31	SP	< LOD	34	< LOD	83	185	25	< LOD	7
DPM32	SP	< LOD	44	< LOD	83	493	37	8	4
DPM33	SP	< LOD	37	< LOD	90	558	41	< LOD	7
DPM34	SP	< LOD	40	< LOD	81	238	26	< LOD	6
DPM35	SP	< LOD	37	< LOD	81	176	24	< LOD	6
DPM36	SP	< LOD	33	< LOD	79	314	31	< LOD	6
DPM37	SP	< LOD	40	< LOD	77	300	29	< LOD	6
DPM38	SP	< LOD	33	< LOD	87	249	28	< LOD	6
DPM39	SP	< LOD	40	< LOD	76	255	27	< LOD	6
DPM39-2	SP	< LOD	40	< LOD	76	276	28	< LOD	6
McK1	SP	< LOD	41	< LOD	80	468	35	< LOD	6
McK2	SP	< LOD	39	< LOD	80	506	37	< LOD	6
McK3	SP	< LOD	43	< LOD	82	432	34	38	6
McK4	SP	< LOD	40	< LOD	78	253	26	< LOD	6
McK5	SP	< LOD	40	< LOD	92	879	48	< LOD	7
McK6	SP	< LOD	37	< LOD	82	509	37	< LOD	6
McK7	SP	< LOD	38	< LOD	82	337	30	< LOD	6

Sample		V		W		Zn		Zr	
Sample #	District	V	± 2σ	W	± 2σ	Zn	± 2σ	Zr	± 2σ
McK8	SP	< LOD	39	< LOD	80	341	31	< LOD	6
McK9	SP	< LOD	35	< LOD	81	426	35	< LOD	7
McK10	SP	< LOD	41	< LOD	84	634	41	< LOD	7
McK11	SP	< LOD	37	< LOD	81	394	33	< LOD	6
McK12	SP	< LOD	56	< LOD	83	457	34	< LOD	6
McK13	SP	< LOD	43	< LOD	78	387	32	< LOD	7
McK15	SP	< LOD	42	< LOD	82	340	30	< LOD	7
Pink1	SP	< LOD	40	< LOD	85	588	40	< LOD	6
Pink2	SP	< LOD	45	< LOD	82	402	33	< LOD	6
Pink3	SP	< LOD	47	< LOD	79	465	35	< LOD	6
Pink4	SP	< LOD	38	< LOD	81	446	34	< LOD	6
Pink7	SP	< LOD	34	< LOD	82	348	33	< LOD	7
Pink8	SP	< LOD	43	< LOD	76	334	29	< LOD	6
Pink9	SP	< LOD	34	< LOD	79	436	35	< LOD	6
Pink10	SP	< LOD	45	< LOD	73	428	32	< LOD	6
Pink11	SP	< LOD	42	< LOD	94	558	43	< LOD	7
Pink12	SP	< LOD	37	< LOD	80	320	30	< LOD	6
JAPM2	TB (IG)	< LOD	46	< LOD	80	227	25	< LOD	6
JAPM8	TB (IG)	< LOD	41	< LOD	80	213	25	< LOD	6
JAPM9	TB (IG)	< LOD	45	< LOD	75	136	20	< LOD	6
JAPM10	TB (IG)	< LOD	45	< LOD	78	345	30	12	5
JAPM15	TB (IG)	< LOD	46	< LOD	75	200	23	< LOD	6
JAPM17	TB (IG)	< LOD	88	< LOD	94	227	29	< LOD	7
MM1	TB (WV)	< LOD	58	< LOD	60	35	12	6	4
MM2	TB (WV)	< LOD	42	< LOD	62	35	12	< LOD	5
MM3	TB (WV)	< LOD	50	< LOD	57	46	12	< LOD	5
MM4	TB (WV)	< LOD	49	< LOD	62	32	12	7	4
MM5	TB (WV)	< LOD	46	< LOD	63	50	13	7	4
MM6	TB (WV)	< LOD	50	< LOD	58	46	12	< LOD	5
MM7	TB (WV)	< LOD	52	< LOD	61	44	12	< LOD	5

Sample		V		W		Zn		Zr	
Sample #	District	V	± 2σ	W	± 2σ	Zn	± 2σ	Zr	± 2σ
MM8	TB (WV)	< LOD	63	< LOD	57	38	12	< LOD	5
MM9	TB (WV)	< LOD	54	< LOD	63	37	12	< LOD	5
MM10	TB (WV)	< LOD	49	< LOD	61	54	13	< LOD	5
MM11	TB (WV)	< LOD	50	< LOD	61	59	14	< LOD	5
MM13	TB (WV)	< LOD	43	< LOD	61	46	13	8	4
MM14	TB (WV)	< LOD	53	< LOD	58	32	11	< LOD	5
MM15	TB (WV)	< LOD	53	< LOD	65	30	12	7	4
MM16	TB (WV)	< LOD	51	< LOD	62	40	12	8	4
MM24	TB (WV)	< LOD	60	< LOD	58	42	12	< LOD	5
MM28	TB (WV)	< LOD	45	< LOD	66	37	13	10	4
MM31	TB (WV)	< LOD	53	< LOD	61	36	12	< LOD	5
MM32	TB (WV)	< LOD	37	< LOD	64	52	14	< LOD	6
MM33	TB (WV)	< LOD	58	< LOD	61	31	11	< LOD	5
MM34	TB (WV)	< LOD	60	< LOD	62	40	12	7	4
MM35	TB (WV)	< LOD	47	< LOD	64	45	13	< LOD	5
MM36	TB (WV)	< LOD	35	< LOD	68	41	14	< LOD	6
MM37	TB (WV)	< LOD	50	< LOD	66	48	14	22	4
MM40	TB (WV)	< LOD	48	< LOD	58	52	12	< LOD	5
MM42	TB (WV)	< LOD	47	< LOD	64	43	13	< LOD	5
MM45	TB (WV)	< LOD	46	< LOD	61	50	13	< LOD	5
MM47	TB (WV)	< LOD	48	< LOD	58	56	13	< LOD	5
MM48	TB (WV)	< LOD	57	< LOD	62	44	13	11	4
MM50	TB (WV)	< LOD	51	< LOD	60	50	13	< LOD	5
MM51	TB (WV)	< LOD	60	< LOD	57	49	13	17	4
MM58	TB (WV)	< LOD	46	< LOD	66	48	13	6	4
MM59	TB (WV)	< LOD	61	< LOD	63	32	12	< LOD	5
MM66	TB (WV)	< LOD	54	< LOD	61	29	11	8	4
MM69	TB (WV)	< LOD	61	< LOD	57	44	12	< LOD	5
MM73	TB (WV)	< LOD	50	< LOD	60	38	12	< LOD	5
MM74	TB (WV)	< LOD	47	< LOD	62	43	13	< LOD	5

Sample		V		W		Zn		Zr	
Sample #	District	V	± 2σ	W	± 2σ	Zn	± 2σ	Zr	± 2σ
MM76	TB (WV)	< LOD	42	< LOD	64	39	13	7	4
MM86	TB (WV)	< LOD	45	< LOD	61	52	13	< LOD	5
MM93-1	TB (WV)	< LOD	51	< LOD	53	48	12	< LOD	5
MM93-2	TB (WV)	< LOD	54	< LOD	63	54	13	9	4
MM93-3	TB (WV)	< LOD	51	< LOD	59	37	12	8	4
MM93-4	TB (WV)	< LOD	53	< LOD	57	57	13	< LOD	5
MM93-5	TB (WV)	< LOD	54	< LOD	60	45	12	20	4
MM93-6	TB (WV)	< LOD	52	< LOD	58	40	12	< LOD	5
MM93-7	TB (WV)	< LOD	55	< LOD	62	35	12	< LOD	5
MM93-8	TB (WV)	< LOD	53	< LOD	59	51	13	6	4
MM93-9	TB (WV)	< LOD	54	< LOD	59	45	12	< LOD	5
VB2	TB (YV)	< LOD	57	< LOD	61	42	12	< LOD	5
VB3	TB (YV)	64	40	< LOD	59	45	12	< LOD	5
VB6	TB (YV)	< LOD	60	< LOD	60	34	12	11	4
VB7	TB (YV)	< LOD	45	< LOD	62	53	13	< LOD	5
VB9	TB (YV)	< LOD	59	< LOD	67	38	13	47	5
VB10	TB (YV)	< LOD	58	< LOD	61	41	12	< LOD	5
VB11	TB (YV)	< LOD	57	< LOD	62	26	11	7	4
VB14	TB (YV)	< LOD	55	< LOD	63	30	11	< LOD	5

APPENDIX D

ETOWAH MUSCOVITE ARTIFACT DESCRIPTIONS

mineral abbreviations follow Kretz (1983)

Catalogue #: UWG-1017	**Artifact #:** 308-1
Artifact Description: cut(?) mica fragments, village area east of Mound A	
Maximum diameter: 42 mm	**Approximate thickness:** 1 mm
Color: silver	**Cleavage/Structure:** ruled
Staining: light (dirt)	**Spots:** light (Bt/Mag?)
Inclusions: Bt/Mag?	

Catalogue #: UWG-1017	**Artifact #:** 308-2
Artifact Description: cut(?) mica fragments, village area east of Mound A	
Maximum diameter: 46 mm	**Approximate thickness:** 1-3 mm (wedged)
Color: silver	**Cleavage/Structure:** wedged
Staining: light (dirt)	**Spots:** none
Inclusions: Bt/Mag?	

Catalogue #: UWG-1017	**Artifact #:** 308-3
Artifact Description: cut(?) mica fragments, village area east of Mound A	
Maximum diameter: 27 mm	**Approximate thickness:** 2 mm
Color: silver	**Cleavage/Structure:** flat
Staining: light (dirt)	**Spots:** none
Inclusions: Bt, Tur, Mag?, pinholes	

Catalogue #: UWG-1017	**Artifact #:** 308-4
Artifact Description: cut(?) mica fragments, village area east of Mound A	
Maximum diameter: 22 mm	**Approximate thickness:** 2 mm
Color: silver	**Cleavage/Structure:** flat
Staining: moderate (dirt)	**Spots:** none
Inclusions: Bt, Tur, Py	

Catalogue #: UWG-1017	**Artifact #:** 308-5
Artifact Description: cut(?) mica fragments, village area east of Mound A	
Maximum diameter: 35 mm	**Approximate thickness:** 1 mm
Color: silver	**Cleavage/Structure:** flat
Staining: moderate (dirt)	**Spots:** none
Inclusions: Bt, Py?	

Catalogue #: UWG-1017	**Artifact #:** 308-6
Artifact Description: cut(?) mica fragments, village area east of Mound A	
Maximum diameter: 26 mm	**Approximate thickness:** < 1 mm
Color: silver	**Cleavage/Structure:** flat
Staining: light (dirt)	**Spots:** none
Inclusions: Bt (specks)	

Catalogue #: UWG-1017	**Artifact #:** 308-7
Artifact Description: cut(?) mica fragments, village area east of Mound A	
Maximum diameter: 24 mm	**Approximate thickness:** < 1 mm
Color: silver	**Cleavage/Structure:** flat
Staining: moderate (dirt)	**Spots:** none
Inclusions: Bt (specks)	

Catalogue #: UWG-1017	**Artifact #:** 308-8
Artifact Description: cut(?) mica fragments, village area east of Mound A	
Maximum diameter: 26 mm	**Approximate thickness:** 1 mm
Color: silver	**Cleavage/Structure:** flat
Staining: moderate (dirt)	**Spots:** none
Inclusions: none	

Catalogue #: UWG-1017	**Artifact #:** 308-9
Artifact Description: cut(?) mica fragments, village area east of Mound A	
Maximum diameter: 17 mm	**Approximate thickness:** < 1 mm
Color: silver	**Cleavage/Structure:** flat
Staining: moderate (dirt)	**Spots:** none
Inclusions: Bt?	

Catalogue #: UWG-1017	**Artifact #:** 1027
Artifact Description: 1 cut(?) mica sheet, Etowah Mound C	
Maximum diameter: 40 mm	**Approximate thickness:** < 1 mm
Color: silver	**Cleavage/Structure:** flat
Staining: moderate (dirt, clay)	**Spots:** none
Inclusions: Bt (wisps)	

Catalogue #: UWG-1017	**Artifact #:** 1311
Artifact Description: mica	
Maximum diameter: 37 mm	**Approximate thickness:** 2 mm
Color: silver	**Cleavage/Structure:** wavy
Staining: moderate (dirt)	**Spots:** none
Inclusions: Bt, Mag?	
no image	

Catalogue #: UWG-1017	**Artifact #:** 1332
Artifact Description: mica fragment	
Maximum diameter: 35 mm	**Approximate thickness:** < 1-2 mm (wedged)
Color: silver	**Cleavage/Structure:** wedged
Staining: moderate (dirt)	**Spots:** none
Inclusions: Bt/Mag?	

Catalogue #: UWG-1017	**Artifact #:** 1350-1
Artifact Description: cut mica fragments, Mound C	
Maximum diameter: not measured	**Approximate thickness:** not measured
Color: silver	**Cleavage/Structure:** flat
Staining: heavy (dirt, clay)	**Spots:** moderate (Bt)
Inclusions: Bt	

Catalogue #: UWG-1017	**Artifact #:** 1350-2
Artifact Description: wedge-"A" mica sheet	
Maximum diameter: 57 mm	**Approximate thickness:** < 1-2 mm (wedged)
Color: silver	**Cleavage/Structure:** wedge-"A"
Staining: moderate (dirt, clay)	**Spots:** light (Bt)
Inclusions: Bt	

Catalogue #: UWG-1017	**Artifact #:** 1567
Artifact Description: mica disc	
Maximum diameter: 17 mm	**Approximate thickness:** < 0.5 mm
Color: silver	**Cleavage/Structure:** flat
Staining: moderate (dirt)	**Spots:** none
Inclusions: none	

no image

Catalogue #: UWG-1017	**Artifact #:** 1713
Artifact Description: mica sun symbol, covered with black pitch	
Maximum diameter: not measured	**Approximate thickness:** not measured
Color: indeterminate	**Cleavage/Structure:** indeterminate
Staining: indeterminate	**Spots:** indeterminate
Inclusions: indeterminate	

Catalogue #: UWG-1019	**Artifact #:** 2014
Artifact Description: muscovite-tourmaline schist gaming disc	
Maximum diameter: 24 mm	**Approximate thickness:** 5-6 mm
Color: variable	**Cleavage/Structure:** NA
Staining: NA	**Spots:** NA
Inclusions: Ms, Tur, Qtz	

Catalogue #: UWG-1019	**Artifact #:** 2430
Artifact Description: 1 mica sheet, village area east of Mound A	
Maximum diameter: 44 mm	**Approximate thickness:** 1-2 mm
Color: green	**Cleavage/Structure:** flat “A”?
Staining: moderate (dirt)	**Spots:** light (Bt/Mg?)
Inclusions: Bt/Mg?	

Catalogue #: UWG-1019	**Artifact #:** 2445
Artifact Description: 1 mica sheet, village area east of Mound A	
Maximum diameter: 30 mm	**Approximate thickness:** < 1 mm
Color: silver	**Cleavage/Structure:** flat
Staining: light (dirt)	**Spots:** none
Inclusions: none	

Catalogue #: UWG-1019	**Artifact #:** 2518
Artifact Description: 2 mica sheets (same book), village area east of Mound A	
Maximum diameter: 77 mm	**Approximate thickness:** 2 mm
Color: silver	**Cleavage/Structure:** flat
Staining: moderate to heavy (dirt, clay)	**Spots:** none
Inclusions: Bt, pinholes	

Catalogue #: UWG-1019	**Artifact #:** 3236
Artifact Description: cut(?) mica fragment, Mound C	
Maximum diameter: 43 mm	**Approximate thickness:** < 2 mm
Color: silver	**Cleavage/Structure:** ruled
Staining: light (dirt, clay)	**Spots:** none
Inclusions: Bt/Mag?	

Catalogue #: UWG-1019	**Artifact #:** 3949
Artifact Description: perforated mica disc, Mound C	
Maximum diameter: 24 mm	**Approximate thickness:** < 0.5 mm
Color: silver	**Cleavage/Structure:** flat
Staining: light to moderate (dirt)	**Spots:** none
Inclusions: none	

APPENDIX E

R COMMANDS, DFA VALIDATION FUNCTION

```
> lda.reclass <- function(DATA, REP, MIN.N) {
+ library(MASS)
+ library(vegan)
+ resub.std <- c()
+ resub.LOG <- c()
+ resub.logr <- c()
+ CV.std <- c()
+ CV.LOG <- c()
+ CV.logr <- c()
+ bootresub.STD <- c()
+ bootresub.LOG <- c()
+ bootresub.LOGR <- c()
+ bootcross.STD <- c()
+ bootcross.LOG <- c()
+ bootcross.LOGR <- c()
+ opt.STD <- c()
+ opt.LOG <- c()
+ opt.LOGR <- c()
+ boot632.STD <- c()
+ boot632.LOG <- c()
```

```
+ boot632.LOGR <- c()

+

+ for (i in 1:REP) {

+ DATA.SAMPLE <-
rbind(DATA[c(sample(which(DATA[,1]==(levels(DATA[,1])[1])),MIN.N)),],DATA[c(sample(which(
DATA[,1]==(levels(DATA[,1])[2])),MIN.N)),]),DATA[c(sample(which(DATA[,1]==(levels(DATA[,1
])[3])),MIN.N)),])

## the preceding command must be modified for datasets with more than 3 source
## groups; the command of the form rbind(1,2,3,… i), where i =
## DATA[c(sample(which(DATA[,1]==(levels(DATA[,1])[i])),MIN.N)),], must be repeated
## through the given number of source groups

+ trn <- sample(1:length(rownames(DATA.SAMPLE)), length(rownames(DATA.SAMPLE)), replace =
TRUE)

+ std <- scale(DATA.SAMPLE[,-1], center = TRUE, scale = TRUE)

+ LOG <- log10(DATA.SAMPLE[,-1])

+ logr <- (log10((DATA.SAMPLE[,-1])/(DATA.SAMPLE[,which.min(sd(DATA.SAMPLE[,-
1]))+1])))[,-(which.min(sd(DATA.SAMPLE[,-1])))]

+ standardize <- function(DATA.SAMPLE) {(DATA.SAMPLE -
mean(DATA.SAMPLE[trn]))/sd(DATA.SAMPLE[trn])}

+ STD <- apply(DATA.SAMPLE[,-1], MARGIN = 2, FUN = standardize)

+ LOGR <- (log10((DATA.SAMPLE[,-1])/(DATA.SAMPLE[,which.min(sd(DATA.SAMPLE[trn,-
1]))+1])))[,-(which.min(sd(DATA.SAMPLE[trn,-1])))]

+ resub.std[i] <- {

+ std.lda <- lda(std, grouping = DATA.SAMPLE[,1], CV = FALSE)
```

```
+ error.resub.std <- table(DATA.SAMPLE[,1], DATA.SAMPLE[,1]) - table(DATA.SAMPLE[,1],
predict(std.lda, std)$class)

+ 100 * (1 - (sum(error.resub.std[error.resub.std > 0])/sum(table(DATA.SAMPLE[,1],
DATA.SAMPLE[,1]))))

+ }

+ resub.LOG[i] <- {

+ LOG.lda <- lda(LOG, grouping = DATA.SAMPLE[,1], CV = FALSE)

+ error.resub.LOG <- table(DATA.SAMPLE[,1], DATA.SAMPLE[,1]) - table(DATA.SAMPLE[,1],
predict(LOG.lda, LOG)$class)

+ 100 * (1 - (sum(error.resub.LOG[error.resub.LOG > 0])/sum(table(DATA.SAMPLE[,1],
DATA.SAMPLE[,1]))))

+ }

+ resub.logr[i] <- {

+ logr.lda <- lda(logr, grouping = DATA.SAMPLE[,1], CV = FALSE)

+ error.resub.logr <- table(DATA.SAMPLE[,1], DATA.SAMPLE[,1]) - table(DATA.SAMPLE[,1],
predict(logr.lda, logr)$class)

+ 100 * (1 - (sum(error.resub.logr[error.resub.logr > 0])/sum(table(DATA.SAMPLE[,1],
DATA.SAMPLE[,1]))))

+ }

+ CV.std[i] <- {

+ std.lda.CV <- lda(std, grouping = DATA.SAMPLE[,1], CV = TRUE)

+ error.CV.std <- table(DATA.SAMPLE[,1], DATA.SAMPLE[,1]) - table(DATA.SAMPLE[,1],
std.lda.CV$class)
```

```
+ 100 * (1 - (sum(error.CV.std[error.CV.std > 0])/sum(table(DATA.SAMPLE[,1],
DATA.SAMPLE[,1]))))

+ }

+ CV.LOG[i] <- {

+ LOG.lda.CV <- lda(LOG, grouping = DATA.SAMPLE[,1], CV = TRUE)

+ error.CV.LOG <- table(DATA.SAMPLE[,1], DATA.SAMPLE[,1]) - table(DATA.SAMPLE[,1],
LOG.lda.CV$class)

+ 100 * (1 - (sum(error.CV.LOG[error.CV.LOG > 0])/sum(table(DATA.SAMPLE[,1],
DATA.SAMPLE[,1]))))

+ }

+ CV.logr[i] <- {

+ logr.lda.CV <- lda(logr, grouping = DATA.SAMPLE[,1], CV = TRUE)

+ error.CV.logr <- table(DATA.SAMPLE[,1], DATA.SAMPLE[,1]) - table(DATA.SAMPLE[,1],
logr.lda.CV$class)

+ 100 * (1 - (sum(error.CV.logr[error.CV.logr > 0])/sum(table(DATA.SAMPLE[,1],
DATA.SAMPLE[,1]))))

+ }

+ bootresub.STD[i] <- {

+ STD.lda.bootresub <- lda(STD[trn,], grouping = DATA.SAMPLE[trn,1])

+ error.bootresub.STD <- table(DATA.SAMPLE[trn,1], DATA.SAMPLE[trn,1]) -
table(DATA.SAMPLE[trn,1], predict(STD.lda.bootresub, STD[trn,])$class)

+ 100 * (1 - (sum(error.bootresub.STD[error.bootresub.STD >
0])/sum(table(DATA.SAMPLE[trn,1], DATA.SAMPLE[trn,1]))))
```

```
+ }

+ bootresub.LOG[i] <- {

+ LOG.lda.bootresub <- lda(LOG[trn,], grouping = DATA.SAMPLE[trn,1])

+ error.bootresub.LOG <- table(DATA.SAMPLE[trn,1], DATA.SAMPLE[trn,1]) -
table(DATA.SAMPLE[trn,1], predict(LOG.lda.bootresub, LOG[trn,])$class)

+ 100 * (1 - (sum(error.bootresub.LOG[error.bootresub.LOG >
0])/sum(table(DATA.SAMPLE[trn,1], DATA.SAMPLE[trn,1]))))

+ }

+ bootresub.LOGR[i] <- {

+ LOGR.lda.bootresub <- lda(LOGR[trn,], grouping = DATA.SAMPLE[trn,1])

+ error.bootresub.LOGR <- table(DATA.SAMPLE[trn,1], DATA.SAMPLE[trn,1]) -
table(DATA.SAMPLE[trn,1], predict(LOGR.lda.bootresub, LOGR[trn,])$class)

+ 100 * (1 - (sum(error.bootresub.LOGR[error.bootresub.LOGR >
0])/sum(table(DATA.SAMPLE[trn,1], DATA.SAMPLE[trn,1]))))

+ }

+ bootcross.STD[i] <- {

+ STD.lda.bootcross <- lda(STD[trn,], grouping = DATA.SAMPLE[trn,1])

+ error.bootcross.STD <- table(DATA.SAMPLE[,1], DATA.SAMPLE[,1]) - table(DATA.SAMPLE[,1],
predict(STD.lda.bootcross, STD)$class)

+ 100 * (1 - (sum(error.bootcross.STD[error.bootcross.STD >
0])/sum(table(DATA.SAMPLE[,1], DATA.SAMPLE[,1]))))

+ }
```

```
+ bootcross.LOG[i] <- {

+ LOG.lda.bootcross <- lda(LOG[trn,], grouping = DATA.SAMPLE[trn,1])

+ error.bootcross.LOG <- table(DATA.SAMPLE[,1], DATA.SAMPLE[,1]) - table(DATA.SAMPLE[,1],
predict(LOG.lda.bootcross, LOG)$class)

+ 100 * (1 - (sum(error.bootcross.LOG[error.bootcross.LOG >
0])/sum(table(DATA.SAMPLE[,1], DATA.SAMPLE[,1]))))

+ }

+ bootcross.LOGR[i] <- {

+ LOGR.lda.bootcross <- lda(LOGR[trn,], grouping = DATA.SAMPLE[trn,1])

+ error.bootcross.LOGR <- table(DATA.SAMPLE[,1], DATA.SAMPLE[,1]) -
table(DATA.SAMPLE[,1], predict(LOGR.lda.bootcross, LOGR)$class)

+ 100 * (1 - (sum(error.bootcross.LOGR[error.bootcross.LOGR >
0])/sum(table(DATA.SAMPLE[,1], DATA.SAMPLE[,1]))))

+ }

+ opt.STD[i] <- {

+ STD.lda.opt <- lda(STD[trn,], grouping = DATA.SAMPLE[trn,1])

+ bootresub.opt.STD <- {

+ error.bootresub.opt.STD <- table(DATA.SAMPLE[trn,1], DATA.SAMPLE[trn,1]) -
table(DATA.SAMPLE[trn,1], predict(STD.lda.opt, STD[trn,])$class)

+ 100 * (1 - (sum(error.bootresub.opt.STD[error.bootresub.opt.STD >
0])/sum(table(DATA.SAMPLE[trn,1], DATA.SAMPLE[trn,1]))))

+ }
```

```
+ bootcross.opt.STD <- {

+ error.bootcross.opt.STD <- table(DATA.SAMPLE[,1], DATA.SAMPLE[,1]) -
table(DATA.SAMPLE[,1], predict(STD.lda.opt, STD)$class)

+ 100 * (1 - (sum(error.bootcross.opt.STD[error.bootcross.opt.STD >
0])/sum(table(DATA.SAMPLE[,1], DATA.SAMPLE[,1]))))

+ }

+ opt <- bootresub.opt.STD - bootcross.opt.STD

+ resub.std - opt

+ }

+ opt.LOG[i] <- {

+ LOG.lda.opt <- lda(LOG[trn,], grouping = DATA.SAMPLE[trn,1])

+ bootresub.opt.LOG <- {

+ error.bootresub.opt.LOG <- table(DATA.SAMPLE[trn,1], DATA.SAMPLE[trn,1]) -
table(DATA.SAMPLE[trn,1], predict(LOG.lda.opt, LOG[trn,])$class)

+ 100 * (1 - (sum(error.bootresub.opt.LOG[error.bootresub.opt.LOG >
0])/sum(table(DATA.SAMPLE[trn,1], DATA.SAMPLE[trn,1]))))

+ }

+ bootcross.opt.LOG <- {

+ error.bootcross.opt.LOG <- table(DATA.SAMPLE[,1], DATA.SAMPLE[,1]) -
table(DATA.SAMPLE[,1], predict(LOG.lda.opt, LOG)$class)

+ 100 * (1 - (sum(error.bootcross.opt.LOG[error.bootcross.opt.LOG >
0])/sum(table(DATA.SAMPLE[,1], DATA.SAMPLE[,1]))))
```

```
+ }
+ opt <- bootresub.opt.LOG - bootcross.opt.LOG
+ resub.LOG - opt
+ }
+ opt.LOGR[i] <- {
+ LOGR.lda.opt <- lda(LOGR[trn,], grouping = DATA.SAMPLE[trn,1])
+ bootresub.opt.LOGR <- {
+ error.bootresub.opt.LOGR <- table(DATA.SAMPLE[trn,1], DATA.SAMPLE[trn,1]) -
table(DATA.SAMPLE[trn,1], predict(LOGR.lda.opt, LOGR[trn,])$class)
+ 100 * (1 - (sum(error.bootresub.opt.LOGR[error.bootresub.opt.LOGR >
0])/sum(table(DATA.SAMPLE[trn,1], DATA.SAMPLE[trn,1]))))
+ }
+ bootcross.opt.LOGR <- {
+ error.bootcross.opt.LOGR <- table(DATA.SAMPLE[,1], DATA.SAMPLE[,1]) -
table(DATA.SAMPLE[,1], predict(LOGR.lda.opt, LOGR)$class)
+ 100 * (1 - (sum(error.bootcross.opt.LOGR[error.bootcross.opt.LOGR >
0])/sum(table(DATA.SAMPLE[,1], DATA.SAMPLE[,1]))))
+ }
+ opt <- bootresub.opt.LOGR - bootcross.opt.LOGR
+ resub.logr - opt
+ }
```

```
+ boot632.STD[i] <- {

+ STD.lda.632 <- lda(STD[trn,], grouping = DATA.SAMPLE[trn,1])

+ bootresub.632.STD <- {

+ error.bootresub.632.STD <- table(DATA.SAMPLE[trn,1], DATA.SAMPLE[trn,1]) -
table(DATA.SAMPLE[trn,1], predict(STD.lda.632, STD[trn,])$class)

+ 100 * (1 - (sum(error.bootresub.632.STD[error.bootresub.632.STD >
0])/sum(table(DATA.SAMPLE[trn,1], DATA.SAMPLE[trn,1]))))

+ }

+ bootinvert.632.STD <- {

+ error.bootinvert.632.STD <- table(DATA.SAMPLE[-trn,1], DATA.SAMPLE[-trn,1]) -
table(DATA.SAMPLE[-trn,1], predict(STD.lda.632, STD[-trn,])$class)

+ 100 * (1 - (sum(error.bootinvert.632.STD[error.bootinvert.632.STD >
0])/sum(table(DATA.SAMPLE[-trn,1], DATA.SAMPLE[-trn,1]))))

+ }

+ (0.368 * bootresub.632.STD) + (0.632 * bootinvert.632.STD)

+ }

+ boot632.LOG[i] <- {

+ LOG.lda.632 <- lda(LOG[trn,], grouping = DATA.SAMPLE[trn,1])

+ bootresub.632.LOG <- {

+ error.bootresub.632.LOG <- table(DATA.SAMPLE[trn,1], DATA.SAMPLE[trn,1]) -
table(DATA.SAMPLE[trn,1], predict(LOG.lda.632, LOG[trn,])$class)
```

```
+ 100 * (1 - (sum(error.bootresub.632.LOG[error.bootresub.632.LOG >
0])/sum(table(DATA.SAMPLE[trn,1], DATA.SAMPLE[trn,1]))))

+ }

+ bootinvert.632.LOG <- {

+ error.bootinvert.632.LOG <- table(DATA.SAMPLE[-trn,1], DATA.SAMPLE[-trn,1]) -
table(DATA.SAMPLE[-trn,1], predict(LOG.lda.632, LOG[-trn,])$class)

+ 100 * (1 - (sum(error.bootinvert.632.LOG[error.bootinvert.632.LOG >
0])/sum(table(DATA.SAMPLE[-trn,1], DATA.SAMPLE[-trn,1]))))

+ }

+ (0.368 * bootresub.632.LOG) + (0.632 * bootinvert.632.LOG)

+ }

+ boot632.LOGR[i] <- {

+ LOGR.lda.632 <- lda(LOGR[trn,], grouping = DATA.SAMPLE[trn,1])

+ bootresub.632.LOGR <- {

+ error.bootresub.632.LOGR <- table(DATA.SAMPLE[trn,1], DATA.SAMPLE[trn,1]) -
table(DATA.SAMPLE[trn,1], predict(LOGR.lda.632, LOGR[trn,])$class)

+ 100 * (1 - (sum(error.bootresub.632.LOGR[error.bootresub.632.LOGR >
0])/sum(table(DATA.SAMPLE[trn,1], DATA.SAMPLE[trn,1]))))

+ }

+ bootinvert.632.LOGR <- {

+ error.bootinvert.632.LOGR <- table(DATA.SAMPLE[-trn,1], DATA.SAMPLE[-trn,1]) -
table(DATA.SAMPLE[-trn,1], predict(LOGR.lda.632, LOGR[-trn,])$class)
```

```
+ 100 * (1 - (sum(error.bootinvert.632.LOGR[error.bootinvert.632.LOGR >
0])/sum(table(DATA.SAMPLE[-trn,1], DATA.SAMPLE[-trn,1]))))

+ }

+ (0.368 * bootresub.632.LOGR) + (0.632 * bootinvert.632.LOGR)

+ }

+ success <- matrix(c(mean(resub.std), mean(resub.LOG), mean(resub.logr), mean(CV.std),
mean(CV.LOG), mean(CV.logr), mean(bootresub.STD), mean(bootresub.LOG),
mean(bootresub.LOGR), mean(bootcross.STD), mean(bootcross.LOG), mean(bootcross.LOGR),
mean(opt.STD), mean(opt.LOG), mean(opt.LOGR), mean(boot632.STD), mean(boot632.LOG),
mean(boot632.LOGR)), ncol = 6, byrow = FALSE, dimnames = list(c("std", "log",
"logr"),c("Resub", "CV", "BootResub", "BootCross", "Opt", "Boot.632")))

+ success

+ write.csv(success, file = "lda_success.csv", row.names = TRUE)

+ }

+ }
```